
Electroorganic Synthesis Enabled by an Automated Flow Platform



A Thesis Submitted to Cardiff University
in Fulfilment of the Requirements for the
Degree of Doctor of Philosophy by

Nasser Amri

PhD Thesis, October 2021
Cardiff University

Acknowledgments

I am grateful to everyone who has spent their time to help and support me during my PhD studies. Words will never fully express the gratitude I have for everyone who has dedicated a time to me. The list is very long, but I will mention a few of the people who had positively affected my research and my life during my PhD.

First of all, my thanks and gratitude to my supervisor, Professor Thomas Wirth, for giving me the opportunity to work in his research group, for his continuous availability and interest, despite his busy timetable. I am grateful for his guidance during, and also for the freedom he gave me to learn from my mistakes, make my own decisions and build my confidence and experience. He has always encouraged me to develop my own ideas and helped to solve the problems encountered.

Next, I would like to thank all the past and present members of the Wirth group, whom I had the pleasure to share some time with, attended the group meetings and shared the office. Ana, Micol, Tobi, Filipa, Jihan, Haifa, Mekhman, Ziyue, Bethan, Jakob, Rawiyah, Ohud, Huaiyuan, Yu, Abdul, Marina, Tom, Donya, Rossana, Adele, Alena, Stefano, Saira, Guilherme, Frauke, Wenchao, Xiang-Yang, Niklas, Taifur, Jarno, Paulina, Chrissi, Joey, James, Tomas, Weronika, Matthew, Muhammad, Leonardo, Alex, Niklas, Dominic, Lars, Arnaud, Shaun, Simon, Alastair, Matthew, Julian, Alexander, Harry, Tim, Camille, Pankaj, Rojan and Krishna, without you all, without your suggestions, advice, support and company, my studies / life would be harder, less fun.

I would also like to thank Duncan Guthrie, Ryan Skilton, Manuel and Sek from Vapourtec company for our discussions about the reactor development and the automation system training. In particular their flow equipment and automated system were extremely helpful, in particular for all my projects. Thanks to my monitoring panel, Prof. Simon Pope and Dr. Duncan Browne, for their valuable suggestions and discussions about my projects. Thanks to all the technicians from Cardiff University. A special gratitude to Nasim, Tuhin, Beth and Mohamed for correcting and proof-reading this thesis.

I would like to acknowledge the government of Saudi Arabia, and the Jazan University (Saudi Arabia) for the generous financial support, without which this work would not have been possible. Finally, I would like to thank my loving wife, Wejdan and my lovely children Adela and Batil for all the love and joy, they provided endless support and motivation throughout my PhD work. Despite the long distance between us, my lovely Mom, brothers, and sisters have always

supported me in whatever I decided to do and go, therefore, I am forever indebted to them. I would like to thank my late dad, Jaber, whose life was not long enough to see this day. Jaber's life has been a constant source of inspiration for me; he never told how to live and always supported me. There is no way I can thank him except by prayers and raising my children the way he raised me. I would finally like to thank all my family members and friends in Cardiff and in Saudi Arabia for their support, it would have never been the same without all of you.

This PhD-journey would have been a lot harder without each and every one of you.

Thank you.

Nasser

Dedicated to my Mom and my lovely family: Wejdan, Adela, and Batil

List of Abbreviations

°C	Degree Celsius
μL	Microlitre
Ac	Acetyl
AcOH	Acetic acid
A	Ampere
aq.	Aqueous
APCI	Atmospheric pressure chemical ionisation
Ar	Aryl
BDD	Boron Doped Diamond
BPR	Back-pressure regulator
C	Concentration
δ	Chemical Shift
Cat.	Catalytic
Conv.	Conversion
CV	Cyclic voltammetry
<i>d.r.</i>	Diastereomeric ratio
DBU	1,8-Diazabicycloundec-7-ene
DIB	(Diacetoxiodo)benzene
DCE	1,2-Dichloroethane
DME	1,2-Dimethoxyethane
DMF	<i>N,N</i> -Dimethylformamide
DMP	Dess-Martin periodinane
DMSO	Dimethylsulfoxide
EDG	Electron donating group
<i>ee</i>	Enantiomeric excess
<i>e.r.</i>	Enantiomeric ratio
EI	Electron ionisation
eq.	Equivalent(s)
ESI	Electrospray ionisation
Et	Ethyl
EWG	Electron withdrawing group
F mol ⁻¹	Faraday per mole

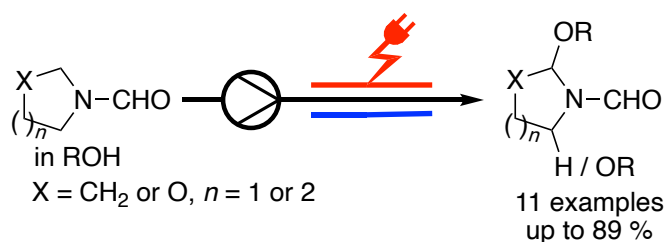
FEP	Fluorinated ethylene propylene
g	Gram
GP	General procedure
GC	Gas chromatography
h	Hour(s)
HFIP	1,1,1,3,3,3-Hexafluoro-2-propanol
HOMO	Highest occupied molecular orbital
HPLC	High performance liquid chromatography
HRMS	High resolution mass spectroscopy
Hz	Hertz
<i>i</i> -Pr	Iso-propyl
IR	Infrared
J	Coupling constant
L	Ligand
LDA	Lithium diisopropylamide
LUMO	Lowest unoccupied molecular orbital
M	Molarity
mA	Milliamperes
m.p.	Melting point
m/z	Mass over charge ratio
<i>m</i> -CPBA	<i>m</i> -Chloroperbenzoic acid
Me	Methyl
Mes	Mesityl
MHz	Megahertz
min	Minute(s)
mL	Millilitre
mmol	Millimole
mol%	Mole percentage
N	Normality
nm	nanometre
<i>n</i> -BuLi	<i>n</i> -butyllithium
NMR	Nuclear magnetic resonance
psi	Pounds per square inch

<i>p</i> -TsOH	<i>p</i> -Toluenesulfonic acid
PEEK	Polyether ether ketone
PTFE	Polytetrafluoroethylene
R _f	Retention factor (TLC)
rt	Room temperature
sat.	Saturated
<i>t</i> -Bu	tert-butyl
TEMPO	2,2,6,6-Tetramethylpiperidine-1-oxyl
Tf	Trifluoromethanesulfonate
TFA	Trifluoroacetic acid
TFE	2,2,2-Trifluoroethanol
TfOH	Trifluoromethanesulfonic acid
THF	Tetrahydrofuran
TLC	Thin layer chromatography
TMSOTf	Trimethylsilyl trifluoromethanesulfonate
r.t.	Residence time (Flow system)
Ts	<i>p</i> -toluenesulfonyl
vs	versus
V	Volts
λ	Wavelength

Abstract

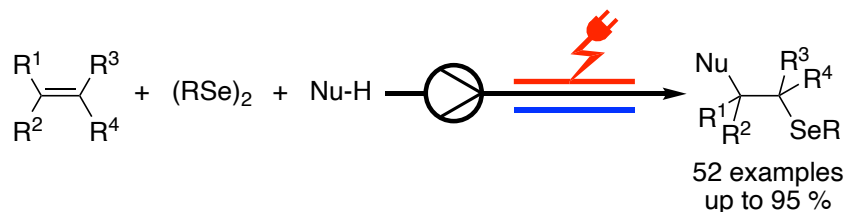
Lately, electroorganic chemistry has received the attention of chemists due to its efficiency and ability to form organic molecules by adding or removing electrons. In addition, microreactors and flow platforms are successfully engaged to offer practical solutions for the typical limitations of batch electrolysis. Our laboratory has made significant contributions to this area by developing and producing home-made electrochemical flow reactors and showing their applications in various synthetic transformations. These developments were successfully achieved but the developed reactors suffered from some limitations that affect standardization of the reaction process development.

The continuous quest to develop standard electrochemical equipment, led to development of the Ion electrochemical reactor by the flow technology company, Vapourtec, in collaboration with our laboratory. This reactor was developed to be more robust and easier to use. The first part of my work was the assessment of the performance and reliability of the Ion reactor prototype before its commercialization. The Shono oxidation was used as a model reaction (Scheme i) and the results were compared to the previously published results for the same reaction using other flow electrochemical reactors.^[1]



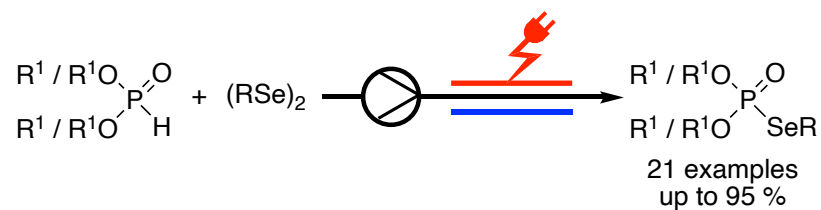
Scheme i. Alkoxylation of *N*-formylpyrrolidine.

The Ion reactor was then integrated with a fully automated flow system. This platform was utilised for selenenylation reactions of alkenes (Scheme ii).^[2] The automation allowed multiple electrochemical reactions to be performed in a fully autonomous way.



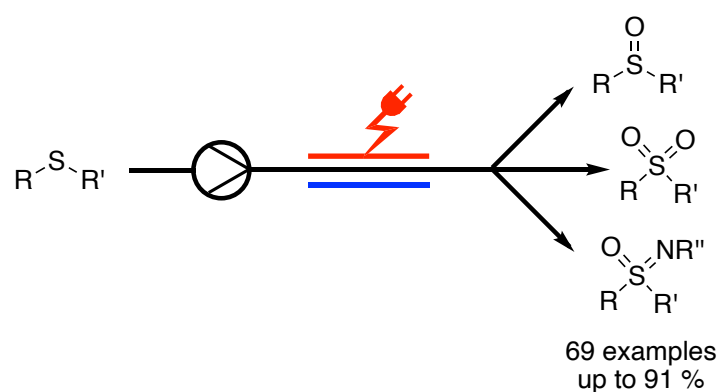
Scheme ii. Electrochemical Selenenylation of alkenes.

Similarly, the automated electrochemical flow system has been utilised for chalcogenophosphite formation (Scheme iii).^[3]



Scheme iii. Flow electrochemical synthesis of chalcogenophosphites.

Also, an efficient electrochemical flow processes for the selective oxidation of sulfides to sulfoxides and sulfones, in addition to oxidation of sulfoxides to *N*-cyanosulfoximines have been developed.^[4] The synthesis was facilitated by the fully automated electrochemical protocol.



Scheme iv. Flow electrochemical diversification of sulfides.

Publications

- [1] N. Amri, R. A. Skilton, D. Guthrie, T. Wirth, *Synlett* **2019**, *30*, 1183–1186.
- [2] N. Amri, T. Wirth, *Synthesis (Stuttg)*. **2020**, *52*, 1751–1761.
- [3] N. Amri, T. Wirth, *Synlett* **2020**, *31*, 1894–1898.
- [4] N. Amri, T. Wirth, *J. Org. Chem.* **2021**, *86*, 15961–1597.
- [5] N. Amri, T. Wirth, *Chem. Rec.* **2021**, *21*, 2526–2537.

Table of Contents

CHAPTER 1: General Introduction	1
1.1. Electrolysis and organic synthesis	3
1.2. Basic requirements	6
1.2.1. The power supply	6
1.2.2. The electrolysis cells.....	6
1.2.3. The electrodes.....	6
1.2.4. The electrolyte.....	7
1.3. Types of electrolysis cells	7
1.3.1. Undivided cells.....	7
1.3.2. Divided cells.....	9
1.3.3. Quasi-divided cell.....	9
1.3.4. Flow cells	10
1.4. Control modes of electrolysis	11
1.4.1. Constant potential electrolysis (Potentiostatic operation).....	11
1.4.2. Constant current electrolysis (Galvanostatic operation).....	13
1.4.3. Alternating current electrolysis	14
1.5.1. Direct electrolysis	18
1.5.2. Indirect electrolysis.....	19
1.5.3. Paired electrolysis.....	21
1.5.3.1. Parallel paired electrolysis	21
1.5.3.2. Divergent paired electrolysis	23
1.5.3.3. Convergent paired electrolysis.....	24
1.5.3.4. Sequential paired electrolysis (Domino paired electrolysis)	26
1.5.3.5. Linear paired electrolysis (200% current efficiency)	27
1.6. High-Throughput experimentation in electrochemistry	30
1.7. Electroorganic synthesis: the other face of the coin	31
1.8. Flow Electroorganic Synthesis	32
1.8.1. Flow electrochemical cells.....	33
1.9. Development of Ion electrochemical reactor.....	53
1.9.1. Reactor designed.....	53
1.9.2. Flow tube connectors.....	53
1.9.3. Electrode wire connection.....	54

1.9.4. Spacer and flow channel.....	55
1.9.5. Temperature control.....	56
1.10. Automation.....	57
2.4.1. RS-400 – Automated System.....	58
1.11. Conclusion and outlook.....	59
1.12. References.....	61
 CHAPTER 2: Electrochemical Alkoxylation of <i>N</i>-Formylpyrrolidine in Flow Cell .. 68	
2.1. Introduction.....	70
2.2. Different synthetic methods of <i>N</i> -acyl- <i>N,O</i> -acetals	70
2.3. Electrochemical synthesis of <i>N</i> -acyl- <i>N,O</i> -acetals	72
2.4. Flow electrochemical alkoxylation of <i>N</i> -acetylpyrrolidine	75
2.5. Results and Discussion	77
2.6. Conclusion	82
2.7. References.....	83
 CHAPTER 2: Electrochemical Selenofunctionalization of Alkenes 87	
3.1. Introduction.....	89
3.2. Different methods for selenofunctionalization of alkenes.....	91
3.2.1. Oxyseleenylation of alkene	91
3.2.2. Aminoseleenylation of alkene.....	94
3.2.3. Selenocyclization of alkenes	96
3.3. Electrochemical selenofunctionalization of alkenes	98
3.4. Flow electrochemical selenofunctionalization of alkenes	100
3.5. Results and discussion	101
3.5.1. Reaction optimization	102
3.5.1.1. Current screening	102
3.5.1.2. Solvents screening	102
3.5.1.3. Supporting electrolytes screening.....	103
3.5.1.4. Flow rate/residence time effect.....	104
3.5.1.5. Electrodes screening	104
3.5.2. Substrate scope	105

3.5.3. Reaction mechanism	108
3.6. Conclusion and outlook	110
3.7. References	112
CHAPTER 4: Electrochemical Synthesis of Chalcogenophosphites.....	117
4.1. Introduction	119
4.2. Typical processes for the synthesis of chalcogenophosphites	119
4.3. Electrochemical processes for the synthesis of chalcogenophosphites	121
4.3.1. Electrochemical oxygen–phosphorus formation	121
4.3.2. Electrochemical sulfur–phosphorus formation	123
4.3.3. Electrochemical selenium–phosphorus formation	125
4.4. Flow electrochemical synthesis of chalcogenophosphites.....	126
4.4.1. Results and discussions.....	127
4.4.1.1. Optimisation of the reaction conditions	127
4.4.1.2. Substrate scope	128
4.4.1.3. Reaction mechanism	130
4.5. Conclusion and outlook	131
4.6. References	133
CHAPTER 5: Electrochemical oxidation of organosulfur compounds	136
5.1. Organosulfur compounds	138
5.2. Results and discussion	139
5.2.1. Electrochemical oxidation of sulfides to sulfoxides.....	140
5.2.1.1. Electrode screening	140
5.2.1.2. Solvent screening	141
5.2.1.3. Flow rate screening	142
5.2.1.4. Concentration screening	143
5.2.1.5. Substrate scope.....	144
5.2.2. Electrochemical oxidation of sulfides to sulfones.....	146
5.2.2.1. Effect of charge on the selectivity of the anodic oxidation of sulfides	147
5.2.2.2. Substrate scope.....	148
5.2.3. Electrochemical oxidation of sulfoxides to sulfoximines.....	149
5.2.3.1. Electrode screening	150
5.2.3.2. Solvent and supporting electrolyte screening	150

5.2.3.3. Flow rate and charge screening.....	151
5.2.3.4. Substrate scope.....	153
5.2.4. Reaction mechanism	155
5.3. Conclusions and outlook	157
5.4. References	158
CHAPTER 6: Experimental Part.....	161
6.1. General methods.....	163
6.2. Automated flow and electrochemical reactor setup	165
6.3. Experimental Data for Chapter 2.....	167
6.3.1. Synthesis of <i>N,O</i> -acetals	167
6.3.1.1. Monoalkoxylation of <i>N</i> -Formylpyrrolidine.....	167
6.3.1.2. Dialkoxylation of <i>N</i> -Formylpyrrolidine.....	169
6.4. Experimental Data for Chapter 3.....	173
6.4.1. Oxyselelenylations of alkenes	173
6.4.2. Intramolecular selenocyclisations of alkenes.....	191
6.5. Experimental Data for Chapter 4.....	194
6.6. Experimental Data for Chapter 5.....	202
6.6.1. Electrochemical oxidation of sulfides to sulfoxides.....	202
6.6.2. Electrochemical oxidation of sulfides to sulfones.....	212
6.6.3. Electrochemical imination of sulfoxides.	221
6.6.4. Reduction of <i>N</i> -cyanosulfoximines.	227
6.7. References.....	230
Appendix: GC Method and Data for Chapter 2.....	233

CHAPTER 1

General Introduction

CHAPTER 1: General Introduction.....	1
1.1. Electrolysis and organic synthesis	4
1.2. Basic requirements.....	7
1.2.1. The power supply	7
1.2.2. The electrolysis cells.....	7
1.2.3. The electrodes.....	7
1.2.4. The electrolyte.....	8
1.3. Types of electrolysis cells	8
1.3.1. Undivided cells.....	8
1.3.2. Divided cells.....	10
1.3.3. Quasi-divided cell.....	10
1.3.4. Flow cells	11
1.4. Control modes of electrolysis	12
1.4.1. Constant potential electrolysis (Potentiostatic operation).....	12
1.4.2. Constant current electrolysis (Galvanostatic operation).....	14
1.4.3. Alternating current electrolysis	15
1.5.1. Direct electrolysis.....	19
1.5.2. Indirect electrolysis.....	20
1.5.3. Paired electrolysis.....	22
1.5.3.1. Parallel paired electrolysis	22
1.5.3.2. Divergent paired electrolysis	24
1.5.3.3. Convergent paired electrolysis.....	25
1.5.3.4. Sequential paired electrolysis (Domino paired electrolysis)	27
1.5.3.5. Linear paired electrolysis (200% current efficiency)	28
1.6. High-Throughput experimentation in electrochemistry	31
1.7. Electroorganic synthesis: the other face of the coin	32
1.8. Flow Electroorganic Synthesis	34
1.8.1. Flow electrochemical cells.....	34
1.9. Development of Ion electrochemical reactor.....	54
1.9.1. Reactor designed	54
1.9.2. Flow tube connectors.....	54
1.9.3. Electrode wire connection.....	55
1.9.4. Spacer and flow channel	56

1.9.5. Temperature control.....	57
1.10. Automation:	58
2.4.1. RS-400 – Automated System	59
1.11. Conclusion and outlook.....	60
1.12. References	62

1.1. Electrolysis and organic synthesis

Although electrochemistry was born as a synthetic method (by Faraday, Kolbe, Haber, and many others),^[1,2] the synthetic applications of electrochemistry and the development of electroorganic synthesis were much way behind the analytical and physical electrochemical studies and applications. It took almost two centuries for electroorganic synthesis to come to the forefront of organic synthesis and becoming one of its mainstreams. This lag could be due to the unfamiliarity of synthetic organic chemists with electricity and electrochemical setups and the lack of standardised equipment and techniques which result in difficulties in reproducing results sometimes. This image is completely flipped in the 21st century and the field is flourishing and becoming one of the mainstreams of synthetic organic chemistry with a burst of publications and the development of tremendous electroorganic synthesis methodologies and the development and commercialisation of standardised electrolysis cells and equipment for synthetic purposes under both batch and flow conditions.^[3–7]

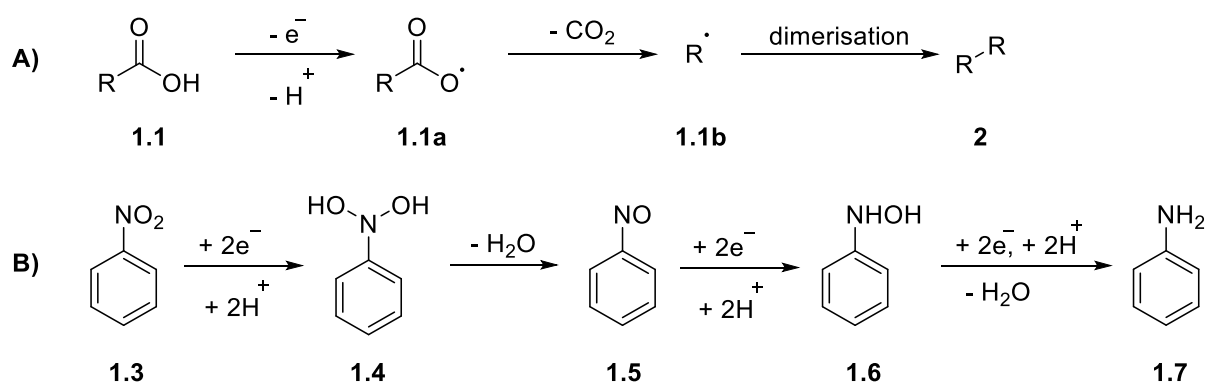
The current interest and developments in electroorganic synthesis can be attributed to two main driving forces: sustainable eco-friendly synthesis and the search for new reactivity, selectivity, and better understanding and control of chemical reactions.

The scientific community generally and the chemical society in its heart is not isolated from the ecological challenges the humanity is facing and the increased global awareness and social movements for combating climate change and developing sustainable economy that guarantee prosperity and at the same time preserves the environment, resources, and reduces waste production. Electroorganic synthesis is the construction of organic molecules using electricity as a ‘reagent’ *via* achieving oxidation and reduction of organic compounds at electrodes. Therefore, using electricity in organic synthesis eliminates hazardous, toxic, and sometimes expensive chemical oxidants and reductants and their direct chemical waste. In addition, electricity is cheap and can be produced from sustainable, renewed energy sources rather than fossil fuel. Hence, electroorganic synthesis is inherently green and is an efficient tool for achieving sustainable eco-friendly organic synthesis.^[2,4]

Electroorganic synthesis is also a powerful tool available for organic chemists in their continuous search for new reactivities, better selectivity and control over reaction pathways. Electron transfer at the electrode surface is a fast phenomenon and electrochemical reactions are generally mild as they are usually run under ambient conditions. As the oxidation and reduction processes take place at the electrode surface, the two redox events are isolated and can be used for productive formation of the desired product(s) (paired electrolysis) and high degrees of selectivity can be achieved by controlling the applied potential at the working

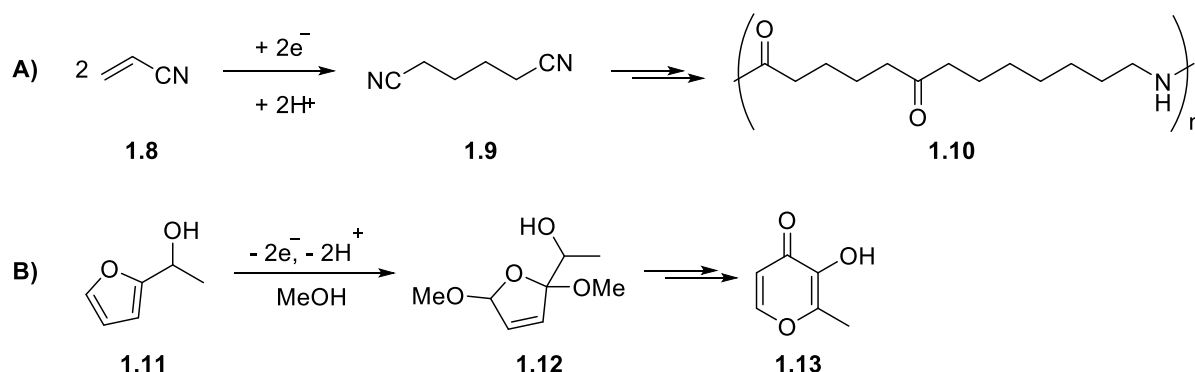
electrode, the composition of the electrolytic solution and the electrode material. In addition, the generation of reactive species and hazardous / toxic reagents can be achieved in a highly controlled way by controlling the rate of charge passage through the solution and the electrode potential. The advantages of electroorganic synthesis are clear and vast but it does not come without a cost. As the electric conductivity of organic solvents is poor, the use of large amounts of supporting electrolytes is inevitable to facilitate the passage of charge and to run the reactions under practical cell potentials in addition to corrosion and erosion of electrodes have its implications on the safety, cost, time, and the burden of removing it from the product. Over oxidation of the desired product(s) sometimes and the restriction of the electron transfer processes to the limited electrode surface poses some challenges, especially for scaling-up.^[1,2,5] But, some of these problems could be minimised and sometimes avoided completely by performing the electrolysis under flow conditions, a technique that is gaining popularity and attention lately.^[8–11]

The history of electroorganic synthesis can be traced back to the pioneering work of Faraday and Kolbe on the electrolysis of carboxylic acids done in the mid of the 19th century. The well-known reaction, referred to as Kolbe electrolysis, is a very powerful tool for synthesis of hydrocarbons *via* dimerization of alkyl radicals generated by anodic decarboxylation of carboxylic acids (Scheme 1.1 A). The work of Haber by the end of the 19th century on the electrochemical reduction of nitrobenzene (**1.3**) is another remarkable early example of the power and potential of electrolysis in organic synthesis. Haber demonstrated the importance of the applied potential in controlling the reaction outcome and selectivity, applying different potential values lead to the isolation of the different reduction products of nitrobenzene: nitrosobenzene (**1.5**), phenylhydroxylamine (**1.6**), and aniline (**1.7**) (Scheme 1.1 B).



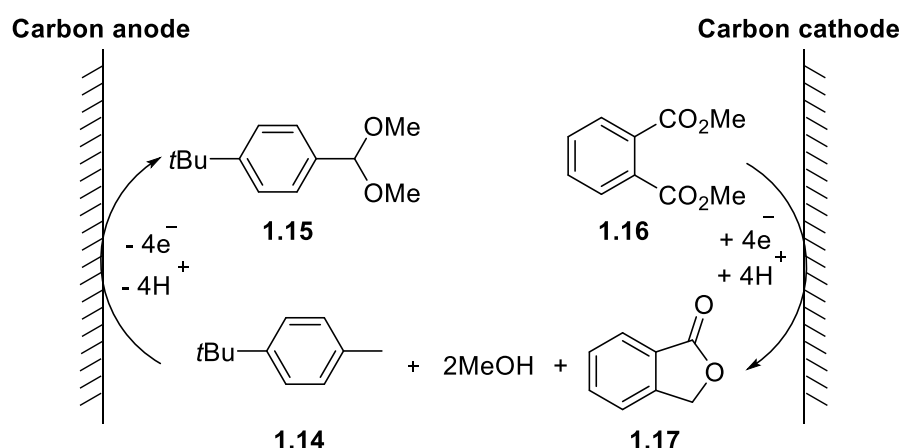
Scheme 1.1. Examples of pioneering work on electroorganic synthesis: A) Kolbe electrolysis; B) Haber's reduction of nitrobenzene.

Several electrochemical processes for commercial production of organic chemicals are known.^[12] For example, adiponitrile (**1.9**), an important intermediate in the production of nylon-6,6 (**1.10**) is produced on a scale > 100,000 ton/year^[5] by electrochemical hydrodimerization of acrylonitrile (**1.8**), the ‘Monsanto’ process (Scheme 1.2A). The reaction was known since 1940s but it was improved by Baizer and commercialised by Monsanto in the 1960s.^[2,13] Another example of industrial electrochemical process for organic compounds is the electrochemical methoxylation of 1-(furan-2-yl)ethan-1-ol (**1.11**) adopted by the Japanese to produce ~150 ton/year of the methoxylated product (**1.12**), a precursor for the food additive maltol (**1.13**) (Scheme 1.2b).^[12]



Scheme 1.2. Examples of electrochemical process for commercial production of organic chemicals: A) The ‘Monsanto’ process; B) Otsuka maltol production.

BASF process for production of 4-(*t*-butyl)benzaldehyde dimethyl acetal (**1.15**) and phthalide (**1.17**) is a remarkable commercial (~30.000 ton/year) example of exploiting both half-cell reactions (paired electrolysis) to produce value-added chemicals at the anode and the cathode simultaneously (Scheme 1.3).^[12]



Scheme 1.3. Schematic representation of the BASF process for electrochemical production of **1.15** and **1.17**.

1.2. Basic requirements

In electrochemical reactions the electrodes replace chemical oxidants and reductants where electron transfer takes place heterogeneously at the electrode surface leading to oxidation at the anode and reduction at the cathode. Usually, the reaction at one electrode (the working electrode) only is intended and leads to the desired product, while the reaction at the other electrode (the counter electrode) is sacrificial, but it is possible to get benefit of the two half-cell reactions simultaneously. Hence, to achieve electrochemical reaction at least two electrodes are needed, positive electrode (the anode) where oxidation takes place and negative electrode (the cathode). The two electrodes need to be connected to the power source and a supporting electrolyte is usually needed to facilitate the passage of the electric charge through poorly conductive organic solvents. The laboratory setup for electrolysis varies from very simple one (a beaker with two electrodes immersed in the solution) to sophisticated instruments, but regardless of being simple or complex the various setups has common basic requirements needed for successful electrolysis.

1.2.1. The power supply

A power supply is a source of electricity that maintains a continuous flow of electrons through the cell by exerting voltage enough to overcome the cell resistance. It come with a wide and variable range of capabilities and costs, from extremely cheap small batteries to high-end expensive sophisticated programable electronic devices that can precisely control the current and voltage over a wide range of values and feed various cells at the same time.

1.2.2. The electrolysis cells

The cell is a vessel that holds the electrolytic solution and at least two electrodes. Like the power supply it can be as simple as an open beaker or a flask with two electrodes connected to a power source or especially designed cell with various shapes, materials, and degrees of sophistication according to the needs, in addition to flow electrochemical cells. More detailed discussion of cell designs and types in section 1.3.

1.2.3. The electrodes

In principle, electrodes can be made of any conductive or semiconductive material and like the cell and the power supply it can vary from cheap graphite (a pencil), aluminium foil or metallic cutlery to highly expensive or boron-doped diamond (BDD). As the electron transfer takes place at the electrode surface, electrodes are the most characteristic component of the cell, and they are of outmost importance for successful electrochemical transformation. In addition to having sufficient electric conductivity, electrode material should have sufficient corrosion

stability and chemical 'inertness'.^[1,14] Electrode passivation, due to the formation of an insulating layer on the electrode surface that reduces its activity because of complete or partial blockage of the electrode surface is the main electrode related problems encountered during electrolysis. The passive layer could be a metal oxide or polymeric film that is formed due to oxidation of electron rich organic molecules, especially olefins and aromatic compounds. Electrode passivation can be alleviated by reversing the electrode polarity periodically - requires the same material for both the anode and the cathode- or using additive to increase the solubility of the polymeric material.^[1]

1.2.4. The electrolyte

In electrolysis, electrolyte is the mixture subjected to electrolysis (the reaction mixture). It consists of the solvent or solvents mixture, supporting electrolytes, reactants, catalysts, additives, and products. The solvent system is a highly important parameter for the success of the electrolysis and obtaining the desired product. In electroorganic synthesis, the electrolysis is usually performed in organic solvents which generally have poor electric conductivity necessitating addition of supporting electrolytes to decrease the cell resistance and make the electrolysis practical. The supporting electrolyte is a chemical, usually, a salt (organic or inorganic) that is added to facilitate the passage of electricity through the poorly conductive reaction medium. Sometimes, one or more of the reactants and / or additives needed for the desired chemical reaction are ionisable and can have a dual role as reactants and enhance the mixture conductivity eliminating or minimising the need of added supporting electrolytes. Supporting electrolytes can be inorganic salts such as LiClO_4 or organic salts such as pyridinium and quaternary ammonium salts. The organic salts such as Bu_4NBF_4 and related compounds have the advantage of easy solubility in organic solvents, but their removal from the product is sometimes problematic.^[1,2]

1.3. Types of electrolysis cells

As mentioned earlier, electrolysis cells can vary from very simple beaker-type cells to elaborate especially designed cells. In this section the basic types of electrolysis cells commonly encountered in synthetic organic chemistry laboratories will be described, flow electrolysis cells will be discussed briefly in section 1.3.4 and in depth in section 1.8.

1.3.1. Undivided cells

The simplest cell design is the undivided cell (Figure 1.1). In an undivided cell the two electrodes -usually parallel plates- are immersed in the electrolytic solution contained in a vial, beaker, flask or more elaborate especially made glassware or other materials, the distance

between the two electrodes should be kept as small as possible to minimise the cell resistance. The electrode surface area and hence the cell productivity can be increased by using a series of parallel plates.^[15] In undivided cells, there is no physical separation between the anode and the cathode, therefore the components of the electrolyte can reach both electrodes. Hence, the reactive intermediates or the desired product(s) formed at one electrode should not undergo a reverse reaction at the counter electrode, otherwise, a “chemical short-cut” is established leading to non- or less productive process. A situation that is usually avoided by choosing an easy sacrificial (non-productive) counter reaction such as hydrogen gas evolution from the reduction of protic solvents or acids at the cathode in case of anodic oxidation. Sometimes the counter reaction can be productive (paired electrolysis) leading to the formation of a reagent or a reactive species needed for the formation of the desired product, or it can be used to produce a second desired product from the same cell, like the BASF process mentioned earlier (Section 1.1, Scheme 1.3).

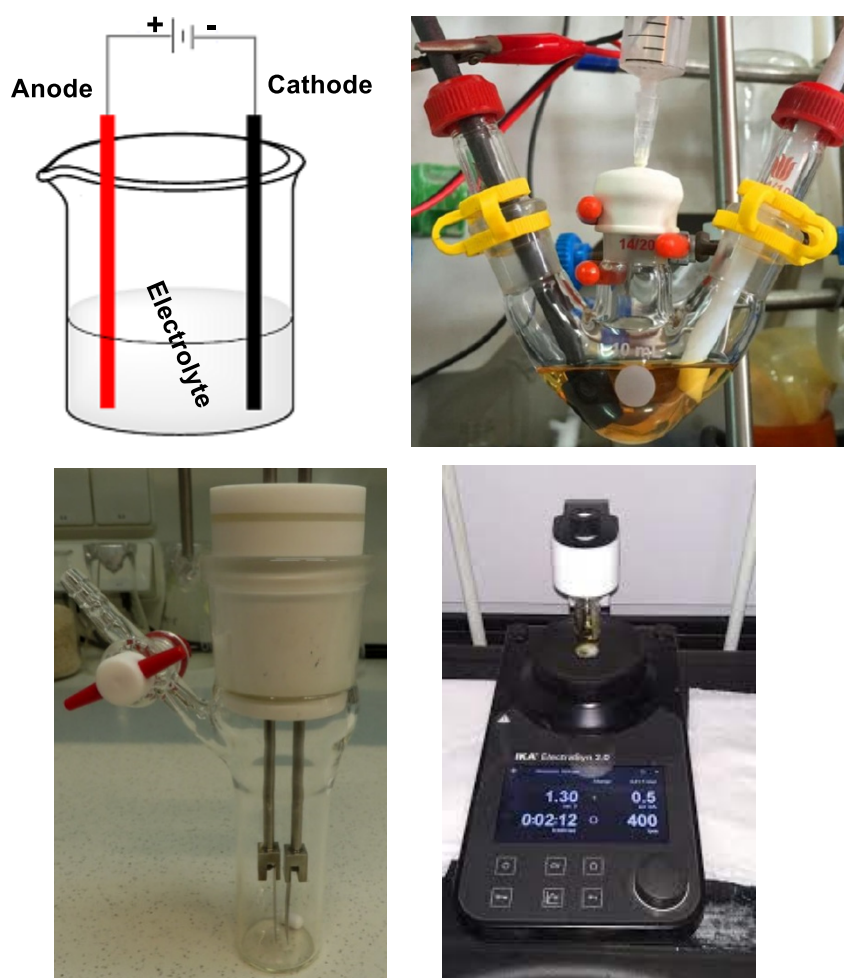


Figure 1.1. Undivided cell setup. Top left: schematic representation; top right: home-made; bottom left: home-made; Commercially available Electrasyn from IKA.

1.3.2. Divided cells

Sometimes it is necessary to physically separate the anode from the cathode, to prevent a “chemical short-cut” or undesired reaction at the counter electrode. In such cases a more elaborate divided cell design, also known as H-cell is used (Figure 1.2). The divided cell is composed of two compartments physically separated by a porous material such as sintered glass or ceramics or ion exchange membrane such as Nafion membranes, these separators allow the exchange of ions between the two separated compartments and hence allowing the conductivity, but prevent mixing chemicals (substrates, reagents, product) from one compartment with the other. One compartment is equipped with the anode and charged with anodic electrolyte (anolyte) and the other compartment is equipped with the cathode and charged with the cathodic electrolyte (catholyte). Although the divided cell is more elaborate and is more complicated compared to a basic undivided cell, its use is sometimes inevitable, in addition, the physical separation of the anolyte and the catholyte can allow paired electrolysis easily and simplify the isolation of the products.

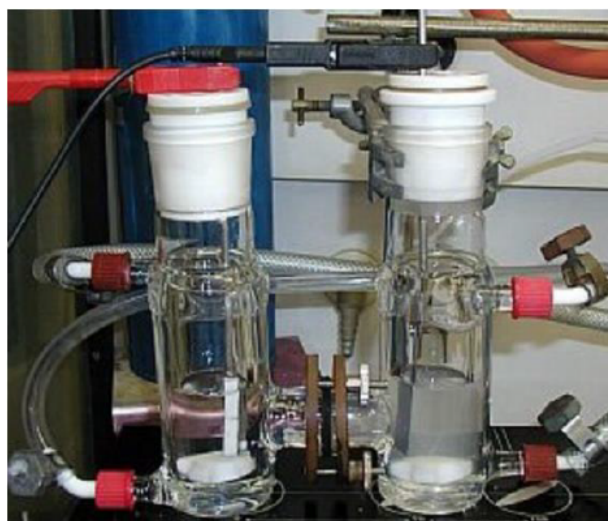
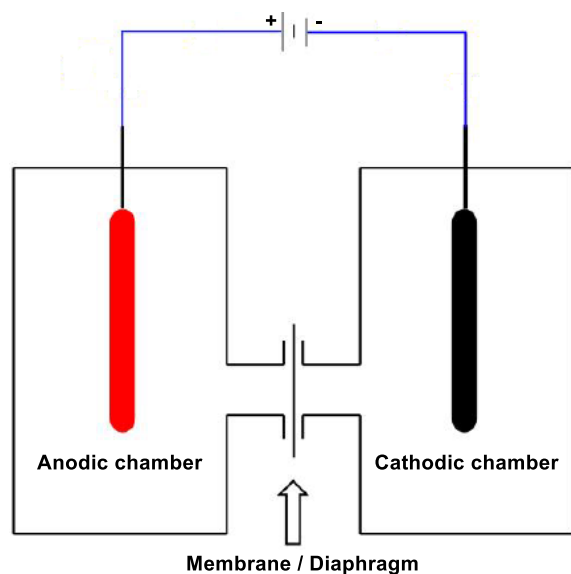


Figure 1.2. Divided cell setup.

1.3.3. Quasi-divided cell

Quasi-divided cell design is characterised by working electrode of very large surface area relative to a small surface area counter electrode usually a wire (Figure 1.3) and the electrolysis is done under low constant current (e.g 10 mA). At the working electrode the current density is low and the substance with the lowest redox potential undergoes electron transfer. At the counter electrode and because of its low surface area the current density is relatively very high, and the mass transfer is poor, hence, the current is used to electrolyze the solvent preventing electrolysis of starting material or product at the counter electrode, avoiding, or largely

minimizing side reactions or chemical short-cut. Therefore, quasi-divided cell design combines the advantages of both divided and undivided-cell designs.

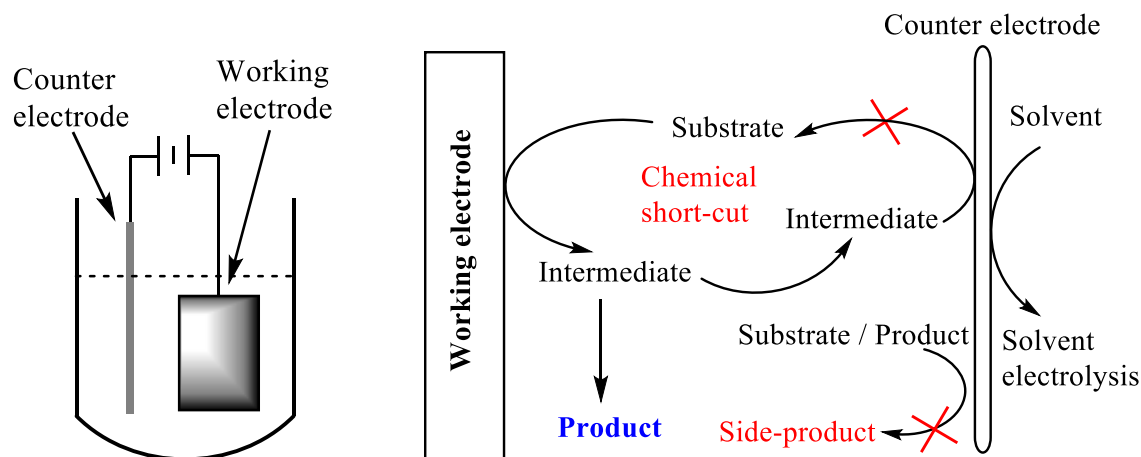


Figure 1.3. Quasi-divided cell. Left: Setup schematic representation; Right: Working principle schematic representation.

1.3.4. Flow cells

Electrolysis under flow conditions can be done simply by pumping the reactant(s) solution between two electrodes fixed on a very short distance from each other. The narrow gap between the two electrodes reduces the cell resistance: hence, the electrolysis can be performed without supporting electrolytes or using much way lower concentrations of added electrolytes compared to batch-type electrolysis. In addition, under flow conditions the reaction mixture is removed continuously reducing the opportunity of overoxidation, which is considered one of the main drawbacks of electrolysis in batch-type cells. A simplified schematic representation of electrolysis under flow conditions is depicted in figure 1.4.^[8–10]

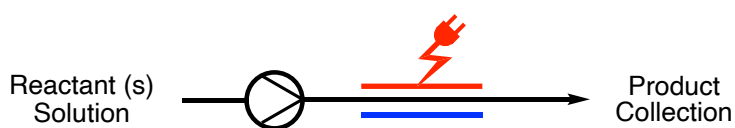


Figure 1.4. Simplified schematic representation of electrolysis under flow conditions.

Several implementations of the above arrangement (Figure 1.4) have been developed by various research groups, leading to the design and production of many electrochemical flow cells, that have been utilized in a wide range of electrochemical reactions.^[16–22] In addition, some designs of electrochemical flow cells have been commercialised^[23–25] which has prompted more laboratories to consider electrolysis under flow conditions as a viable

alternative in organic synthesis. In this context, our laboratory has developed several generations of electrolysis flow cells that have been utilized in the development of a wide range of electrochemical methodologies for organic synthesis.^[8]

The various types and designs of electrochemical flow cells and examples of their applications in organic synthesis will be discussed in detail in section 1.8.

1.4. Control modes of electrolysis

Electrochemical reactions can be controlled by electrical parameters. The basic concepts of electrolysis can be deduced from Ohm's law ($V = IR$) which is applicable to all kinds of electrolysis. Based on that electrolysis cells can operate under different control modes as follows:

1.4.1. Constant potential electrolysis (Potentiostatic operation)

Under potentiostatic mode of operation the electrolysis is performed at a constant potential applied over the whole electrolysis time, using a potentiostat as a power supply (Figure 1.5).

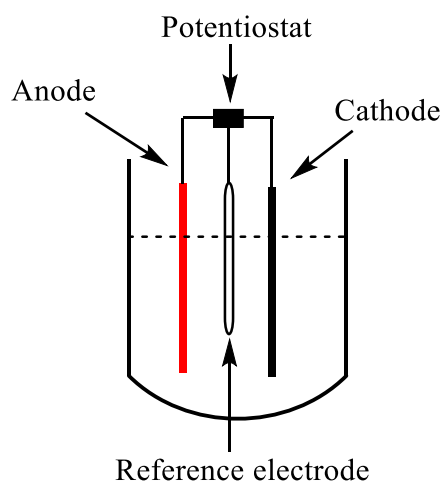


Figure 1.5. Schematic representation of electrolysis under potentiostatic mode of operation.

The applied potential is set to a specific value that matches the redox potential of a specific substrate in the reaction mixture. Hence, the redox potential of the desired substrate must be known in the same solvent system used for the reaction which can be achieved by running cyclic voltammetry experiment before the electrolysis (Figure 1.6).

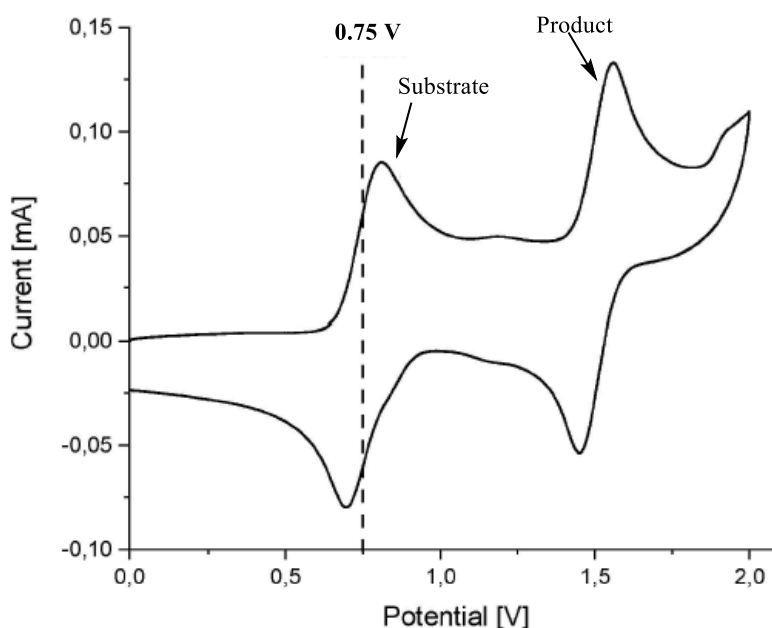


Figure 1.6. Determination of redox potential by cyclic voltammetry. Reproduced from reference [14] under Creative Commons CC BY license.

Under this operation mode, at the beginning, the substrate concentration is high, and the mass transport is sufficient to keep the cell current constant to some extent. With the progress of the reaction and consumption of the starting material its concentration decreases, and the mass transfer becomes insufficient, therefore the cell current drops reaching the endpoint of the electrolysis when the cell current is about only 5% of the initial value which corresponds to consumption of about 98% of the starting material (Figure 1.7).

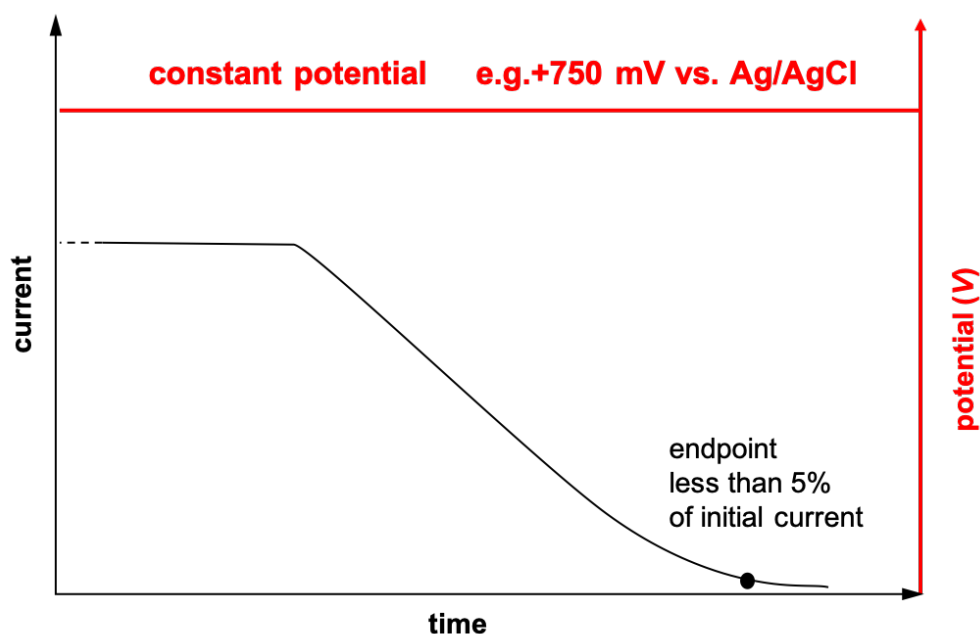


Figure 1.7. Change of cell current over potentiostatic electrolysis. Reproduced from reference [14] under Creative Commons CC BY license.

From mere electrochemical point of view, potentiostatic mode of operation is the optimal control mode as selective electron transfer can be achieved and the maximum possible reaction rate (current density) is automatically adjusted independent of other variables, under the application of constant potential corresponding to the redox potential of the desired substrate.^[1] But this operation mode is more complicated than the galvanostatic mode (*vide infra*) and is relatively expensive, especially in large-scale cells. As the electrochemical potential is a relative value, a third electrode (reference electrode) is necessary. Calomel electrode and Ag/AgCl electrode are widely used reference electrodes. For reproducible results, the applied potential and the type of the reference electrode used must be reported.

1.4.2. Constant current electrolysis (Galvanostatic operation)

Under the galvanostatic mode of operation, the electrolysis is performed at a constant current applied over the whole electrolysis time, using a galvanostat as a power supply.^[1] This mode of operation is simpler compared to potentiostatic mode requiring only two electrodes, anode and cathode, and an inexpensive power supply (Figure 1.8).

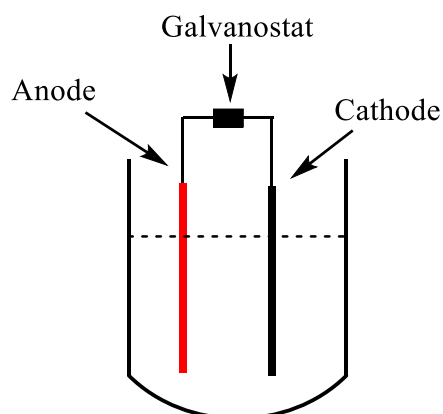


Figure 1.8. Schematic representation of electrolysis under galvanostatic mode of operation.

The potential (V) of the transformation is not controlled under galvanostatic mode of operation, therefore, at low current densities electrochemical transformation of the substrate of the lowest redox potential takes place. But the concentration of that substance decreases over time and at some point, the concentration becomes insufficient (Figure 1.9).

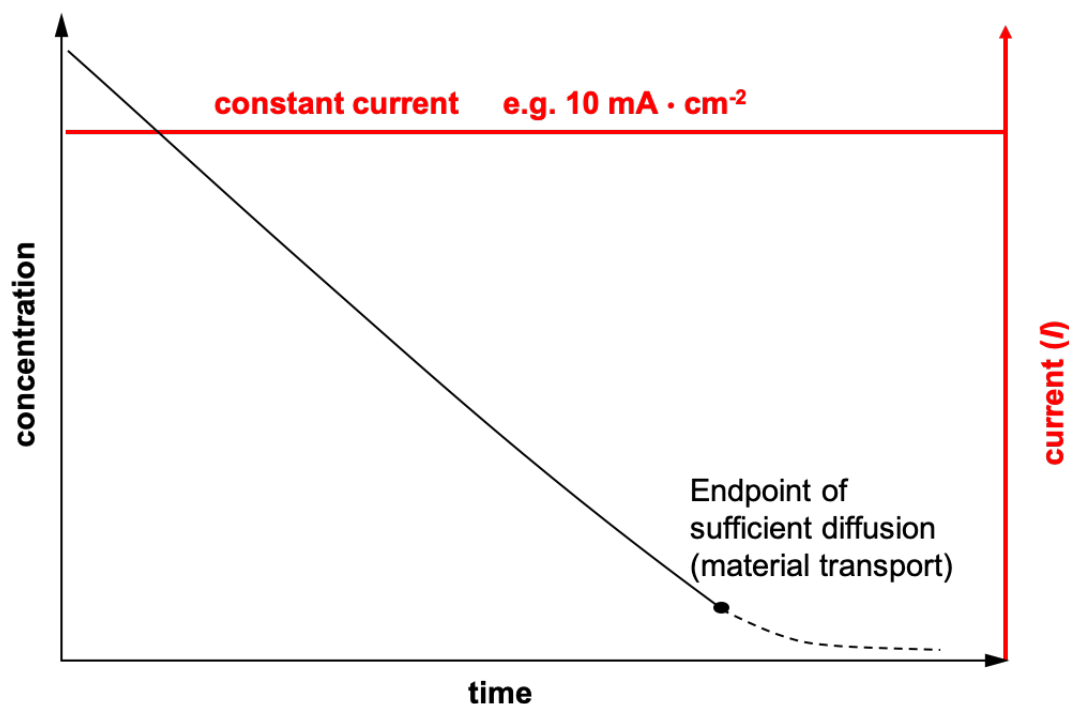


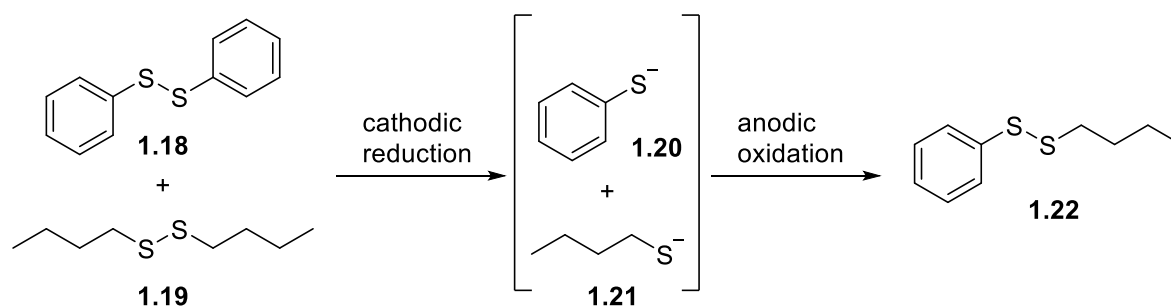
Figure 1.9. Change of substrate concentration over galvanostatic electrolysis. Reproduced from reference [14] under Creative Commons CC BY license.

If the electrolysis continued beyond that point, the galvanostat will increase the applied potential to keep the applied current constant leading to electrochemical transformation of the substance that has the next lowest redox potential, which could result in over-oxidation of the product if that substance happens to be the desired product. Under this mode of operation, it is important to report the applied current, the dimensions of the electrodes (the immersed area), the total charge (F/mol) or the time to ensure reproducibility of the results. It is also desirable to report the gap between the electrodes and the cell design.^[14]

1.4.3. Alternating current electrolysis

The above two modes of operation; potentiostatic and galvanostatic electrolysis, rely on direct current where the polarity of each electrode remains fixed over the whole electrolysis time. Doing the electrolysis using alternating current or periodically alternating the electrode polarity is not common and its applications in organic synthesis are scarce. In organic synthesis, electrolysis with alternating polarity is mainly used to overcome electrode passivation due to deposition of solids or formation of polymeric films on the electrode surface.

Recently, electrolysis using alternating current has gained some momentum. In 2019 Hilt and co-workers^[26] reported the application of alternating current electrolysis in the synthesis of libraries of unsymmetrical disulfides starting from readily available symmetric disulfides through sulfur-sulfur bond metathesis (Scheme 1.4).



Scheme 1.4. Electrochemical reduction-oxidation cycle for formation of mixed disulfides *via* sulfur-sulfur bonds metathesis.

The authors reported that it was possible to form a dynamic library of mixed disulfides using a matrix of up to six symmetrical disulfides under alternating polarity conditions. Where the electrolyte mixture was subjected to constant current pulse for a specific period (t_1) followed by a period with no current (t_2) then the polarity of electrodes is reversed for a period of t_1 (Figure 1.10).

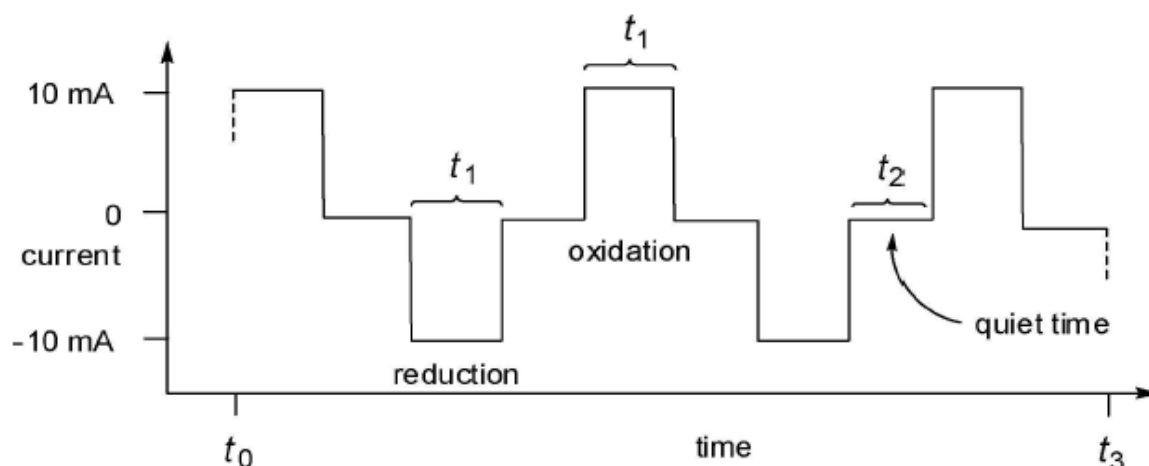
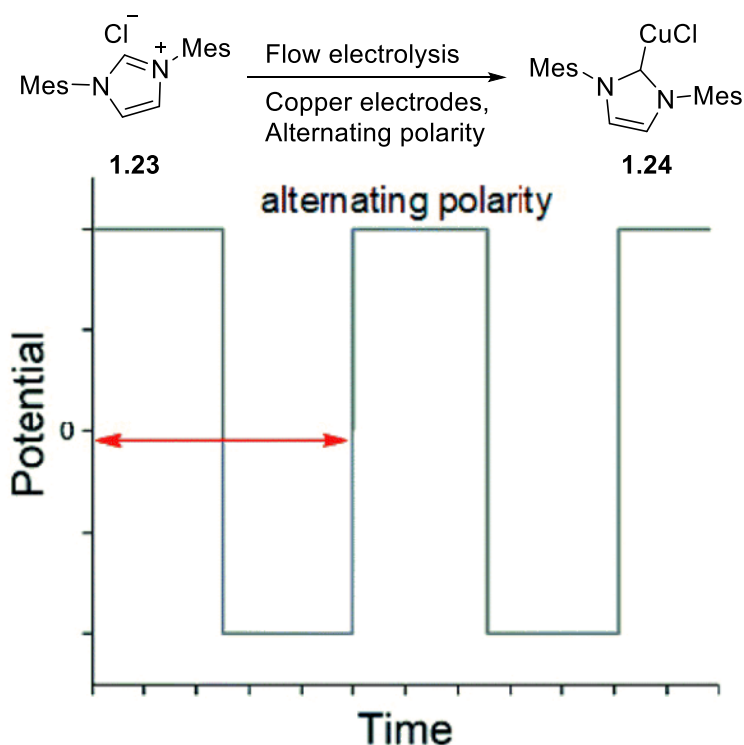


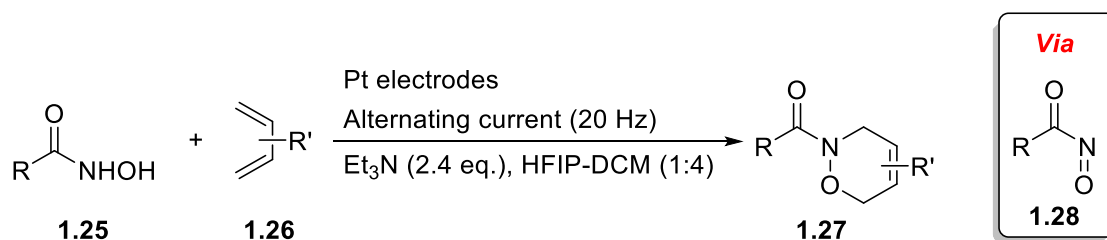
Figure 1.10. Alternating current profile for synthesis of mixed disulfides by sulfur-sulfur bonds metathesis of a mixture of symmetrical disulfides. Reproduced from reference [26] under Creative Commons CC-BY-NC-ND license.

In another report, Schotten *et. al.*^[27] highlighted a significant enhancement of the electrochemical synthesis of metal-NHC complexes (Scheme 1.5) under flow conditions using alternating polarity protocol. Where, application of alternating polarity enhanced the stability of the continuous synthesis of Cu(I)-NHC complexes, as both electrodes' surfaces were used evenly, and short-circuiting due to the build-up of metal dendrites was avoided.



Scheme 1.5. Electrochemical synthesis of Cu(I)-NHC complexes using alternating polarity.^[27]

Recently, Fährmann and Hilt^[28] reported electrochemical synthesis of 1,2-oxazines *via* Diels-Alder reaction of anodically generated acyl nitroso intermediates **1.28** and dienes **1.26** (Scheme 1.6). Hydroxamic acid derivatives **1.25** were oxidised at the anode to the corresponding acyl nitroso dienophiles **1.28**. Performing the reaction using direct current led to decomposition of the hydroxamic acid substrate without formation of the desired cycloadduct. On the other hand, doing the electrolysis using alternating current led to oxidation of the hydroxamic substrate without decomposition of the generated intermediate **1.28** that underwent a successful Diels-Alder reaction forming the desired 1,2-oxazine cycloadducts **1.27** in high yields.



Scheme 1.6. Electrochemical synthesis of 1,2-oxazines **1.27** *via* Diels-Alder reaction of dienes and electrochemically generated dienophile **1.28**.

Lately, Baran and co-workers^[29] reported a new method for controlling chemoselectivity *via* rapid alternating polarity (rAP). rAP is a type of alternating current achieved by alternating the polarity of an electrode in the millisecond timescale while keeping either the potential or current fixed. The authors hypothesised that if the rate of alternating polarity is faster than the

rate of certain redox reactions, this could enable suppression a slower subset of electrochemical processes. In other words, rAP would enable chemoselective electrosynthesis because of differentiation of redox reactions based on their relative reaction rate (Figure 1.11). Such a technique could open a new dimension to reaction control.

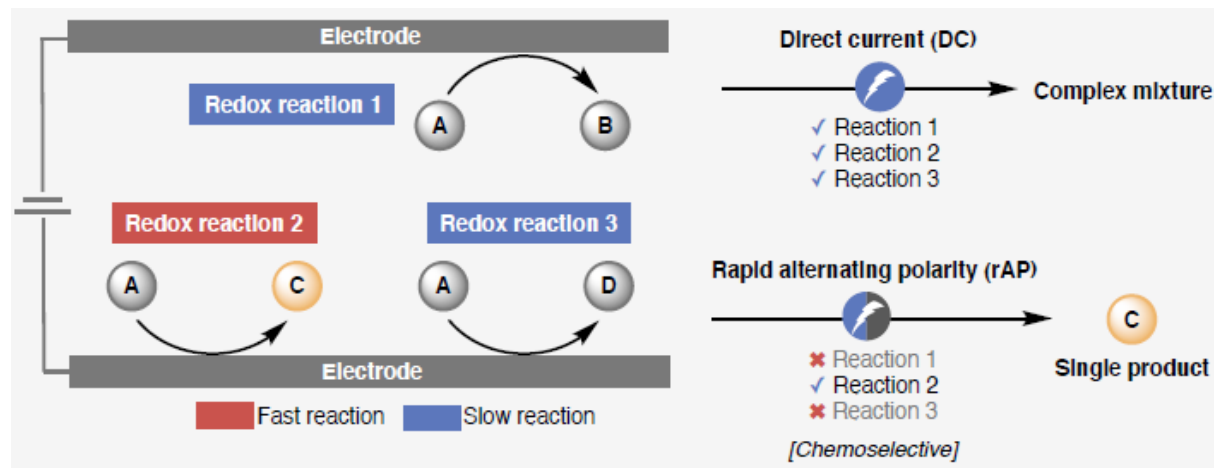
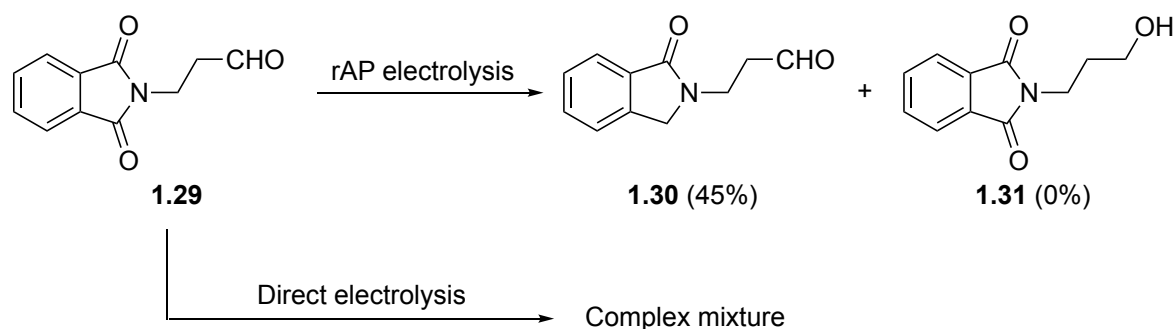


Figure 1.11. Schematic representation of the hypothesis of chemoselectivity *via* application of rapid alternating polarity (rAP).

The authors proved the viability of this new method for controlling chemoselectivity of many electrochemical reactions. For example, a striking chemoselectivity was observed with phthalimide **1.29** which underwent selective deoxygenation of the phthalimide moiety under rAP conditions without affecting the alkyl aldehyde part. While conventional direct electrolysis of **1.29** under the same condition resulted in decomposition leading to a complex mixture (Scheme 1.7).



Scheme 1.7. Chemoselective reduction of phthalimide derivative **1.29** under rapid alternating polarity (rAP) conditions.

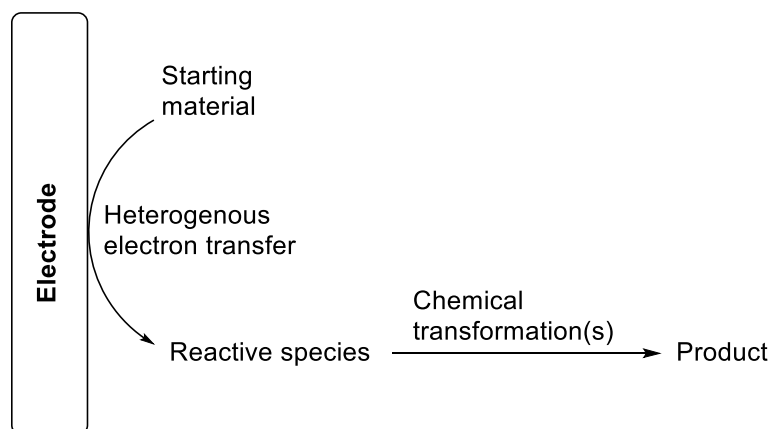
1.5. Electrolysis techniques

In electrochemistry, electron transfer processes at the electrode surface are heterogenous. But different electrolysis techniques can be realized depending on the mode of electron transfer from/to the electrode surface and chemicals in the bulk solution and the following chemical

transformations. Generally, the electron transfer process could be direct or indirect. In the following sections the different techniques of electrolysis will be discussed.

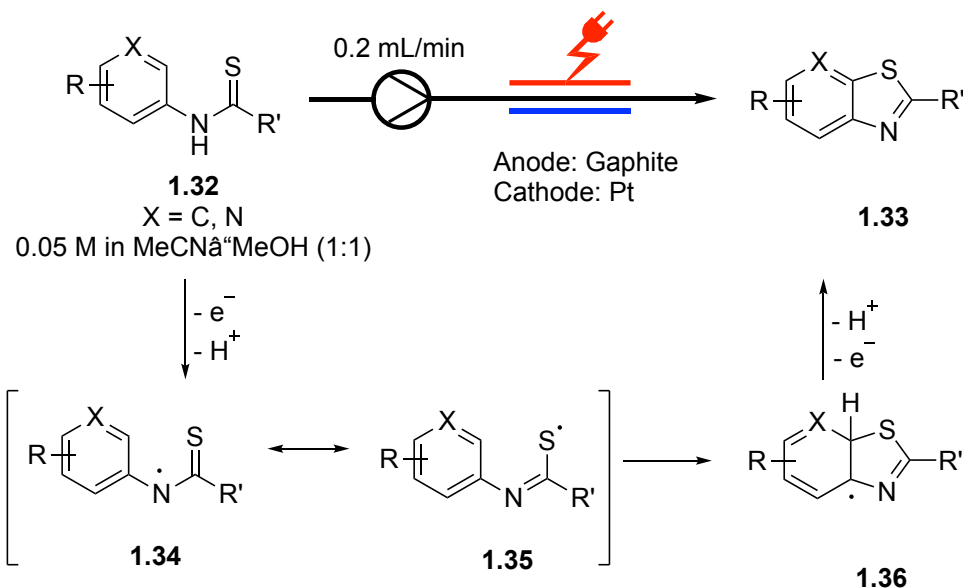
1.5.1. Direct electrolysis

Direct electrolysis involves direct heterogenous electron transfer between the electrode and the chemical substrate at the electrode surface. This heterogenous electron transfer leads to activation of the starting material generating reactive species that undergoes chemical transformations leading to the final product (Scheme 1.8).



Scheme 1.8. Schematic representation direct electrolysis.

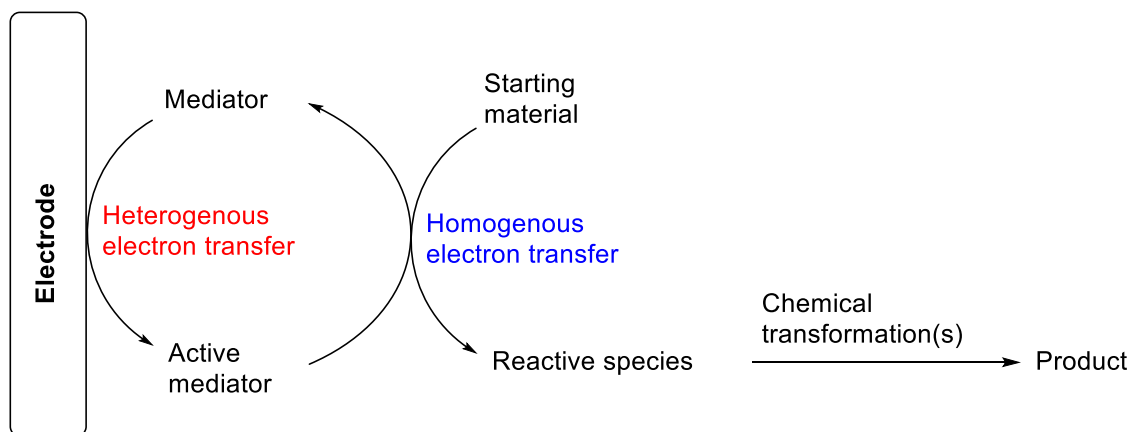
Electrochemical synthesis of benzothiazoles and thiazolopyridines *via* anodic oxidation / cyclization of thioamide derivatives is an example of direct electrochemical processes (Scheme 1.9). The starting material, thioamide **1.32**, is oxidised directly at the anode surface - heterogenous electron transfer- forming radical species **1.34** that undergoes intramolecular heterocyclization forming intermediate **1.36** that undergoes a second one-electron anodic oxidation giving the final product **1.33** after rearomatization.^[30]



Scheme 1.9. Flow electrochemical synthesis of benzothiazoles and thiazolopyridines *via* anodic oxidation / cyclization of thioamide derivatives.

1.5.2. Indirect electrolysis

Sometimes the direct heterogenous electron transfer between the electrode and the substrate is sluggish and inefficient. In some other cases, the direct electrolysis could lead to the formation of polymeric films -oxidation of pyrrole and aniline for example- that covers the electrode surface reducing the conductivity and sometimes leading to complete passivation of the electrode. In such scenarios, where the direct electrolysis is problematic, indirect electrolysis could offer the solution. In indirect electrolysis, a redox active mediator is used as electron carrier. The mediator gets activated through a heterogenous electron transfer at the electrode surface then undergoes homogenous electron transfer with the substrate in the bulk solution (Scheme 1.10).^[31]



Scheme 1.10. Schematic representation indirect electrolysis.

Indirect electrolysis has two different modes: in-cell and ex-cell. In the in-cell mode the mediator and the substrate are present in the electrolysis cell from the beginning of the electrolysis and the reaction ends by the end of electrolysis. On the other hand, in the ex-cell mode only the mediator is electrolysed to form a reactive form of it then the substrate is added after the electrolysis is finished (Figure 1.12).

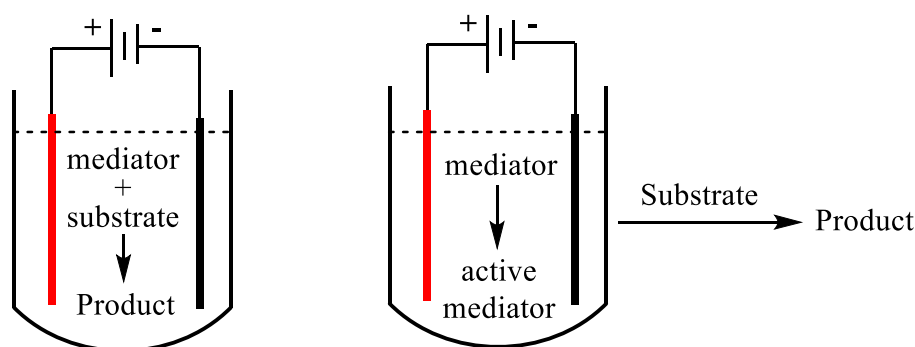
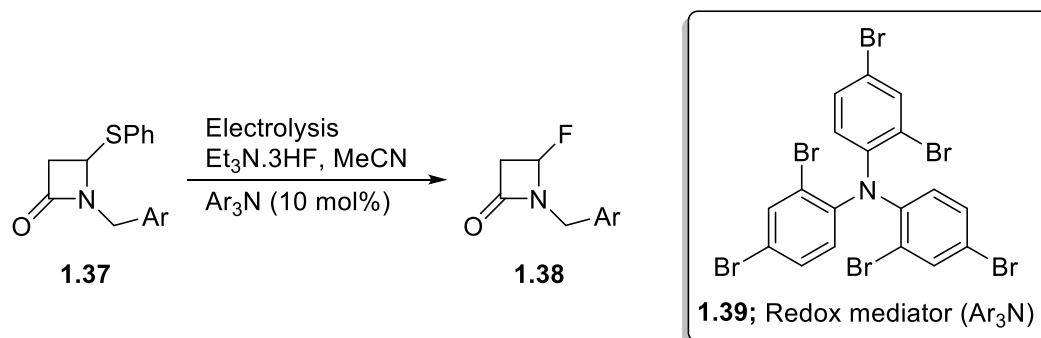


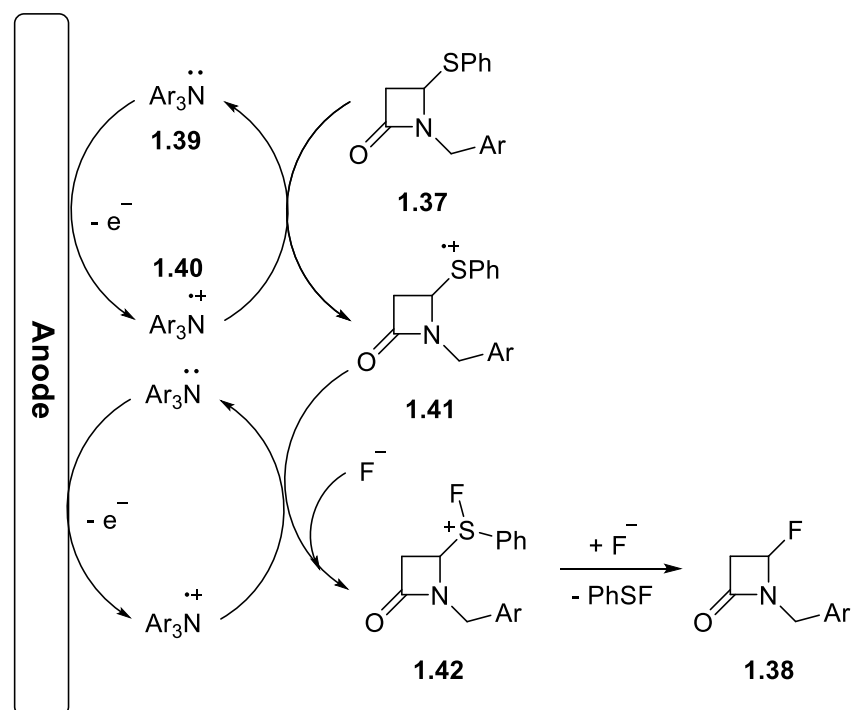
Figure 1.12. Indirect electrolysis. Left: in-cell mode; right: ex-cell mode.

Electrochemical fluordesulfurisation of β -phenylsulfenyl β -lactams **1.37**, presented in Scheme 1.11 is an example of in-cell indirect (mediated) electrolysis.^[32]



Scheme 1.11. In-cell tertiaryarylamine mediated electrochemical fluordesulfurisation of β -phenylsulfenyl β -lactams **1.37**.

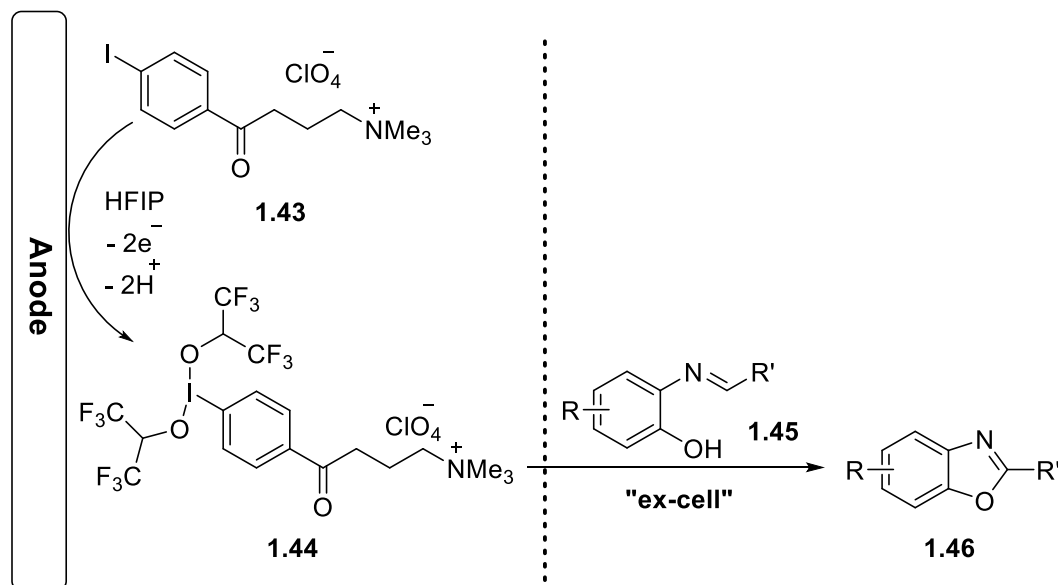
Direct anodic oxidation of sulfur-containing organic compounds is sometimes sluggish and leads to electrode passivation. In the above reaction, in contrast to direct electrolysis, using 10 mol% of tertiary arylamine redox mediator **1.39** leads to a smooth fluordesulfurisation of lactam substrates in very good yields avoiding electrode passivation. The reaction mechanism is presented in Scheme 1.12.



Scheme 1.12. Mechanism of fluordesulfurization of β -phenylsulfenyl β -lactams **1.37**.

The indirect electrochemical synthesis of benzoxazoles from imines is an example of excellent mediated process. In this reaction the iodoarene derivative **1.43** is anodically oxidised to the

corresponding hypervalent iodine species **1.44**. After completion of the electrolysis, imine substrates **1.45** were added to react with the electrochemically generated species **1.44** forming benzoxazole products **1.46** *via* hypervalent iodine mediated oxidative heterocyclisation (Scheme 1.13).



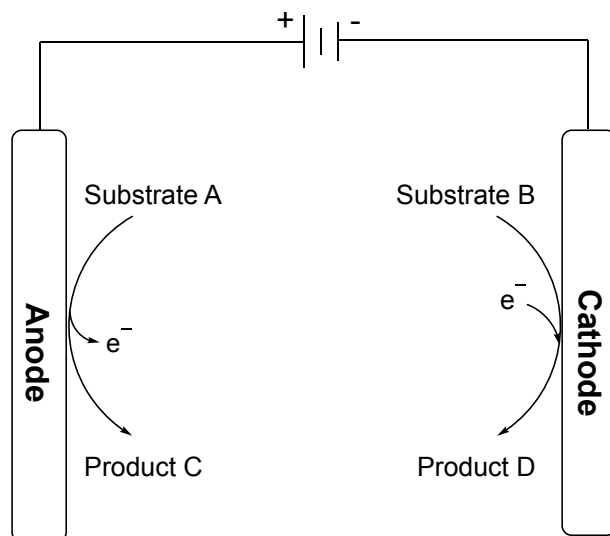
Scheme 1.13. Ex-cell indirect electrochemical synthesis of benzoxazoles **1.46** *via* electrochemically generated hypervalent iodine species **1.44**.

1.5.3. Paired electrolysis

In the vast majority of reported organic electrochemical methods, only one-half cell reaction (anodic oxidation or cathodic reduction) is productive, and the other half reaction is sacrificial, usually decomposition of the solvent. But in principle the two half reactions could be both productive leading to value added products, this approach is called paired electrolysis.^[4,14,33] Highly sustainable synthetic methods can be achieved *via* paired electrolysis that is characterised by highly efficient use of energy and chemicals and waste minimization. Paired electrolysis methodologies can be categorised into five types.

1.5.3.1. Parallel paired electrolysis

Parallel paired electrolysis is an electrolysis technique in which two substrates are transformed concurrently without interaction to produce two products one at the anode and the other one at the cathode (Scheme 1.14). In other words, the two-half-cell reactions are productive and lead simultaneously to two desired products. Parallel paired electrolysis can be done in both divided and undivided electrolysis cells.



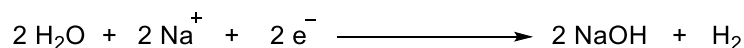
Scheme 1.14. Schematic representation of parallel paired electrolysis.

One of the largest electrochemical processes that is of utmost importance to a wide range of our daily life products, the chlor-alkali process is one of the most important examples of parallel paired electrolysis, where millions of tons of chlorine and sodium hydroxide are produced from brine at the anode and cathode, respectively (Scheme 1.15).

Anodic oxidation

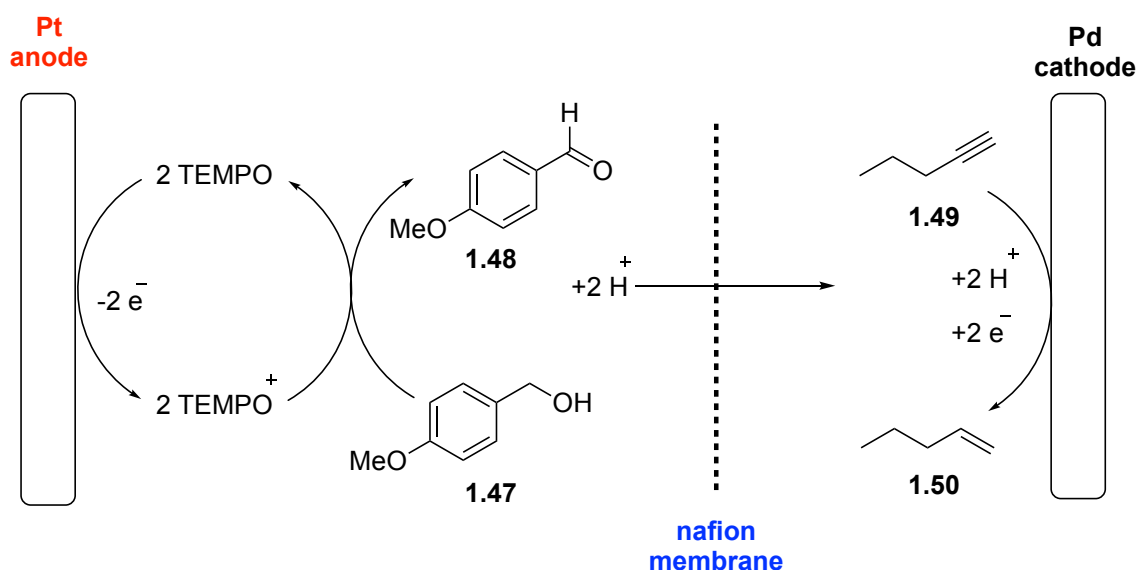


Cathodic reduction



Scheme 1.15. The two-half reactions of the chlor-alkali process.

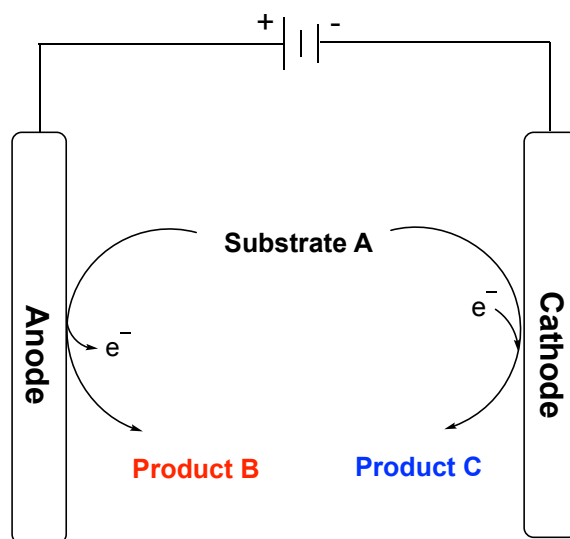
An impressive large scale industrial application of paired parallel electrolysis in commercial production of organic chemicals is the BASF electrochemical process for 4-(*t*-butyl)benzaldehyde dimethyl acetal (**1.15**) and phthalide (**1.17**) presented in scheme 1.3 (*vide supra*). Hydrogen gas evolution at the cathode is the most encountered sacrificial half-reaction in synthetic applications relying on anodic oxidation of organic compounds. The Berlinguette group reported^[34,35] elegant synthetic applications of electrochemically generated hydrogen in hydrogenation reactions (Scheme 1.16).



Scheme 1.16. Parallel paired electrolysis: using electrochemically generated hydrogen for hydrogenation reactions.

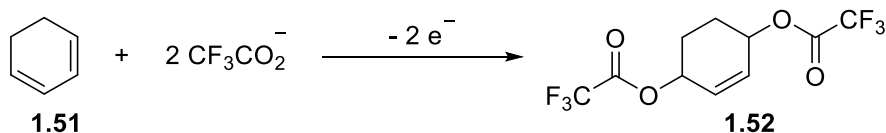
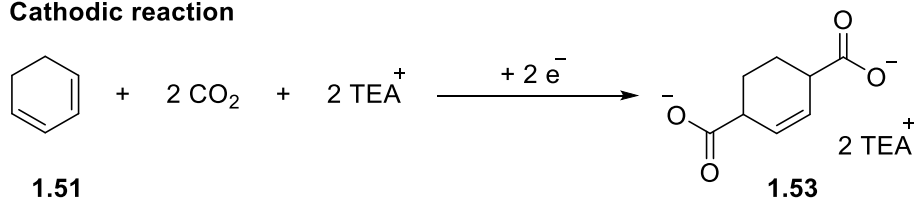
1.5.3.2. Divergent paired electrolysis

In divergent paired electrolysis two different products arise from a common substrate that undergoes simultaneous oxidation at the anode and reduction at the cathode giving a different product at each electrode (Scheme 1.17). The divergent paired electrolysis is limited to substrates containing function groups that can undergo both oxidation and reduction.



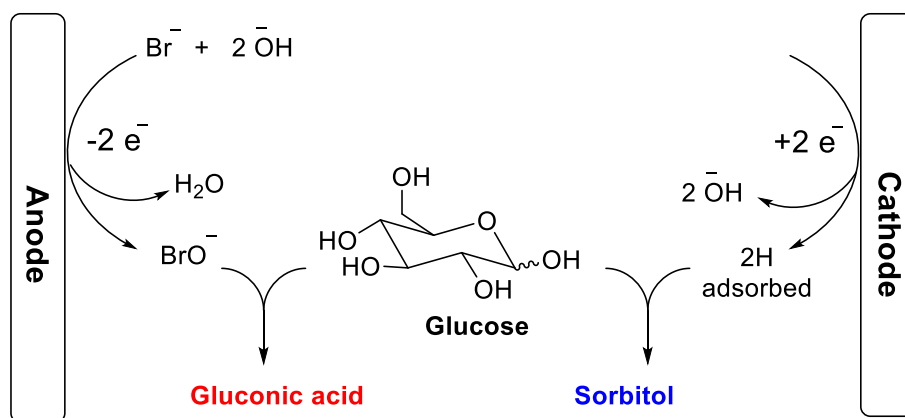
Scheme 1.17. Schematic representation of divergent paired electrolysis.

One example of divergent paired electrolysis is the simultaneous anodic acetoxylation and cathodic carboxylation of conjugated dienes^[36] to form 1,4-diol derivatives **1.52** and 1,4-dicarboxylates **1.53**, respectively (Scheme 1.18).

Anodic reaction**Cathodic reaction**

Scheme 1.18. Divergent paired electrolysis of dienes **1.51** to diol derivatives **1.52** and dicarboxylates **1.53**.

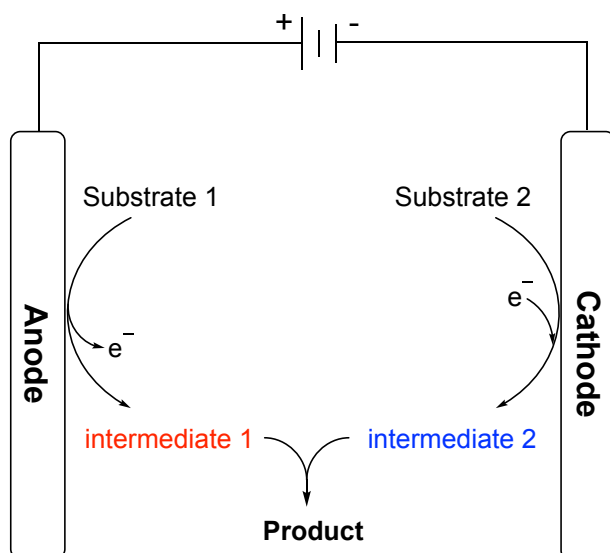
Another example is the anodic oxidation of glucose to gluconic acid and its cathodic reduction to sorbitol (Scheme 1.19).^[37,38]



Scheme 1.19. Synthesis of gluconic acid and sorbitol from glucose *via* divergent paired electrolysis.

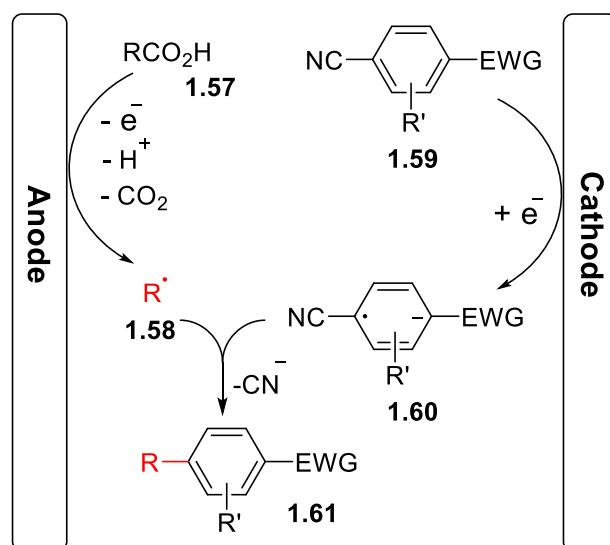
1.5.3.3. Convergent paired electrolysis

In convergent paired electrolysis the product is formed by the combination of two intermediates, one is generated *via* anodic oxidation and the other one is generated *via* cathodic reduction (Scheme 1.20).



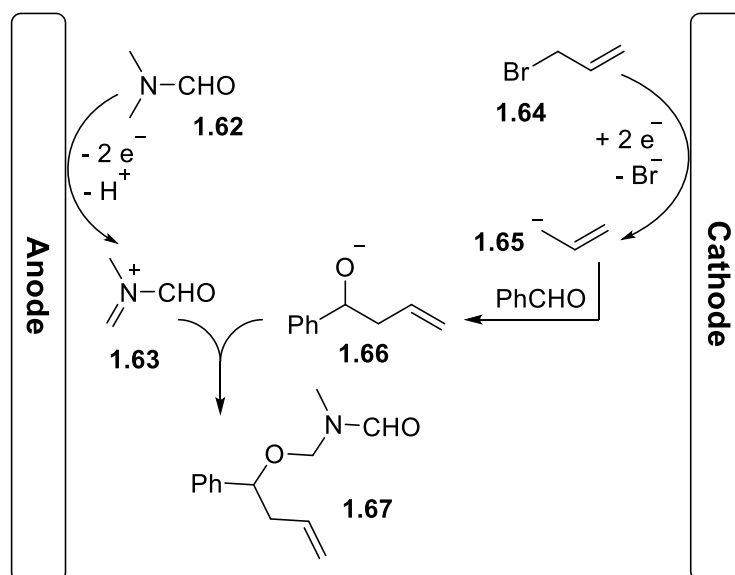
Scheme 1.20. Schematic representation of convergent paired electrolysis.

The combination of carbon-centred radicals generated simultaneously at the anode and the cathode is an interesting application of convergent paired electrolysis for carbon-carbon bond formation as demonstrated by Jensen and Buchwald in 2020^[39] (Scheme 1.21).



Scheme 1.21. Convergent paired electrolysis: carbon-centred radical coupling for C-C bond formation.

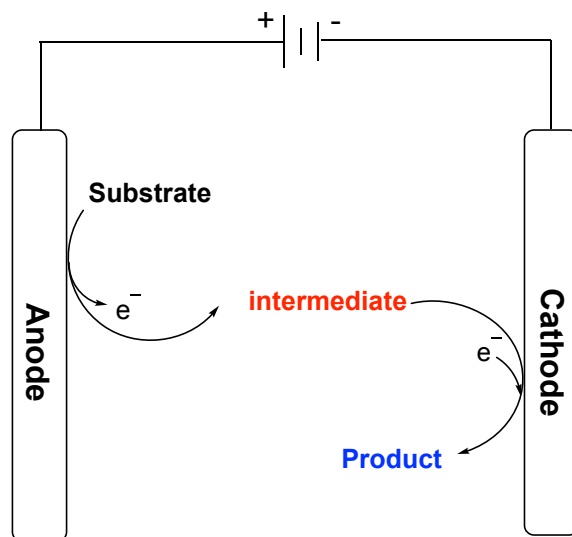
Another interesting example is the synthesis of *N*-*O*-acetal derivatives **1.67** via three-component convergent paired electrolysis depicted in Scheme 1.22.^[40] The reaction proceeds through the formation of allyl anion **1.65** at the cathode via cathodic reduction of allyl bromide **1.64**. The electrochemically generated anion reacts with benzaldehyde to form intermediate **1.66** which reacts with iminium ion derivative **1.63** generated at the anode by anodic oxidation of the solvent, DMF.



Scheme 1.22. Convergent paired electrolysis: synthesis of *N*-*O*-acetal derivatives **1.67**.

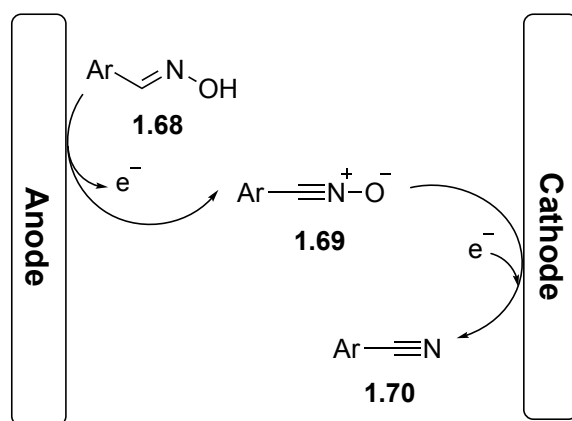
1.5.3.4. Sequential paired electrolysis (Domino paired electrolysis)

In sequential paired electrolysis, a substrate undergoes anodic oxidation to generate an intermediate that is sequentially transformed to the product at the cathode or the other way around (Scheme 1.23). For this kind of electrolysis to be successful, the initially generated intermediate should be stable enough to migrate to the counter electrode to undergo the subsequent transformation.



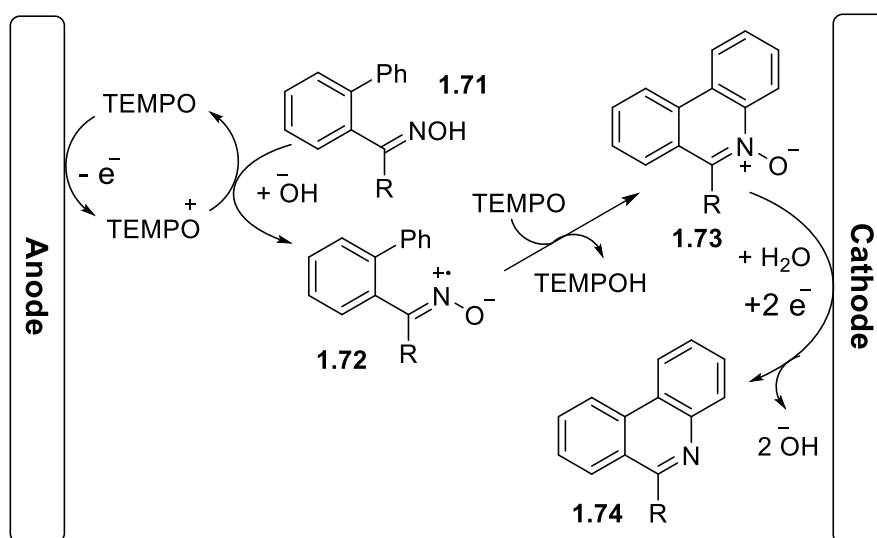
Scheme 1.23. Schematic representation of sequential paired electrolysis.

Waldvogel *et. al*^[41] reported a sequential paired electrolysis route for aryl nitriles (Scheme 1.24). The starting aldoximes **1.68** were anodically oxidised to the corresponding nitrile oxides **1.69** that have enough stability to travel to the cathode and undergo reduction give the nitrile final products **1.70**.



Scheme 1.24. Synthesis of aryl nitriles *via* sequential paired electrolysis.

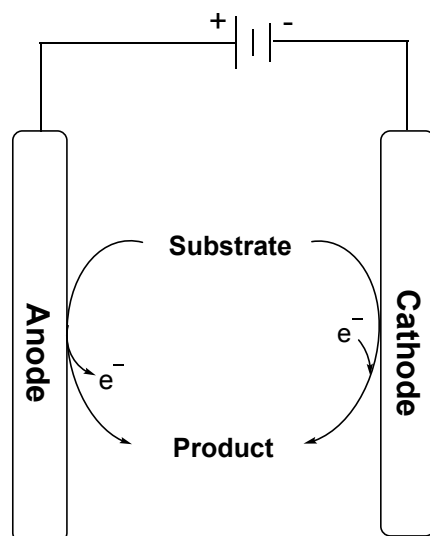
Conversion of biaryl ketoximes **1.71** to polycyclic *N*-heteroaromatic compounds **1.74** was reported Xu and co-workers ^[42] in 2018 *via* sequential paired electrolysis (Scheme 1.25).



Scheme 1.25. Synthesis of polycyclic *N*-heteroaromatic compounds **1.74** *via* sequential paired electrolysis.

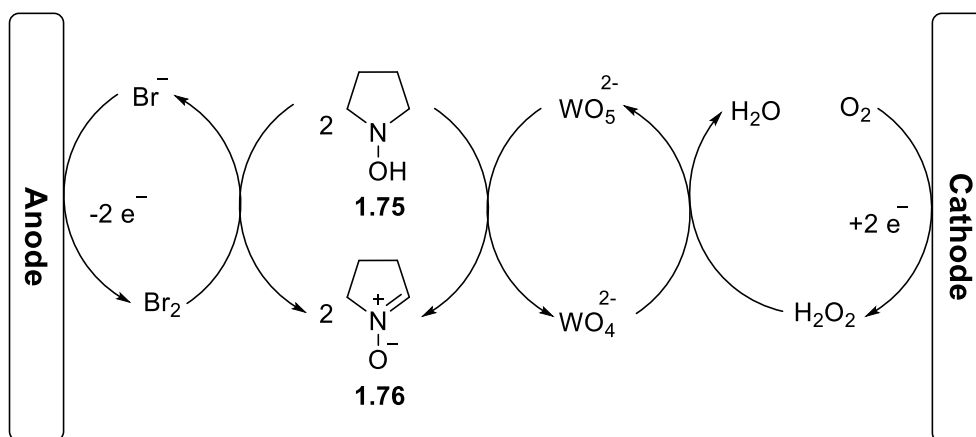
1.5.3.5. Linear paired electrolysis (200% current efficiency)

Paired electrolysis can in principle achieve 200% current yield (current efficiency) that is so called linear paired electrolysis. For this to happen a starting material must be converted to the same product in both anodic and cathodic reactions (Scheme 1.26). Achieving up to 200% current efficiency is more complicated and is only possible through mediated processes that can generate an oxidizing species at the cathode or a reducing species at the anode.



Scheme 1.26. Schematic representation of linear paired electrolysis (200% cell).

Li and Nonaka reported a seminal example for such a linear paired electrolysis with a theoretical 200% current efficiency in 1999.^[43] The authors investigated the conversion of hydroxylamines to nitrones through anodic oxidation and a cathodic oxidation system and reported the formation of the desired nitrones in up to 185% current efficiency (Scheme 1.27).

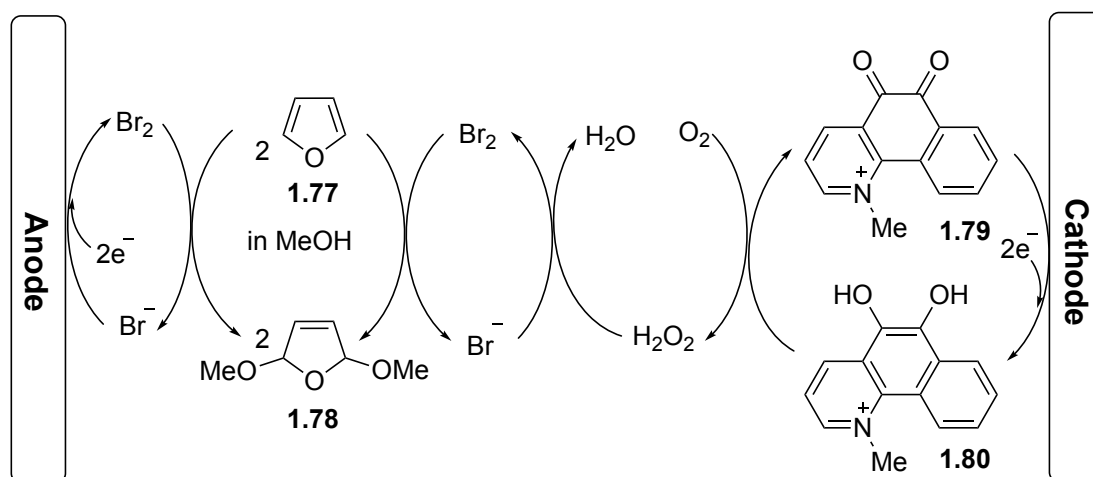


Scheme 1.27. Linear paired electrolysis of hydroxylamines.

The hydroxylamine derivative **1.75** is oxidized to the corresponding nitrone **1.76** at the anode mediated by anodically generated bromine from bromide ions. At the cathode molecular oxygen is reduced forming hydrogen peroxide that oxidises tungstenate to peroxo-tungstenate, oxidising species that is proposed to oxidize **1.75** to **1.76**. The overall process shows that a flow of only two electrons led to a 4e oxidation process (200% theoretical current yield).

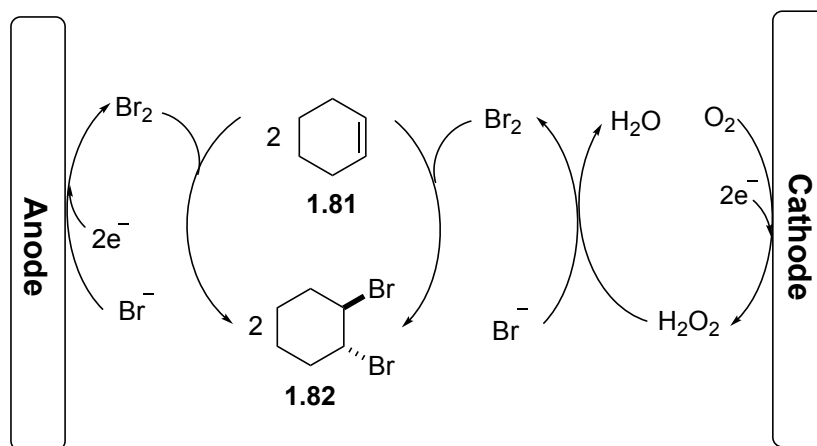
Another synthetic applications of linear paired electrolysis (200% cell), is the bromine-mediated oxidation of furane **1.77** in methanol to form the dimethoxy derivative **1.78** in up to 195% current yield (Scheme 1.28).^[44] The anodic reaction involves oxidation of bromide to

bromine that oxidises furan in methanol to the dimethoxy derivative **1.78**. At the cathode, *N*-methyl-1,10-phenanthroline-5,6-dione catalyst **1.79** mediates reduction of molecular oxygen to hydrogen peroxide that oxidises bromide to bromine that oxidizes furan to the same product **1.78**. The overall is that flow of only two electron leads to generation of two molecules of bromine that oxidizes two molecules of furan to two molecules of product **1.78** i.e. only two electron result in a four electron oxidation process.



Scheme 1.28. Linear paired electrolysis of furan.

The above reaction represents the basis of another example published recently by Hilt and co-workers (Scheme 1.29).^[44] The same principle was applied to generate bromine from both the anodic and cathodic reactions, the generated bromine adds to alkenes giving the corresponding dibromo products, reaching up to 200% current yield.



Scheme 1.29. Bromination of alkenes *via* linear paired electrolysis.

1.6. High-Throughput experimentation in electrochemistry

Organic electrochemical reactions comprise complex variable interactions. In addition to universal chemical reaction parameters such as stoichiometry, concentrations, temperature, solvents, reagents, catalysts, and additives, using electricity in organic synthesis adds more parameters including electrode material, supporting electrolytes, charge, current density, cell design and electrolysis mode. Therefore, the development of a reliable and scalable electrochemical process can currently be challenging. Hence, high-throughput experimentation (HTE) is of great importance for rapid and robust optimisation of electrochemical reactions.^[45] In 2020 Jensen and co-workers^[46] described an automated multifunctional microfluidic platform for HTE application in electroorganic synthesis (Figure 1.13). The developed HTE platform enabled rapid screening and optimisation of various radical–radical cross-coupling reactions. In principle this system could be expanded to other electrochemical reactions and could be of great benefit for the growing electroorganic synthesis field.

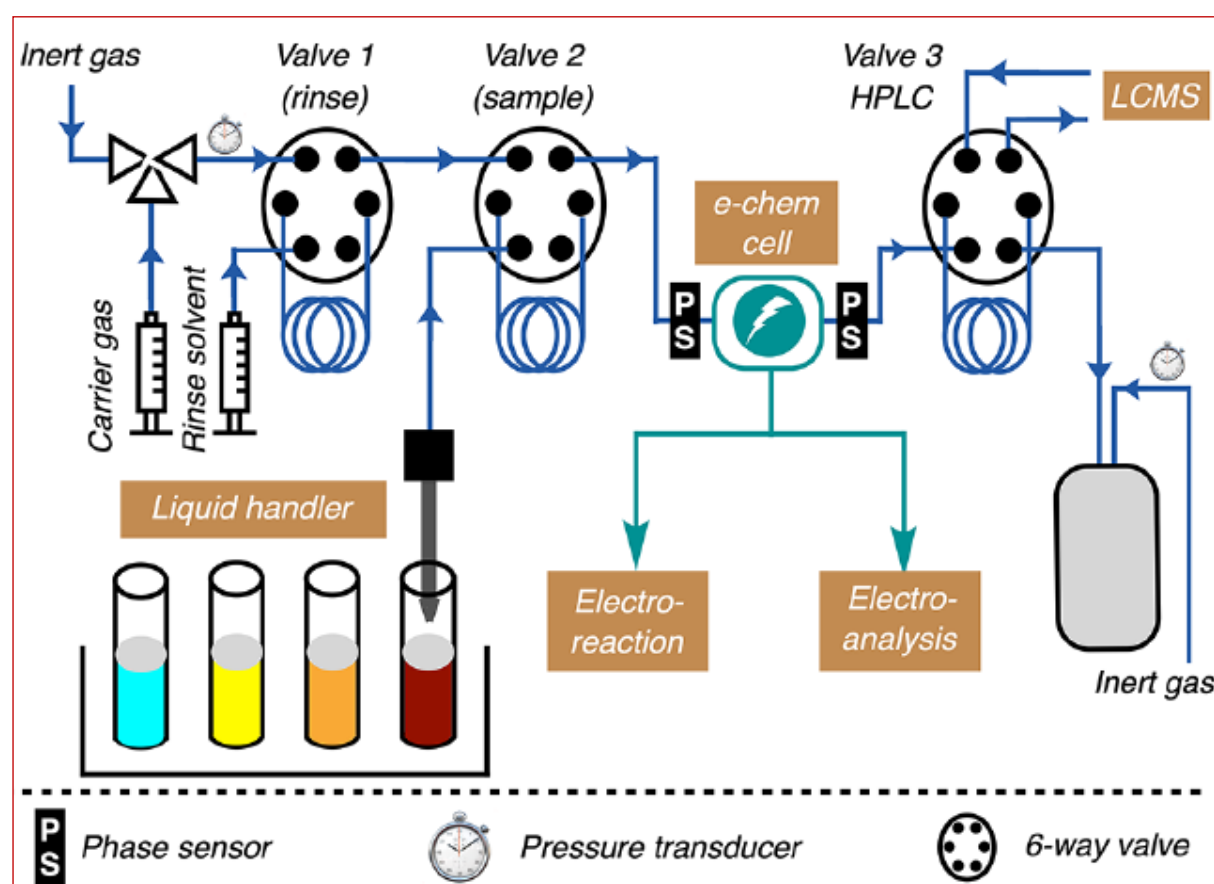
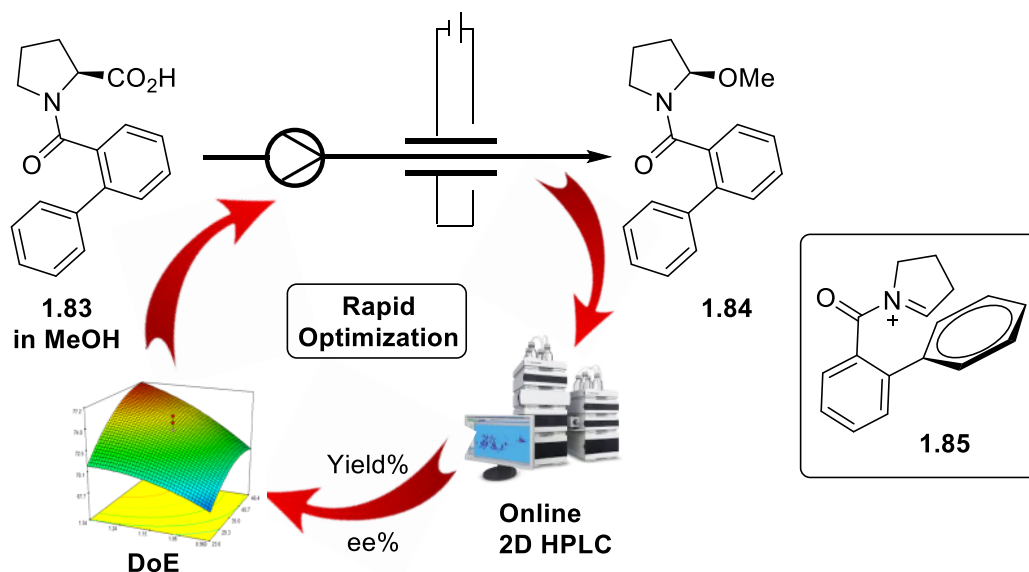


Figure 1.13. Schematic representation of microfluidic electrochemical HTE platform developed by Jensen and co-workers.^[46]

Recently, we have demonstrated in our laboratory the power of combining flow electrochemical reactor, 2D-HPLC, and Design of Experiment (DoE) approach in the rapid

development and optimisation of stereoselective electrochemical alkoxylation of amino acids (Scheme 1.30).^[47]



Scheme 1.30. Memory of Chirality: rapid optimization with online 2D-HPLC and DoE approach.

Nowadays, various automated high-throughput experimentation (HTE) platforms are commercially available from commercial suppliers such as IKA and Vapourtec.^[45]

1.7. Electroorganic synthesis: the other face of the coin

As discussed throughout this chapter, electroorganic synthesis is undoubtedly inherently green, efficient, reliable, and advantageous. But is it always green and advantageous? Is it free of limitations? The short answer for the two questions is definitely no.

Although electroorganic synthesis itself is inherently green as it replaces chemical oxidants and reductants and the inevitable accompanying waste with traceless holes and electrons, this does not necessarily guarantee that all electricity driven chemical reactions have no ecological footprint or that they are always environmentally more benign compared to traditional methods. Large quantities of hazardous supporting electrolytes are inevitable in most batch electrochemical methods, a problem that could be minimised under flow conditions. Flammable, corrosive, or toxic reagents and solvents and environmentally hazardous additives are also used in electrochemical methods and result in the production of waste, negatively impacting the safety and the ‘greenness’ of the overall process, the same way they do in traditional methods.^[48]

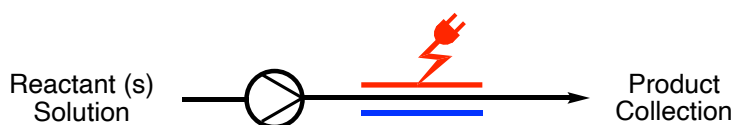
Apart from the above safety and environmental issues, electroorganic synthesis suffers from some other practical limitations and drawbacks. Again, the inevitable large amounts of supporting electrolytes are sometimes hard to separate from the desired product due to their

amphiphilic nature. Precipitation of chemicals or formation of polymeric films on electrode surfaces and leaching of metals from some electrode materials are some of the electrode related problems that could lead to sluggish impractical reactions sometimes. Metal catalysis is relatively not easy under the simple cheap undivided cells due to the easy reduction of the metal cations at the cathode which requires the use of expensive ion exchange membranes in the more complicated divided cells. In addition, lack of equipment and / or the high cost of some electrochemical setups and electrode materials limit exploring electroorganic synthesis in some synthetic organic chemistry laboratories.^[48,49]

1.8. Flow Electroorganic Synthesis

The electrochemical flow reactor techniques to organic chemistry have gained widespread attention because of their capability to produce improved conversions and selectivity in product generation. Under similar conditions compared to batch electrolysis, electrolysis in microflow should provide improved yields and selectivity. This requires development of a flow cell that avoid the drawback of traditional beaker cells that show slow rates of conversion, use of excess supporting electrolytes and longer reaction times.^[50,51]

In flow electrolysis the reaction mixtures flows through a setup of closely spaced electrodes.^[8,9,52] The small gap between the two electrodes leads to reducing the electric resistance. Hence, the electrolysis can be done at very low supporting electrolyte concentration or even without using any supporting electrolyte. Furthermore, one of the major issues with batch electrolysis is overoxidation, which could be minimised or avoided under flow circumstances by removing the reaction mixture continuously from the cell. Scheme 1.31 shows a generalized version of such configuration.



Scheme 1.31. Simplified diagram of electrolysis under flow conditions.

Various groups have documented the progress and usage of microflow cells in electrosynthesis under continuous flow.^[16,20,22,27,53,54] Our group has also contributed to the development of electrochemical microflow cells.^[55,56] The most relevant and emerging technologies of electrochemical microflow cell designs including our developments will be discussed in detail in this chapter.

1.8.1. Flow electrochemical cells

In 2015, Waldvogel and co-workers reported an electrochemical microflow reactor designed for dehalogenation reactions.^[57] This development allowed to increase the productivity of the desired reaction, previously performed under batch conditions.

This electrochemical microflow cell was made up as a divided cell assembly of two blocks of Teflon[®], which are attached by two stainless steel plates. Each Teflon[®] part contains a small space where the electrodes and reaction chambers can be placed. The cathode is made of leaded

bronze (15% Pb), while the anode is made of graphite felt. Nafion[®] membrane was used to separate the anodic and cathodic chambers. (Figure 1.14).

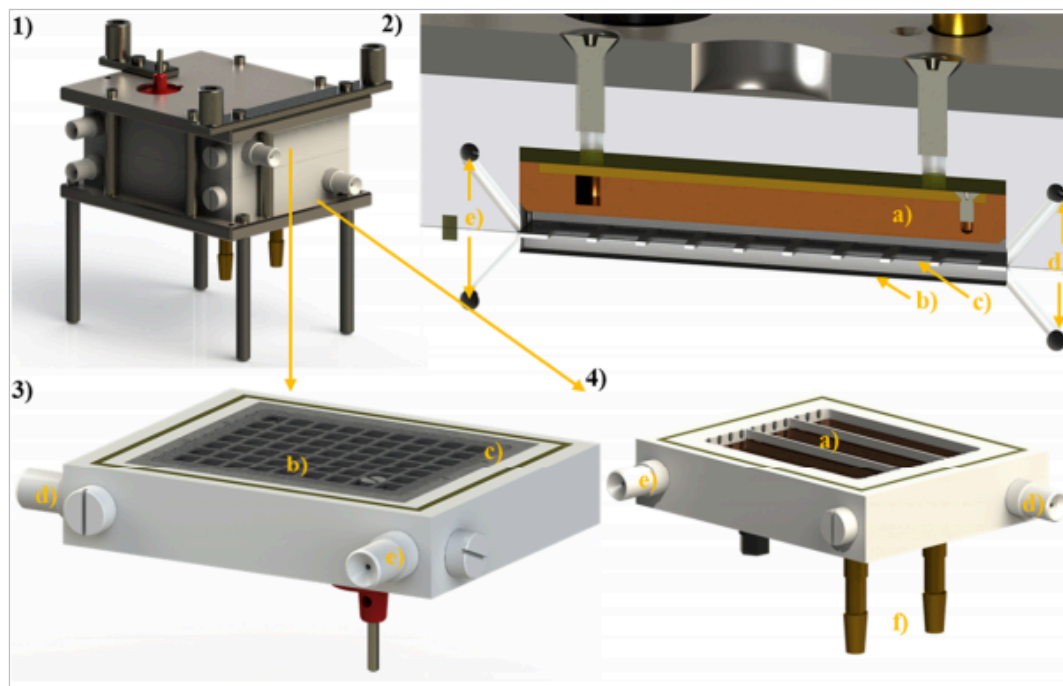
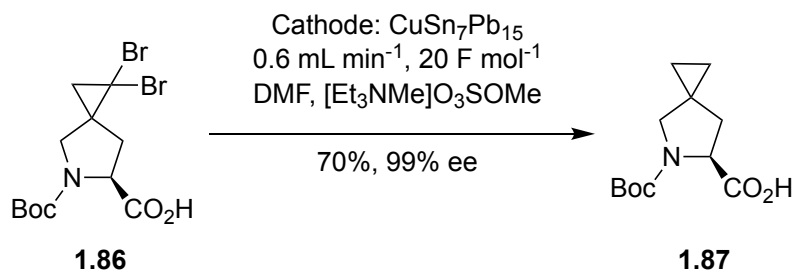


Figure 1.14. (1) Overall view of the flow cell, (2) cross section of the whole cell, (3) anodic half-cell and Nafion[®] separator, (4) cathodic half-cell: (a) cathode, CuSn₇Pb₁₅; (b) anode, graphite; (c) Nafion[®] membrane; (d) inlets for electrolyte; (e) outlets for electrolyte; (f) contacts for cooling media.^[57] Copyright (2015) American Chemical Society.

Using the reactor shown in Figure 1.14 they synthesised compound **1.87** from the dibrominated spirocyclopropane-proline derivative **1.86** in good yields and high selectivity (Scheme 1.32).



Scheme 1.32. Flow electrochemical dehalogenation.^[57]

Methanol was utilised as a sacrificial reagent, which was continuously oxidised at the anode and recirculated, while the catholyte was collected and the product was separated after a single pass through the microflow cell (Figure 1.15).

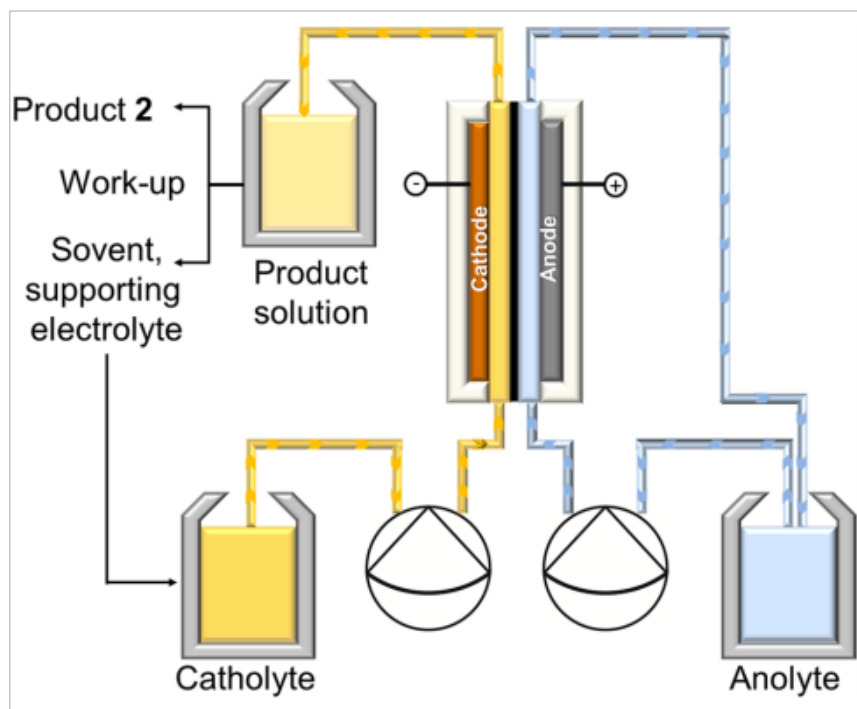


Figure 1.15. Schematic setup of the flow electrochemical cell and the recycling streams.^[57] Copyright (2015) American Chemical Society.

In 2020, Waldvogel and co-workers described a scalable flexible parallel-plate electrochemical microflow cell (Figure 1.16).^[58] Two Teflon[®] half-cells (170 mm x 30 mm x 5 mm) were sandwiched between two stainless steel covers to form the cell using 10 bolts. This setup allowed to avoid the extension of Teflon[®] during the use of chilling by using the bolts adjustment. Many electrode materials combinations can be used and placed simply. Also, the channel between two the electrodes can be controlled by different Teflon[®] spacer thickness (0.12 mm – 2.0 mm) which allowed minimization or complete waiver of supporting electrolyte. This microflow cell may also be operated as a divided cell by inserting an ion exchange membrane between two spacers.

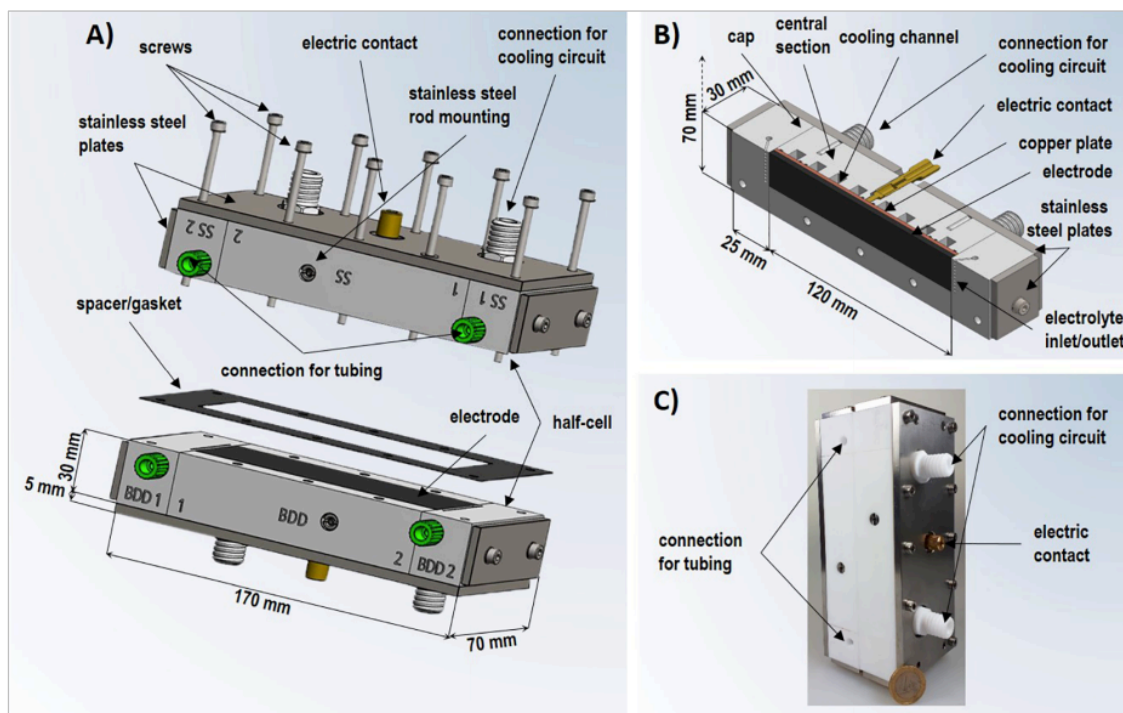
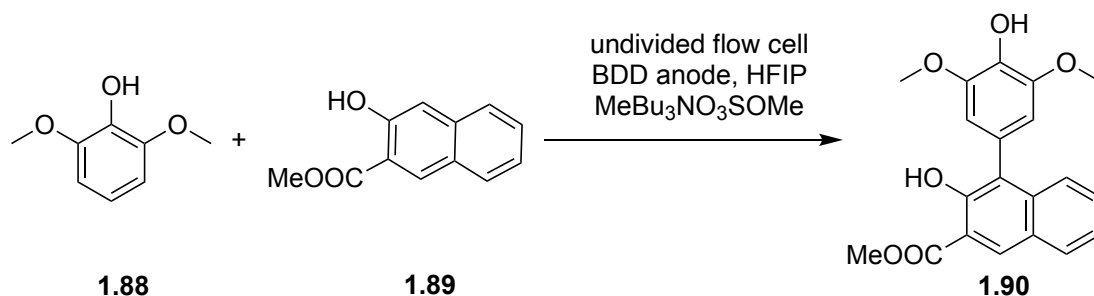


Figure 1.16. (A) Partly exploded drawing of the full-featured flow cell. (B) Cross-section of one half-cell. (C) Completely mounted 4 cm × 12 cm flow cell and a Euro coin (diameter: 23.25 mm) for comparison.^[58] Copyright (2020) American Chemical Society.

The undivided microflow cell (4 cm × 12 cm) was tested for the coupling of 2,6-dimethoxyphenol **1.88** and 3-hydroxy-2-naphthoate **1.89**.^[58] The higher mass transformation was achieved by using thin spacer (0.25 mm), leading to 94% yield of the desired product **1.90** with a current density of 15 mA/cm² (Entry 3, Table 1.1). However, the efficient mass transfer between both electrode surfaces depends on the microflow cell geometry, which is judiciously designed in this case.

Table 1.1. Overview of the optimized conditions of each Electrolysis Cell and the corresponding yields for anodic Cross-Coupling of **1.88** with Methyl 3-hydroxy-2-naphthoate **1.89**.^[58]



Entry	Cell type	T [°C]	Supporting Electrolyte	Yield [%]	Productivity [g/h]
1	beaker-type cell (25 mL)	30	0.09 M MeBu ₃ NO ₃ SOMe	86	0.27
2	flow cell (2 cm × 6 cm)	rt	0.005 M MeBu ₃ NO ₃ SOMe	86	0.24
3	flow cell (4 cm × 12 cm)	10	0.005 M MeBu ₃ NO ₃ SOMe	94	3.15

To show the microflow reactor productivity, the reaction has been tested using smaller and commercially available microflow cell (ElectraSyn) that developed by the same group and IKA Ltd[®] with dimensions of 2 cm × 6 cm (Figure 1.17) and 86% of desired product **1.90** was obtained.^[16,57,59] Also, the targeted product **1.90** was obtained in 86% yield using beaker-type cell (25 mL).

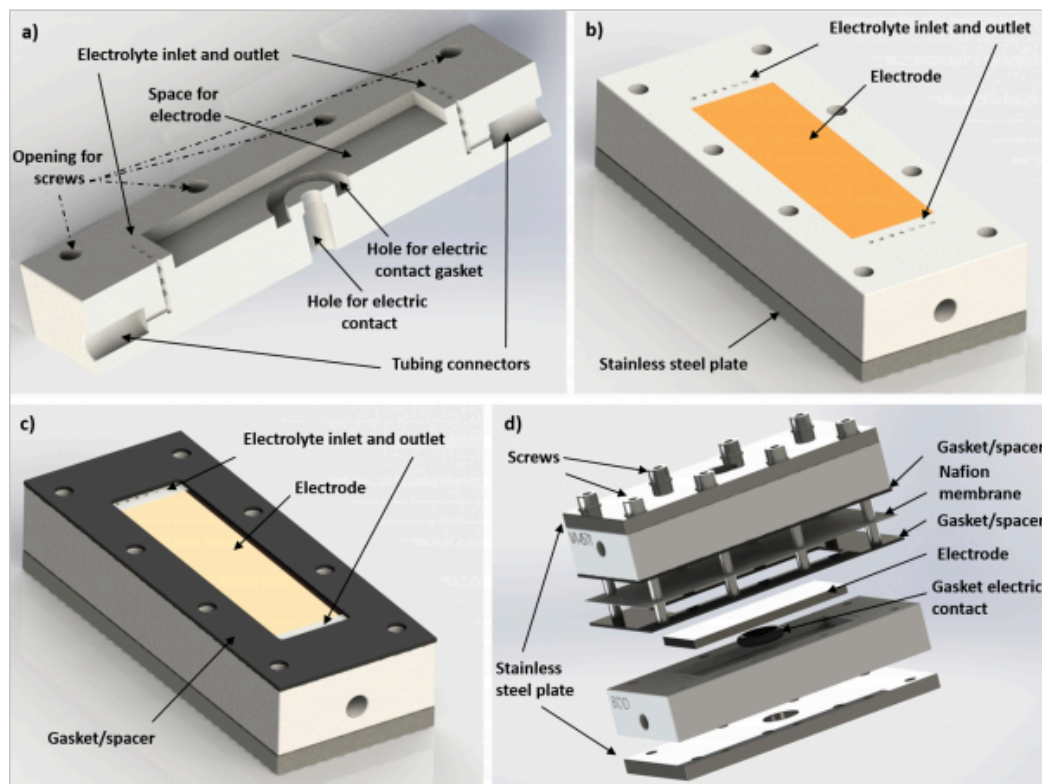


Figure 1.17. a) Cross-section of the Teflon[®] block; b) half-cell with the stainless-steel plate, the Teflon[®] block and the electrode placed in the Teflon[®] block; c) half part of the cell with the gasket; d) Complete reactor as a divided cell. For an undivided cell, only one gasket is needed, the second one and the Nafion[®] membrane are excluded.^[16] Copyright (2017) American Chemical Society.

Robertson and co-workers (2018) have designed a simple electrochemical flow reactor.^[60] The reactor was proposed using simple software and 3D printer. The reactor house is made up of polyether ether ketone (PEEK) materials with a suitable groove in the middle for the electrodes (Figure 1.18). The electrodes are held to the PEEK with Araldite[®] epoxy resin glue in this slot, which features a series of grooves. With a typical pitch spacing of 2.54 mm, three spring-loaded pins (Preci-dip) were used to connect the electrodes and were hidden within a straight socket to ease cable connection. Two threaded ports were made to flow into and out the cell through PTFE tube. Appropriate gaskets with different thickness (25–100 mm) were cut from a variety of materials, including FEP, PEEK, PTFE, and Kapton. To use in electrochemical transformations, the cell is held together by ten screws.

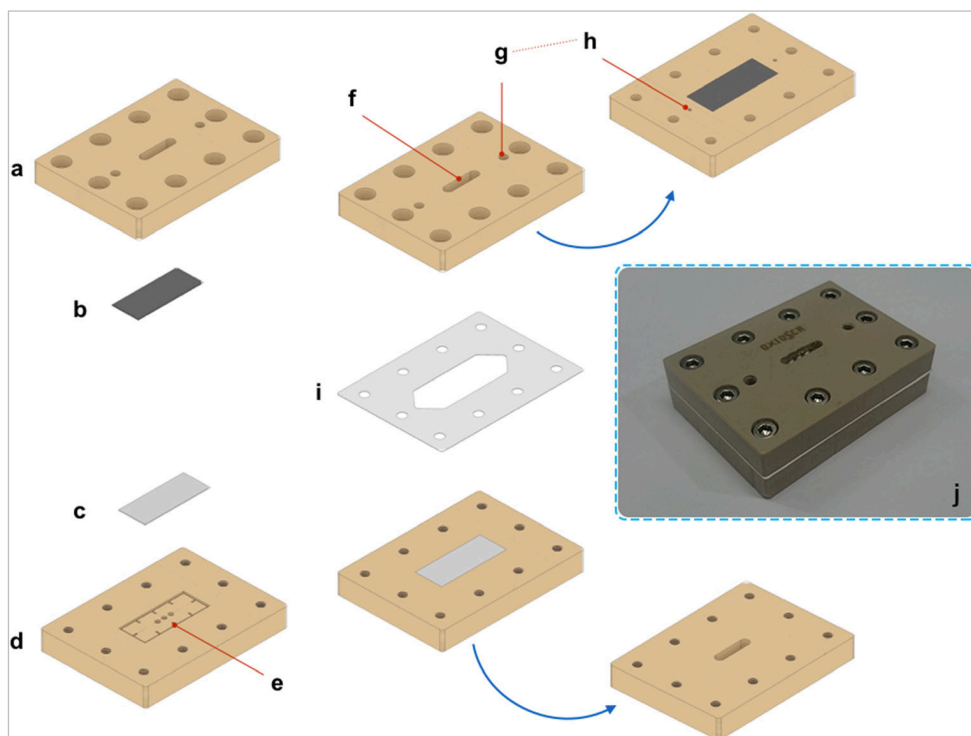
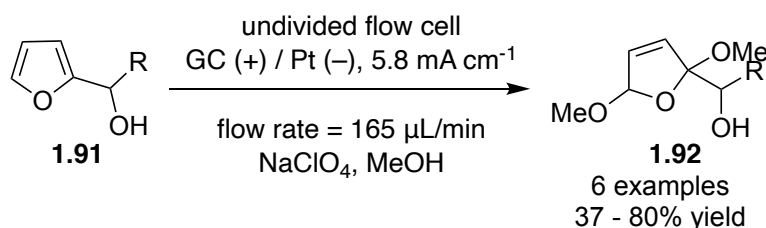


Figure 1.18. Flow cell schematic. a) PEEK mount; b) glassy carbon anode; c) platinum cathode; d) PEEK mount showing a recess e) for the electrodes; f) port for electrical connection; g) and h) the inlet ports for the reaction solution; i) gasket; j) the complete assembly.^[60] Copyright (2018) Springer Link.

This flow electrochemical reactor was examined by effecting anodic oxidation of furfuryl alcohols **1.91** in methanol into hydroxypyrones. Different functional group and phenyl ring bearing side-chain of furfuryl alcohols were well tolerated and products were obtained in good yield up to 80 % (Scheme 1.33).^[60]



Scheme 1.33. Flow anodic oxidation of furfuryl alcohols.^[60]

In 2018, Noël and co-workers designed an electrochemical microflow cell using cheap and solvent-resistant materials that allowed performing reactions at small and large scale (Figure 1.19).^[62] The reactor is robust and flexible to use different spacer thickness and simple and variable electrodes forms. The reactor consists of rectangular insulator (160 mm× 95 mm×10 mm) made from polytetrafluoroethylene (PTFE) pressed between two stainless-steel parts using eight bolts. The Super Flangeless Nuts (PEEK, 1/4–28 Flat bottom, for 1/16" OD) were used to inject the reaction mixture into the cell.

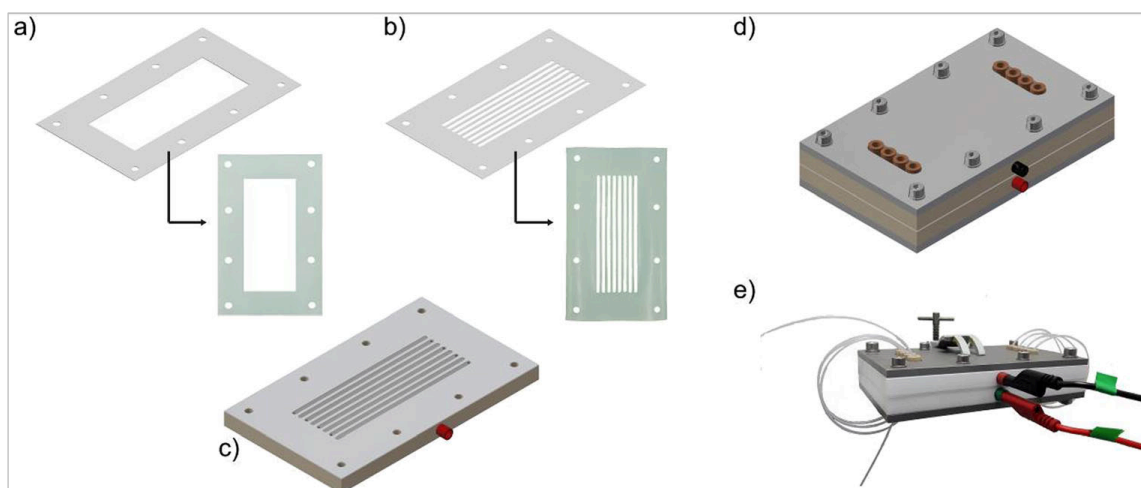
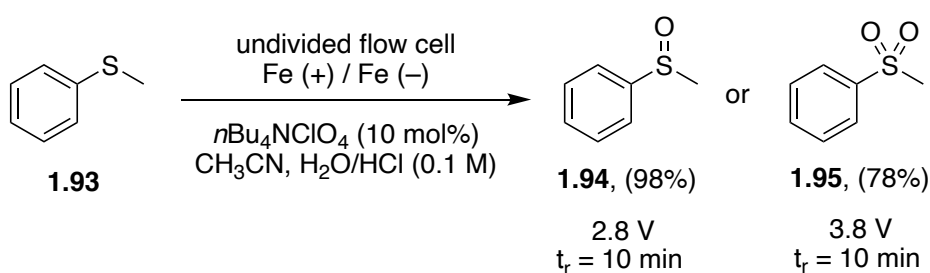


Figure 1.19. Schematic representation of electrochemical flow reactor. (a) open-channel gasket design; (b) 8-channel gasket design; (c) bottom plate with electrode and 8-channel gasket; (d) schematic representation of the complete device; (e) picture of the assembled electrochemical flow reactor with banana cables to establish the electric connections.^[62] Copyright (2018) Springer Link.

This homemade reactor was applied for sulfides oxidation and compared with previous reported results that done in the same group using a commercial electrochemical microflow reactor that supplied by Syrris Asia Flux.^[62,63] Under flow reaction conditions, potentiostatic electrolysis is used to selectively oxidise sulfide **1.93** to the corresponding sulfoxide **1.94** or sulfone **1.95**. Different parameters such as spacer thickness, residence time and electrolyte concentration were screened. The reaction uses stainless-steel as electrodes and $n\text{Bu}_4\text{NClO}_4$ (10 mol%) as supporting electrolyte; the best results were obtained by adjusting the applied voltage and residence time. (Scheme 1.34).

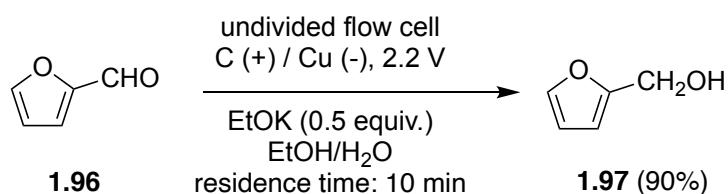


Scheme 1.34. Electrochemical oxidation of thioethers to sulfoxides and sulfones in flow electrochemistry using potentiostatic reaction conditions.^[62]

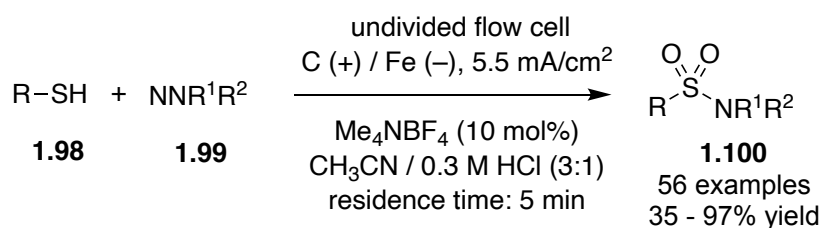
The microflow cell was used for several types of transformations, using either a divided reactor or an undivided cell setup by the same group.^[22,62,64–67] For the use of the undivided cell, potentiostatic reduction of furfural to corresponding furfuryl alcohol (Scheme 1.35.a),^[22] synthesis of sulfonamide through oxidative coupling of thiols and amines (Scheme 1.35.b),^[66] synthesis of sulfonyl fluoride through oxidative coupling of thiols with potassium fluoride

(Scheme 1.35.c)^[65] and aziridination of alkenes via oxidative coupling of alkenes and alkylamines (Scheme 1.35.d)^[67] were successfully achieved. Additionally, using the paired setup of the microflow cell, an electrochemical transformation of furfural to produce useful derivatives by using a membrane separated the cathode and anode was developed (Scheme 1.35.e).^[64]

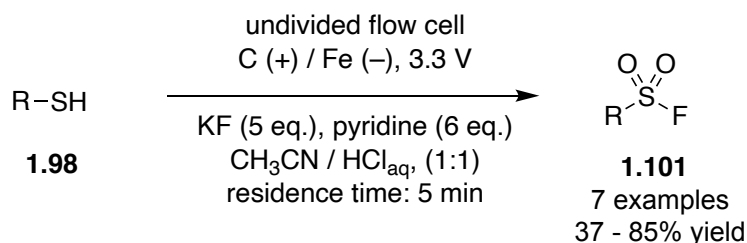
(a) Electrocatalytic reduction of furfural to furfuryl alcohol



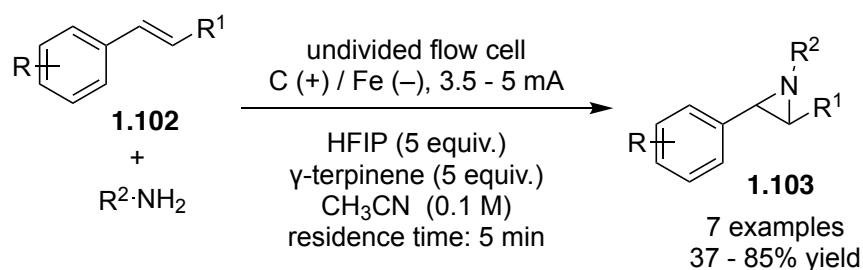
(b) Electrochemical oxidative coupling of thiols and amines

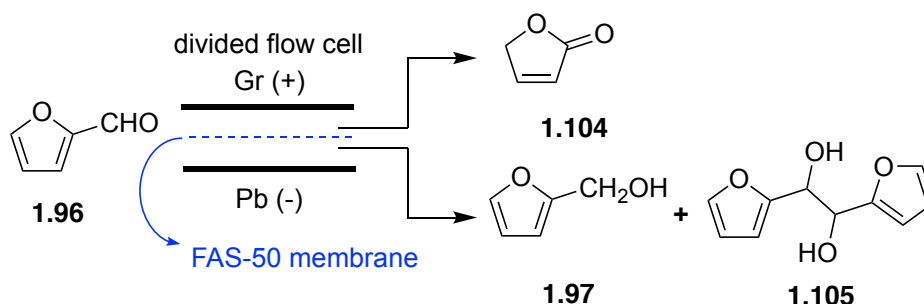


(c) Electrochemical oxidative coupling of thiols and potassium fluoride



(d) Aziridination of alkenes via oxidative coupling of alkenes and alkylamines



(e) Electrochemical transformation of furfural to produce useful derivatives

Scheme 1.35. Different kinds of synthesis using microflow cell (Figure 1.19).

Lately (2021), Kappe and co-workers developed an economical and simple microflow cell that can be easily manufactured (Figure 1.20).^[68] The reactor involves two sheets electrodes divided by a flexible spacer as flow channel (Mylar films). The Mylar films can be cut to different geometry by laser-cutting and variety of spacer thicknesses can be easily prepared. The spacer material has the ability to avoid the reaction mixture solution leakage and solvent resistance. The reactor cover made from aluminium which can be threaded taps by drill. All the equipment that used to construct the reactor are simple, inexpensive and without the necessity of complicated machine. The reactor design is useful for a variety of synthesis processes, using either a divided or undivided cell configuration.

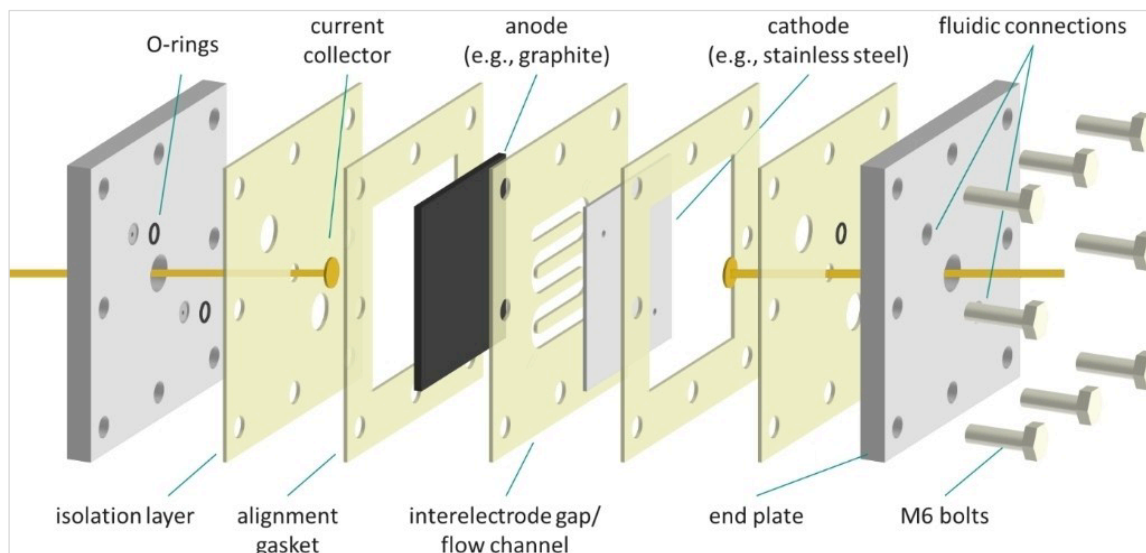
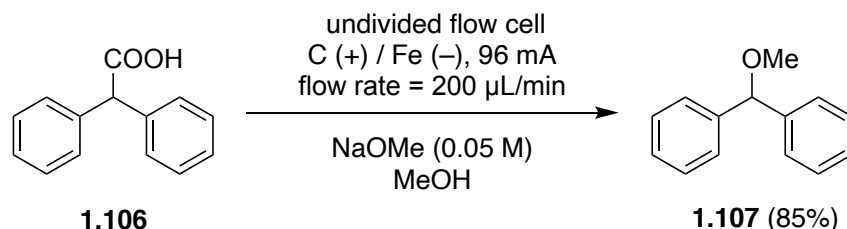


Figure 1.20. Exploded view of the flow electrolysis cell, based on a parallel plate arrangement and consisting of a stack of insulating, chemically resistant Mylar foils.^[68] Copyright (2021) Wiley).

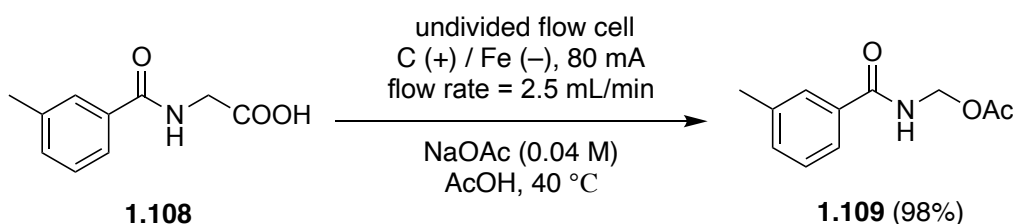
To show the performance of this reactor, the decarboxylative methoxylation of diphenylacetic acid **1.106** as typical reaction has been demonstrated (Scheme 1.36a).^[68] Several flow reactor parameters such as channel geometry, total flow charge and flow rates were optimized and the highest yield of benzhydrol methyl ether **1.107** in a single pass was 85% under constant current

of 96 mA and 200 $\mu\text{L}/\text{min}$ flow rate.^[68] Likewise, the same reactor have been used also for anodic decarboxylative acetoxylation reaction (Scheme 1.36b).^[69] Methylhippuric acid **1.108** was converted into **1.109** in a very high yield (98%).

(a) Electrochemical decarboxylative methoxylation of diphenylacetic acid



(b) Electrochemical decarboxylative acetoxylation of methylhippuric acid



Scheme 1.36. Electrochemical decarboxylation using the flow electrolysis cell.

Willans and co-workers developed three generations of microflow cells to increase synthetic process effectiveness and scalability.^[27,70] The first generation electrochemical microflow cell consists of two PTFE plates with two copper electrodes (surface area of each electrode 7.6 cm^2) separated by a linear 2.5 mm interelectrode distance, flow channel covered using stainless steel plates (Figure 1.21a).^[70] Using IMes•HCl (**1.23**) as the starting material, this reactor effectively produced the required Cu(I) – NHC complex and [Cu (IMes)Cl]. In addition, [Cu(IMes)₂]Cl and bis-NHC complex has been synthesised with the same setup. The targeted mono-NHC complex was carried out with a yield of 82% in a single pass through the flow cell (Scheme 1.17a) and 98% yield by recirculating the reaction mixture (Scheme 1.37b).^[70]

The second-generation microflow cell has manufactured similar to the first-generation cell but with higher electrode surface and volume (Figure 1.21b).^[70] The microflow cell is made up of two electrodes with PTFE flow channel spacers (1 mm) between them. Depending on the application type, the reactor volume can be adjusted by stacking more electrodes. The electrodes and spacers are covered by stainless steel block similar to the first-generation reactor. The reactor design has the flexibility to increase the surface area of the electrodes as well as the volume of the reactor suitable for scale-up. The efficiency of the microflow reactor was demonstrated by the production of Cu (IMes)Cl complex, with full conversion (94 % yield) accomplished in a single pass. (Scheme 1.37c).^[70]

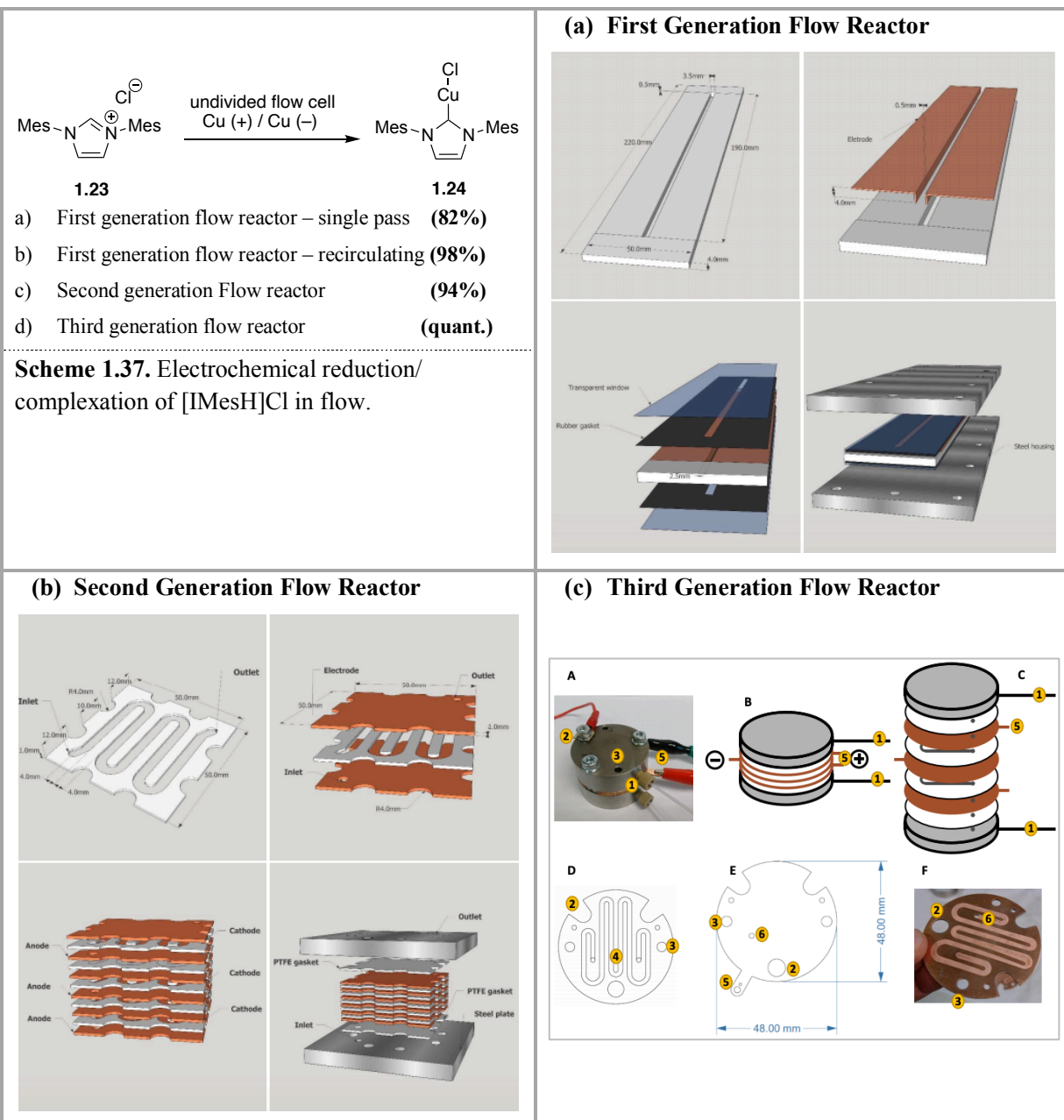


Figure 1.21. Three generations of electrochemical flow reactors used for the synthesis of transition metal complexes. (Reproduced with permission from ref.^[27,70] Copyright (2015 and 2021) Royal Society of Chemistry.

Very recently, the third-generation microflow cell was designed that allows fast screening of derived catalysts under electrochemical arrangement (Figure 1.21c).^[27] The microflow cell is constructed similar to the second-generation flow cell with assembled electrodes and PTFE spacers (0.25 mm) that covered by two stainless steel plates. The reactor is designed to minimize reaction volume for high production screening. The Cu (IMes)Cl complex has been formed and demonstrated over extended reaction times using the third generation microflow cell that can be operated to reach full conversion (Scheme 1.37d).^[27]

The commercial electrochemical reactor Asia Flux established by Syrris Ltd[®] (Figure 1.22)^[71] has been used to study different electrochemical transformations in numerous research laboratories.^[63,72–74] The Asia Flux module consists of two electrodes divided by a snaking channel of volume 225 μL . Various range of electrodes can be used and replaced without requiring any complex tools. This reactor can withstand pressures of up to 5 bar and temperatures ranging from 0 to 60 $^{\circ}\text{C}$.

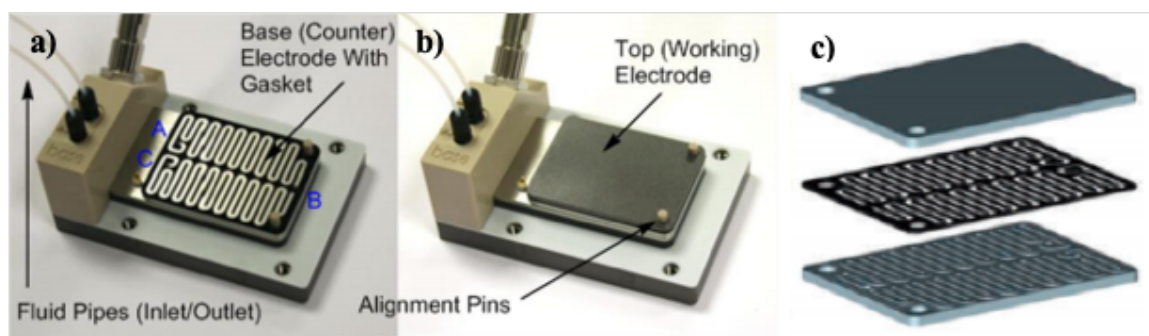
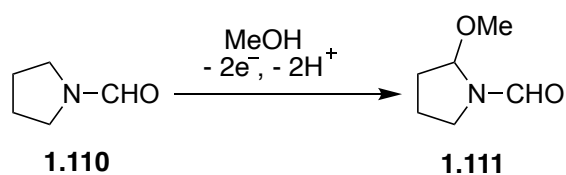


Figure 1.22. Asia Flux module for continuous flow electrochemistry, provided by Syrris Ltd. a) Internal picture of the reactor showing the grooved electrode and elastomer gasket to form meandered channel; b) cell with the top electrode in place; c) schematic picture of the grooved electrode and top electrode, with the gasket in between them.^[52]

Brown and co-workers have made substantial contributions to developing flow electrosynthesis technology in recent years. Several electrochemical flow cells have been established and designed to reach an electrochemical transformation rate of multigrams per hour. In order to study the capability and productivity of the various microflow electrochemical cells, electrochemical methoxylation of *N*-formylpyrrolidine (**1.110**) was utilised as an exemplar substrate (Scheme 1.38).^[53,54,75–77]



Scheme 1.38. Methoxylation of *N*-formylpyrrolidine.

In order to obtain high selectivity and conversion in one pass, reaction time and the amount of supporting electrolyte have been optimised using four different microflow electrolytic reactors. In 2011, a star-moulded microflow electrochemical cell with a channel (600 mm x 1 mm) and a 500 μm interelectrode distance was constructed and utilised to methoxylate *N*-formylpyrrolidine (Figure 1.23a).^[53] A commercially offered microflow electrochemical reactor provided by Syrris Ltd (Figures 1.23b and 1.23c) was used for investigating the same

reaction by the same group. The same authors examined the same reaction process using an electrochemical flow reactor provided by Syrris Ltd. (Figures 1.23b and 1.23c), with (700 mm length x 1.5 mm width) and 200 μm interelectrode gap, resulting in a larger reaction volume. This cell allows to produce the required product in shorter time.^[75]

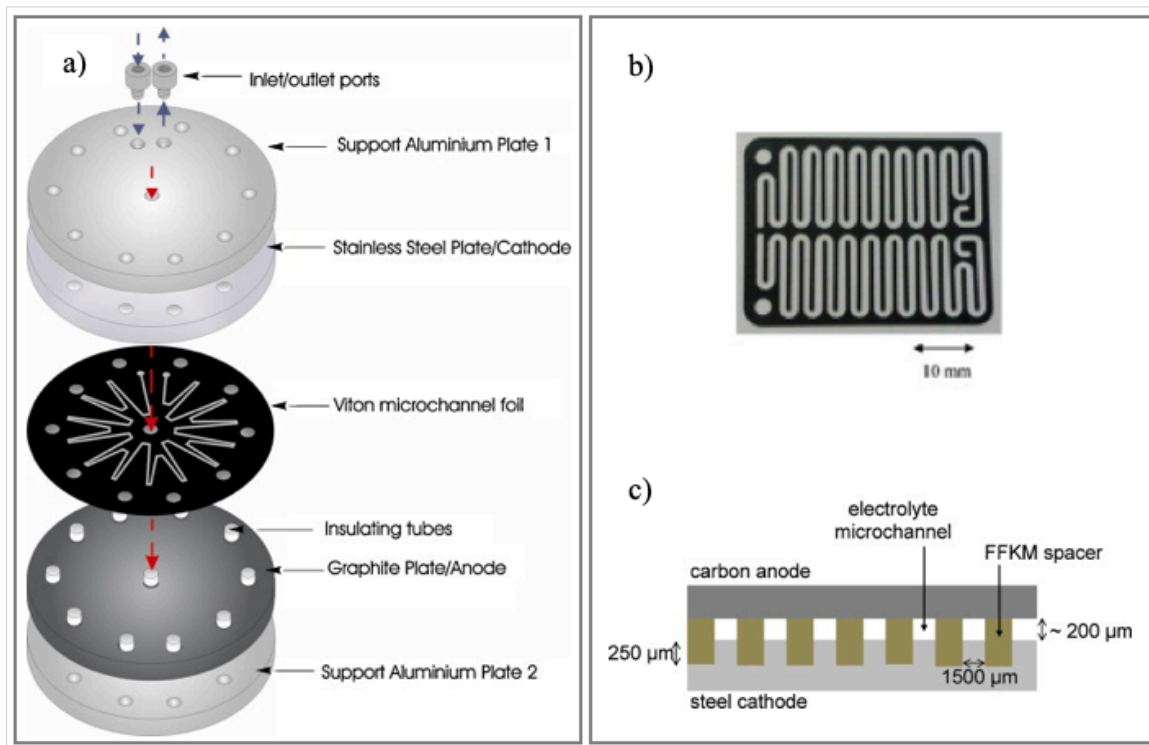


Figure 1.23. a) Microflow reactor with the main components of the cell, b) cell spacer for the Syrris Flux module, c) flow electrolytical cell diagram. ^[53,75] Copyright (2011 and 2012) Elsevier.

Two sizes of Ammonite cell have been designed by Cambridge Reactor Design Ltd, Cambridge, UK.^[54,77] First, flow electrolysis reactor (Ammonite 15) was manufactured.^[54] The reactor consists of two circular electrodes ($\varnothing = 149$ mm), spiral channel (2.0 m long and 5 mm wide) between two electrodes with an interelectrode gap of 500 μm and a 5 mL internal volume (Figure 1.24). The Ammonite 15 electrolysis reactor allows to produce a multigram scale synthesis up to 20 grams per hour.

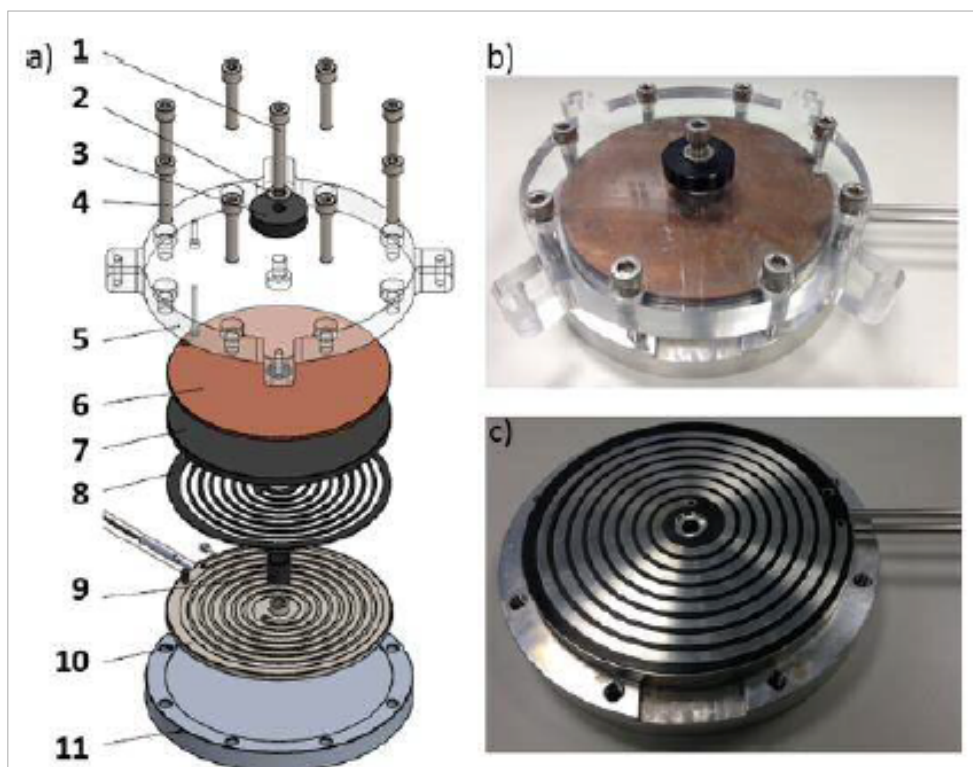


Figure 1.24. Ammonite 15 electrolysis cell: a) Components of the flow electrolysis cell; 1. Central bolt; 2. Washer; 3. Insulating tube; 4. Peripheral bolt; 5. Perspex top plate; 6. Cu baking plate; 7. Carbon/polymer anode plate; 8. Perfluoroelastomer gasket; 9. Insulating tube around central bolt; 10. Stainless steel cathode plate with spiral groove; 11. Aluminium base plate. b) Picture of the assembled reactor. c) Picture of the open reactor with gasket fitted into the cathode plate (spiral channel).^[54] Copyright (2015) American Chemical Society.

A second version of the Ammonite reactor is the Ammonite 8 was also proposed and manufactured by Cambridge Reactor Design Ltd in 2016. The reactor designed for use in a synthetic chemistry laboratory. The reactor capacity has been reduced to 1 mL, and the flow channel has been lengthened to 1.0 m long and 2 mm broad, with a spacer thickness and groove depth making the interelectrode gap at 0.5 mm, providing a thinner flow route that can improve the reaction.^[77] The reactor has been used in two electrolysis transformations; the methoxylation of *N*-formylpyrrolidine (**1.110**) and the cleavage 4-methoxybenzyl groups from ethers to form deprotected alcohols, giving high yields and production rate >1 g/h with flow rates up to 3 mL/min.

Brown and co-workers (2020) developed a small flow reactor with a rectangle shape that manufactured and assembled in a simple workshop (Figure 1.25).^[76] The reactor comprises of a copper plate (70 mm long × 40 mm wide × 3 mm thick); The copper plate contains two holes for inlet and outlet of the solution as well as two ears for electrical connection. RVC block (30

mm \times 20 mm \times 10 mm) was fitted in the middle section (30 mm long 20 mm wide). The anode electrode part comprising of a PTFE plate (70 mm long \times 40 mm wide \times 3 mm thick) with the middle section made to permit solution flow. The cathode electrode was made of 316 stainless steel plate (70 mm 40 mm 3 mm thick) with two ears for electrical connection and two holes (diameter 4.77 mm) for solution inlet and outlet. All components were clamped with aluminium plates with 6 screws. This cell was operated as divided and undivided cell.

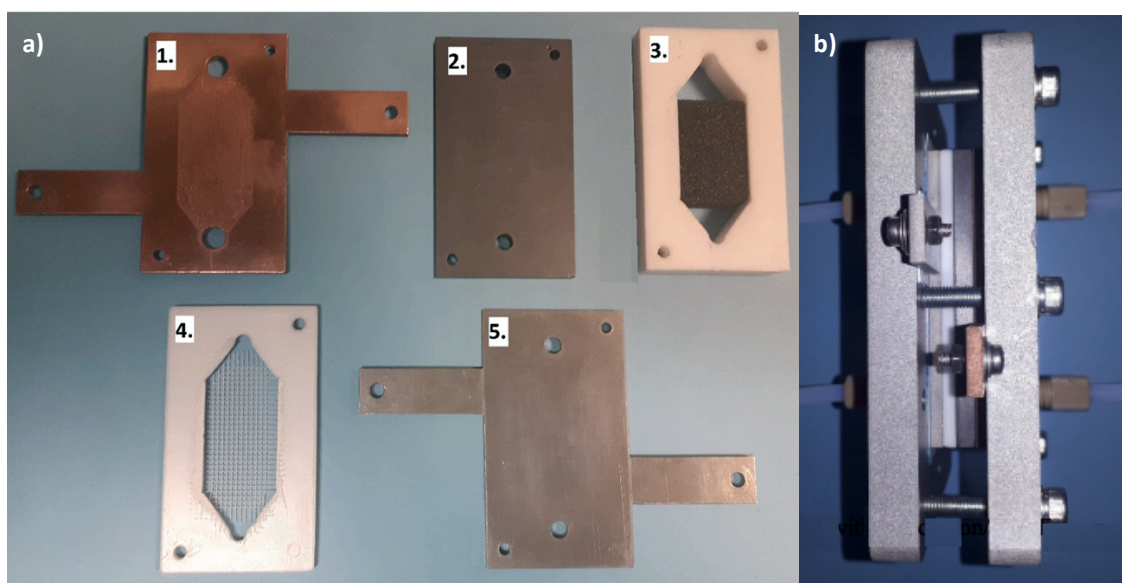
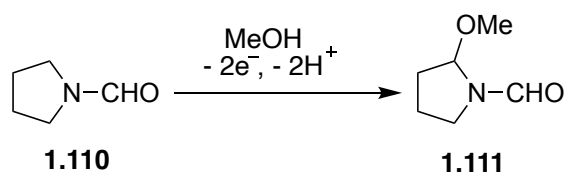


Figure 1.25. (a) Picture of the components of the cell with RVC electrode: 1. Copper plate current connector 2. Carbon/PVDF composite plate; 3. PTFE working electrode compartment with RVC anode in place; 4. PTFE counter electrode compartment filled with stack of fine polymer meshes; 5. Stainless steel plate cathode. (b) Picture of the cell assembled with flat carbon/PVDF composite plate anode.^[76] Copyright (2020) Royal Society of Chemistry.

The results of the five flow electrochemical reactors mentioned above for the methoxylation of *N*-formylpyrrolidine **1.110** are summarized in Table 1.2.

Table 1.2. Comparison of the outcome of the different flow electrochemical reactors. [4-7]

Entry	Cell description	Flow rate (mL min ⁻¹)	Conversion (%)	Rate max ^a (g h ⁻¹)	Ref
1	Star shaped microchannel: 600 mm long x 1 mm wide	0.1	96	0.078	[53]
	(500 μm interelectrode gap)	3.5	33	0.95	
2	Patterned recessed channel: 700 mm long x 1.5 mm wide	3	>95	1.8	[75]
	(200 μm interelectrode gap)				
3	Spiral shaped microchannel: 2000 mm long x 5 mm wide	16	88	20.7	[54]
	(500 μm interelectrode gap)				
4	Spiral shaped microchannel: 1000 mm long x 2 mm wide	1	82	3.16	[77]
	(500 μm interelectrode gap)				
5	Middle part microchannel: 70 mm long x 40 mm wide	36	86	0.44	[76]
	(1000 μm aperture)				

^a Maximum rate of product formation

In the last decade, our lab has made significant contributions in this area by developing and producing microflow electrosynthesis reactors and showing their application in various synthetic transformations. The first generation microreactor was established in 2011 (Figure 1.26) and the microreactor has been applied for the synthesis of diaryliodonium salts **1.115**. The flow reactor made up of two rounded platinum electrodes (0.1 mm thick) that are divided by using different thicknesses of a fluorinated ethylene propylene (FEP) as flow channels where the reaction mixture can pass through the channels.^[56] The two electrodes and the FEP spacer (3 × 30 mm) were sandwiched using two round aluminum bodies.

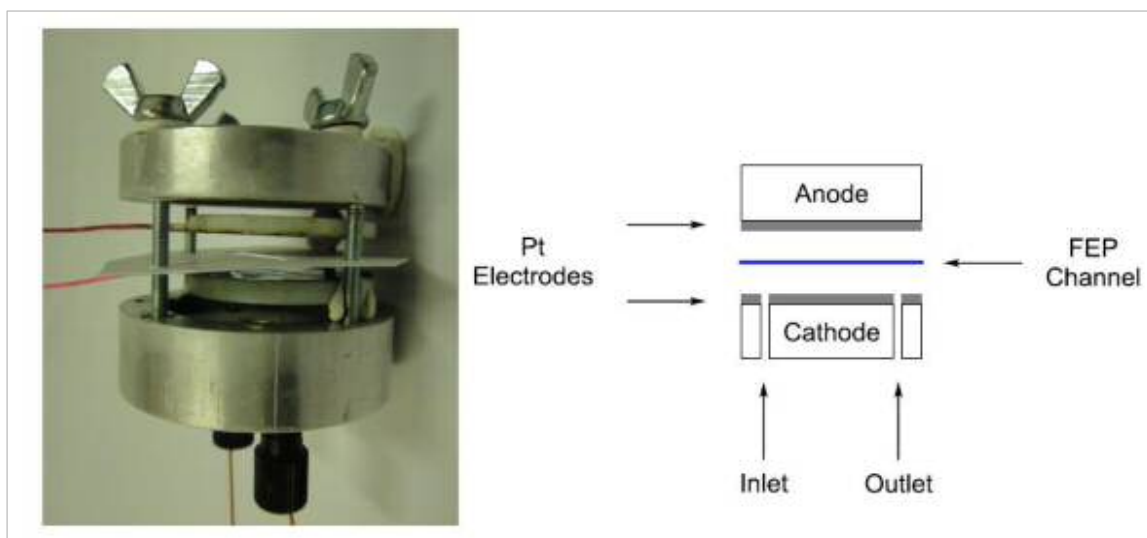
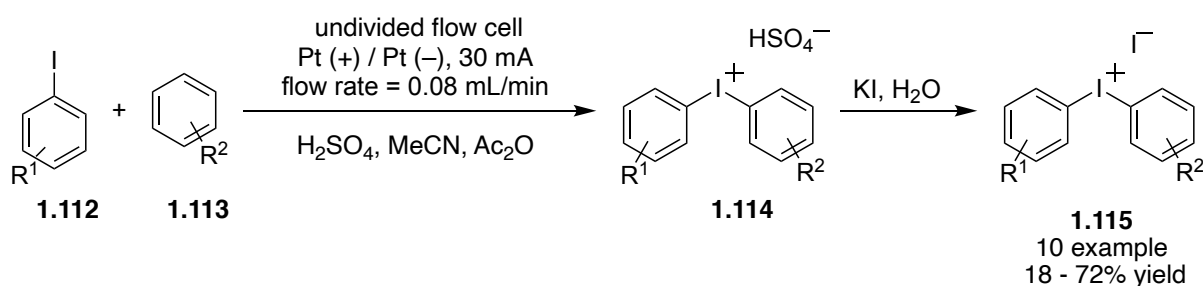


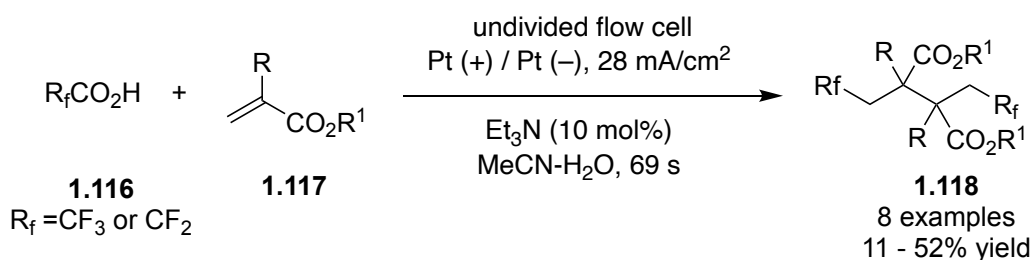
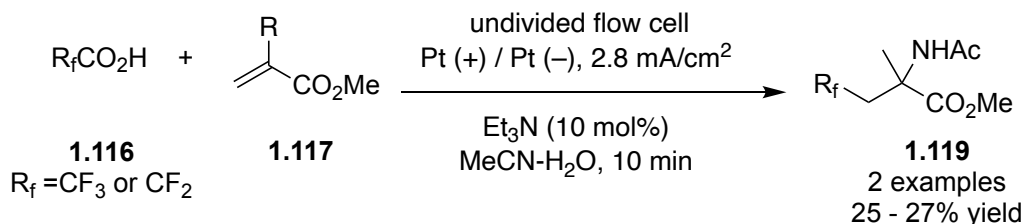
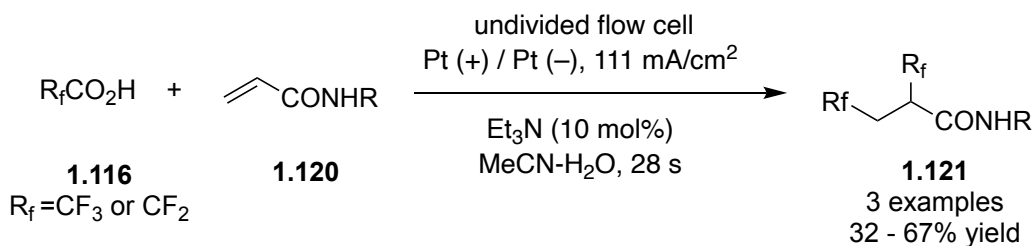
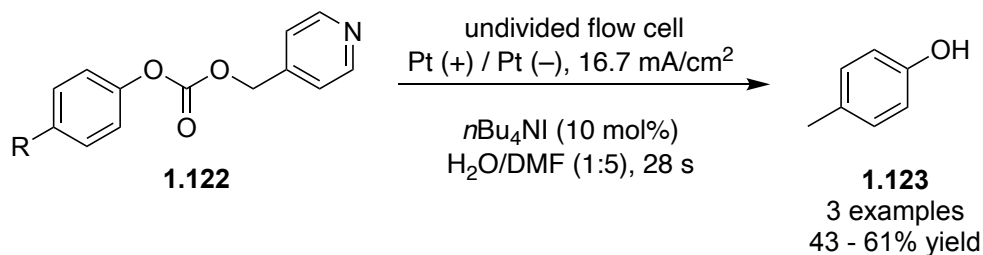
Figure 1.26. First generation electrochemical flow microreactor.^[56] Copyright (2011) Beilstein-Institut.

The diaryliodonium salts were synthesized in a single pass of an iodoarenes **1.112** in the presence of **1.113** through electrochemical oxidation and avoiding the use of harmful chemical oxidants (Scheme 1.39).^[56]



Scheme 1.39. Electrochemical generation of diaryliodonium salts.

In addition, the reactor is utilised for a variety of processes such as difluoro- and trifluoromethylation of alkenes (Scheme 1.40a-c),^[78] and the deprotection of the isonicotinoyloxycarbonyl (*i*Noc) protecting group from carbonates and thiocarbonates (Scheme 1.40d).^[78]

a) Di- and trifluoromethylation of acrylates**b) Di- and trifluoromethylation of methyl methacrylate****c) Di- and trifluoromethylation of acrylamide****d) Electrochemical cleavage of the *i*Noc protecting group**

Scheme 1.40. Electrochemical generation of CF_3 and CHF_2 radicals for the addition to electron-deficient alkenes and deprotection of the isonicotinylloxycarbonyl (*i*Noc) protecting group.

Although the reactor described above was employed successfully in numerous potential transformations, it had certain drawbacks. Only platinum electrodes were permitted to use, and replacing or repairing the bonded thin platinum foils was a time-consuming operation. The circular cell design resulted in the loss of a costly electrode cut off material, as well as overly brittle electrical connections to the electrode. A second-generation microreactor was planned and built.^[55] The second-generation reactor (Figure 1.27) is made up of two square aluminium blocks ($75 \times 75 \times 25 \text{ mm}^3$) with a square area in the center ($50 \times 50 \text{ mm}^2$, variable depth) for

the electrodes. To connect the electrodes, copper plates or stainless-steel sheets are welded to copper wires, which are then connected to the power supply. The two electrodes are divided by a FEP gasket, and the reaction takes place in a passage carved out of the FEP spacer. The new design resilience and versatility allowed easy switching to any electrode material based on user choice. This resulted in considerably easier and more efficient screening of reaction conditions, as well as extended operating durations with less maintenance and easy cleaning. Furthermore, the reactor body composition may be changed from aluminium material to polymeric material, allowing easy customization or modification using low-cost manufacturing (3D printing).

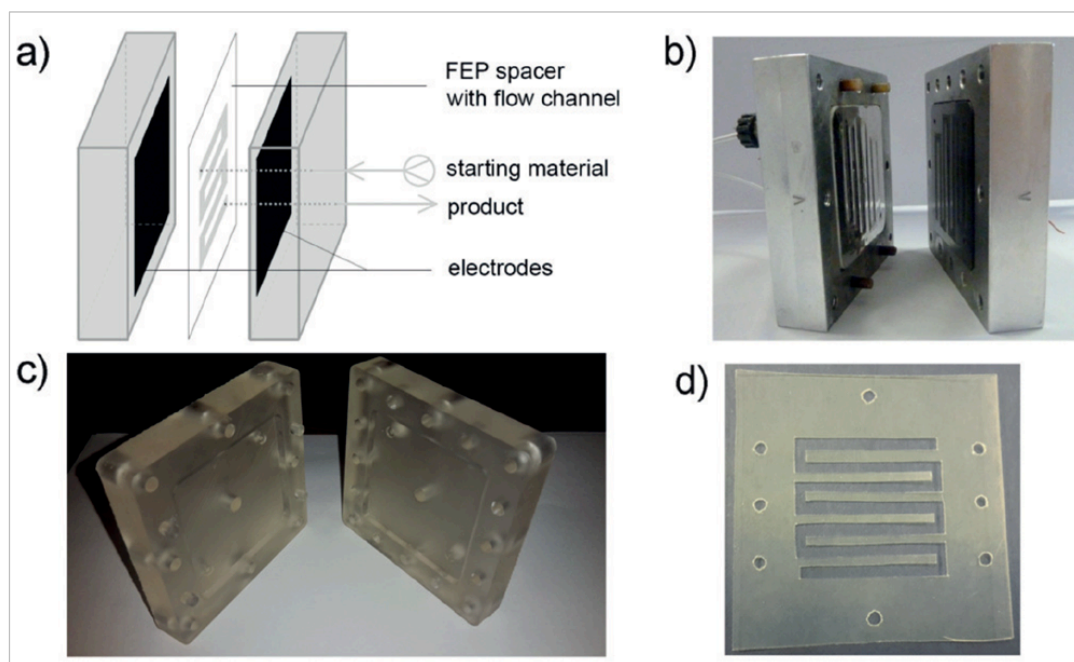


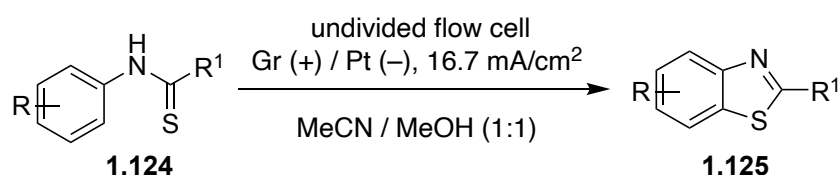
Figure 1.27. Second generation electrochemical flow cell. (a) Schematic representation, (b) aluminum reactor, (c) reactor made by additive manufacturing (3D printing) using resins consisting of methacrylic acid esters, and (d) FEP spacer with flow channel.^[55] Copyright (2017) Wiley.

The second generation microflow reactor's efficiency and reliability was successfully demonstrated by the synthesis of isoindolinones^[55] and benzothiazoles.^[79] Benzothiazoles and thiazolopyridines (Scheme 1.41a) were synthesized simply under flow electrochemical conditions without using any catalyst or supporting electrolyte. Furthermore, scaling up to the gram scale in high yield was easy by simply utilizing the same reactor for a longer duration.^[79] The same reaction has been done using batch cell electrochemically in good efficiency. Although TEMPO as a mediator and supporting electrolytes were required, the scalability was limited. The current efficiency under flow conditions was better than the batch electrolysis for the synthesis of benzothiazoles.^[79]

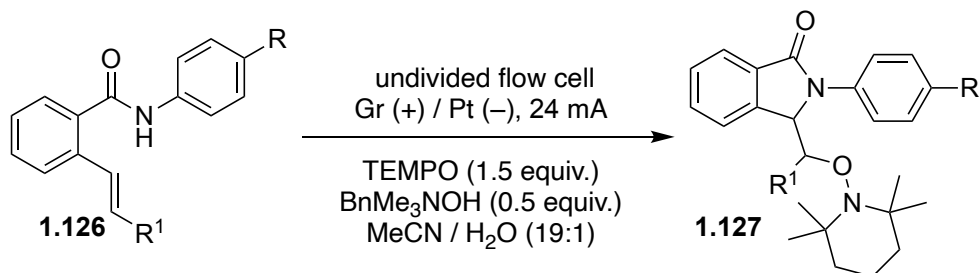
For the synthesis of isoindolinones (Scheme 1.41b), an online mass spectrometer was connected to second generation microflow reactor through an automatic sampling valve, monitoring the starting material and targeted product intensity peaks. This allowed to accelerate the optimization process.^[79]

Interestingly, the second generation microflow reactor has been reprinted by Prof. Xu and co-workers and used for intramolecular dehydrogenative C–S coupling to produce benzofused six-membered S-heterocycles (Scheme 1.41c).^[80]

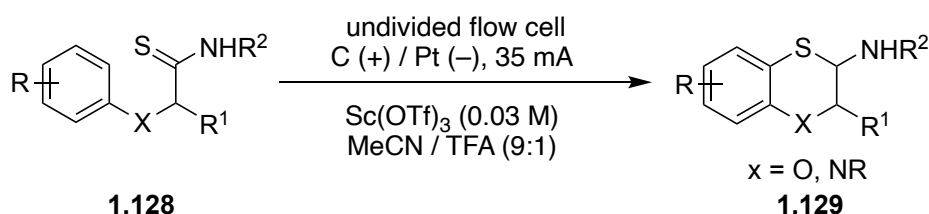
a) Electrochemical synthesis of benzothiazoles and thiazolopyridines



b) Electrochemical synthesis of isoindolinones



c) Electrochemical synthesis of benzofused six-membered S-heterocycles



Scheme 1.41. Flow electrochemical synthesis of benzothiazoles **1.125**, isoindolinones **1.126** and benzofused six-membered S-heterocycles **1.127**.

The successful applications, efficiency and reliability of the second-generation reactor has prompted the flow technologies company Vapourtec Ltd. to collaborate and develop the third generation flow electrochemical reactor based on the second-generation reactor design.

The essential collaboration between Prof. Wirth and Vapourtec Ltd. company led to the manufacture and commercialisation of the third generation flow electrochemical reactor, the Ion reactor. The Ion electrochemical reactor has two versions for standalone (Figure 1.28a) or integrated with Vapourtec heating and cooling module (Figure 1.28b).^[81]

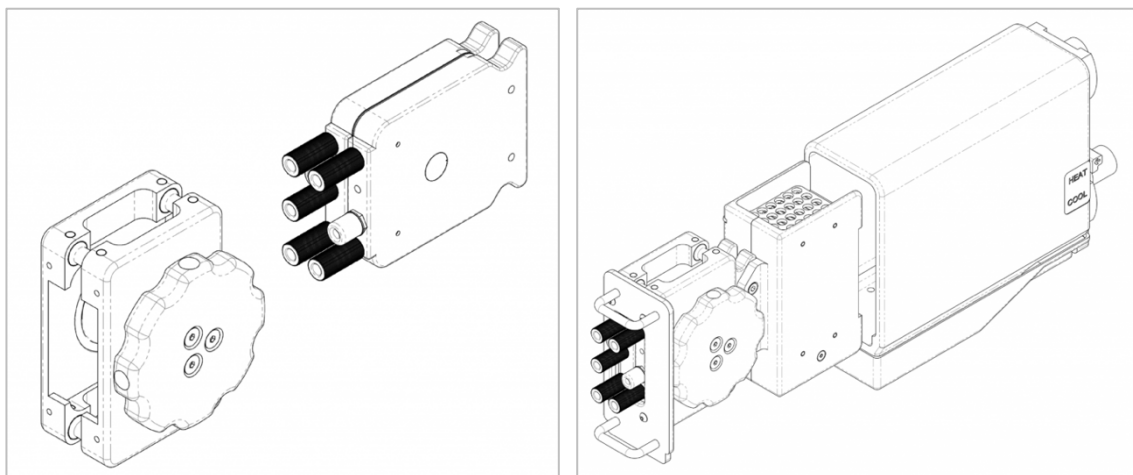


Figure 1.28. Vapourtec Ion electrochemical reactor. (a) Standalone reactor (b) Reactor integrated with Vapourtec cooling and heating module.^[81] Copyright Vapourtec Ltd. Company.

1.9. Development of Ion electrochemical reactor

As described above, the first- and second-generation reactors have been used for a variety of fascinating transformations, but there were certain aspects that were improved in the third-generation electrochemical reactor.

1.9.1. Reactor designed

The reactor was designed and built using two square stainless steel bodies with plastic stake, where the electrodes are placed (Figure 1.29a). Each stainless steel body is surrounded by solvent resistant rubber seals in order to avoid the electrical spark and reaction solution leakage. The whole device is held together by one clamp with a center male handwheel (Figure 1.16b), tightening manually using the hand without any need of screwdriver or kit is a major advantage of this reactor compared to other the pervious reactors, published or commercially available that use many bolts for holding.

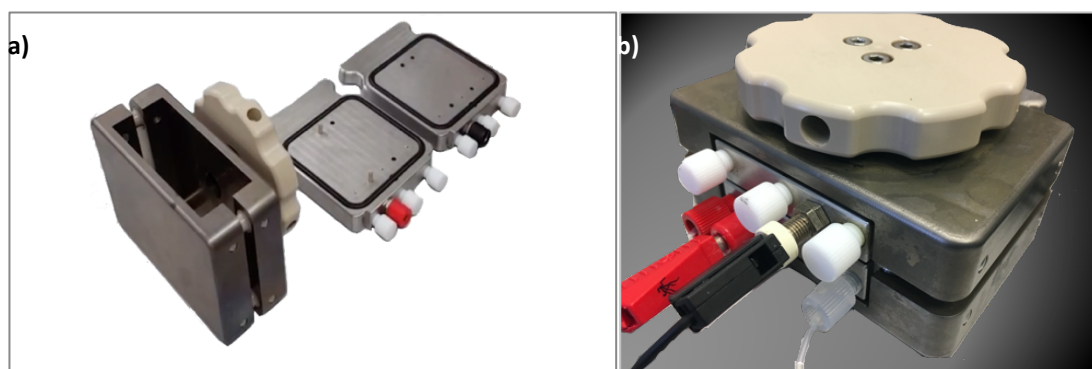


Figure 1.29. (a) Reactor bodies and clamp (b) Vapourtec Ion electrochemical reactor.

1.9.2. Flow tube connectors

In the first- and second-generation reactor, the tube was connected by ferrule (e.g coned PEEKTM HPLC) and this led to occasional leakage between the copper plates and the electrodes or copper plates and the bodies. To avoid this problem, well-knitted plastic fittings were built in the bodies and encompassed rubber seals to get a well sealing at the inflow and outflow of the reactor (Figure 1.30). Also, an extra inlet was added in the middle of the reactor that can be used to add a second stream of flow during electrolysis in the reactor.

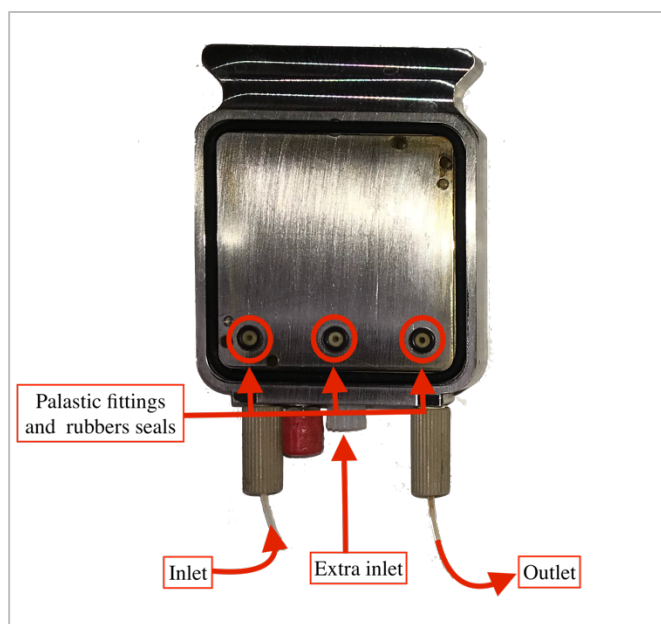


Figure 1.30. Inlet and out let plastic fittings and rubber seals.

1.9.3. Electrode wire connection

The electrodes have to be linked to the power supply through a copper wire for electrical connection. In the first generation reactor, the wires were connected to the platinum sheets *via* drilled bores in the PTFE body. It deformed the platinum sheets, making the region, where the wire was located uneven. A similar approach was used in the second generation reactor, but rather than drilling a bore in the PTFE part randomly, the wire was taped or glued to the center of the electrode. The platinum electrode connects to the wire was glued on the PTFE piece which led to deform it after a while of use. In both reactors, the wire was one of the problematic parts which was fragile and need to be replaced or fixed after regularly. These problems have been solved efficiently in the third generation reactor. The wires were connected straightforwardly via holes in the reactor, using banana plugs wires which are commercially available. Two inlets have been made in the body of the reactor and assigned with different colors for working and counter electrode (Figure 1.31). This design allows to use of the reactor safely without any special care.

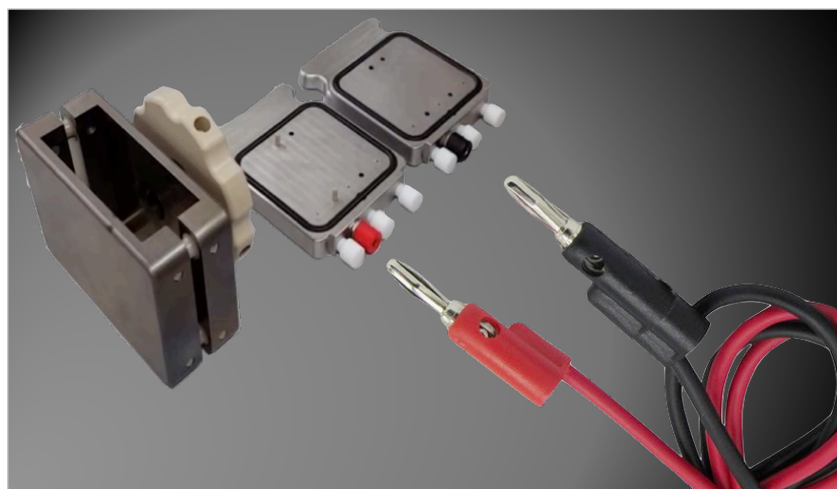


Figure 1.31. Counter and auxiliary wires connection.

1.9.4. Spacer and flow channel

The distance and the flow channel between the electrodes have defined by an inert FEP (fluorinated ethylene propylene) membrane. A range of membrane thicknesses can be used and easily replaced (Table 1.3). The membrane was designed with sinuous shape, allowing good mixing of the reaction mixture and use the maximum electrodes area (Figure 1.32). Also, a small gap between the electrodes can effectively nullify or minimize the amount of supporting electrolyte depending on the reaction conditions. This microflow cell can also be operated as a divided cell if an ion exchange membrane is inserted among two gaskets.

Table 1.3. Electrochemical reactor volumes and membrane thickness

Membrane thickness (mm)	Electrode area (cm ²)	Reactor volume (ml)
0.125	12.07	0.15
0.25	12.07	0.30
0.5	12.07	0.60
1	12.07	1.20



Figure 1.32. FEP spacer with flow channel design.

1.9.5. Temperature control

The Ion reactor has been developed with additional cooling and heating part that allow to cool and heat the cell in the temperature range from -10 to $+100$ °C (Figure 1.33). This part covered by housing made from plastic, integrating with Vapourtec E-Series or R-Series systems. The set-up is controlled and stabilised by temperature sensor that is connected to the reactor via a hole. This feature was not present in the first- and second- generation.

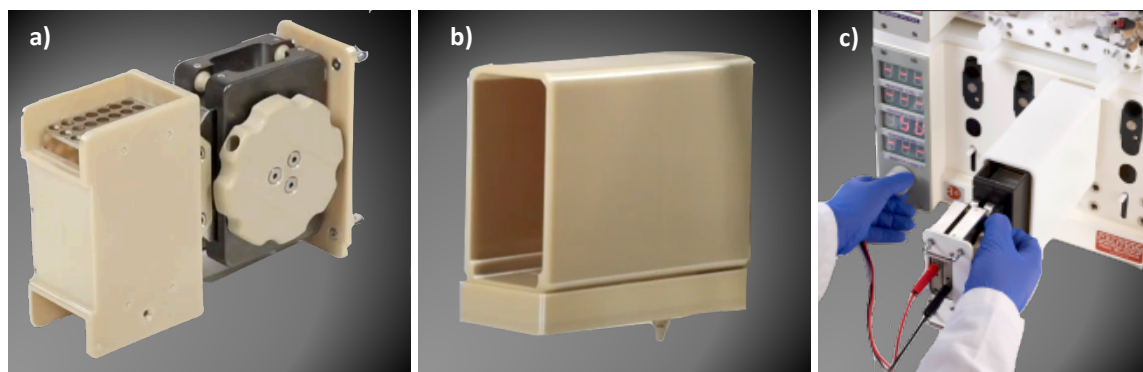
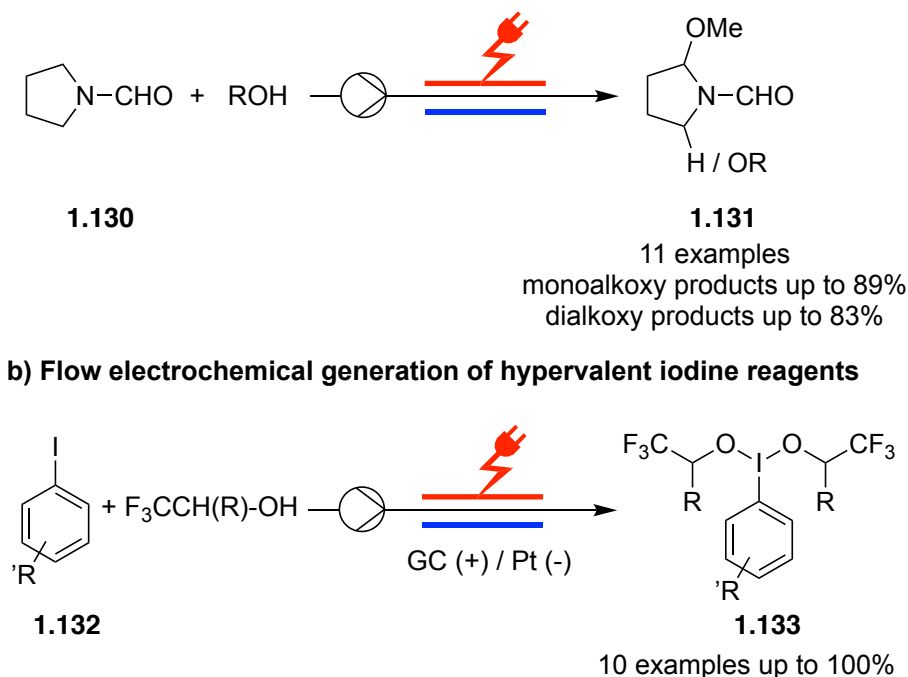


Figure 1.33. (a) Reactor with cooling and heating part; (b) Reactor house, and (c) Reactor integrated with Vapourtec cooling and heating module.^[81]

The Shono oxidation was used as a model reaction to assess the performance of the Vapourtec electrochemical Ion microreactor (Scheme 1.42a).^[82] This study was first reported for this reactor even before its commercialisation. Many aspects and parameters were evaluated to identify their impacts on the reaction, which will additionally control the productivity of the developed reactor (explained in Chapter 2 in detail). Subsequently, the synthesis of iodine(III) reagents through anodic oxidation using Ion electrochemical microreactor was achieved (Scheme 1.42b).^[61] Several iodoarenes **1.132** have been oxidised to the hypervalent iodine reagents **1.133** in good to excellent yields. Various hypervalent iodine mediated oxidative

transformations were obtained in good to excellent yields by combining a second flow of the substrate with the flow electrolysis setup.



Scheme 1.42. (a) Flow electrochemical alkoxylation of Pyrrolidine-1-carbaldehyde and (b) Flow electrochemical generation of hypervalent iodine reagents.

After successful development of the third-generation electrochemical reactor (Ion reactor) by flow technology company Vapourtec Ltd., the challenging aspect was to integrate the Ion electrochemical reactor with automated machine.

1.10. Automation:

Automated flow synthesis platform plays an important role in the transformation from laboratory chemistry processes to industrial-scale processes.^[83–86] The automation of continuous flow setup has the potential to accelerate the synthesis process, to scaling up the reaction, to reduce the required manpower, to avoid human errors, and to make a positive contribution towards sustainable and green chemistry by minimizing waste. The automated flow technologies have been used in several chemical applications. Several automated platforms such as the AFRICA flow systems,^[87] Uniqsis Flow-Synch reactor systems,^[88] the Advion Nanotec reactor systems,^[89] and the Vapourtec R2+/R4 systems^[90] have been manufactured and provided for the needs of researchers. Different reactors such as heated flow coil, glass column, and sample loop have been integrated with such a machine.^[91–93]

Integration of electrochemical reactor with automation machine hasn't been done with all the reported reactors. To the best of our knowledge, the Vapourtec electrochemical Ion reactor is

the first use of a flow electrochemical reactor integrated in an automated system RS-400. Certainly, remotely controlled self-optimization to accelerate various transformations under electrochemical conditions could be achieved using such technology. Vapourtec generously supplied RS-400 automated system in addition to the electrochemical reactor including full instructions regarding its operation.

2.4.1. RS-400 – Automated System

The RS-400 is a complex system, It is consisting of 4 pumps (2 HPLC pumps and 2 V3 pumps), reactors heater, external chiller, power supply, liquid handler (loading and collection), and autosampler, that are controlled automatically using Flow Commander™ software via touch screen (Figure 1.34).^[94] Also, this machine can be integrated with different analysis machines such as HPLC, IR, UV and Mass spectroscopy. A sequence of reactions with varying conditions can be pre-programmed and executed without human interaction.

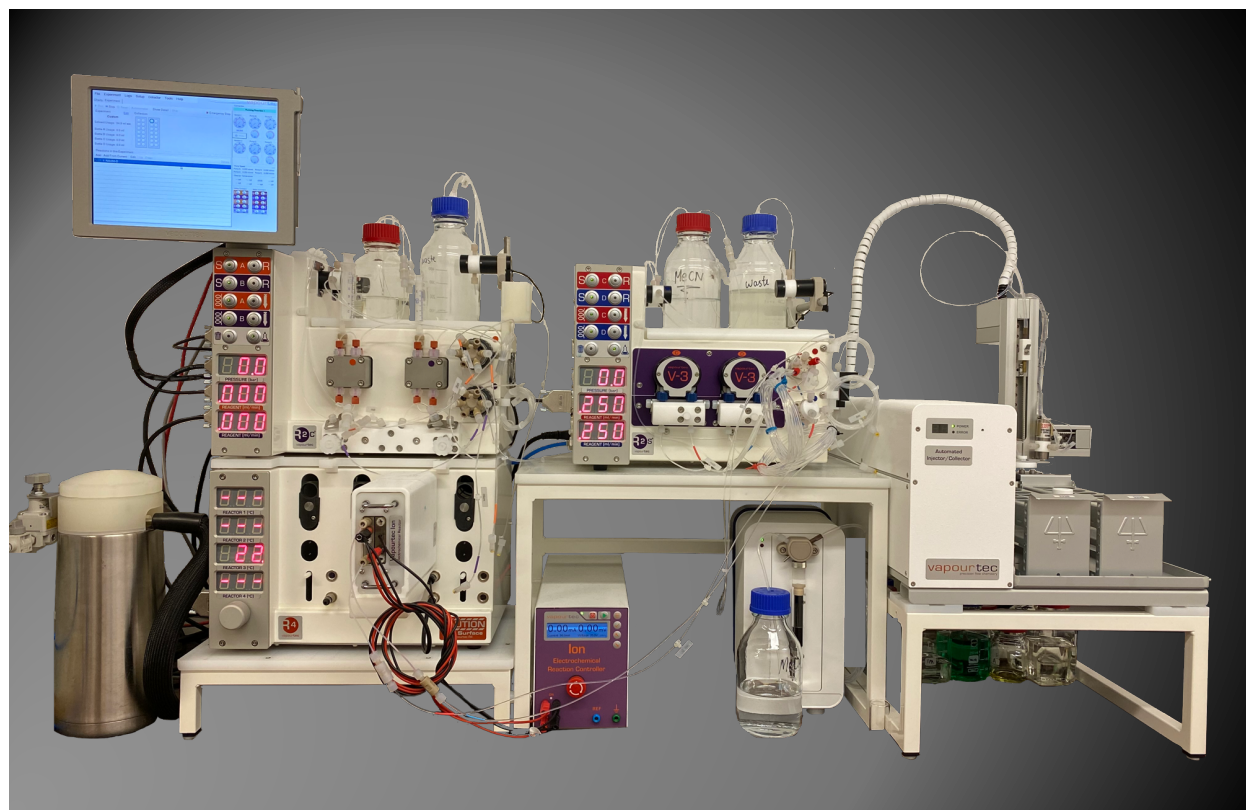


Figure 1.34: Automated Vapourtec R-Series Flow System integrated with Ion electrochemical reactor.

As a follow-up to our group's previous work on flow electrochemical reactor design and flow electrolytic transformation developments, the integration of automated system with flow electrochemical reactor and its application in different organic transformations will be discussed in chapters 3 to 5.

1.11. Conclusion and outlook

Electroorganic synthesis is witnessing a renaissance and is becoming a mainstream in synthetic organic chemistry. A wide range of electrochemical transformations and efficient methodologies were developed using batch and / or flow electrolysis cells. The applications of electroorganic synthesis are not limited to small laboratory scale, but some large-scale production processes are already developed and participate in producing value added chemicals on industrial scale. Under electrolysis conditions electron transfer takes place on the electrode surface enabling selective redox chemical transformations without using exogenous oxidising and / or reducing agents, hence, prevents the formation of chemical waste associated with the traditional methods. Therefore, electroorganic synthesis is intrinsically greener than traditional chemical methods and reduces the environmental burden of chemical processes. On the other hand, electrochemical methods are not always green or are not always that green as large amounts of hazardous supporting electrolytes are necessary in most organic electrochemical transformations, especially under batch conditions. In addition, environmentally stressful additives and hazardous, corrosive, or toxic solvents used in traditional chemical methods are also used in electrochemical processes posing the same safety and environmental concerns.

Despite the efficiency, reliability and relative 'greenness' of electroorganic synthesis and the burst of reports, publications and research efforts, the field is still in its infancy and various aspects and challenges need more interest and research in order to achieve more efficient and greener electroorganic synthetic methods and processes. Some of such aspects and challenges include but not limited to: 1) Eliminating or reducing the burden of supporting electrolytes; 2); paying more attention to electrochemical reduction reactions as cathodic reactions are less studied and exploited in organic synthesis compared to the extensively studied anodic reactions; 3); another underdeveloped area in electroorganic synthesis is asymmetric electrochemical protocols which are extremely limited and sporadic; 4); the vast majority of synthetic electrochemical methods benefit of one half of the cell only, either the anodic or the cathodic reaction is involved in the production of the desired product while the other half is sacrificial. Some paired electrolysis protocols that benefit from the two halves of the cell are already reported but they are extremely limited, more attention and efforts are needed to develop paired electrolysis and push it to the mainstream of electroorganic synthesis; 5) design and production of more efficient continuous flow electrochemical cells and expanding electroorganic synthesis under flow conditions; 6) development of new materials for electrodes and ion exchange membranes.

Over the last few decades, flow electrochemistry techniques became a useful tool as a viable alternative methodology in organic synthesis. Electrolysis under the flow conditions can be completed using low concentrations of supporting electrolyte or even without adding supporting electrolyte, due to the short distance between the electrodes, which along with large surface to volume ratio are major advantages of such techniques over batch-type electrolysis. In addition, removing the reaction mixture continuously under flow conditions minimises the opportunity of overoxidation, that is one of the main problems of electrolysis under batch conditions.

Various research laboratories have developed their own electrochemical flow cells, that were applied successfully in a various electrochemical transformation. Also, some electrochemical flow cells have been commercialized which encouraged more research groups to consider flow electrochemistry as a feasible alternative in organic synthesis.

Our group has developed microflow electrosynthesis reactors showing their applications in various synthetic transformations over the last 10 years. Two generations of our flow electrochemical reactor with different shapes and features have been designed and produced in-house with low cost. Furthermore, a fruitful collaboration with the flow technology company, Vapourtec, resulted in an improved third generation (Ion Reactor) that has been produced and commercialized. The design of the ion reactor is based on the design of our second-generation reactor but avoiding its limitations and adding new features such cooling and heating capabilities, in addition to the ability to combine additional flow stream to the middle of the reactor.

The Ion electrochemical reactor has been designed to be combined easily with automation platforms. Using the automation approach in combination with flow electrochemical reactor for rapid and robust optimisation of electrochemical transformations is a very attractive research area that requires more efforts to be developed as a standard technique in synthetic organic chemistry laboratories.

1.12. References

- [1] O. Hammerich, B. Speiser, Editors, *Organic Electrochemistry: Revised and Expanded, Fifth Edition*, CRC Press, **2016**.
- [2] T. Fuchigami, M. Atobe, S. Inagi, Editors, *Fundamentals and Applications of Organic Electrochemistry: Synthesis, Materials, Devices*, Wiley, **2014**.
- [3] S. D. Minter, P. Baran, *Acc. Chem. Res.* **2020**, *53*, 545–546.
- [4] D. Pollok, S. R. Waldvogel, *Chem. Sci.* **2020**, *11*, 12386–12400.
- [5] D. Pletcher, *Electrochem. Commun.* **2018**, *88*, 1–4.
- [6] R. D. Little, K. D. Moeller, *Chem. Rev.* **2018**, *118*, 4483–4484.
- [7] M. Yan, Y. Kawamata, P. S. Baran, *Angew. Chemie Int. Ed.* **2018**, *57*, 4149–4155.
- [8] M. Elsherbini, T. Wirth, *Acc. Chem. Res.* **2019**, *52*, 3287–3296.
- [9] T. Noël, Y. Cao, G. Laudadio, *Acc. Chem. Res.* **2019**, *52*, 2858–2869.
- [10] D. Pletcher, R. A. Green, R. C. D. Brown, *Chem. Rev.* **2018**, *118*, 4573–4591.
- [11] M. Atobe, H. Tateno, Y. Matsumura, *Chem. Rev.* **2018**, *118*, 4541–4572.
- [12] D. Pletcher, F. C. Walsh, *Industrial Electrochemistry*, Springer Netherlands, Dordrecht, **1993**.
- [13] M. M. Baizer, *Naturwissenschaften* **1969**, *56*, 405–409.
- [14] G. Hilt, *ChemElectroChem* **2020**, *7*, 395–405.
- [15] M. Elsherbini, W. J. Moran, *Org. Biomol. Chem.* **2021**, *19*, 4706–4711.
- [16] C. Gütz, A. Stenglein, S. R. Waldvogel, *Org. Process Res. Dev.* **2017**, *21*, 771–778.
- [17] R. A. Green, R. C. D. Brown, D. Pletcher, B. Harji, *Org. Process Res. Dev.* **2015**, *19*, 1424–1427.
- [18] R. A. Green, R. C. D. Brown, D. Pletcher, *J. Flow Chem.* **2016**, *6*, 191–197.
- [19] R. Horcajada, M. Okajima, S. Suga, J. Yoshida, *Chem. Commun.* **2005**, 1303–1305.
- [20] D. Wang, P. Wang, S. Wang, Y.-H. Chen, H. Zhang, A. Lei, *Nat. Commun.* **2019**, *10*, 2796.
- [21] F. Amemiya, K. Fuse, T. Fuchigami, M. Atobe, *Chem. Commun.* **2010**, *46*, 2730.
- [22] Y. Cao, T. Noël, *Org. Process Res. Dev.* **2019**, *23*, 403–408.
- [23] “IKA ElectraSyn Flow,” can be found under <https://www.ikaprocess.com/en/Products/Electro-synthesis-cph-45/ElectraSyn-flow-csb-ES/>.
- [24] “Cambridge Reactor design - Ammonite,” can be found under

- <https://www.cambridgereactordesign.com/ammonite/>.
- [25] “Asia Flux,” can be found under <https://syrris.com/product/asia-electrochemistry-flow-chemistry-system/>.
- [26] L. E. Sattler, C. J. Otten, G. Hilt, *Chem. – A Eur. J.* **2020**, *26*, 3129–3136.
- [27] C. Schotten, C. J. Taylor, R. A. Bourne, T. W. Chamberlain, B. N. Nguyen, N. Kapur, C. E. Willans, *React. Chem. Eng.* **2021**, *6*, 147–151.
- [28] J. Fährmann, G. Hilt, *Angew. Chemie Int. Ed.* **2021**, *60*, 20313–20317.
- [29] Y. Kawamata, K. Hayashi, E. Carlson, S. Shaji, D. Waldmann, B. J. Simmons, J. T. Edwards, C. W. Zapf, M. Saito, P. S. Baran, *J. Am. Chem. Soc.* **2021**, *143*, 16580–16588.
- [30] A. A. Folguez-Amador, X. Y. Qian, H. C. Xu, T. Wirth, *Chem. - A Eur. J.* **2018**, *24*, 487–491.
- [31] R. Francke, R. D. Little, *Chem. Soc. Rev.* **2014**, *43*, 2492.
- [32] T. Fuchigami, M. Tetsu, T. Tajima, H. Ishii, *Synlett* **2001**, 1269–1271.
- [33] W. Zhang, N. Hong, L. Song, N. Fu, *Chem. Rec.* **2021**, *21*, 2574–2584.
- [34] R. S. Sherbo, A. Kurimoto, C. M. Brown, C. P. Berlinguette, *J. Am. Chem. Soc.* **2019**, *141*, 7815–7821.
- [35] R. S. Sherbo, R. S. Delima, V. A. Chiykowski, B. P. MacLeod, C. P. Berlinguette, *Nat. Catal.* **2018**, *1*, 501–507.
- [36] R. Matthesen, J. Fransaer, K. Binnemans, D. E. De Vos, *ChemElectroChem* **2015**, *2*, 73–76.
- [37] K. Park, P. N. Pintauro, M. M. Baizer, K. Nobe, *J. Electrochem. Soc.* **1985**, *132*, 1850–1855.
- [38] J. C. Yu, M. M. Baizer, K. Nobe, *J. Electrochem. Soc.* **1988**, *135*, 1400–1406.
- [39] Y. Mo, Z. Lu, G. Rughoobur, P. Patil, N. Gershenfeld, A. I. Akinwande, S. L. Buchwald, K. F. Jensen, *Science (80-.)*. **2020**, *368*, 1352–1357.
- [40] G. Hilt, *Angew. Chemie Int. Ed.* **2003**, *42*, 1720–1721.
- [41] M. F. Hartmer, S. R. Waldvogel, *Chem. Commun.* **2015**, *51*, 16346–16348.
- [42] H. Zhao, P. Xu, J. Song, H. Xu, *Angew. Chemie* **2018**, *130*, 15373–15376.
- [43] W. Li, T. Nonaka, *J. Electrochem. Soc.* **1999**, *146*, 592–599.
- [44] J. Strehl, M. L. Abraham, G. Hilt, *Angew. Chemie Int. Ed.* **2021**, *60*, 9996–10000.
- [45] A. G. Wills, S. Charvet, C. Battilocchio, C. C. Scarborough, K. M. P. Wheelhouse, D. L. Poole, N. Carson, J. C. Vantourout, *Org. Process Res. Dev.* **2021**, DOI: [acs.oprd.1c00167](https://doi.org/10.1021/acs.oprd.1c00167).
- [46] Y. Mo, G. Rughoobur, A. M. K. Nambiar, K. Zhang, K. F. Jensen, *Angew. Chemie Int.*

- Ed.* **2020**, 59, 20890–20894.
- [47] M. Santi, J. Seitz, R. Cicala, T. Hardwick, N. Ahmed, T. Wirth, *Chem. – A Eur. J.* **2019**, 25, 16230–16235.
- [48] Y. Yuan, A. Lei, *Nat. Commun.* **2020**, 11, 802–804.
- [49] J. P. Barham, B. König, *Angew. Chemie Int. Ed.* **2020**, 59, 11732–11747.
- [50] J. Yoshida, *Flash Chemistry*, John Wiley & Sons, Ltd, Chichester, UK, **2008**.
- [51] T. Wirth, Ed., *Microreactors in Organic Chemistry and Catalysis*, Wiley-VCH Verlag GmbH & Co. KGaA, Weinheim, Germany, **2013**.
- [52] D. Pletcher, R. A. Green, R. C. D. Brown, *Chem. Rev.* **2018**, 118, 4573–4591.
- [53] J. Kuleshova, J. T. Hill-Cousins, P. R. Birkin, R. C. D. Brown, D. Pletcher, T. J. Underwood, *Electrochim. Acta* **2011**, 56, 4322–4326.
- [54] R. A. Green, R. C. D. Brown, D. Pletcher, B. Harji, *Org. Process Res. Dev.* **2015**, 19, 1424–1427.
- [55] A. A. Folguez-Amador, K. Philipps, S. Guilbaud, J. Poelakker, T. Wirth, *Angew. Chemie Int. Ed.* **2017**, 56, 15446–15450.
- [56] K. Watts, W. Gattrell, T. Wirth, *Beilstein J. Org. Chem.* **2011**, 7, 1108–1114.
- [57] C. Gütz, M. Bänziger, C. Bucher, T. R. Galvão, S. R. Waldvogel, *Org. Process Res. Dev.* **2015**, 19, 1428–1433.
- [58] B. Gleede, M. Selt, C. Gütz, A. Stenglein, S. R. Waldvogel, *Org. Process Res. Dev.* **2020**, 24, 1916–1926.
- [59] “IKA. Electrochemistry Screening System,” can be found under <https://www.ikaprocess.com/en/Products/Electro-synthesis-cph-45/ElectraSyn-flow-csb-ES/> (accessed June 28, 2021).
- [60] L.-D. Syntrivanis, F. Javier del Campo, J. Robertson, *J. Flow Chem.* **2018**, 8, 123–128.
- [61] M. Elsherbini, B. Winterson, H. Alharbi, A. A. Folguez-Amador, C. Génot, T. Wirth, *Angew. Chemie Int. Ed.* **2019**, 58, 9811–9815.
- [62] G. Laudadio, W. de Smet, L. Struik, Y. Cao, T. Noël, *J. Flow Chem.* **2018**, 8, 157–165.
- [63] G. Laudadio, N. J. W. Straathof, M. D. Lanting, B. Knoops, V. Hessel, T. Noël, *Green Chem.* **2017**, 19, 4061–4066.
- [64] Y. Cao, J. Knijff, A. Delparish, M. F. N. D’Angelo, T. Noël, *ChemSusChem* **2021**, 14, 590–594.
- [65] G. Laudadio, A. de A. Bartolomeu, L. M. H. M. Verwijlen, Y. Cao, K. T. de Oliveira, T. Noël, *J. Am. Chem. Soc.* **2019**, 141, 11832–11836.
- [66] G. Laudadio, E. Barmpoutsis, C. Schotten, L. Struik, S. Govaerts, D. L. Browne, T. Noël, *J. Am. Chem. Soc.* **2019**, 141, 5664–5668.

- [67] M. Ošeka, G. Laudadio, N. P. van Leest, M. Dyga, A. de A. Bartolomeu, L. J. Gooßen, B. de Bruin, K. T. de Oliveira, T. Noël, *Chem* **2021**, *7*, 255–266.
- [68] W. Jud, C. O. Kappe, D. Cantillo, *Chem. Methods* **2021**, *1*, 36–41.
- [69] M. Köckinger, P. Hanselmann, D. M. Roberge, P. Geotti-Bianchini, C. O. Kappe, D. Cantillo, *Green Chem.* **2021**, *23*, 2382–2390.
- [70] M. R. Chapman, Y. M. Shafi, N. Kapur, B. N. Nguyen, C. E. Willans, *Chem. Commun.* **2015**, *51*, 1282–1284.
- [71] “Asia Flux electrochemical reactor,” can be found under <https://www.syrris.com/product/asia-electrochemistry-flow-chemistry-system/> (accessed June 28, 2021).
- [72] G. P. Roth, R. Stalder, T. R. Long, D. R. Sauer, S. W. Djuric, *J. Flow Chem.* **2013**, *3*, 34–40.
- [73] R. Stalder, G. P. Roth, *ACS Med. Chem. Lett.* **2013**, *4*, 1119–1123.
- [74] R. Green, R. Brown, D. Pletcher, *J. Flow Chem.* **2015**, *5*, 31–36.
- [75] J. Kuleshova, J. T. Hill-Cousins, P. R. Birkin, R. C. D. Brown, D. Pletcher, T. J. Underwood, *Electrochim. Acta* **2012**, *69*, 197–202.
- [76] A. A. Folgueiras-Amador, A. E. Teuten, D. Pletcher, R. C. D. Brown, *React. Chem. Eng.* **2020**, *5*, 712–718.
- [77] R. A. Green, R. C. D. Brown, D. Pletcher, B. Harji, *Electrochem. Commun.* **2016**, *73*, 63–66.
- [78] H. Hoffelner, H. W. Lorch, H. Wendt, *J. Electroanal. Chem. Interfacial Electrochem.* **1975**, *66*, 183–194.
- [79] A. A. Folgueiras-Amador, X.-Y. Qian, H.-C. Xu, T. Wirth, *Chem. - A Eur. J.* **2018**, *24*, 487–491.
- [80] C. Huang, X. Qian, H. Xu, *Angew. Chemie Int. Ed.* **2019**, *58*, 6650–6653.
- [81] “Ion electrochemical reactor,” can be found under <https://www.vapourtec.com/products/flow-reactors/ion-electrochemical-reactor-features/> (accessed June 28, 2021).
- [82] N. Amri, R. A. Skilton, D. Guthrie, T. Wirth, *Synlett* **2019**, *30*, 1183–1186.
- [83] C. A. Shukla, A. A. Kulkarni, *Beilstein J. Org. Chem.* **2017**, *13*, 960–987.
- [84] D. C. Fabry, E. Sugiono, M. Rueping, *React. Chem. Eng.* **2016**, *1*, 129–133.
- [85] Jamison, Koch, Eds., in *Flow Chem. Org. Synth.*, Georg Thieme Verlag, Stuttgart, **2018**.
- [86] C. Mateos, M. J. Nieves-Remacha, J. A. Rincón, *React. Chem. Eng.* **2019**, *4*, 1536–1544.
- [87] “AFRICA flow systems,” can be found under <https://www.syrris.com/> (accessed July 2, 2021).

-
- [88] “Uniqsis Flow-Synch reactor systems,” DOI <https://www.uniqsis.com/> (accessed July 2, 2021).
- [89] “Advion Nanotec reactor systems,” can be found under <https://www.advion.com/> (accessed July 2, 2021).
- [90] “Vapourtec R2+/R4,” can be found under <https://www.vapourtec.com/> (accessed July 2, 2021).
- [91] D. L. Browne, J. L. Howard, C. Schotten, in *Compr. Med. Chem. III*, Elsevier, **2017**, pp. 135–185.
- [92] J. C. Pastre, D. L. Browne, S. V. Ley, *Chem. Soc. Rev.* **2013**, 42, 8849.
- [93] A. Gioiello, A. Piccinno, A. M. Lozza, B. Cerra, *J. Med. Chem.* **2020**, 63, 6624–6647.
- [94] “RS-400 – Automated System,” can be found under <https://www.vapourtec.com/products/r-series-flow-chemistry-system-overview/> (accessed July 2, 2021).

CHAPTER 2

Electrochemical Alkoxylation of *N*-Formylpyrrolidine in a Flow Cell

CHAPTER 2: Electrochemical Alkoxylation of <i>N</i> -Formylpyrrolidine in Flow Cell	68
2.1. Introduction	70
2.2. Different synthetic methods of <i>N</i> -acyl- <i>N,O</i> -acetals	70
2.3. Electrochemical synthesis of <i>N</i> -acyl- <i>N,O</i> -acetals	72
2.4. Flow electrochemical alkoxylation of <i>N</i> -acylpyrrolidine	75
2.5. Results and Discussion	77
2.6. Conclusion	82
2.7. References	83

2.1. Introduction

The *N*-acyl-*N,O*-acetal moieties have received much attention as a key structural motif in organic chemistry due to their medicinal bioactivity and uses as synthetic building blocks in complex compounds.^[1] The cytotoxic compounds Pederin (**2.1**) and Pysmberin (**2.2**) are two examples of bioactive natural chemicals having an *N,O*-acetal moiety (Figure 2.1).^[2,3] Furthermore, Floreancig and coworkers have shown that the *N,O*-acetal moiety of (**2.1**) and (**2.2**) is required for their bioactivity in structural activity investigations.^[4]

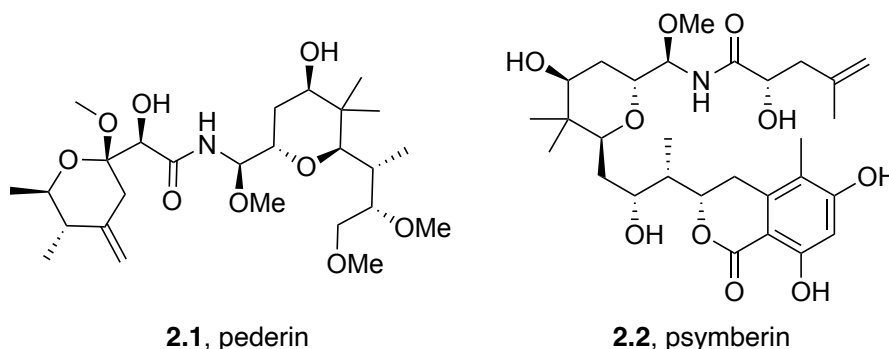
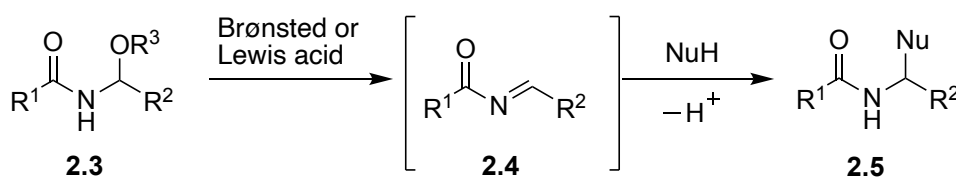


Figure 2.1. Bioactive natural products containing *N*-acyl-*N,O*-acetals.

In addition to being important building blocks in organic chemistry, *N*-acyl-*N,O*-acetals are also particularly useful reactive intermediates to unstable *N*-acylimines (**2.4**) as water, air, and light stable precursors. The carbonyl group on the nitrogen has electron-attracting properties making the iminium carbon of *N*-acyliminium ions more electron-deficient. It has more cationic character which is a more reactive electrophile than simple *N*-alkyliminium compounds.^[5–7] Treatment of *N*-acyl-*N,O*-acetals **2.3** with Brønsted or Lewis acids produces the reactive intermediate *N*-acylimines **2.4**, that undergo nucleophilic substitution forming products of type **2.5** (Scheme 2.1).^[7–9]



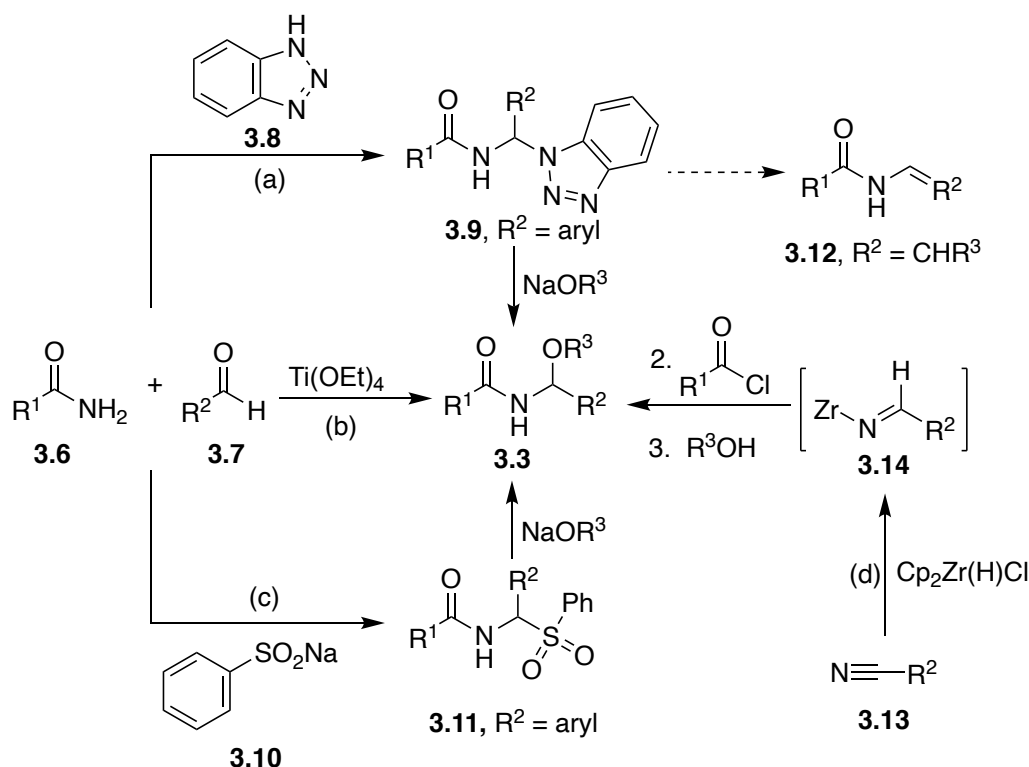
Scheme 2.1. Reactive *N*-acylimines generation from *N*-acyl-*N,O*-acetals.

2.2. Different synthetic methods of *N*-acyl-*N,O*-acetals

Several synthetic approaches to synthesise *N,O*-acetals have been established. Katritzky's benzotriazole approach and the production *via* amido-sulfones are two of the most widely used synthetic methods.^[10,11] Amides **2.6** and aldehydes **2.7** condense to produce imines, that are attacked by nucleophilic benzotriazole (**2.8**) to form α -substituted amides **2.9** (Scheme 2.2a) or benzenesulfinic acid salt **2.10** to form α -amido sulfones **2.11** (Scheme 2.2c). Both **2.9** and **2.11**

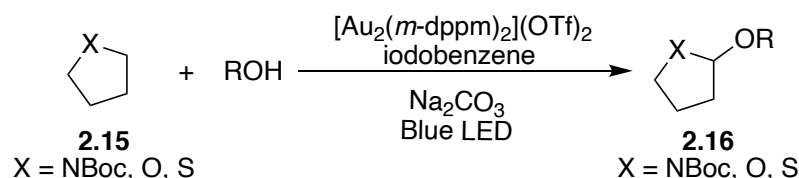
are then treated with sodium alkoxides to provide the corresponding *N,O*-acetals **2.3**.^[11,12] Nevertheless, these reactions are restricted to aromatic aldehydes, leading to the production of enamides **2.12** when aliphatic aldehydes were used.^[13]

Another one-pot strategy involving hydrozirconization of nitriles **2.13**, followed by acylation and alcohol trapping of the *N*-acylimine intermediates **2.14** have been described by Wen and co-workers in 2007 (Scheme 2.2d).^[8] Also, Wen and co-workers have disclosed a simple titanium-ethoxide mediated approach in which *N*-acyl-*N,O*-acetals **2.3** were prepared in a single step, starting with amides **2.6** and aldehydes **2.7**. A broad range of substrates including both aliphatic and aromatic aldehydes were successfully incorporated (Scheme 2.2b).^[5]



Scheme 2.2. Different synthetic approaches of *N*-acyl-*N,O*-acetals **2.3**.

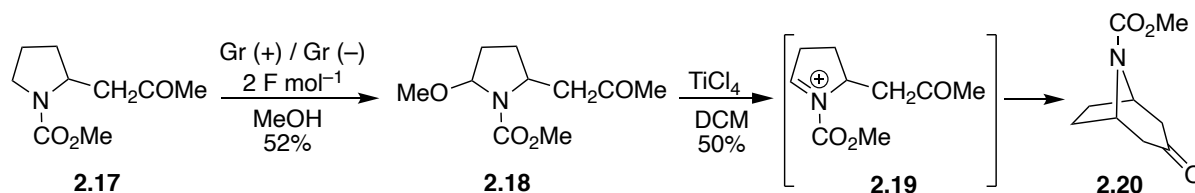
Photochemistry has also contributed to carry out *N*-acyl-*N,O*-acetals reactions.^[14,15] Recently, in 2020, Hashmi and co-workers developed a photochemical pathway for α -alkoxylation of pyrrolidines via $C(sp^3)-H$ dehydrogenative cross-couplings of pyrrolidines **2.15**.^[15] The reaction performed under visible light irradiation by using iodobenzene and an in situ-formed gold complex. A variety of alcohols were investigated to produce the corresponding α -alkoxylated pyrrolidines **2.16** in good to excellent yield. The synthesis of cyclic ether acetals and thioacetals were also achieved under the optimal conditions.



Scheme 2.3. α-alkoxylation of pyrrolidines under visible-light irradiation.

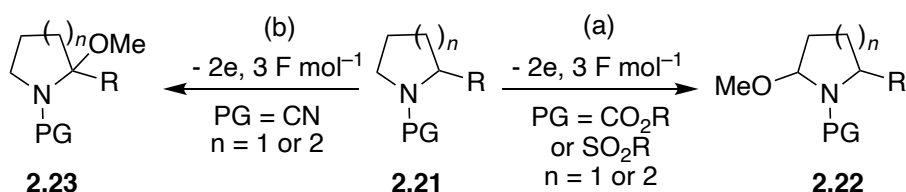
2.3. Electrochemical synthesis of *N*-acyl-*N,O*-acetals

The application of anodic oxidation in selective C–H bond functionalization next to *N*-protected cyclic amine derivatives is well known.^[16] The first direct electrochemical example for the synthesis of *N,O*-acetal **2.18** *via* anodic α-methoxylation of amide **2.17** was reported by Shono and co-workers (Scheme 2.3).^[17,18] After the electrolysis step, the reactive intermediate, *N*-acyliminium ion **2.19**, was generated using titanium(IV) chloride as a Lewis acid.



Scheme 2.4. Electrochemical methoxylation of amide **2.17**.^[17]

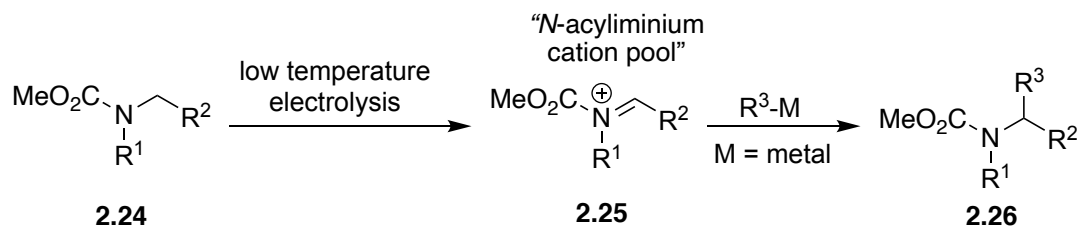
Onomura and co-workers have also investigated the effect of the protecting group on nitrogen on the product of a variety of *N*-acylated cyclic amines.^[17] It was proposed that the generated *N*-acyliminium ion would be stabilised by different protecting groups, changing the regioselectivity of the product (Scheme 2.5). It was discovered that the kinetically controlled product **2.22** was only produced for ring size $n = 1$ or 2 with carbonyl or sulfonyl-based protecting groups (Scheme 2.5a). Conversely, the thermodynamically controlled product **2.23** was produced when the cyano group was used (Scheme 2.5b). Computational studies have shown that the cyano group significantly stabilises the more substituted iminium ion, promoting the regioselectivity switch for methoxylation.



Scheme 2.5. The effect of the amino protecting group on anodic methoxylation.

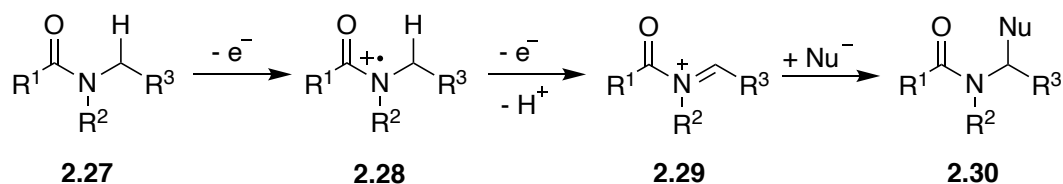
Yoshida and co-workers reported the electrochemical generation of *N*-acyl iminium cation **2.25** using the “cation pool” method (Scheme 2.6).^[19] The “cation pool” technique, in which the anodic oxidation is performed at low temperature, allows the production of iminium ions. Subsequently, these extremely reactive intermediates can be attacked by different nucleophiles

offering *N,O*-acetal products **2.26** in several transformations. Such methods have been extensively investigated.^[20–23]



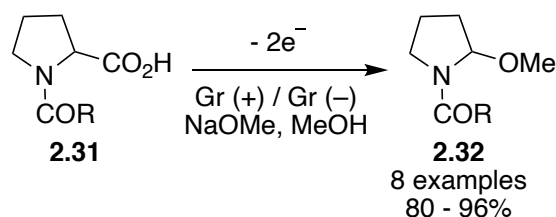
Scheme 2.6. The cation pool strategy in Shono oxidation.

Mechanistically, *N*-centred radical cations **2.28** are formed *via* one-electron anodic oxidation of amides. The reactive intermediates **2.28** undergoes a second one-electron oxidation and loss of proton to generate iminium ions **2.29**, which then reacts with nucleophiles such as MeOH to provide the corresponding *N,O*-acetal products **2.30** (Scheme 2.7).^[17,24]



Scheme 2.7. The classical Shono oxidation mechanism.

In addition to the Shono anodic oxidation for direct α -methoxylation of amides, the electrochemical methoxylation of amino acids to synthesize *N,O*-acetals has also been utilized, known as non-Kolbe oxidation. Miyoshi and co-workers described another electrochemical method for alkoxylation of *N*-acylprolines derivatives through non-Kolbe electrolysis (Scheme 2.8).^[25] The *N,O*-acetals **2.32** were obtained in good to excellent yields by electrolysis of the *N*-acyl prolines **2.31** in methanol with sodium methoxide as a base and a supporting electrolyte.

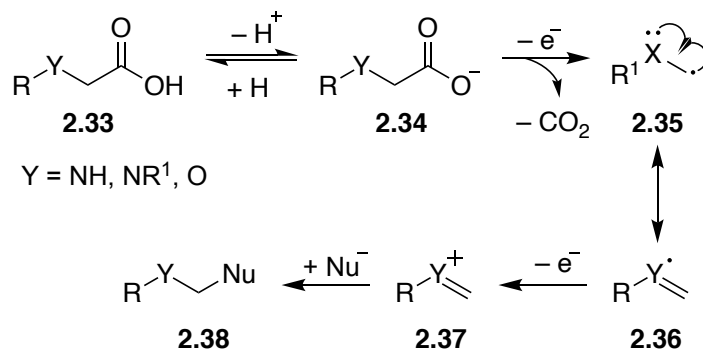


Scheme 2.8. Electrochemical methoxylation of amino acid derivatives to synthesize *N,O*-acetals.

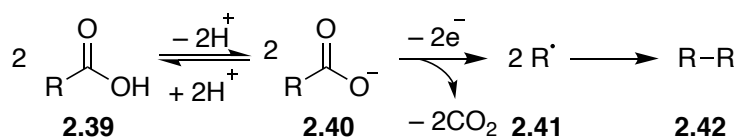
The non-Kolbe oxidation mechanism has been proposed^[26] in which initially the *N*-acyl amino acid **2.33** undergoes one electron oxidation under electrochemical conditions, followed by decarboxylation, providing the radical intermediate **2.35** (Scheme 2.9). Subsequently, the *N*-acyliminium ion **2.37** is formed after a second one-electron oxidation, which reacts with the nucleophile to produce final product **2.38**. In contrast, with anodic decarboxylation, the

conventional Kolbe reaction allows for the production of the dimerized product **2.42** via coupling of two generated radicals **2.41**.^[27,28]

Non-Kolbe Electrolysis:

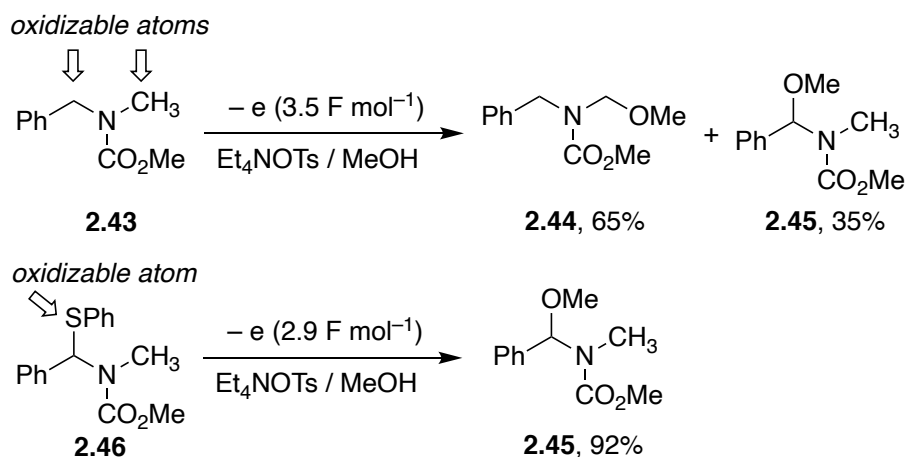


Kolbe Electrolysis:



Scheme 2.9. Non-Kolbe and Kolbe electrolysis mechanism.

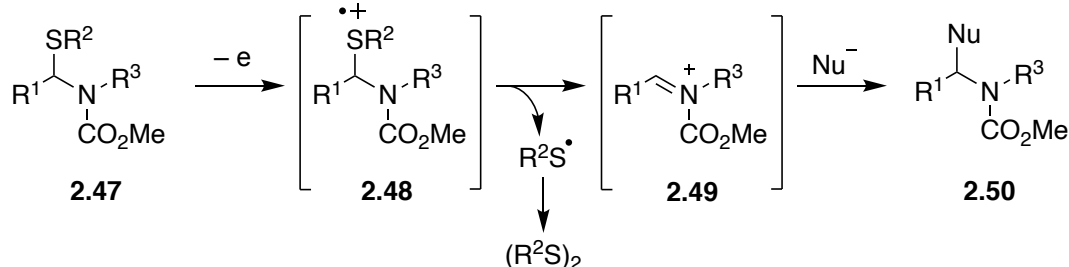
Moreover, Yoshida and coworkers have reported an indirect Shono-type oxidation using electroauxiliaries (Scheme 2.10).^[29] Sulfur-based electroauxiliaries in organic molecules are used to control the electron transfer and decrease the oxidation to produce the required products in exclusive regioselectivity. The α -organothio carbamate **2.46** is first anodically oxidised and cleaved to generate carbocations, followed by the introduction of a methoxy group as nucleophile.



Scheme 2.10. Regioselective anodic oxidation with the use of a thiophenyl electroauxiliary.

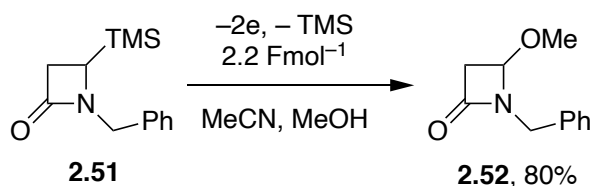
Such a method is beneficial for developing highly regioselective transformations through carbamate oxidation. The suggested mechanism of this transformation follows radical formation exactly where the organothio group is connected and the organothio group generates

the diorganodisulfide by-product through homocoupling (Scheme 2.11).^[29] Initially, the iminium cation **2.49** and the organothio radical is generated from the radical cation intermediate **2.48** through the breakage of the carbon-sulfur bond. Subsequently, a methoxy group attacks **2.49** to afford *N,O*- acetal product **2.50**.



Scheme 2.11. Organothio electroauxiliary reaction mechanism.

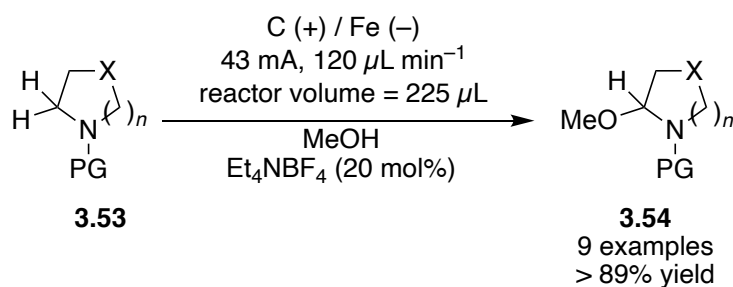
This electrochemical methoxylation is reported for acyclic amino compounds or 4–6-membered cyclic amino derivatives. For larger ring systems such as 7-membered rings electroauxiliary is necessary for successful transformation.^[30,31] Silicon derivatives are also used as electroauxiliaries. For example, β -lactams (4-membered rings) **2.51** undergoes anodic oxidation of the carbon directly attached to silicon and the silyl group is replaced by the methoxy group to yield the α -methoxylated product **2.52** (Scheme 2.12).^[32,33]



Scheme 2.12. Electrochemical methoxylation of 4-membered ring.

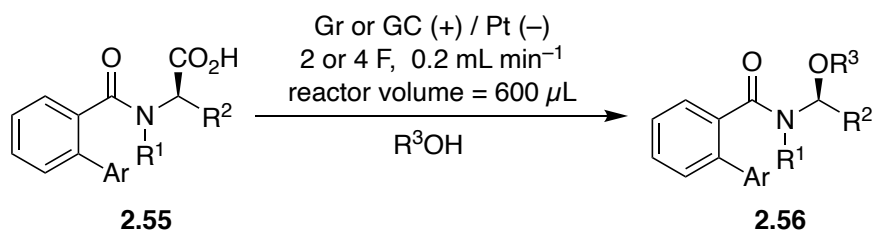
2.4. Flow electrochemical alkoxylation of *N*-acylpyrrolidine

In the last decade, the anodic oxidation of *N*-acyl prolines has been used as an exemplar substrate to study the reliability and the productivity of different flow electrochemical reactors in several labs. In 2014, Ley and co-workers developed the α -methoxylation of *N*-protected cyclic amines under flow electrochemical conditions using the Asia Flux electrochemical module from Syrris Ltd (Scheme 2.13).^[34] The optimal conditions were employed for the α -methoxylation of several types of cyclic amino acids, with different ring size and protecting groups. The efficient methoxylation of *N*-protected pyrrolidine, piperidine, azepane, and morpholine derivatives **2.53** was successfully demonstrated, offering the α -methoxyamine products **2.54** in up to 98% yield.



Scheme 2.13. α -Methoxylation of *N*-protected cyclic amines.

In 2019, Wirth and co-workers developed a useful method for studying the stereoselective electrochemical α -alkoxylation of amino acid derivatives with online analysis (Scheme 2.14).^[35] The iminium ion is formed by electrochemical decarboxylation of **2.55** which is then trapped by alcohols. The reaction is carried out using the Vapourtec Ion electrochemical reactor and the percentage enantiomeric excess is monitored by a 2D HPLC system through an automatic sampling valve. With the coupled system, the Design of Experiments (DoE) approach was used to accelerate the reaction screening and to identify the best reaction conditions. High yields (up to 100%) and enantioselectivities (up to 70% *ee*) for the *N*-acyl-*N,O*-acetal **2.56** was achieved in a very short time. The optimal conditions were successfully applied for various protecting groups and alcohols.

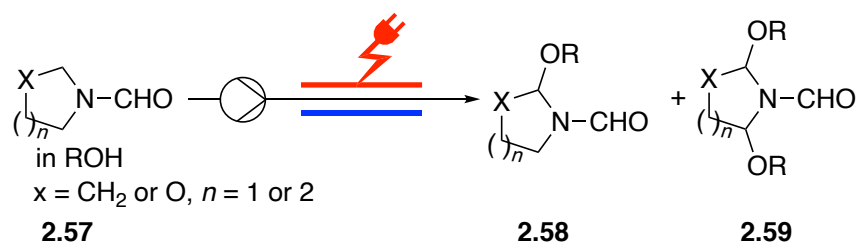


Scheme 2.14. Flow electrochemical α -alkoxylation of amino acids reported by Wirth *et al.*

Other studies of the α -methoxylation of *N*-formylpyrrolidine (**2.57**) have been done by Brown and co-workers.^[36–40] This reaction has been used to test the performance of several modules of flow electrochemical reactors such as the Star shaped microchannel,^[36] Asia Flux module,^[37] Ammonite 8 reactor,^[39] Ammonite 15 reactor^[38] and a homemade electrochemical cell^[40] (explained in Chapter 1).

2.5. Results and Discussion

In this chapter, we focus on the development and performance of the Ion electrochemical reactor^[41] that was developed by Vapourtec (explained in details in Chapter 1), using the Shono oxidation.^[42] The regioselective alkoxylation of the pyrrolidine **2.57** to the monoalkoxylated compound **2.58** or the dialkoxylated product **2.59** was performed under flow electrochemical conditions.



Scheme 2.15. Alkoxylation of *N*-formylpyrrolidine (**2.57**) using the Ion electrochemical microreactor.

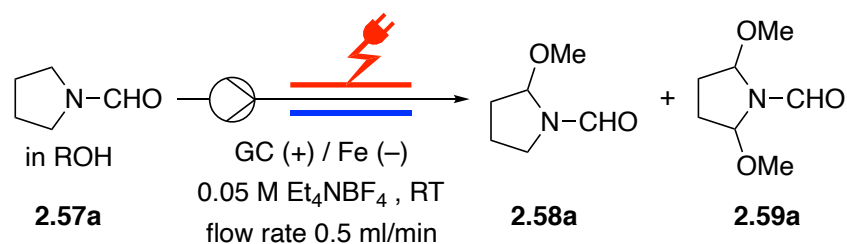
As previously mentioned, the alkoxylation of the pyrrolidine derivatives has been investigated under batch and flow electrolysis conditions. It was shown that the productivity and reaction time of such reactions varies, depending on the type of the reactor. However, the use of flow reactors has numerous advantages compared to batch reactors, especially in the case of reactive or unstable intermediates. The high surface area to volume ratio in and the short distance between the anode and the cathode enhance the mass transfer and allows for the reduction or even elimination of added electrolytes. With the aim of exploring the performance of the Ion electrochemical reactor for high selectivity and productivity, various flow electrochemical parameters and reaction optimisation were studied using pyrrolidine-1-carbaldehyde (**2.57a**) as a model substrate.

First, Glassy Carbon (GC) was employed as anode and stainless steel as cathode for the initial optimization of the electrochemical oxidation of *N*-formylpyrrolidine (**2.57a**) to the corresponding methoxylated product **2.58a**. A teflon spacer (0.5 mm), resulting in a channel volume of 0.6 mL was used, resulting in an exposed electrode surface of 12 cm². A solution **2.57a** (0.1 M) in methanol containing tetraethylammonium tetrafluoroborate (Et₄NBF₄) as supporting electrolyte (0.05 M) was injected at a flow rate of 0.5 ml/min. Using these conditions, 75% of the desired product **2.58a** was generated using 100 mA current (1.25 F) and a residence time of 1.2 minutes at room temperature (Table 2.1, entry 1). Keeping all the parameters constant and increasing the current from 100 mA to 140 mA (Table 2.1, entries 2-4), the reaction resulted in an increase in yield to 90% for the mono-methoxylated product **2.58a**, with generation of a side product **2.59a**, which is methoxylated at positions 2 and 5 in

approximately 2% as detected by GC. With a further increase in current, the yield of the monomethoxylated product **2.58a** dropped and the yield of the dimethoxylated product **2.59a** increased (Table 2.1, entries 6 and 9). When the substrate concentration was increased to 1 M, the reaction followed the same pattern whereby the yield of product **2.58a** was not improved and dimethoxylated product **2.59a** was observed (Table 2.1, entry 10). Carrying out the reaction at room temperature, 30 °C or 60 °C, the reaction outcomes were identical (Table 2.1, entries 7, 12, 13). The use of a graphite electrode was shown to reduce the formation of the dimethoxylated product **2.59a** (Table 2.1, entry 7). A divided electrolysis approach is feasible using the same reactor^[41] by separating the anodic and the cathodic reaction using a Nafion membrane. A methanolic solution of 0.05 M tetraethylammonium tetrafluoroborate (Et₄NBF₄) was used as the catholyte and cathodic hydrogen generation was observed, while the anodic half reaction produced 80% yield of product **2.58a** and 6% yield of the undesired product **2.59a** (Table 2.1, entry 8). Unfortunately, in divided electrolysis, higher selectivity could not also be achieved.

All of the findings and screening in Table 2.1 did not provide a product **2.56a** with complete conversion without the generation of the undesired product **2.59a**. However, increasing the current to 640 mA (8 F) lead in 83% conversion to the dimethoxylated product **2.59a** with just 8% yield of the monomethoxylation product **2.58a** in the reaction mixture (Table 2.1, entry 14). Applying a higher flow rate with higher current to the reactor led to heat generation. The temperature was stabilized at 25 °C by using a cooling system for the reactor, resulting in a conversion of **2.58a** in 94% (87% isolated yield) and a production rate of 1.35g/h (Table 2.1, entry 10).

The monomethoxylation product **2.58a** was achieved selectively but with incomplete conversion of the starting material **2.57a** (Table 2.1, entry 7). This was further improved by connecting a sequential second Ion electrochemical reactor with identical parameters. So far, only a few reactions have been investigated using two electrochemical serial microreactors in line.^[43] Furthermore, recirculating the reaction mixture in the electrochemical microreactor until complete conversion could be accomplished, or stacking multiple electrochemical microreactors in one device are two more methods for optimizing electrochemical reactors.^[44]

Table 2.1. Optimized conditions of electrochemical methoxylation of *N*-formylpyrrolidine **2.57a**.

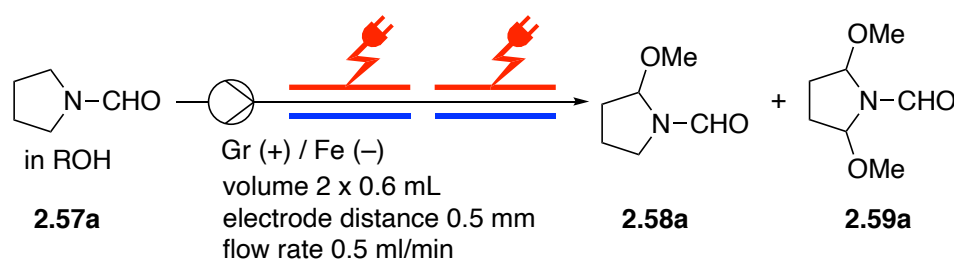
Entry	Anode	Conditions	Conv. of 2.58a [%] ^[a]	Conv. of 2.59a [%] ^[a]
1	glassy C	100 mA (1.25 F)	75	0
2	glassy C	120 mA (1.5 F)	84	0
3	glassy C	130 mA (1.6 F)	86	0
4	glassy C	140 mA (1.75 F)	91	2
5	glassy C	150 mA (1.88 F)	89	3
6	glassy C	160 mA (2 F)	90	3
7	Gr	160 mA (2 F)	85	0
8	Gr	160 mA (2 F) ^[b]	80	6
9	glassy C	320 mA (2 F) ^[c]	76	12
10	glassy C	1250 mA (2 F) ^[d]	94 (87 ^[h])	3
11	Gr	1600 mA (2 F) ^[e]	73	18
12	Gr	160 mA (2 F) ^[f]	88	0
13	Gr	160 mA (2 F) ^[g]	86	0
14	glassy C	640 mA (8 F)	8 ^[h]	83 ^[h]

General Procedure: Reactions were performed using a stainless steel as cathode, a FEP spacer (0.5 mm thickness; reactor volume: 600 μ L; working area: 12 cm²); [a] GC yield of the crude product solution. [b] Divided cell. [c] Flow rate: 1.0 mL/min. [d] Flow rate: 2 mL/min, cooling applied. [e] Concentration of **2.57a**: 1 M in MeOH. [f] 30 °C. [g] 60 °C. [h] Isolated yield.

In the sequential configuration of two electrochemical reactors, four different current values were examined (Table 2.2). The reaction was not completed after the first reactor at a flow rate of 0.5 mL/min with the use of graphite (Gr) electrode as anode (Table 2.2, entries 1-4). After optimization, 150 mA could be used to obtain almost complete conversion after the second reactor (Table 2.2, entry 3). Full conversion of **2.57a** to the monomethoxylation product **2.58a** and a small amount of the dimethoxylated product **2.59a** was detected when 160 mA (4 F) current was applied to each reactor (Table 2.2, entry 4). By changing the anode to glassy carbon (GC) and applying 120 mA current, 83% conversion of product **2.58a** was observed after the first reactor and products **2.58a** and **2.59a** were observed after the second reactor in 53% and

47% yields, respectively (Table 2.2, entry 5). However, full conversion is required since chromatographic separation of the starting material **2.57a** from **2.58a** was difficult. If only one reactor is employed for these experiments, half the flow rate (0.25 mL/min) will offer the same amount of electric charge to the substrate for the course of the reaction (residence) time. Only 80% conversion to desired product **2.58a** was achieved by applying 2 F (80 mA) and both the products **2.58a** and **2.59a** were produced with 78% and 16% conversion, respectively. When 4F (160 mA) was applied, the starting material **2.57a** was still present.

Table 2.2. Optimized conditions for the methoxylation of *N*-formylpyrrolidine (**2.57a**) using two sequential flow electrochemical reactors.



Entry	Conditions	Conv. after first reactor	Conv. after second reactor
		2.58a + 2.59a [%] ^[a]	2.58a + 2.59a [%] ^[a]
1	100 mA (2.5 F)	66 + 0	90 + 0
2	130 mA (3.2 F)	77 + 0	94 + 0
3	150 mA (3.76 F)	80 + 0	95 + 2
4	160 mA (4 F)	84 + 0	95 + 5
5	120 mA (3 F) ^[b]	83 + 0	53 + 47

[a] GC yield of the crude product solution. [b] Glassy carbon anode

Under the optimal conditions, *N*-formylpyrrolidine (**2.57**) with various alcohols provided the corresponding mono- or dialkoxylation products on a larger scale (5.5 mmol). The monoalkoxylation compounds **2.58a**, **2.58b**, **2.58c**, **2.58d** and **2.58e** have been prepared in good yields (Figure 2.2). While the reactor residence time is only 2.4 minutes, the reaction time for feeding 5.5 mmol starting material is 110 min. In addition, *N*-formylmorpholine also reacted to form the corresponding methoxylated product (**2.58f**) in 67% yield. Due to the limited rotation around the amide bond, two atropisomers combination of the compound **2.58f** were detected which have already been characterized.^[45,46]

The reaction was also performed in a batch electrochemical cell with the same concentration of starting materials using identical electrode materials of graphite (1 cm²) and 304 stainless

steel under constant current of 10 mA, until 2 F/mol of charge was passed. Only 60% conversion to methoxylated product **2.57a** was achieved after 160 minutes.

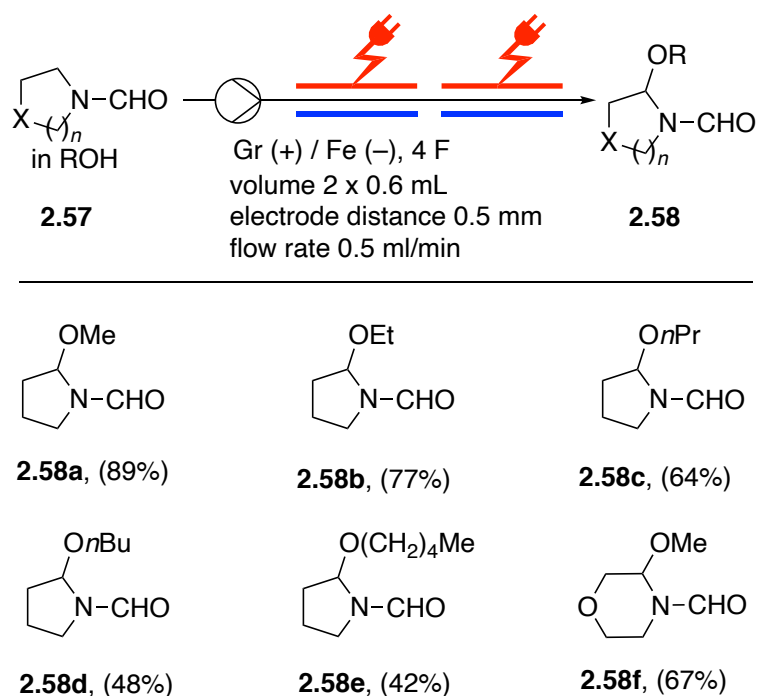


Figure 2.2. Monoalkoxylation of *N*-formylpyrrolidine.

Double alkoxylation was achieved using the reaction conditions for one electrochemical reactor provided in Table 2.1, entry 12, and have been carried out on a 5.5 mmol scale, yielding products **2.59a**, **2.59b**, and **2.59c** as illustrated in Figure 2.3. However, use of *n*-butanol and *n*-pentanol under the same conditions for the double alkoxylation process using one electrochemical reactor was not successful. With 640 mA (8 F), the conductivity was very low which led to high cell voltage. As the carbon chain increases the conductivity decreases with higher alcohols. To improve the yield, two electrochemical reactors were connected and a current of 320 mA was applied to each reactor. This has diminished the conductivity problems which in turn increased the yield of the compounds **2.59d** and **2.59e** as shown in Figure 2.3. While compound **2.59a** has an approximately 1:2 ratio of the *cis* and *trans*-stereoisomer, compounds **2.59b**, **2.59c**, **2.59d**, and **2.59e** only have one stereoisomer (not assigned) as determined by ¹H NMR spectroscopy.

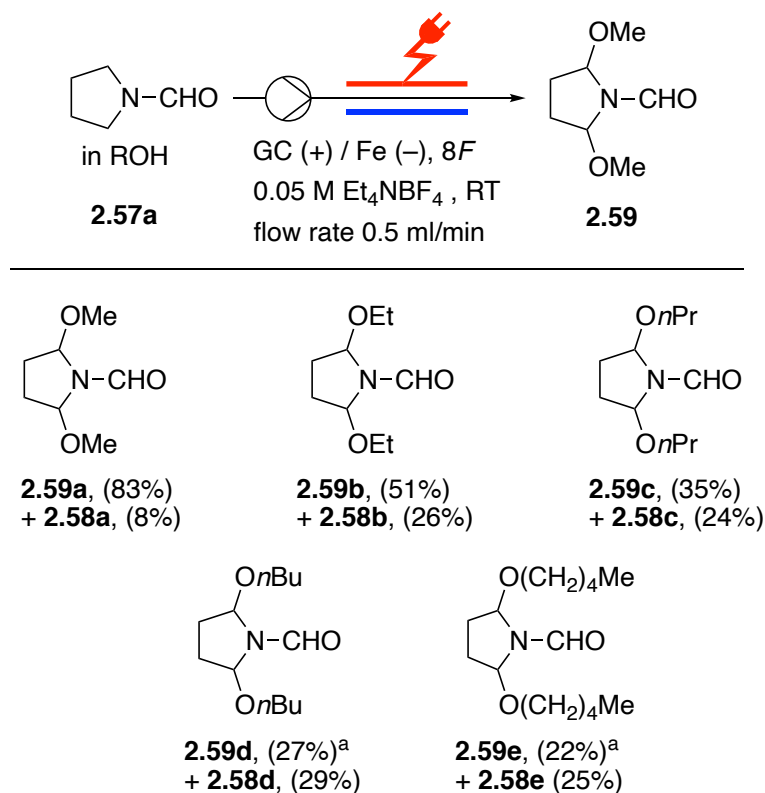


Figure 2.3. Dialkoxylation of *N*-formylpyrrolidine. (a) two reactors, 320 mA.

2.6. Conclusion

To conclude, the selective mono- or dialkoxylation of *N*-formylpyrrolidine as a model substrate was optimized to evaluate the performance of the Ion electrochemical microreactor designed by Vapourtec. The Ion microreactor showed high performance providing the methoxylated product **2.58a** arising from pyrrolidine-1-carbaldehyde (**2.57a**) in 94 % yield, in a single flow at a reasonably high flow rate (2 mL/min), using the system's cooling capabilities. Different alcohol nucleophiles including methanol, ethanol, *n*-propanol, *n*-butanol, and *n*-pentanol were successfully employed in this reaction. Furthermore, dialkoxylation products were selectively achieved by using serial coupled reactors in good to high yield.

This work has already been published.^[42]

2.7. References

- [1] J. Halli, K. Hofman, T. Beisel, G. Manolikakes, *Eur. J. Org. Chem.* **2015**, 4624–4627.
- [2] G. R. Pettit, J.-P. Xu, J.-C. Chapuis, R. K. Pettit, L. P. Tackett, D. L. Doubek, J. N. A. Hooper, J. M. Schmidt, *J. Med. Chem.* **2004**, 47, 1149–1152.
- [3] R. A. Mosey, P. E. Floreancig, *Nat. Prod. Rep.* **2012**, 29, 980–995.
- [4] S. Wan, F. Wu, J. C. Rech, M. E. Green, R. Balachandran, W. S. Horne, B. W. Day, P. E. Floreancig, *J. Am. Chem. Soc.* **2011**, 133, 16668–16679.
- [5] M. Li, B. Luo, Q. Liu, Y. Hu, A. Ganesan, P. Huang, S. Wen, *Org. Lett.* **2014**, 16, 10–13.
- [6] P. Gizecki, R. Dhal, C. Poulard, P. Gosselin, G. Dujardin, *J. Org. Chem.* **2003**, 68, 4338–4344.
- [7] N. Yamazaki, T. Ito, C. Kibayashi, *Org. Lett.* **2000**, 2, 465–467.
- [8] S. Wan, M. E. Green, J.-H. Park, P. E. Floreancig, *Org. Lett.* **2007**, 9, 5385–5388.
- [9] R. W. Bates, Y. Lu, M. P. Cai, *Tetrahedron* **2009**, 65, 7852–7858.
- [10] A. R. Katritzky, J. Pernak, W. Q. Fan, F. Saczewski, *J. Org. Chem.* **1991**, 56, 4439–4443.
- [11] A. R. Katritzky, W. Q. Fan, M. Black, J. Pernak, *J. Org. Chem.* **1992**, 57, 547–549.
- [12] N. George, M. Bekkaye, G. Masson, J. Zhu, *Eur. J. Org. Chem.* **2011**, 3695–3699.
- [13] A. Bayer, M. E. Maier, *Tetrahedron* **2004**, 60, 6665–6677.
- [14] L. Li, G. Zhang, A. Savateev, B. Kurpil, M. Antonietti, Y. Zhao, *Asian J. Org. Chem.* **2018**, 7, 2464–2467.
- [15] X. Si, L. Zhang, Z. Wu, M. Rudolph, A. M. Asiri, A. S. K. Hashmi, *Org. Lett.* **2020**, 22, 5844–5849.
- [16] O. Hammerich, B. Speiser, Eds., *Organic Electrochemistry*, CRC Press, **2015**.
- [17] T. Shono, Y. Matsumura, K. Tsubata, *J. Am. Chem. Soc.* **1981**, 103, 1172–1176.
- [18] T. Shono, H. Hamaguchi, Y. Matsumura, *J. Am. Chem. Soc.* **1975**, 97, 4264–4268.
- [19] S. Suga, M. Okajima, J. Yoshida, *Tetrahedron Lett.* **2001**, 42, 2173–2176.
- [20] A. Nagaki, K. Kawamura, S. Suga, T. Ando, M. Sawamoto, J. Yoshida, *J. Am. Chem. Soc.* **2004**, 126, 14702–14703.
- [21] T. Maruyama, Y. Mizuno, I. Shimizu, S. Suga, J. Yoshida, *J. Am. Chem. Soc.* **2007**, 129, 1902–1903.
- [22] T. Maruyama, S. Suga, J. Yoshida, *J. Am. Chem. Soc.* **2005**, 127, 7324–7325.
- [23] S. Suga, Y. Kageyama, G. Babu, K. Itami, J. Yoshida, *Org. Lett.* **2004**, 6, 2709–2711.

- [24] T. Shono, *Tetrahedron* **1984**, *40*, 811–850.
- [25] T. Iwasaki, H. Horikawa, K. Matsumoto, M. Miyoshi, *J. Org. Chem.* **1979**, *44*, 1552–1554.
- [26] H.-J. Schäfer, in *Electrochem. IV*, Ed.: E. Steckhan, Springer Berlin Heidelberg, Berlin, Heidelberg, **1990**, pp. 91–151.
- [27] S. D. Ross, M. Finkelstein, *J. Org. Chem.* **1969**, *34*, 2923–2927.
- [28] H. Kolbe, *Ann. chem. Pharm.* **1849**, *69*, 257–294.
- [29] M. Sugawara, K. Mori, J.-I. Yoshida, *Electrochim. Acta* **1997**, *42*, 1995–2003.
- [30] M. David, H. Dhimane, *Synlett* **2004**, 1029–1033.
- [31] T. Golub, J. Y. Becker, *J. Electrochem. Soc.* **2013**, *160*, G3123–G3127.
- [32] K. Suda, K. Hotoda, F. Iemuro, T. Takanami, *J. Chem. Soc., Perkin Trans. 1* **1993**, 1553–1555.
- [33] K. Suda, K. Hotoda, J. Watanabe, K. Shiozawa, T. Takanami, *J. Chem. Soc., Perkin Trans. 1* **1992**, 1283.
- [34] M. A. Kabeshov, B. Musio, P. R. D. Murray, D. L. Browne, S. V. Ley, *Org. Lett.* **2014**, *16*, 4618–4621.
- [35] M. Santi, J. Seitz, R. Cicala, T. Hardwick, N. Ahmed, T. Wirth, *Chem. Eur. J.* **2019**, *25*, 16230–16235.
- [36] J. Kuleshova, J. T. Hill-Cousins, P. R. Birkin, R. C. D. Brown, D. Pletcher, T. J. Underwood, *Electrochim. Acta* **2011**, *56*, 4322–4326.
- [37] J. Kuleshova, J. T. Hill-Cousins, P. R. Birkin, R. C. D. Brown, D. Pletcher, T. J. Underwood, *Electrochim. Acta* **2012**, *69*, 197–202.
- [38] R. A. Green, R. C. D. Brown, D. Pletcher, B. Harji, *Org. Process Res. Dev.* **2015**, *19*, 1424–1427.
- [39] R. A. Green, R. C. D. Brown, D. Pletcher, B. Harji, *Electrochem. Commun.* **2016**, *73*, 63–66.
- [40] A. A. Folgueiras-Amador, A. E. Teuten, D. Pletcher, R. C. D. Brown, *React. Chem. Eng.* **2020**, *5*, 712–718.
- [41] “Ion electrochemical reactor,” can be found under <https://www.vapourtec.com/products/flow-reactors/ion-electrochemical-reactor-features/> (accessed Jul 28, 2021).
- [42] N. Amri, R. A. Skilton, D. Guthrie, T. Wirth, *Synlett* **2019**, *30*, 1183–1186.
- [43] F. Amemiya, T. Kashiwagi, T. Fuchigami, M. Atobe, *Chem. Lett.* **2011**, *40*, 606–608.
- [44] M. R. Chapman, Y. M. Shafi, N. Kapur, B. N. Nguyen, C. E. Willans, *Chem.*

Commun. **2015**, *51*, 1282–1284.

- [45] F. Liebner, P. Schmid, C. Adelwöhrer, T. Rosenau, *Tetrahedron* **2007**, *63*, 11817–11821.
- [46] W. E. Stewart, T. H. Siddall, *Chem. Rev.* **1970**, *70*, 517–551.

CHAPTER 3

Electrochemical Selenofunctionalization of Alkenes

CHAPTER 3: Electrochemical Selenofunctionalization of Alkenes.....	87
3.1. Introduction.....	89
3.2. Different methods for selenofunctionalization of alkenes.....	91
3.2.1. Oxyselenenylation of alkene.....	91
3.2.2. Aminosenenylation of alkene.....	94
3.2.3. Selenocyclization of alkenes.....	96
3.3. Electrochemical selenofunctionalization of alkenes.....	98
3.4. Flow electrochemical selenofunctionalization of alkenes.....	100
3.5. Results and discussion.....	101
3.5.1. Reaction optimisation.....	102
3.5.1.1. Current screening.....	102
3.5.1.2. Solvents screening.....	102
3.5.1.3. Supporting electrolytes screening.....	103
3.5.1.4. Flow rate/residence time effect.....	104
3.5.1.5. Electrode screening.....	104
3.5.2. Substrate scope.....	105
3.5.3. Reaction mechanism.....	108
3.6. Conclusion and outlook.....	110
3.7. References.....	112

3.1. Introduction

Organoselenium compounds have a long history that can be dated back to first organoselenium compound synthesized by F. Wöhler and C. Siemens in 1847.^[1,2] Until the discovery of selenoxide eliminations in the 1970s,^[3–5] organoselenium chemistry progressed slowly. As early in the 1930s, it was discovered that organoselenium reagents are hazardous, but the toxicity is lower than inorganic selenium compounds.^[6,7]

The properties of selenium compounds are similar to sulfur and tellurium counterparts. However, the chemistry of sulfur compounds have been vastly investigated, while reactions of selenium and tellurium compounds are less studied and are receiving more attention recently. The C–Se bond is weaker than the C–S bond. So, the elimination of selenium-containing functionalities occurs easily under mild conditions compared to those needed for the sulfur compounds.^[8,9]

Organoselenium compounds has been extensively studied in recent decades, with their unique reactivity and structural properties they became useful tools in organic synthesis. They have been used as ligands and catalysts in asymmetric synthesis and selective functionalizations of molecules, allowing valuable synthetic targets to be achieved.^[10–12] They are also interesting molecules due to their relevance in medical and biological activities such as, anti-oxidant,^[13,14] anti-inflammatory,^[15,16] anxiolytic effects,^[17] anticancer,^[16,18] and antinociceptive activities^[19] (Figure 3.1).

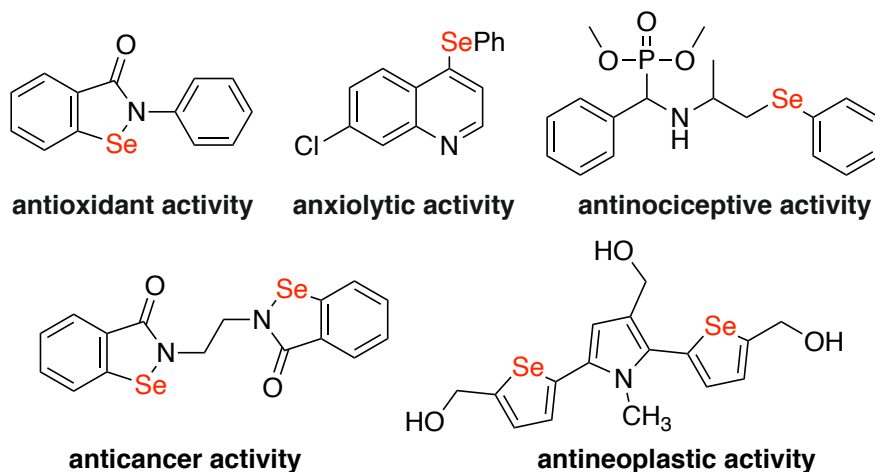


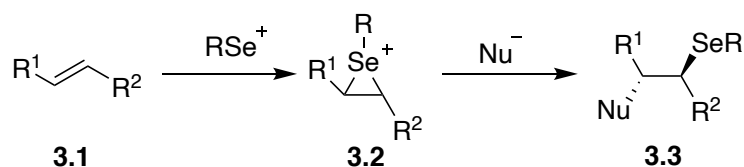
Figure 3.1. Bioactive molecules containing selenium.

Organic selenium reagents are typically utilised to catalyse organic processes. In organic synthesis, electrophilic organoselenium reagents are commonly employed to introduce new functional groups into organic molecules. The most common application of this functionality is the electrophilic addition of selenyl functional group to alkenes **3.1** in the presence of an

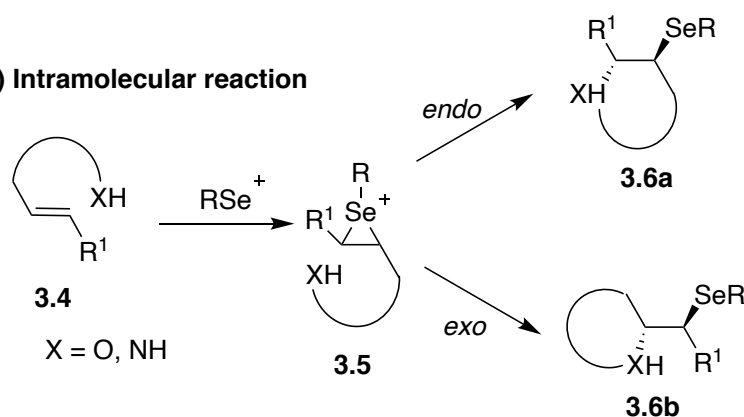
internal or external nucleophile, emphasising their dual roles as protective groups and reactive electrophiles intermediates (Scheme 3.1).^[20]

Mechanistically, the seleniranium ion **3.2** is generated through reaction of the electrophilic selenium with the carbon-carbon unsaturated bond. Then regioselective attack from the nucleophile provides the final product **3.3**. Such reaction can also occur in an intramolecular fashion, providing a powerful route for heterocycles synthesis (Scheme 3.1b). The contain selenium molecules can be utilised for additional various applications resulting to non-selenium-containing products.

(a) Intermolecular reaction

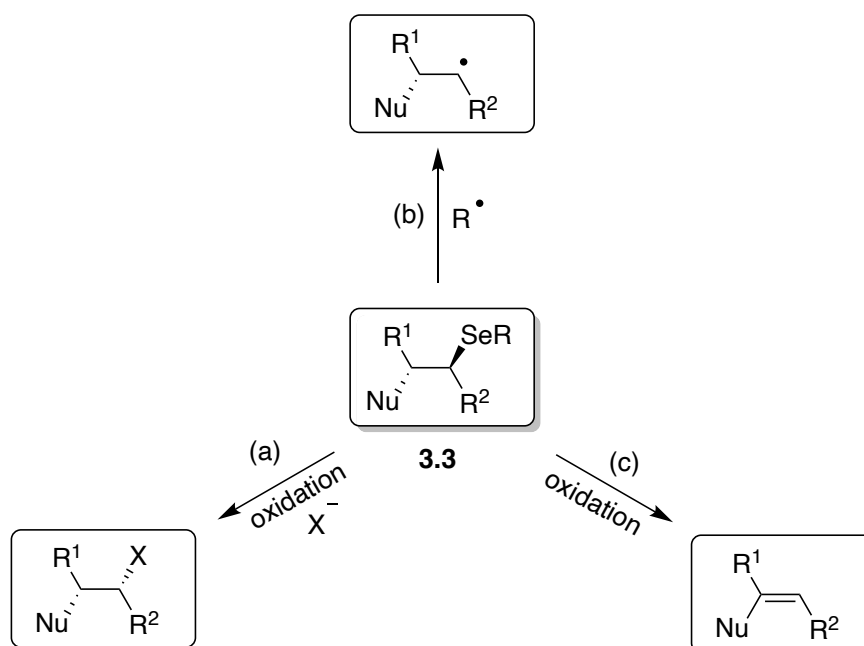


(b) Intramolecular reaction



Scheme 3.1. Activation of alkenes using selenium electrophiles.

Compounds **3.3** can be utilised to substitute the selenide group with functional groups in organic synthesis. Selenid can be used in various transformations such as: nucleophilic substitution (a), radical reactions by cleavage of the carbon–selenium bond (b), and oxidation process to form double bonds (c) (Scheme 3.2).^[21]



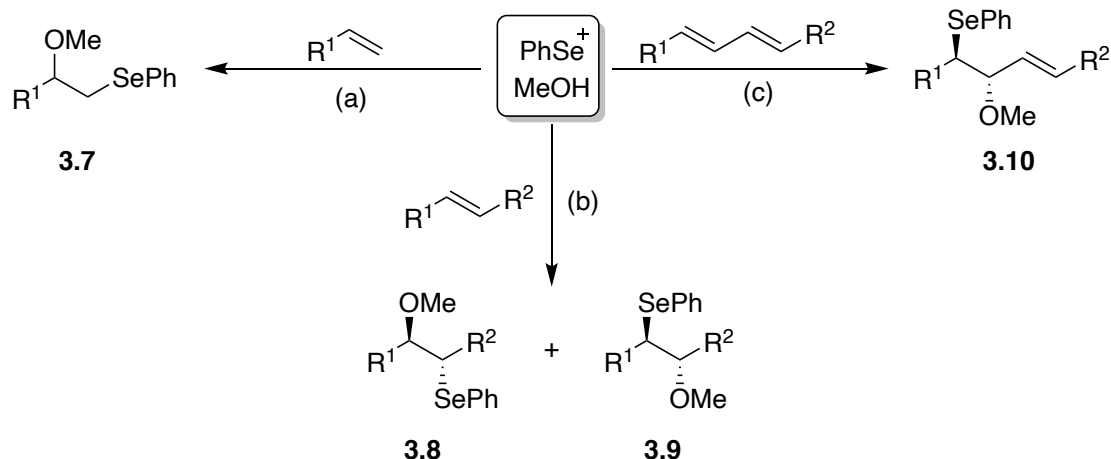
Scheme 3.2. General application of organoselenium compounds.

3.2. Different methods for selenofunctionalization of alkenes

The selenofunctionalization of alkenes is the reaction between unsaturated bond with selenyl functionality in the presence of different nucleophilic sources such as: (a) water, alcohols or acids producing oxyselenation products; (b) amines, producing aminoselenation products; (c) azides, producing azidoselenylation products. All these vicinal difunctional alkanes, β -substituted selenides containing two different functional groups (α -OR or α -NR² and β -SeR) at the same single bond might be used as significant intermediates for further transformation via the selective cleavage of the C–O or C–Se bonds. The homolytic cleavage of the C–Se bond is a relatively easy process, which can be initiated either photochemically or thermally.^[9,22]

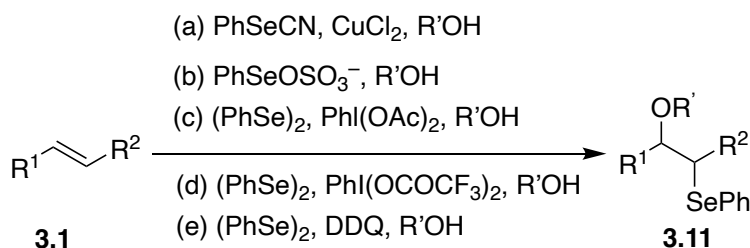
3.2.1. Oxyselenenylation of alkene

Various synthetic methods for intermolecular oxyselenenylations of alkene have been developed. Commonly, the *anti*-addition of an alkyl- or arylseleno functionality in presence of an oxygen containing solvent including hydroxy-, alkoxy-, or acetoxy nucleophile are known. The production of β -methoxyselenides is traditionally achieved with the use of methanol as a solvent and PhSeCl as an electrophile.^[23,24] Generally, the regiochemistry for terminal alkene addition follows the Markovnikov rule to afford product class **3.7**, (Scheme 3.3a).^[25] In contrast, the use of internal alkenes can lead to a mixture of regioisomers (**3.8**, **3.9**) (Scheme 3.3b). Interestingly, the use of conjugated dienes provide the 1,2 addition products (**3.10**) with Markovnikov selectivity (Scheme 3.3c).^[26,27]



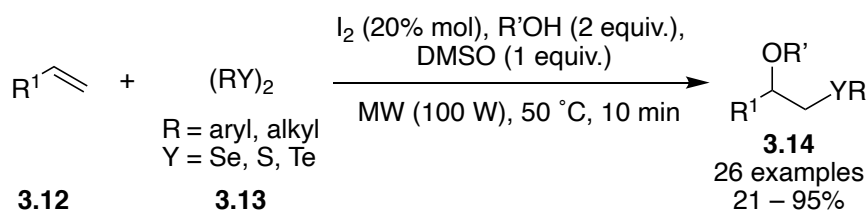
Scheme 3.3. Regioselectivity of oxyselenylation of alkenes.

Several synthetic methods for β -alkoxyselenides **3.11** starting from cyclic and acyclic alkenes have been published (Scheme 3.4). Common methods include the reaction of an unsaturated olefinic substrates **3.1** with PhSeCN in the presence of a Cu(II) or Ni(II) catalyst and alcohol as solvent (Scheme 3.4.a).^[28,29] Tiecco *et al.* reported the use of PhSeOSO₃H as the electrophile. This is produced by the oxidation of diphenyl diselenide with ammonium persulfate in alcohol or a combination of dichloromethane and alcohol (Scheme 3.4.b).^[30] Another method for β -alkoxyselenide synthesis is the oxidation of diphenyl diselenide to generate selenenylating species by using different oxidants such as hypervalent iodine reagents ((diacetoxyiodo)benzene, (Scheme 3.4.c) or Iodobenzene trifluoroacetate (Scheme 3.4.d)) or 2,3-dichloro-5,6-dicyano-1,4-benzoquinone (DDQ, Scheme 3.4.e).^[31–33]



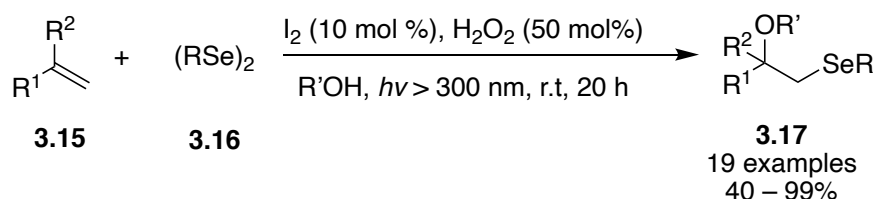
Scheme 3.4. Different methods for the synthesis of β -alkoxyselenides compounds.

In 2015, Braga and co-workers have reported such methodology employing molecular iodine (I₂) as a catalyst under microwave irradiation (Scheme 3.5).^[34] This approach was applied on different styrene derivatives **3.12** and nucleophiles, offering the β -alkoxyselenated products **3.1** in good to excellent yields.



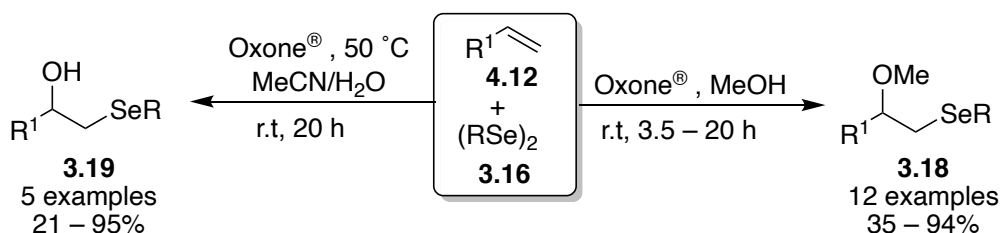
Scheme 3.5. Synthesis of β -alkoxyselenides under microwave irradiation.

An alternative route for the selenoalkoxylation of olefins **3.15** using molecular iodine (I_2) as catalyst and 0.5 equiv. of hydrogen peroxide (H_2O_2) under visible light irradiation has been developed by Jiang and co-workers in 2018 (Scheme 3.6).^[35] The amount of H_2O_2 was controlled to avoid the overoxidation of diselenides to achieve the high selectivity. Under ambient conditions, the use of different diselenides **3.16** and alcohols was successfully achieved, leading to the formation of selenoalkoxylated products **3.17** in good to high yields.



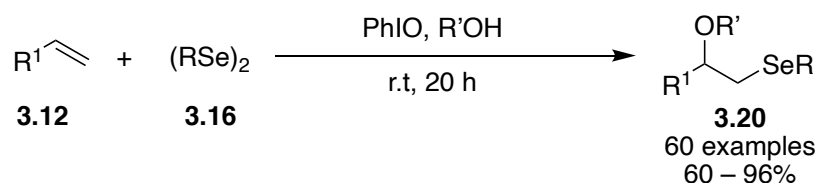
Scheme 3.6. Synthesis of β -alkoxyselenides under visible light irradiation.

In 2018, Santi *et al.* published the generation of β -oxyselenated products starting from alkenes **3.12** and diorganyl diselenides **3.16** using stoichiometric amount of Oxone[®] as an oxidant at different temperatures (Scheme 3.7).^[36] Under these conditions, high selectivity for β -alkoxyselenation **3.18** was obtained when methanol was used as the solvent. Also, β -hydroxyselenated products **3.19** were achieved in good to excellent yields when a mixture of MeCN/ H_2O was used as a solvent.



Scheme 3.7. Oxyselenation of olefins using oxone.

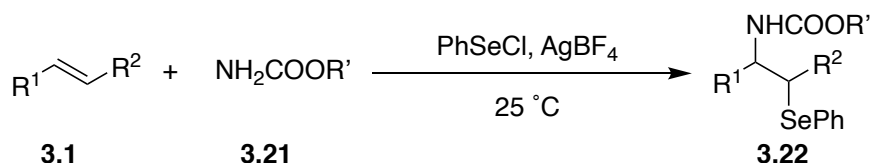
Very recently (2021), Ling and co-workers developed an alternative approach by using a simple and commercially available hypervalent iodine(III) reagent, iodosylbenzene (PhIO), as the oxidant (Scheme 3.8).^[37] A wide range of selenofunctionalized products **3.20** was obtained under the optimum conditions with good to excellent yields, using a combination of alkene **3.12**, diselenide **3.16** and a nucleophilic source.



Scheme 3.8. Synthesis of selenofunctionalized products **3.17** using PhIO, as oxidant.

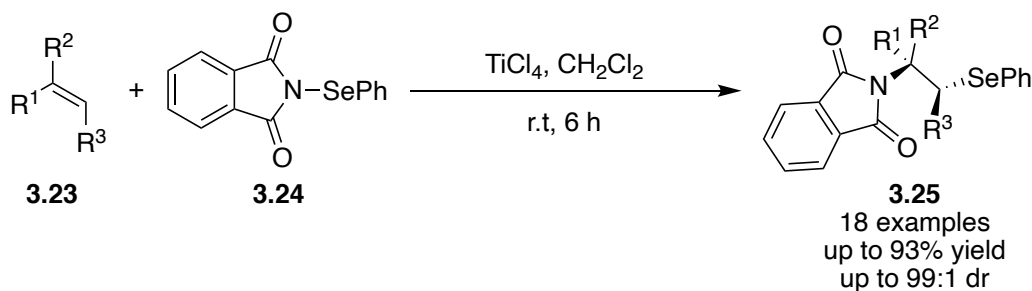
3.2.2. Aminoselenenylation of alkene

The aminoselenenylation of alkenes has been less studied compared to the oxyselenenylation of alkenes, despite the relevant synthetic usefulness for the production of biologically relevant compounds. In most cases the reaction needs additional activation methods. For instance, the addition of carbamate **3.21** as nucleophilic source and PhSeCl as selenyl functional group to alkene **3.21** was developed using silver tetrafluoroborate (AgBF_4) as an activating agent (Scheme 3.9).^[38]



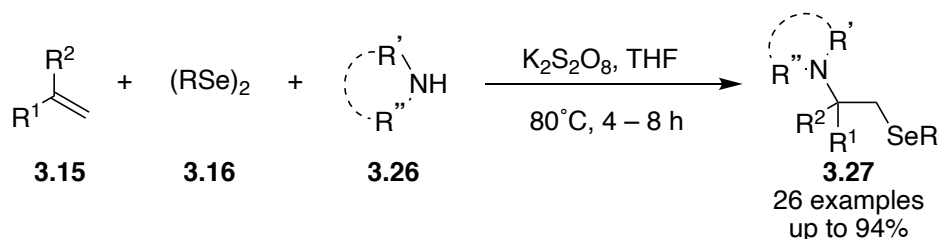
Scheme 3.9. Synthesis of β -phenylseleno carbamates **3.22** by using AgBF_4 .

In the last decade, development of simple and sustainable methods for aminoselenenylation of alkenes have drawn more attention. In this regard, in 2015 Tang *et al.* reported a process for amidoselenenylation of alkenes using a Lewis acid catalyst (TiCl_4) and *N*-(phenylseleno)-phthalimide (**3.24**) as a nitrogen and selenium source (Scheme 3.10).^[39] A vast range of alkenes **3.23** were used to generate amidoselenenylation products **3.25** with high regioselectivity and diastereoselectivity.



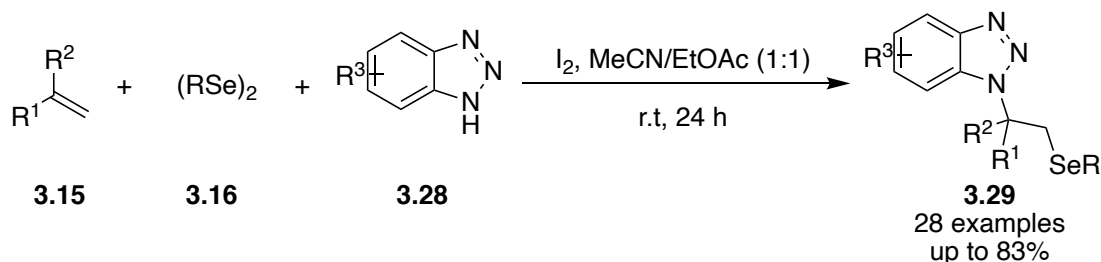
Scheme 3.10. Amidoselenenylation of alkenes using TiCl_4 .

Subsequently, in 2016 Sun and co-workers described another synthetic method for selenoamination of alkenes affording amidoselenide-containing sulfamides and azoles **3.27** using potassium peroxodisulfate ($K_2S_2O_8$) as oxidant (Scheme 3.11).^[40] The broad reaction scope was achieved with the use of olefins **3.15** in the presence of amino sources **3.26** as nucleophiles and diphenyl diselenide (**3.16**) as source of selenyl functionality.



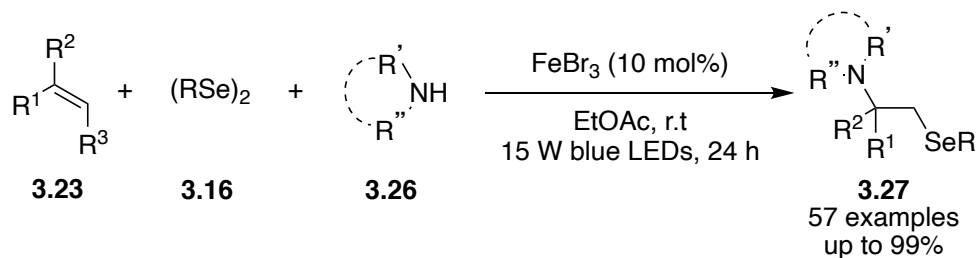
Scheme 3.11. Aminoselenenylation of alkenes using $K_2S_2O_8$.

The aminoselenenylation of alkenes has been also achieved through molecular iodine (I_2) as a mediator at room temperature by Yan and co-workers in 2017.^[41] In this reaction, only benzotriazole derivatives **3.28** were used as nitrogen source in the presence of diselenides **3.16**, providing the corresponding aminoselenenides **3.29** in good yields.



Scheme 3.12. Aminoselenenylation of alkenes using I_2 .

Very recently in 2020, Xia and co-workers described a visible-light mediated iron catalysed process for the aminoselenenylation of alkenes **3.23** with amines **3.26** and diselenides **3.16** (Scheme 3.13).^[42] The key intermediate, the photo-excitable Fe-amine $[FeBr_3 \cdot NHRAr]$ is generated *in situ* by mixing of amine and $FeBr_3$. A broad variety of alkenes, diselenides, primary and secondary amines were evaluated under air atmosphere at room temperature, yielding the corresponding aminoselenenylation products **3.27** in good to excellent yields.



Scheme 3.13. Aminoselenenylation of alkenes under visible-light irradiation.

3.2.3. Selenocyclization of alkenes

Heterocycles play an important role in the agrochemical, pharmaceutical and medicinal industries (Figure 3.2).^[43–48]

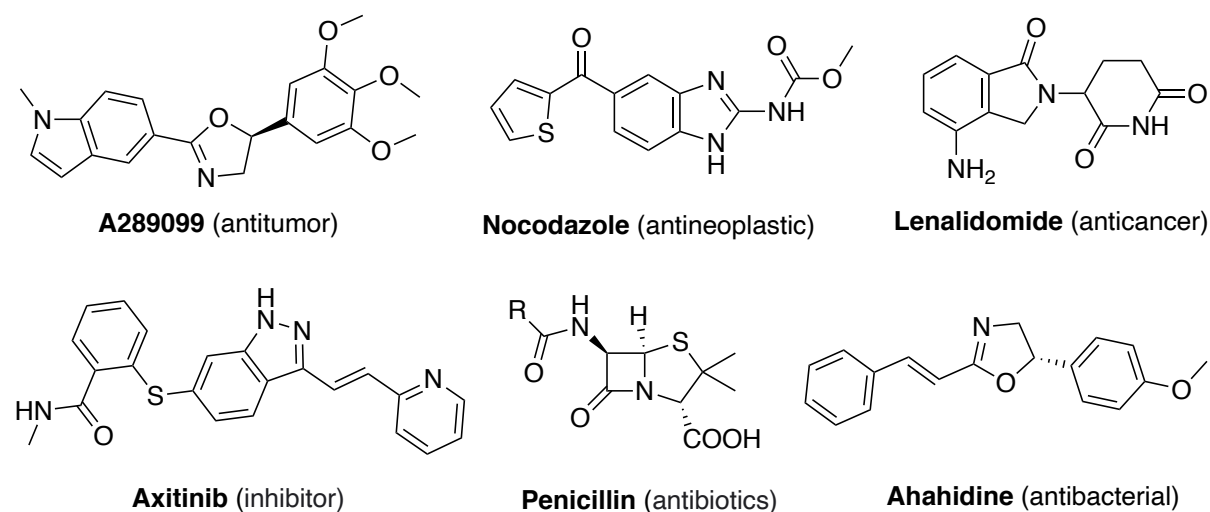
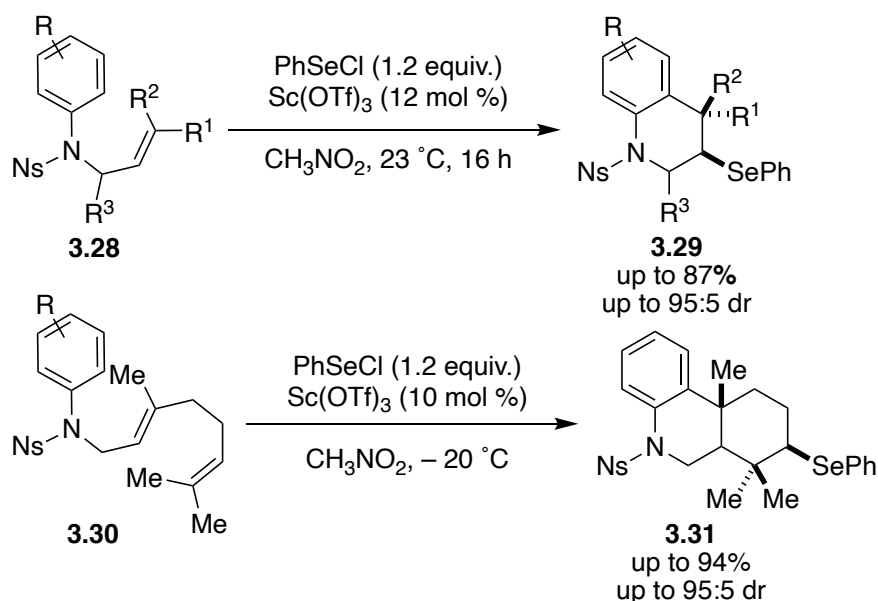


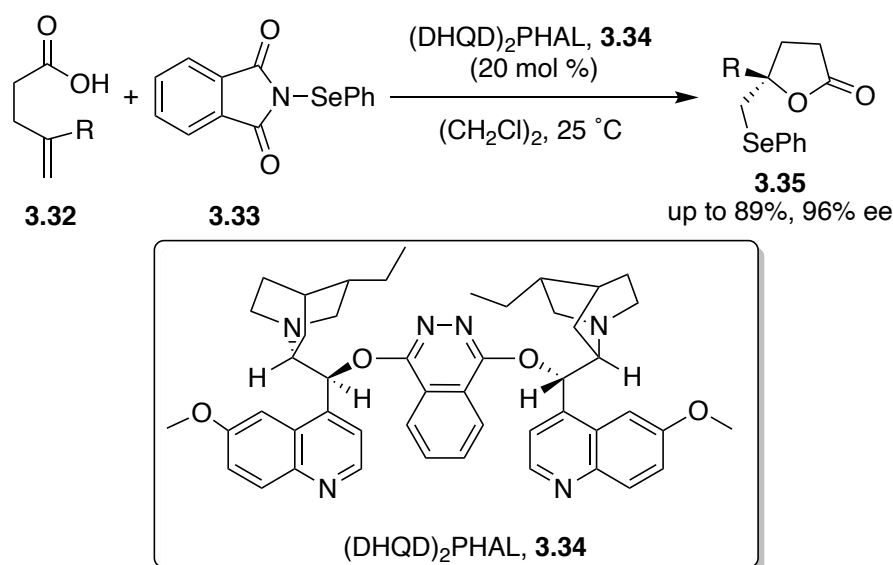
Figure 3.2. Examples of biologically active heterocyclic agents.

The selenium functionality can play an important role to generate such heterocyclic cores through intramolecular selenofunctionalisation. In 2013, Shaw and co-workers described the synthesis of polysubstituted tetrahydroquinoline **3.29** and octahydrophenanthridine **3.31** through the reaction of alkene (**3.28** or **3.30**) and PhSeCl using catalytic amounts of a Lewis acid (Sc(OTf)₃).^[49] Two rings, three bonds, and three stereogenic centres were produced in a single reaction process with good stereo- and regio-control (Scheme 3.14).



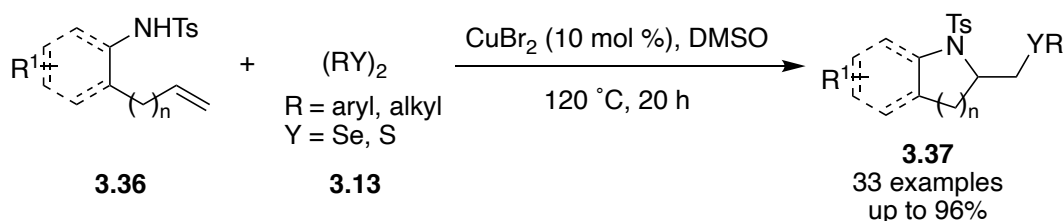
Scheme 3.14. Mono- and Bi-selenocyclization reactions of alkenes.

Subsequently in 2015, Yeung *et al.* explored an enantioselective selenolactonization of olefinic acids **3.32** in presence of *N*-phenylselenophthalimide (NPSP) (**3.33**) as the electrophilic selenium source using hydroquinidine 1,4-phthalazinediyl diether (DHQD)₂PHAL (**3.34**) as chiral catalyst (Scheme 3.15).^[50] This catalytic reaction protocol tolerated a vast range of functional groups, providing the selenolactones **3.35** in good to excellent yields and up to 96% *ee*. Also, heteroaromatic substrates were successfully prepared using this condition.



Scheme 3.15. Enantioselective Selenolactonization of olefinic acids **3.32**.

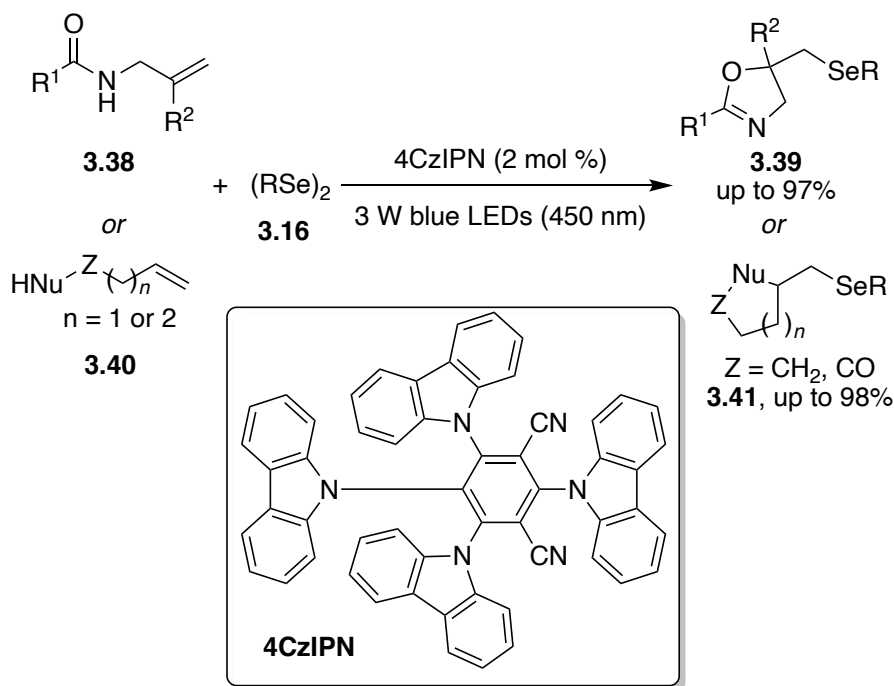
In 2018, Yang *et al.* published an interesting process for the intramolecular selenoamination of alkenes **3.36** using a copper catalyst to generate seleno-*N*-heterocycles products **3.37** in moderate to excellent yields (Scheme 3.16).^[51] The proposed mechanism showed that oxygen and DMSO act as co-oxidants and play important roles for these cyclization processes.



Scheme 3.16. Intramolecular selenoamination of **3.36** using copper catalyst.

Photochemistry has also contributed to carry out selenocyclization reactions. Recently, in 2019, Liu and co-workers developed a photochemical pathway for selenocyclisation of *N*-allylamides in the presence of diselenides **3.16** and photoredox catalyst, 4CzIPN (2 mol%) under visible-light irradiation (Scheme 3.17).^[52] Under the optimal reaction conditions, broad range of allylic amides **3.38** and different diselenide substrates **3.16** successfully provided selenocyclized products **3.39** in moderate to high yields. Various unsaturated compounds containing different

nucleophiles **3.40** were investigated to produce the corresponding selenoheterocycle products **3.41** in good yields.

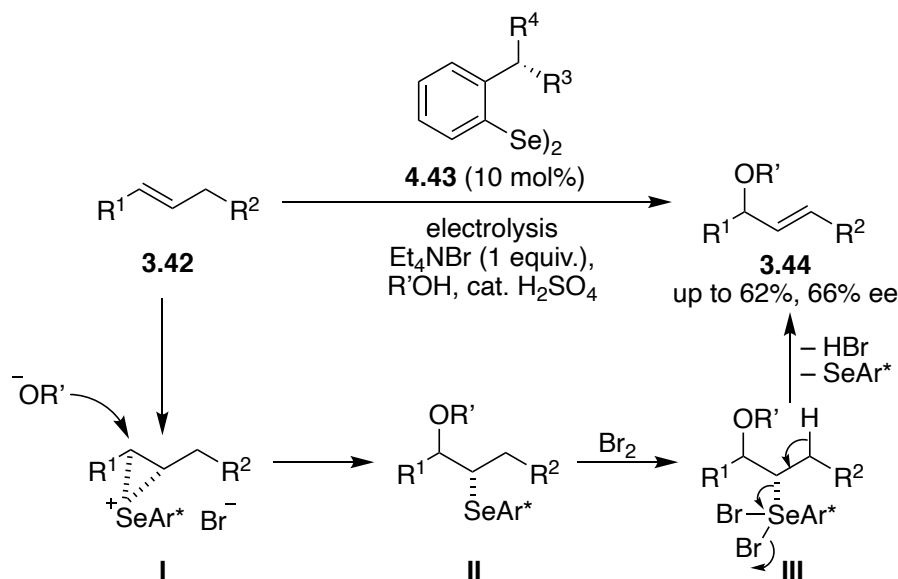


Scheme 3.17. Intramolecular selenocyclization under visible-light irradiation.

3.3. Electrochemical selenofunctionalization of alkenes

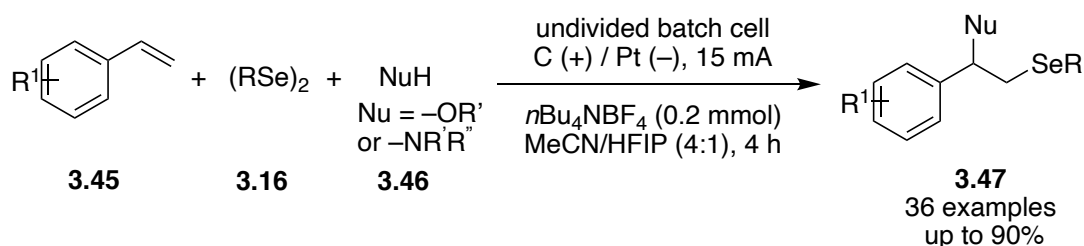
In the last decades, the conventional and electrochemical synthetic methods for the functionalization of the alkenes have been widely explored, but electrochemical methods for the selenofunctionalization of alkenes are relatively uncommon. However, few developments for such reaction including oxyselenenylation, aminoselenenylation and selenocyclization starting from alkene have been conducted.

In 2006, Wirth and co-workers have described the electrochemical selenenylation–elimination of alkenes in a single reaction process using catalytic amount of chiral diselenide (Scheme 3.18).^[53] The reaction of alkene **3.42**, electrophilic selenium precursor **3.43** and alcohols or water affords the alkoxy- or hydroxyselenenylated intermediate (**II**). In this reaction, tetraethylammonium bromide (Et_4NBr) was utilized as a redox catalyst as well as the supporting electrolyte. Subsequently, the allylic alcohol or ether **3.44** were rapidly formed *via* the second oxidation process and the electrophilic selenium reagents were regenerated.



Scheme 3.18. Electrochemical oxyselenenylation and deselenenylation of alkenes.

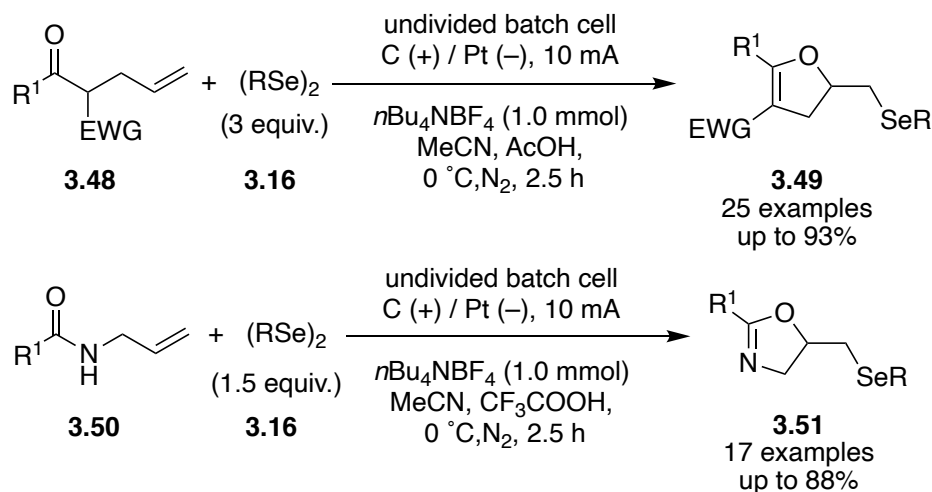
In 2019, Lei *et al.* reported an electrochemical selenofunctionalisation of styrenes to afford the aminoselenation and oxyselenation products **3.47** (Scheme 3.19).^[54] The reaction was performed in an undivided cell under constant current of 15 mA using graphite (Gr) electrode as the anode and a platinum plate (Pt) as the cathode with *n*Bu₄NBF₄ as the supporting electrolyte. A solvent combination of CH₃CN/HFIP mixture was used in a 4:1 ratio where the co-solvent HFIP is proposed to stabilise the radical. Various functional groups attached to styrene substrates **3.45**, diselenide **3.16**, and different nucleophiles **3.46** including amines, alcohols, carboxylic acids and water delivered the desired products **3.47**. However, this method was limited to substituted-styrene substrates.



Scheme 3.19. Electrochemical selenofunctionalization of styrenes in an undivided batch cell.

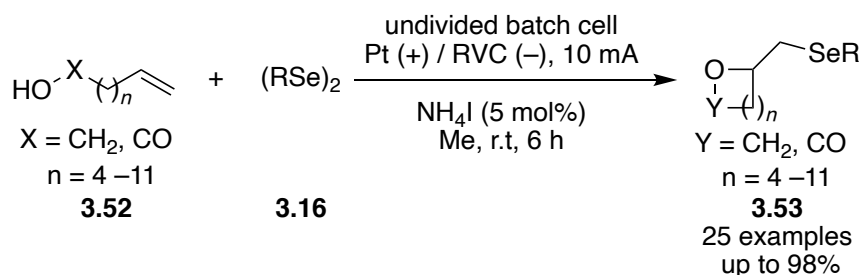
In 2019, Lei *et al.* also demonstrated an electrochemical oxidative selenocyclisation between olefinic carbonyls **3.48** and diaryl diselenides **3.16**, offering a sustainable route to the production of selenium-functionalized dihydrofurans **3.49** (Scheme 3.20).^[55] This reaction process was carried out in MeCN/AcOH solvent combinations with *n*Bu₄NBF₄ as supporting electrolyte, graphite as the anode and platinum as the cathode. Various substituents on the olefinic carbons of **3.48** delivered the selenylated dihydrofurans compounds **3.49** in moderate

to good yields. Likewise, the unsaturated amides **3.50** also returned the corresponding selenylated oxazolines **3.51** in moderate to excellent yields.



Scheme 3.20. Electrochemical synthesis of selenylated dihydrofurans and oxazolines in an undivided batch cell.

Another electrochemical selenocyclization of olefins **3.52** in the presence of diselenides **3.16** was developed by Pan and co-workers to produce seleno-substituted cyclic lactones or ethers **3.53** (Scheme 3.21).^[56] In this approach, olefins such as unsaturated alcohols and unsaturated carboxylic acids **3.52**, were transformed into selenocyclic products **3.53** under mild electrochemical conditions in good yields. Furthermore, medium-sized ethers (7-, 9-, and 11-membered rings) and 4–6-membered lactones were synthesized easily using this optimized condition.



Scheme 3.21. Electrochemical synthesis of selenylated ethers, lactones and isobenzofuranones in an undivided batch cell.

3.4. Flow electrochemical selenofunctionalization of alkenes

As described in the previous sections of this chapter, several conventional and electrochemical synthetic processes for the selenofunctionalization of alkenes have been developed. Many of these methods are limited to the use of toxic or metallic reagents, high temperature and long reaction times. Based on these inferences, the main aim of this project is to improve the

throughput of selenofunctionalization of alkenes by using the Ion electrochemical flow reactor and the Vapourtec automated flow machine that is explained in chapter 1. The starting alkene, the diselenide as selenenylating reagent, and the nucleophile can all be selected in the automated setup. Also, various product solutions can be collected separately when different combinations are used. Vast range of substrates and nucleophiles will be screened to achieve the synthesis of different molecules including oxyselenenylation, aminoselenenylation and selenocyclization in a robot like fashion in a very short time. A simplified schematic representation of the selenenylation reactions through electrolysis under automated flow conditions is shown in Figure 3.3.

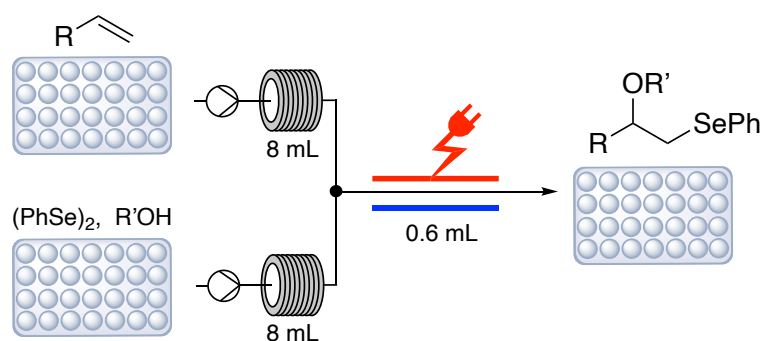
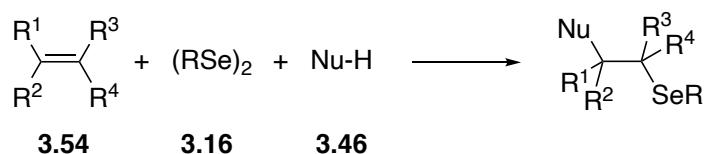


Figure 3.3. Simplified schematic representation of selenenylation of alkene under automated electrochemical flow conditions.

3.5. Results and discussion

The three-component reaction; the alkenes **3.54**, diselenide **3.16**, and various nucleophiles **3.46** were used in the initial studies to determine optimum reaction conditions (Scheme 3.22). Different reaction parameters were quickly and robotically screened by using the automated flow system with an integrated Ion electrochemical flow reactor. The system software allowed the automatic design of multiple reactions, applying several reaction parameters and collecting the specific reaction products in an automated mode. The most essential parameters such as electrical currents, solvents, supporting electrolytes, electrodes materials and flow rates were tested separately in order to identify the best conditions for performing this reaction in the electrochemical flow reactor. These parameters will be explained in details in the following sections.



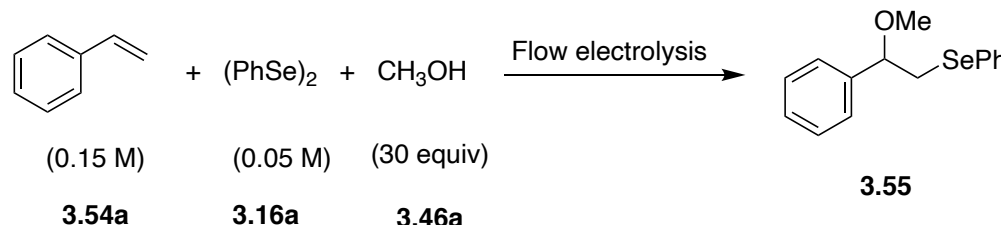
Scheme 3.22. Selenenylation of alkenes.

3.5.1. Reaction optimisation

3.5.1.1. Current screening

As a standard reaction, styrene (**3.54a**, 0.15 M), diphenyl diselenide (**3.16a**, 0.05 M) and MeOH (30 equiv.) in MeCN were reacted to generate methoxyselenenylated product **3.55** using graphite (Gr) as anode and platinum (Pt) as cathode, with a flow rate of 0.1 mL/min, and 5 mM tetrabutylammonium tetrafluoroborate (Bu_4NBF_4) as the supporting electrolyte (Table 3.1). Only 32% of the targeted product **3.55** was produced when a residence time of 6 minutes and a current of 16 mA (2.0 F) were applied at room temperature (Table 3.1, entry 1). Theoretically, the two-electron oxidation requires a charge of only 2.0 F per mol. However, it has been noted that increasing the current from 16 mA to 32 mA (4 F) led to improve the yield from 32 % to 66 % along with unreacted starting materials (Table 3.1, entry 2). Reduced yield of the intended product (**3.55**) was observed when the charge was increased beyond 4.0 F (Table 3.1, entries 3-5).

Table 3.1. Screening of current for the methoxyselenenylation of styrene (**3.54a**) to methoxyselenenylated product **3.55** under the flow conditions.

				
Entry	Current (mA)	Current density (mA/cm ²)	3.55 Yield (%) ^[a]	
1	16	1.33	32	
2	32	2.66	66	
3	48	4	40	
4	64	5.33	33	
5	80	6.66	20	

[a] The yield was determined using ¹H NMR with 1,3,5-trimethoxybenzene as internal standard.

3.5.1.2. Solvents screening

The impact of the solvent was also investigated by using the best condition in Table 3.1 with different solvents. Several solvents and solvent mixtures such as acetonitrile (Table 3.2, entry 1), tetrahydrofuran (Table 3.2, entry 2), methanol (Table 3.2, entry 3), and mixtures of acetonitrile/tetrahydrofuran (Table 3.2, entry 4) were screened. It was discovered that acetonitrile was the best solvent for this reaction.

Table 3.2. Screening of solvents for the methoxyselenenylation of styrene (**3.54a**) to methoxyselenenylated product **3.55** under the flow conditions.

Entry	Solvent	3.55 Yield (%) ^[a]
1	MeCN	66
2	THF	49
3	MeOH	45
4	MeCN/THF (1:1)	58

[a] The yield was determined using ¹H NMR with 1,3,5-trimethoxybenzene as internal standard.

3.5.1.3. Supporting electrolytes screening

Lei and co-authors described an oxyselenenylation of styrene in a batch electrochemical process using excess tetrabutylammonium tetrafluoroborate (*n*Bu₄NBF₄) as a supporting electrolyte.^[54] Under flow conditions, we observed that only small amounts of *n*Bu₄NBF₄ were required to achieve identical results in a faster reaction time under flow conditions. The reaction under flow condition still produced a yield of 32 % even without the addition of electrolyte. The amount of electrolyte has a great impact on the yield. Different supporting electrolytes were screened at low concentrations, including *n*Bu₄NBF₄, *n*Bu₄NOTs, *n*Et₄NCl, *n*Bu₄NBr, KI, and *n*Bu₄NI. Among them, *n*Bu₄NI delivered the highest yield of 87 % (Table 3.3, entry 8). This also confirms that *n*Bu₄NI played an important role in the formation of methoxyselenenylated product **3.55**, which will be explained in details in section 3.5.3.

Table 3.3. Screening of supporting electrolytes for the methoxyselenenylation of styrene (**3.54a**) under flow conditions.

Entry	Electrolyte (M)	3.55 Yield (%) ^[a]
1	Without supporting electrolyte	23
2	<i>n</i> Bu ₄ NBF ₄ (0.005)	66
3	<i>n</i> Bu ₄ NBF ₄ (0.005)	73 ^[b]
4	<i>n</i> Bu ₄ NBr (0.005)	78
5	<i>n</i> Bu ₄ NBr (0.05)	39
6	Me ₄ NPF ₆ (0.005)	59
7	<i>n</i> Et ₄ NCl (0.005)	78
8	<i>n</i> Bu ₄ NI (0.005)	87
9	<i>n</i> Bu ₄ NI (0.05)	43
10	KI (0.005)	85

[a] The yield was determined using ¹H NMR with 1,3,5-trimethoxybenzene as internal standard. [b] at 40 °C.

3.5.1.4. Flow rate/residence time effect

The impact of flow rate/residence time on product yield was also studied in order to find the best flow rate to avoid mass-transfer limitations.^[57] Surprisingly, increasing the flow rate to 0.2 – 0.6 mL/min resulted in full conversion with a yield of >99%. Further increase in the flow rate beyond 0.6 mL/min resulted in a decrease of the yield. This might be attributed to a decreased conductivity with increase flow rate. A quantitative yield was observed at flow rates up to 0.6 mL/min, equivalent to an estimated residence time of 1.0 minute by increasing the electrolyte concentration from 5 mM to 7.5 mM (Figure 3.4). The actual residence time is shorter due to hydrogen gas production. The increase in electrolyte concentration allowed a further reduction of the reaction time.

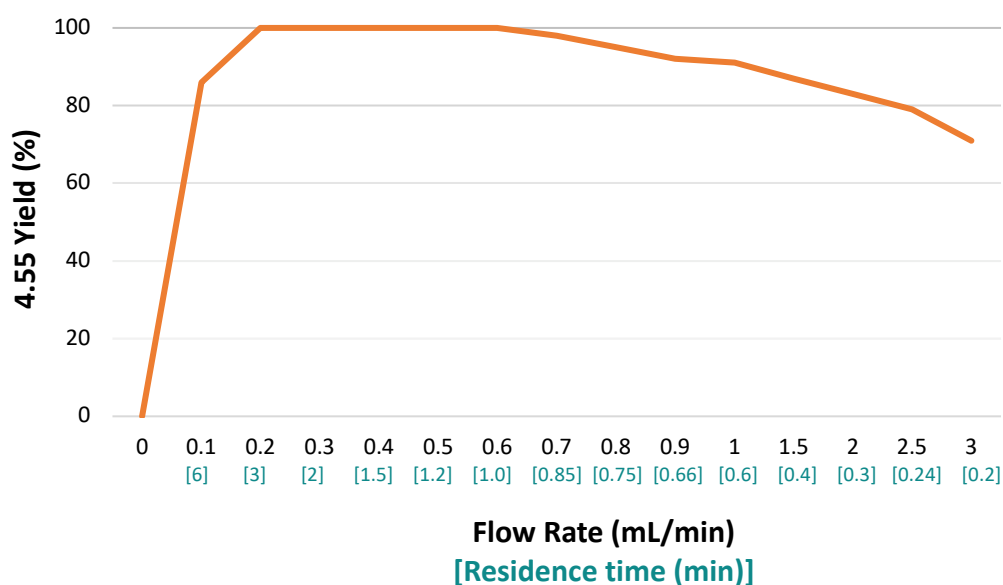


Figure 3.4: Effect of residence time and flow rate on the yield of **3.55**.

3.5.1.5. Electrode screening

The electrode materials employed in an electrochemical transformation are critical to the outcome of the reaction. Therefore, screening of different electrode materials as anode and cathode were also accomplished in a flow setup to transform the styrene (**3.54a**) to the methoxyselenenylated product **3.55** (Figure 3.5). Initially, platinum (Pt) was used as cathode and various anode materials such as graphite (Gr), glassy carbon (GC), boron-doped diamond (BDD), Panasonic carbon, PTFE carbon, stainless steel (Fe), and nickel (Ni) were screened. Among these, Gr as anode was found to be most efficient.

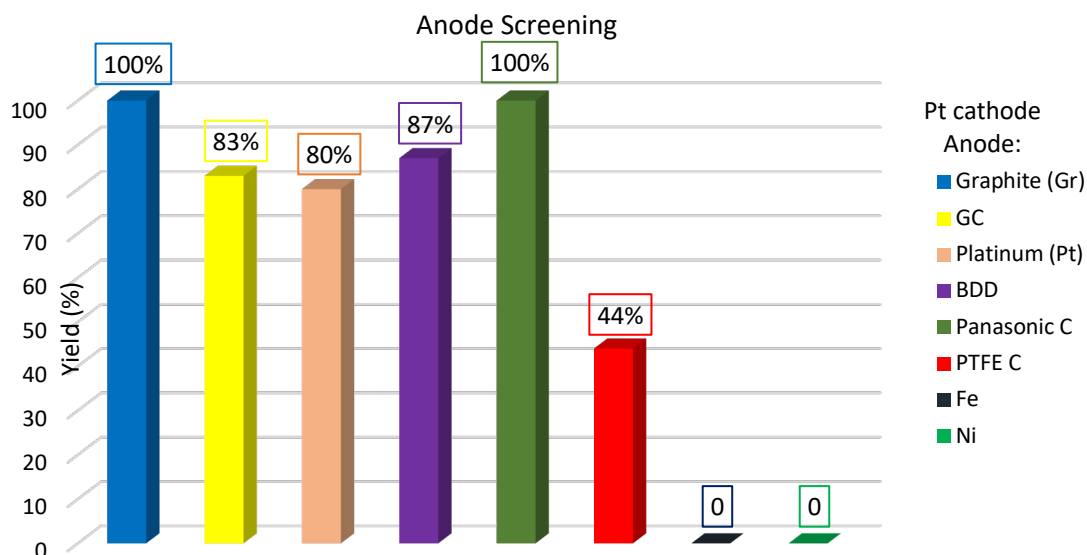


Figure 3.5. Anode electrode material screening.

Furthermore, Gr as anode was then screened against various cathodes such as Pt loaded on Nb, Pt loaded on Ti, Ni, Fe, Gr, GC, and Zn (Figure 3.6). From this screening it was found that Gr as anode and Pt as cathode constituted an optimal combination. A low-cost electrode (Pt loaded on Nb) still gave 95% yield. The same trend was observed for Gr as a cathode and anode.

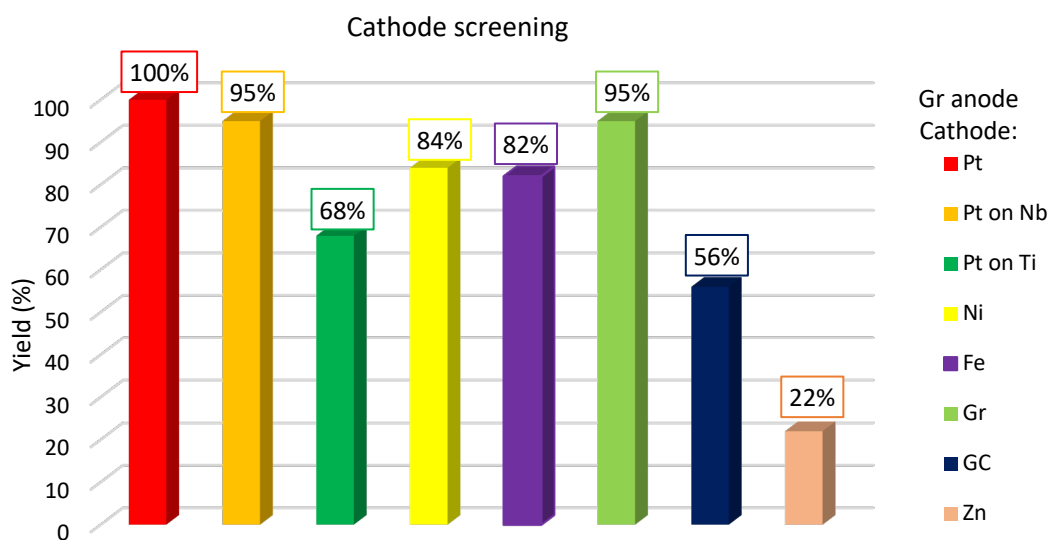


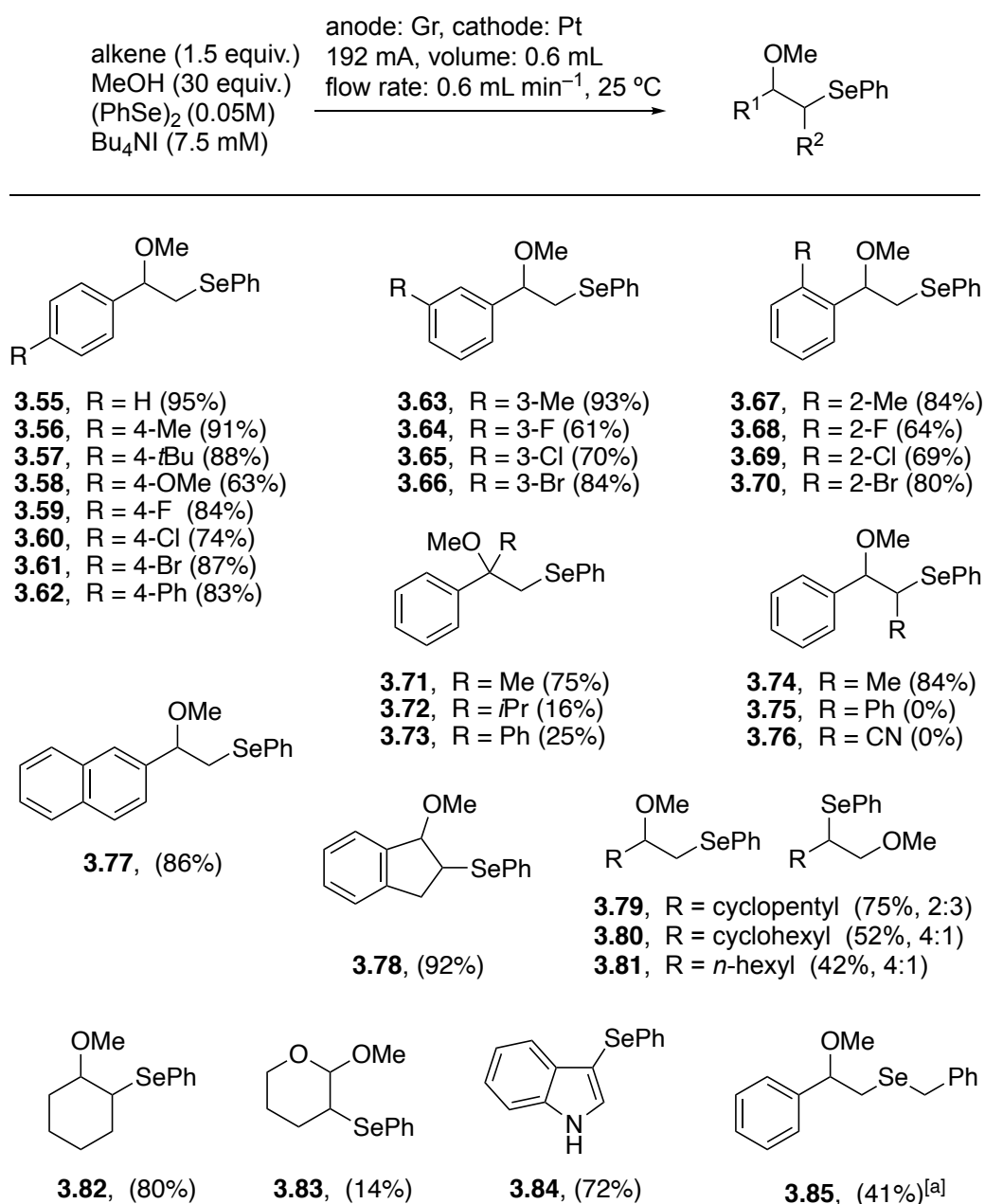
Figure 3.5. Cathode electrode materials screening.

3.5.2. Substrate scope

With the optimised reaction conditions in hand, an investigation of the scope and general applicability of this methodology using different alkenes, alcohols, and diselenides was performed in an automated way. Loading different alkenes, alcohols and diselenides into the auto-sampler allowed the reaction products shown in Schemes 3.23 and 3.24 and Scheme 3.25

to be obtained in a fully automated way without additional manual interference. The different product solutions obtained were purified by using a Biotage Isolera chromatography system. Due to the automated protocol, all reactions shown were performed using identical amounts and concentrations of reagents and 1.2 mmol alkene was used in each experiment.

Pleasingly, the electrochemical reaction of many different substituted styrene derivatives gave the desired products in good to excellent yields **3.55** – **3.78**. However, for **3.72** and **3.73**, the yields were low. No product formation was observed with disubstituted alkenes **3.75** and **3.76** (Scheme 3.23).

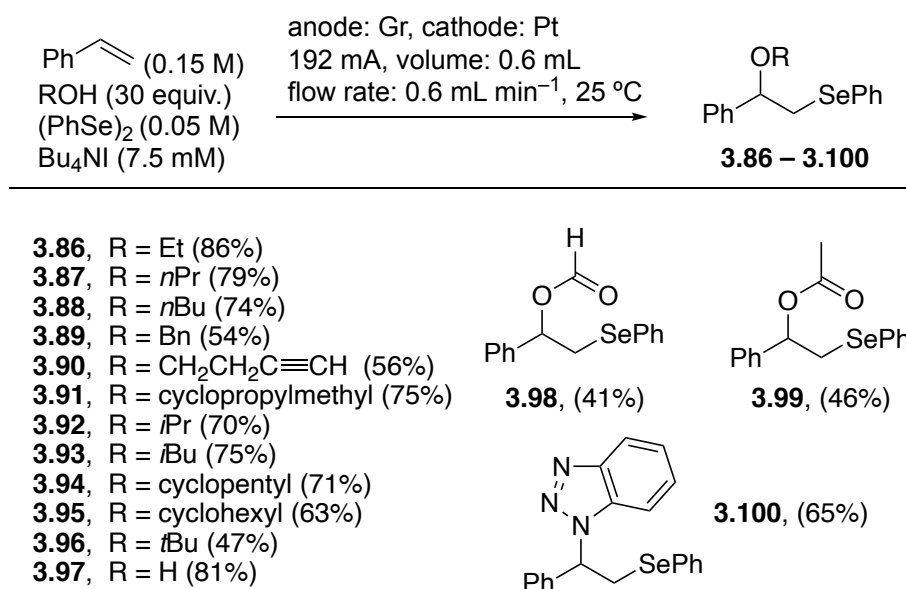


Scheme 3.23. Scope and limitations of the electrochemical methoxyselenenylation of alkenes. [a]

Dibenzyl diselenide was used instead of diphenyl diselenide.

Alkyl-substituted alkenes led to regioisomeric mixtures **3.79** – **3.81** as previously reported.^[27] 3,4-Dihydro-2*H*-pyran delivered **3.83** as a 1:1 mixture of *cis* and *trans* isomers in 14% combined yield as observed previously.^[58] Indole was selenenylated in the 3-position leading to **3.84**.^[59] Other diselenides such as dibenzyl diselenide can also be used for the synthesis of **3.85** using MeCN/THF solvent mixture (1:1) for optimum yield.

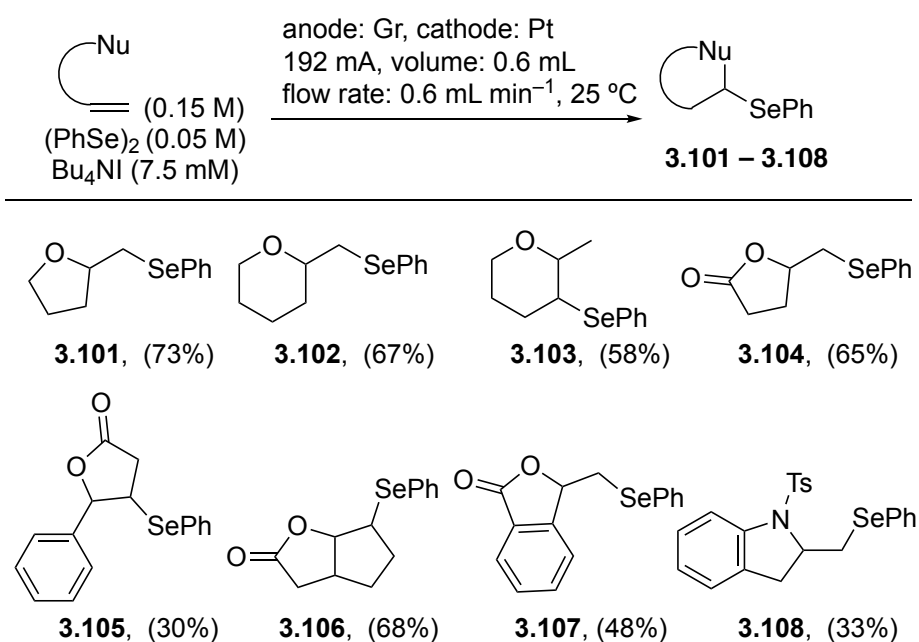
Variations of nucleophiles in the selenenylation are shown in Scheme 3.24. Primary, secondary, and tertiary alcohols can be used in the selenenylation reactions as shown in the formation of products **3.86** – **3.96**. Even water, formic acid, and acetic acid can be used, leading to products **3.97** – **3.99**. Benzotriazole also participated as an *N*-nucleophile in this reaction to form the aminoselenenylated product **3.100** in 65% yield.



Scheme 3.24. Different nucleophiles for the electrochemical selenenylation of styrene.

Cyclic ethers and lactones are important cores in several natural products and important bioactive molecules. This methodology can also be expanded to intramolecular cyclisations and was found to be efficient to obtain a variety of cyclised *O*-heterocycles as shown in Scheme 3.25. The lactones and ethers were obtained in moderate to good yields. Substituted tetrahydrofuran **3.101** was obtained in 73% yield. Functionalised pyrans **3.102** and **3.103** were obtained in 67 and 58% yield, respectively. Different functionalised and fused lactones **3.104** – **3.17** were obtained in good yields. Similarly, dihydroindole **3.108** was obtained in 33% yield. All the synthesised compounds were fully characterised by different spectroscopic techniques. Among them, also a single crystal X-ray analysis was performed for compound **3.72** (see experimental section, chapter 7) that further confirms the formation of the target molecules.^[60]

The selenium cation necessary for the addition and cyclisation reactions described here is believed to be formed through sequential oxidation of diphenyl diselenide as already investigated by Breder, Siewert, and co-workers.^[61] The oxidation potential required for a subsequent elimination of the selenide is not reached here. To further demonstrate the synthetic potential of this protocol, a gram-scale reaction was performed for the synthesis of **3.55**. Encouragingly, 1.52 g of **3.55** was obtained in just 100 minutes (overall yield 87%).



Scheme 3.25. Flow electrochemical selenocyclisations.

3.5.3. Reaction mechanism

In order to further insight about the reaction mechanism, cyclic voltammetry studies of the styrene and diphenyl diselenide were carried out in different solvents. Initially, each substrate was screened individually in absence of *n*Bu₄NI in acetonitrile, one-electron oxidation peaks of styrene (**3.54a**) was observed at *E*_p = 2.2 V (Figure 3.7, red line) and two one-electron oxidation peaks of diphenyl diselenide (**3.16a**) was observed at *E*_p = 1.52 V and *E*_p = 1.82 V (Figure 3.7, blue line). The *n*Bu₄NI has showed two oxidation peaks lower than diphenyl diselenide at *E*_p = 1.0 V and *E*_p = 1.3 V (Figure 3.7, yellow line).

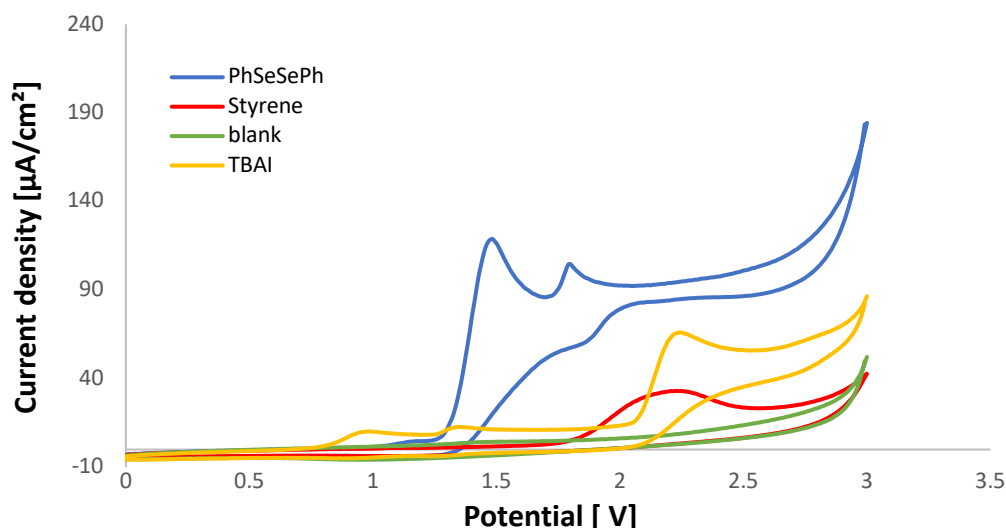


Figure 3.7. Cyclic voltammogram (CV) of substrates, styrene (5 mM); diphenyl diselenide (5 mM) and $n\text{Bu}_4\text{NI}$ (5 mM) in 0.1 M $n\text{Bu}_4\text{NClO}_4$ / MeCN electrolyte (20 mV s^{-1} scan rate). Working electrode: glassy carbon electrode tip (3 mm diameter); Counter electrode: platinum wire; Reference electrode: Ag/AgCl in 3 M KCl.

The oxidation potential of $n\text{Bu}_4\text{NI}$ is lower than styrene (**3.54a**) and diphenyl diselenide (**3.16a**), indicates that the oxidation of iodide should proceed first in the galvanostatic setup. However, similar peaks were observed when styrene (**3.54a**) and $n\text{Bu}_4\text{NI}$ were combined (Figure 3.8, purple line). Also, the CV of diphenyl diselenide (**3.16a**) and $n\text{Bu}_4\text{NI}$ mixture showed only two oxidation peaks at $E_p = 1.49 \text{ V}$ and $E_p = 1.86 \text{ V}$ with no obvious oxidation peaks for $n\text{Bu}_4\text{NI}$ (Figure 3.8, brown line).

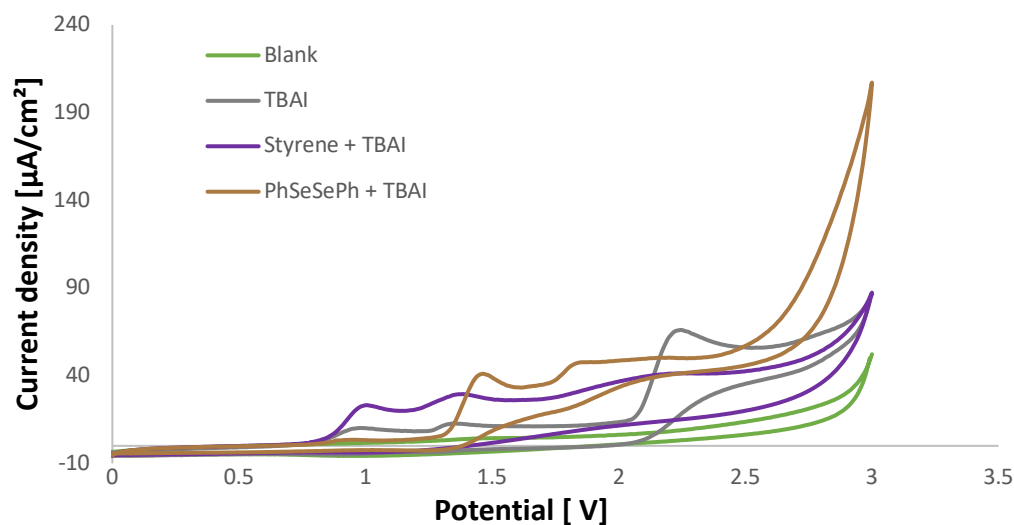
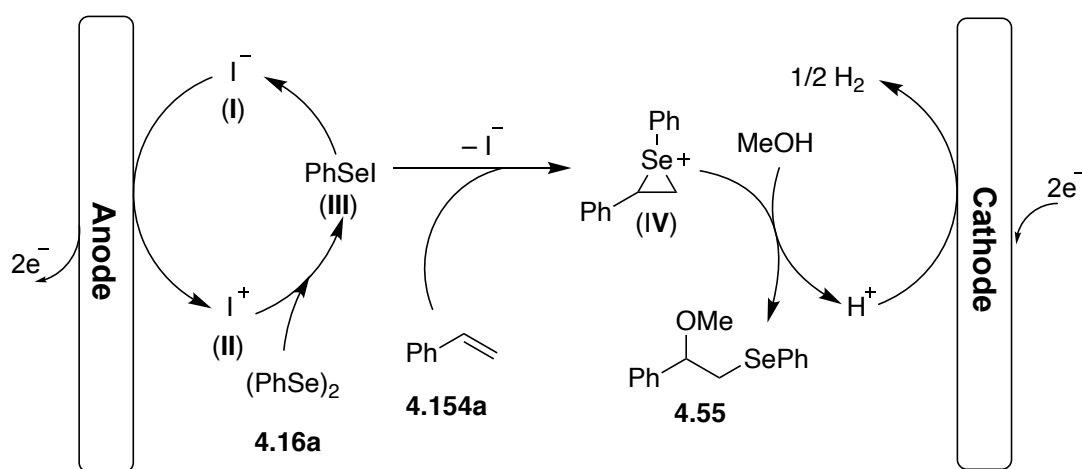


Figure 3.8. Cyclic voltammogram (CV) of substrate styrene (5 mM) with $n\text{Bu}_4\text{NI}$ (5 mM); diphenyl diselenide (5 mM) and $n\text{Bu}_4\text{NI}$ (5 mM) in MeCN with 0.1 M $n\text{Bu}_4\text{NClO}_4$ as electrolyte (20 mV s^{-1} scan

rate). Working electrode: glassy carbon electrode tip (3mm diameter); Counter electrode: platinum wire; Reference electrode: Ag/AgCl in 3 M KCl.

Based on our preliminary studies and according to previous literature reports on the selenenylation of alkene,^[62,63] the possible mechanism for the oxyselenenylation of alkene is shown in Scheme 3.26. At the anode, iodide (**I**) is oxidised sequentially by losing two electrons from iodide to the iodine radical to the iodine cation: $I^- \rightarrow I^\bullet \rightarrow I^+$. The iodine cation (**II**) is known to activate the diphenyl diselenide (**3.16a**) by generating PhSeI (**III**) that reacts with alkene (**3.54a**) to generate seleniranium ion (**IV**). **IV** then reacts with MeOH to form the desired product **3.55**. The proton produced in this process will be finally reduced to hydrogen at the cathode.



Scheme 3.26. Proposed mechanism for the electrochemical oxyselenenylation of styrene.

3.6. Conclusion and outlook

In conclusion, an efficient and straightforward electrochemical synthesis for selenenylations of alkenes in flow electrochemical reactor integrated with remote-controlled synthetic equipment was developed. Using this method, many oxyselenated products were prepared in a short time with minimal humanal interference. Under the optimum conditions, vast range of substrates and nucleophiles were screened, leading to the synthesis a library of 54 molecules including oxyselenenylation, azaselenenylations and selenocyclization. To show the potentials of this electrochemically combined automated flow technology, a gram scale reaction was also carried out. Also, 10 of these reactions were automatically performed in 200 minutes.

In future, different nucleophiles such as carbon-centered nucleophiles can be used to carry out carboselenenylation reaction of alkene. Moreover, asymmetric selenenofunctionalization reactions of alkenes with different nucleophilic compounds through an optically active electrophilic selenium reagents will be a very valuable approach as well. The use of catalytic

amount of diselenide as selenenylating reagent and control for sequential oxidation reaction has been rarely done under electrochemical conditions which can be improved under the flow electrochemical setup with automated flow system. Indeed, the remote-controlled technique has been demonstrated to accelerate the reaction optimization and preparation in a short time. This easy-to-use automated tool can be explored in further electrochemical transformations as well.

This work has already been published.^[64]

3.7. References

- [1] S. Patai, Z. Rappoport, *The Chemistry of Organic Selenium and Tellurium Compounds*, John. Wiley & Sons, Chichester, **1986**.
- [2] F. Wöhler and C. Siemens, *Ann. der Chemie und Pharm.* **1847**, *61*, 360–362.
- [3] K. B. Sharpless, R. F. Lauer, *J. Am. Chem. Soc.* **1973**, *95*, 2697–2699.
- [4] R. Walter, J. Roy, *J. Org. Chem.* **1971**, *36*, 2561–2563.
- [5] D. N. Jones, D. Mundy, R. D. Whitehouse, *J. Chem. Soc. D Chem. Commun.* **1970**, 86.
- [6] C. W. Nogueira, G. Zeni, J. B. T. Rocha, *Chem. Rev.* **2004**, *104*, 6255–6286.
- [7] C. . Nogueira, F. Meotti, E. Curte, C. Pilissão, G. Zeni, J. B. . Rocha, *Toxicology* **2003**, *183*, 29–37.
- [8] V. K. Jain, in *Organoselenium Compd. Biol. Med.*, Royal Society of Chemistry, Cambridge, **2017**, pp. 1–33.
- [9] T. Wirth, Ed. , *Organoselenium Chemistry*, Wiley-VCH Verlag GmbH & Co. KGaA, Weinheim, Germany, **2011**.
- [10] F. V. Singh, T. Wirth, *Catal. Sci. Technol.* **2019**, *9*, 1073–1091.
- [11] A. Braga, D. Lüdtke, F. Vargas, R. Braga, *Synlett* **2006**, 1453–1466.
- [12] F. V. Singh, T. Wirth, in *Organoselenium Chemistry*, Wiley-VCH Verlag GmbH & Co. KGaA, Weinheim, Germany, **2011**, pp. 321–360.
- [13] R. L. Quispe, M. L. Jaramillo, L. S. Galant, D. Engel, A. L. Dafre, J. B. Teixeira da Rocha, R. Radi, M. Farina, A. F. de Bem, *Redox Biol.* **2019**, *20*, 118–129.
- [14] M. Hopanna, L. Kelly, L. Blaney, *Environ. Sci. Technol.* **2020**, *54*, 11271–11281.
- [15] T. Schewe, *Gen. Pharmacol. Vasc. Syst.* **1995**, *26*, 1153–1169.
- [16] J. Rafique, R. F. S. Canto, S. Saba, F. A. R. Barbosa, A. L. Braga, *Curr. Org. Chem.* **2015**, *20*, 166–188.
- [17] M. Pinz, A. S. Reis, V. Duarte, M. J. da Rocha, B. S. Goldani, D. Alves, L. Savegnago, C. Luchese, E. A. Wilhelm, *Eur. J. Pharmacol.* **2016**, *780*, 122–128.
- [18] J. He, D. Li, K. Xiong, Y. Ge, H. Jin, G. Zhang, M. Hong, Y. Tian, J. Yin, H. Zeng, *Bioorg. Med. Chem.* **2012**, *20*, 3816–3827.
- [19] A. Gabriela Vogt, G. Perin, C. Luchese, P. C. da Silva, E. Antunes Wilhelm, M. Santos Silva, *European J. Org. Chem.* **2018**, 627–639.
- [20] M. Kieliszek, *Molecules* **2019**, *24*, 1298.
- [21] T. G. Back, *Organoselenium Chemistry: A Practical Approach*, OUP Oxford, **1999**.
- [22] G. Mugesh, W.-W. du Mont, H. Sies, *Chem. Rev.* **2001**, *101*, 2125–2180.

- [23] W. J. E. Parr, R. C. Crafts, *Tetrahedron Lett.* **1981**, 22, 1371–1372.
- [24] T. Wirth, G. Fragale, M. Spichly, *J. Am. Chem. Soc.* **1998**, 120, 3376–3381.
- [25] T. Takahashi, H. Nagashima, J. Tsuji, *Tetrahedron Lett.* **1978**, 19, 799–802.
- [26] C. Santi, C. Tidei, in *PATAI'S Chem. Funct. Groups*, John Wiley & Sons, Ltd, Chichester, UK, **2013**.
- [27] A. Toshimitsu, S. Uemura, M. Okano, *J. Chem. Soc. Chem. Commun.* **1982**, 965.
- [28] A. Toshimitsu, S. Uemura, M. Okano, *J. Chem. Soc. Chem. Commun.* **1977**, 166.
- [29] A. Toshimitsu, T. Aoai, S. Uemura, M. Okano, *J. Org. Chem.* **1980**, 45, 1953–1958.
- [30] M. Tiecco, L. Testaferri, L. Bagnoli, F. Marini, A. Temperini, C. Tomassini, C. Santi, *Tetrahedron Lett.* **2000**, 41, 3241–3245.
- [31] M. Tiecco, L. Testaferri, A. Temperini, L. Bagnoli, F. Marini, C. Santi, *Synlett* **2001**, 1767–1771.
- [32] M. Tingoli, M. Tiecco, L. Testaferri, A. Temperini, *Synth. Commun.* **1998**, 28, 1769–1778.
- [33] Y. H. Kim, K. R. Roh, H. K. Chang, *Heterocycles* **1998**, 48, 437.
- [34] A. A. Vieira, J. B. Azeredo, M. Godoi, C. Santi, E. N. da Silva Júnior, A. L. Braga, *J. Org. Chem.* **2015**, 80, 2120–2127.
- [35] M. Liu, Y. Li, L. Yu, Q. Xu, X. Jiang, *Sci. China Chem.* **2018**, 61, 294–299.
- [36] G. Perin, P. Santoni, A. M. Barcellos, P. C. Nobre, R. G. Jacob, E. J. Lenardão, C. Santi, *European J. Org. Chem.* **2018**, 1224–1229.
- [37] Z.-P. Liang, W. Yi, P.-F. Wang, G.-Q. Liu, Y. Ling, *J. Org. Chem.* **2021**, 86, 5292–5304.
- [38] C. G. Francisco, E. I. León, J. A. Salazar, E. Suárez, *Tetrahedron Lett.* **1986**, 27, 2513–2516.
- [39] E. Tang, W. Wang, Y. Zhao, M. Zhang, X. Dai, *Org. Lett.* **2016**, 18, 176–179.
- [40] K. Sun, X. Wang, Y. Lv, G. Li, H. Jiao, C. Dai, Y. Li, C. Zhang, L. Liu, *Chem. Commun.* **2016**, 52, 8471–8474.
- [41] X. Wang, H. Li, M. Zhu, J. Yan, *RSC Adv.* **2017**, 7, 15709–15714.
- [42] B. Huang, Y. Li, C. Yang, W. Xia, *Green Chem.* **2020**, 22, 2804–2809.
- [43] H. Luo, Z. Yang, W. Lin, Y. Zheng, S. Ma, *Chem. Sci.* **2018**, 9, 1964–1969.
- [44] H. Newman, A. Krajnc, D. Bellini, C. J. Eyermann, G. A. Boyle, N. G. Paterson, K. E. McAuley, R. Lesniak, M. Gangar, F. von Delft, J. Brem, K. Chibale, C. J. Schofield, C. G. Dowson, *J. Med. Chem.* **2021**, 64, 11379–11394.

- [45] D. Schmidt, T. Rodat, L. Heintze, J. Weber, R. Horbert, U. Girreser, T. Raeker, L. Bußmann, M. Kriegs, B. Hartke, C. Peifer, *ChemMedChem* **2018**, *13*, 2415–2426.
- [46] M. E. Matyskiela, W. Zhang, H.-W. Man, G. Muller, G. Khambatta, F. Baculi, M. Hickman, L. LeBrun, B. Pagarigan, G. Carmel, C.-C. Lu, G. Lu, M. Riley, Y. Satoh, P. Schafer, T. O. Daniel, J. Carmichael, B. E. Cathers, P. P. Chamberlain, *J. Med. Chem.* **2018**, *61*, 535–542.
- [47] H. Park, S. Hong, S. Hong, *ChemMedChem* **2012**, *7*, 53–56.
- [48] Q. Li, K. W. Woods, A. Claiborne, S. L. Gwaltney, II, K. J. Barr, G. Liu, L. Gehrke, R. B. Credo, Y. H. Hui, J. Lee, R. B. Warner, P. Kovar, M. A. Nukkala, N. A. Zielinski, S. K. Tahir, M. Fitzgerald, K. H. Kim, K. Marsh, D. Frost, S.-C. Ng, S. Rosenberg, H. L. Sham, *Bioorg. Med. Chem. Lett.* **2002**, *12*, 465–469.
- [49] J. T. Moore, C. Soldi, J. C. Fettingner, J. T. Shaw, *Chem. Sci.* **2013**, *4*, 292–296.
- [50] W. Niu, Y.-Y. Yeung, *Org. Lett.* **2015**, *17*, 1660–1663.
- [51] Y. Ni, H. Zuo, Y. Li, Y. Wu, F. Zhong, *Org. Lett.* **2018**, *20*, 4350–4353.
- [52] Q.-B. Zhang, P.-F. Yuan, L.-L. Kai, K. Liu, Y.-L. Ban, X.-Y. Wang, L.-Z. Wu, Q. Liu, *Org. Lett.* **2019**, *21*, 885–889.
- [53] O. Niyomura, M. Cox, T. Wirth, *Synlett* **2006**, 251–254.
- [54] L. Sun, Y. Yuan, M. Yao, H. Wang, D. Wang, M. Gao, Y.-H. Chen, A. Lei, *Org. Lett.* **2019**, *21*, 1297–1300.
- [55] Z. Guan, Y. Wang, H. Wang, Y. Huang, S. Wang, H. Tang, H. Zhang, A. Lei, *Green Chem.* **2019**, *21*, 4976–4980.
- [56] X. Meng, P. Zhong, Y. Wang, H. Wang, H. Tang, Y. Pan, *Adv. Synth. Catal.* **2020**, *362*, 506–511.
- [57] T. Noël, Y. Cao, G. Laudadio, *Acc. Chem. Res.* **2019**, *52*, 2858–2869.
- [58] A. Kaye, S. Neidle, C. B. Reese, *Tetrahedron Lett.* **1988**, *29*, 2711–2714.
- [59] A. G. Meirinho, V. F. Pereira, G. M. Martins, S. Saba, J. Rafique, A. L. Braga, S. R. Mendes, *European J. Org. Chem.* **2019**, *2019*, 6465–6469.
- [60] “CCDC-1980248 (3.72) contains the supplementary crystallographic data. These data can be obtained free of charge from The Cambridge Crystallographic Data Centre via,” can be found under www.ccdc.cam.ac.uk/getstructures.
- [61] M. Wilken, S. Ortgies, A. Breder, I. Siewert, *ACS Catal.* **2018**, *8*, 10901–10912.
- [62] J. Chen, L. Mei, H. Wang, L. Hu, X. Sun, J. Shi, Q. Li, *ChemistryOpen* **2019**, *8*, 1230–1234.

- [63] X. Zhang, C. Wang, H. Jiang, L. Sun, *Chem. Commun.* **2018**, 54, 8781–8784.
- [64] N. Amri, T. Wirth, *Synthesis* **2020**, 52, 1751–1761.

CHAPTER 4

Electrochemical Synthesis of Chalcogenophosphites

CHAPTER 4: Electrochemical Synthesis of Chalcogenophosphites	117
4.1. Introduction.....	119
4.2. Typical processes for the synthesis of chalcogenophosphites	119
4.3. Electrochemical processes for the synthesis of chalcogenophosphites	121
4.3.1. Electrochemical oxygen–phosphorus bond formation	121
4.3.2. Electrochemical sulfur–phosphorus bond formation.....	123
4.3.3. Electrochemical selenium–phosphorus bond formation.....	125
4.4. Flow electrochemical synthesis of chalcogenophosphites.....	126
4.4.1. Results and discussions.....	127
4.4.1.1. Optimisation of the reaction conditions	127
4.4.1.2. Substrate scope	128
4.4.1.3. Reaction mechanism	130
4.5. Conclusion and outlook	131
4.6. References	133

4.1. Introduction

Organophosphorus compounds have been established and studied for over a century.^[1,2] It is found in vast a range of different compounds from small molecules to large polymeric molecules. Organophosphorus compounds, especially containing chalcogens such as selenium and sulfur, are widely applied in agriculture, material chemistry and as ligands in organometallic chemistry.^[3,4] Selenium–phosphorus or sulfur–phosphorus bonds are part of a large number of phosphorus compounds that can be found in a variety of biologically active molecules (Figure 4.1).^[5,6]

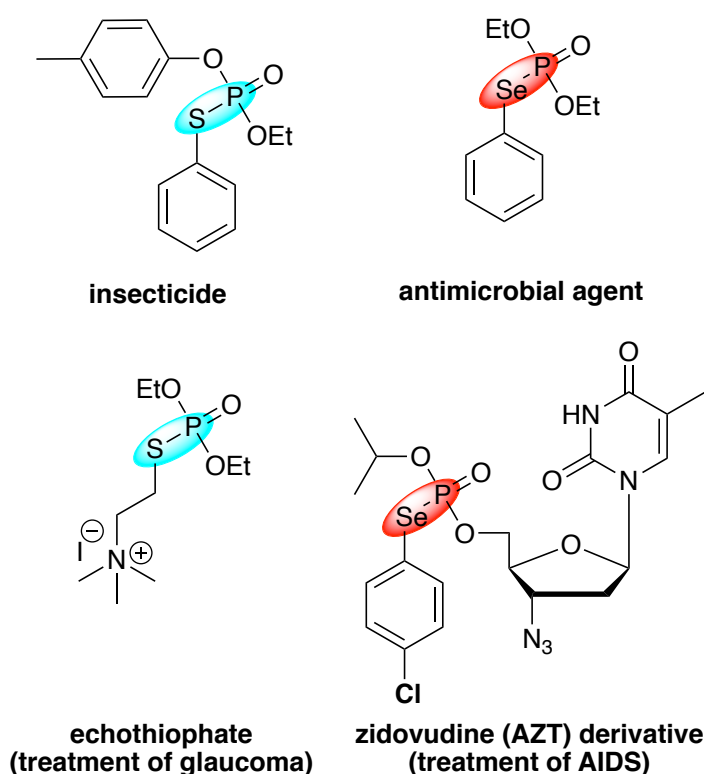


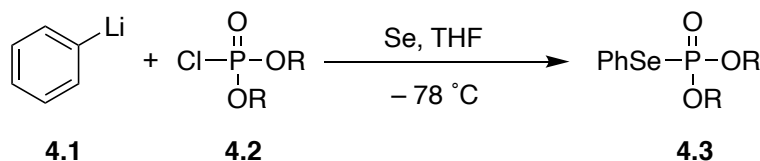
Figure 4.1. Bioactive molecules containing selenium–phosphorus or sulfur–phosphorus bonds.

4.2. Typical processes for the synthesis of chalcogenophosphites

Various reactions processes have been developed for making selenium- or sulfur–phosphorous bonds, but the synthesis of selenophosphonates has received less attention compared to the synthesis of thiophosphonates. The most of these methods are carried out by using expensive metals or toxic reagents.

A classical approach to produce selenophosphites is the coupling of *O,O*-diaryl- or dialkyl-phosphoryl chloride (4.2) with solution of PhSeLi which is *in situ* generated by the reaction of PhLi (4.1) with Se (Scheme 4.1).^[7] However, this reaction is operated at cryogenic temperatures (−78 °C), leading to synthesis of phenylselenophosphites products 4.3 in

moderate yields. The phosphorous-selenium bond is utilized in oxidative additions with Pd(0) and Pt(0) complexes for selenophosphorylation of alkynes.^[7]

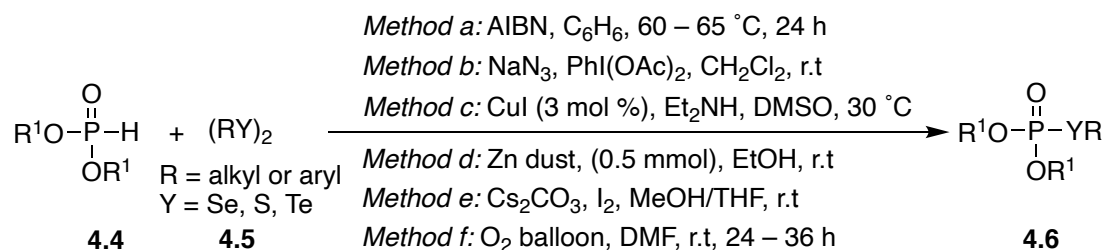


Scheme 4.1. Synthesis of phenylselenenophosphates using PhLi.

In 2003, Huang *et al.* described the synthesis of chalcogenophosphites **4.6** via the coupling of dialkyl phosphites **4.4** with diaryl diselenide **4.5** (Scheme 4.2, method a).^[8] Phosphonyl radicals were generated by using AIBN as the radical initiator for successful trapping by diaryl diselenide to give the aryl-selenophosphates products **4.6** in good to excellent yields. Similarly, the use of diaryldisulfides and diarylditellurides with dialkyl phosphites was also achieved under the optimum condition to produce the corresponding aryl-thiophosphates and aryl-tellurophosphates, respectively. A similar approach for the synthesis of chalcogenophosphites **4.6** using the same starting materials and (diacetoxyiodo)benzene and sodium azide was studied by Chen and co-workers (Scheme 4.2, method b).^[9] However, the substrate scope for both reactions is limited to alkyl-phosphites only.

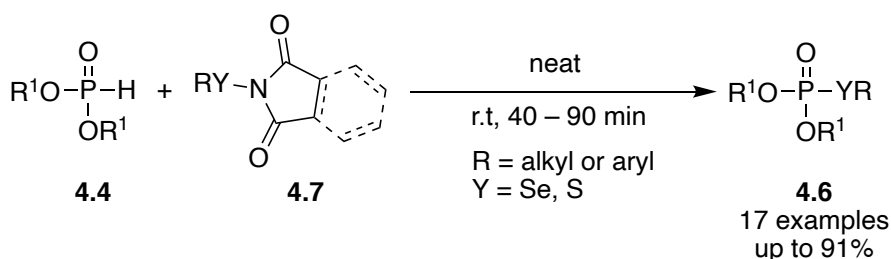
In 2009, Zhao and co-workers also developed an alternative method for the synthesis of chalcogenophosphites **4.6** (Scheme 4.2, method c).^[10] The cross-coupling between the dialkyl phosphite **4.4** and diaryl dichalcogenide **4.5** in DMSO was achieved using copper catalysis, leading to chalcogenophosphites products **4.6** in good yields. However, in this reaction, a stoichiometric amount of organic base and only alkyl-phosphites were utilised. Along the same technique, Hajra and co-workers have used zinc dust (0.5 equiv.) to synthesise the desired chalcogenophosphites **4.6** (Scheme 4.2, method d).^[11] However, zinc dust is quite toxic and undesirable from the standpoint of green chemistry. In a different report, cesium carbonate (Cs₂CO₃) and molecular iodine (I₂) promoted the synthesis of chalcogenophosphites from diaryl dichalcogenide and different phosphites (Scheme 4.2, method e).^[12]

More recently, Jana *et al.* showed an economical method, in which selenophosphites **4.6** are prepared in a single step starting from the phosphite **4.5** and diselenides **4.5** (Scheme 4.2, method f).^[13] The reaction used molecular oxygen as the oxidant at room temperature.



Scheme 4.2. Different processes for the synthesis of selenophosphosphites.

Very recently (2019), Saha and co-workers developed a simple approach by using a *N*-chalcogenoimides **4.7** as chalcogenyl source and oxidant (Scheme 4.3).^[14] Under catalyst, base- and solvent- free conditions, *N*-chalcogenoimides **4.7** were utilised to chalcogenylate phosphite moieties **4.4**, offering selenophosphosphites products **4.6** in good yields.



Scheme 4.3. Chalcogenylation of phosphite **4.4** by using *N*-chalcogenoimides **4.7**.

4.3. Electrochemical processes for the synthesis of chalcogenophosphites

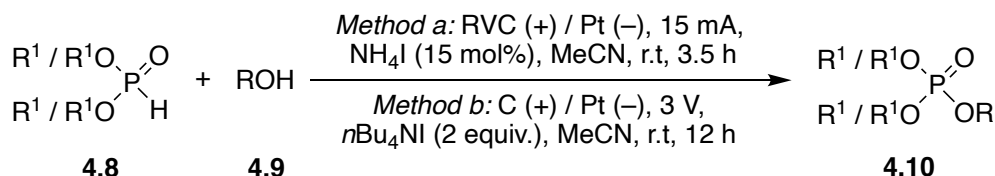
In order to offer ecological and sustainable synthetic methods, electricity has also been utilised for phosphorylation reactions.^[15,16] Different oxygen–phosphorus (O–P), sulfur–phosphorus (S–P) and selenium–phosphorus (Se–P) bonds were formed by using different nucleophiles under electrochemical conditions.

4.3.1. Electrochemical oxygen–phosphorus bond formation

Formation of oxygen–phosphorus (O–P) bond is very significant in biological systems. The Atherton-Todd reaction is a well-known technique for forming P–O bonds.^[17,18] The cross coupling of diaryl phosphites with alcohols has recently been reported in the presence of stoichiometric quantities of oxidants or metals catalysts.

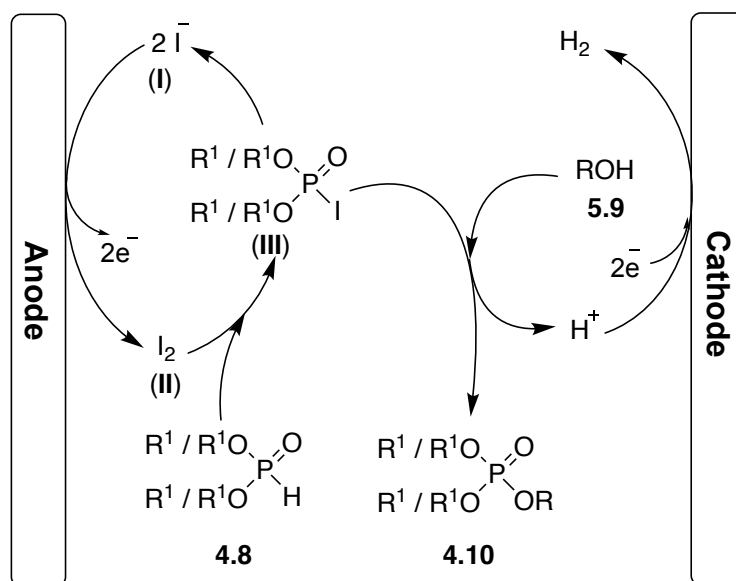
Tang and co-authors demonstrated a sustainable and green process for the synthesis of organophosphites **4.10** through electrochemical oxidative coupling of H-phosphoryl substrates **4.8** with alcohols **4.9** (Scheme 4.4, method a).^[19] The reaction was performed at room temperature in an undivided batch cell under constant current (15 mA) in the presence of ammonium iodide (NH₄I) as mediator and supporting electrolyte. Likewise, Han and co-authors reported the same approach using *n*Bu₄NI as mediator and supporting electrolyte under

constant voltage (3 V) conditions at room temperature (Scheme 4.4, method b).^[20] In both protocols, carbon electrodes were employed as the anode and platinum electrodes as the cathode in an undivided batch cell. A wide range of alkyl and aryl phosphite esters (**4.8**) were converted to their corresponding organophosphate compounds (**4.10**) in the presence of various alcohols.



Scheme 4.4. Electrochemical O–P bond formation *via* iodide mediator.

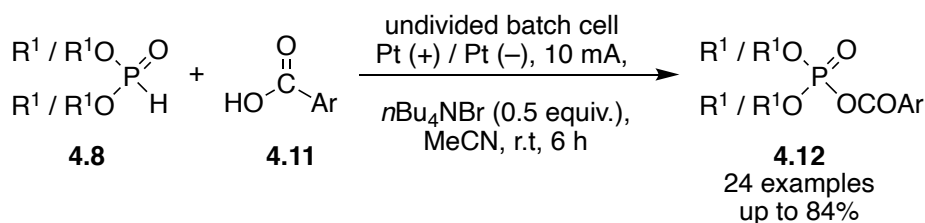
The proposed mechanism for this transformation is identical in both protocols. At the anode, the iodide anion **I** is first oxidised to produce molecular iodine **II**. Then, **II** generates the phosphoryl iodide intermediate **III** *via* iodination of H-phosphite **4.8**. Next, a nucleophilic substitution occurs between intermediate **III** and alcohol **4.9**, resulting in the formation of organophosphinates product **4.10**. At the same time, the proton produced in this process is reduced to hydrogen at the cathode.



Scheme 4.5. Plausible mechanism for electrochemical O–P bond formation *via* iodide mediator.

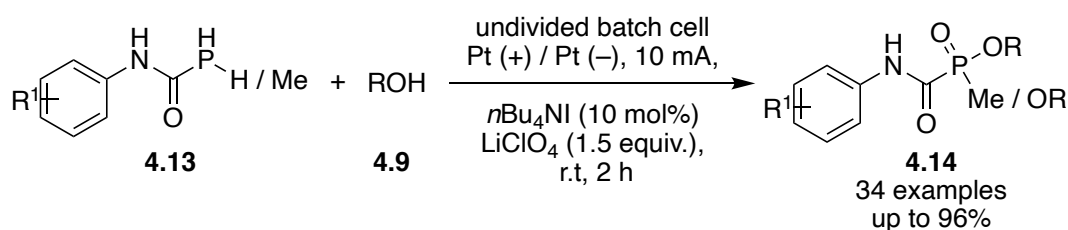
Subsequently in 2020, Cai and co-authors also documented useful electrochemical synthesis of acyl phosphates from phosphites and carboxylic acids in the presence of *n*Bu₄NBr as both mediator and supporting electrolyte (Scheme 4.6).^[21] The reaction was demonstrated in an undivided batch cell with platinum electrodes as anode and cathode under galvanostatic reaction conditions at room temperature for 6 h. The broad scope of carboxylic acids and

phosphite substrates bearing diverse functional groups delivered the acyl phosphates in moderate to excellent yields. The suggested mechanism of this reaction is similar to that shown in Scheme 4.5, in which molecular bromine (Br_2) is produced from bromide anion (Br^-) at the anode, which subsequently oxidises phosphite **4.8** to generate the phosphoryl bromide intermediate, which is then attacked by the acid anion to result in the O–P bonded product **4.12**.



Scheme 4.6. O–P bond formation *via* electrochemical coupling of phosphites with carboxylic acids.

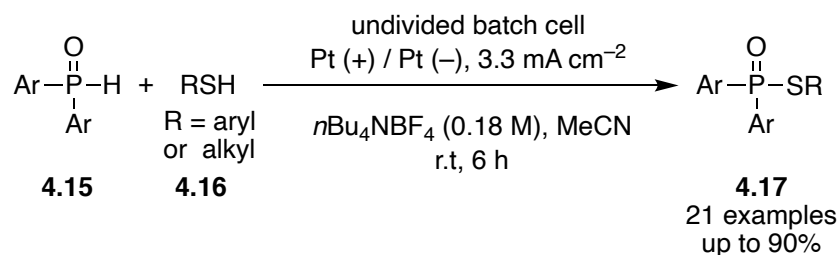
In 2019, Quan and co-authors developed an alternative electrochemical approach for $n\text{Bu}_4\text{NI}$ mediated synthesis of carbamoylphosphonates **4.14** from phosphoramides **4.13** and alcohols **4.9** (Scheme 4.7).^[22] Alcohol was used as a solvent as well as the reagent. The reaction is carried out in an undivided batch cell under galvanostatic reaction conditions with platinum plates as anode and cathode, and LiClO_4 as electrolyte at ambient temperature. A wide range of the desired products (**4.14**) was successfully achieved through this technique in moderate to good yields.



Scheme 4.7. Electrochemical synthesis of carbamoylphosphonates **4.14**.

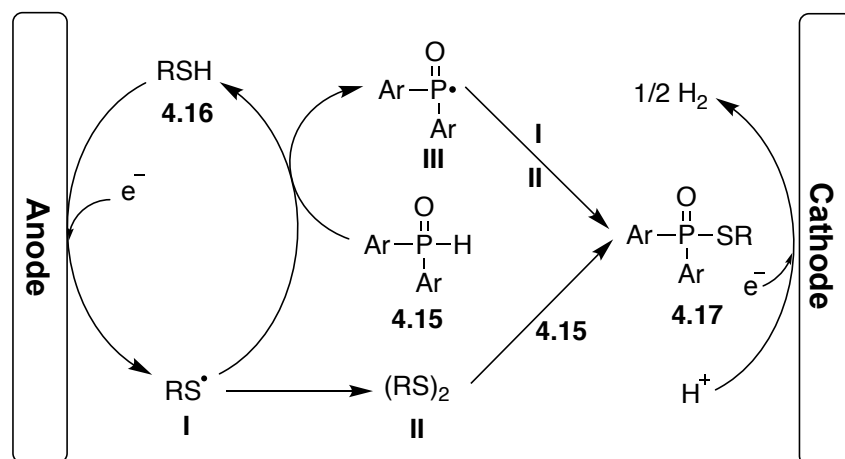
4.3.2. Electrochemical sulfur–phosphorus bond formation

An efficient electrochemical oxidative method for S–P bond production *via* diphenyl phosphine oxides **4.15** and thiol compounds **4.16** was developed in 2019 by Zheng and co-workers (scheme 4.8).^[23] The optimum condition was achieved by using platinum electrodes and $n\text{Bu}_4\text{NBF}_4$ as an electrolyte in MeCN. Different alkyl and aryl substituted thiol substrates were assessed to provide a wide range of corresponding thiophosphates **4.17** in moderate to high yields. In this reaction, the substrate scope is limited to aryl phosphine oxides.



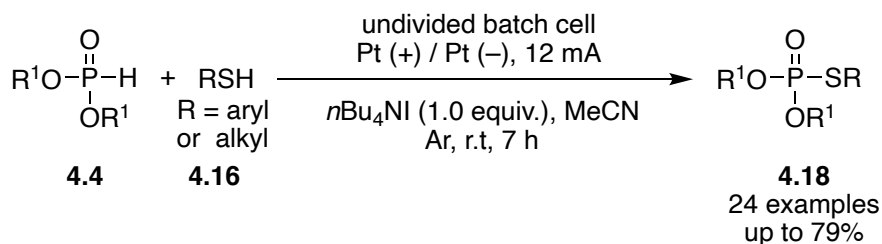
Scheme 4.8. Electrochemical synthesis of thiophosphates **4.17**.

The suggested mechanism for this electrochemical cross-coupling process is illustrated in Scheme 4.9. Initially, sulfur radicals **I** are formed at the anode *via* single-electron-transfer (SET) oxidation of thiols **4.16**. Subsequently, the dimerization of sulfur radicals **I** set an equilibrium to produce disulfides **II**. Meanwhile, **I** also produce the phosphorus radicals intermediate **III** *via* a hydrogen atom transfer (HAT). Then, **III** undergoes direct coupling with sulfur radicals or disulfides to produce the desired product **4.17**.



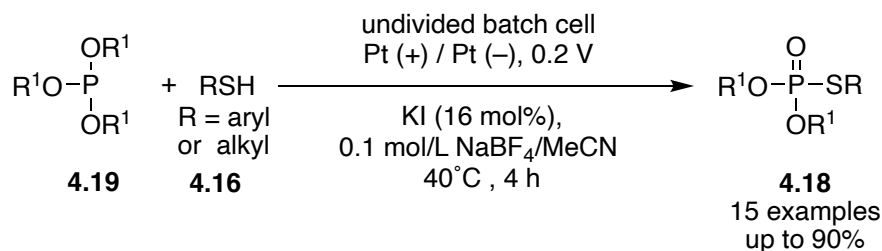
Scheme 4.9. Plausible mechanism for electrochemical synthesis of thiophosphates **4.17**.

At the same year (2019), Lee and co-authors published a similar approach for the synthesis of thiophosphites under electrochemical process in the presence of $n\text{Bu}_4\text{NI}$ as a mediator (Scheme 4.10).^[24] The reaction was implemented in an undivided batch cell with platinum electrodes in MeCN at room temperature. The substrates scope was extended to phosphite derivatives with diverse range of thiols, leading to 24 examples of thiophosphite products in moderate yields.



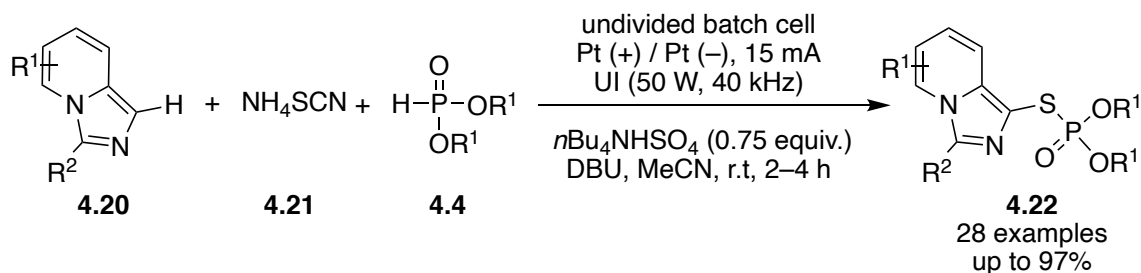
Scheme 4.10. Electrochemical synthesis of thiophosphites **4.18** using $n\text{Bu}_4\text{NI}$ as a mediator.

Very recently in 2021, Le and co-authors established an indirect electrochemical synthesis of thiophosphites **4.18** starting from trialkyl phosphites **4.19** and thiols **4.16** (Scheme 4.11).^[25] The use of KI as a redox mediator plays an important role in this reaction by delivering the products **4.18** at lower potential. The optimal condition for this reaction was carried out in undivided batch cell, with platinum electrodes in 0.1 M solution of NaBF₄ in CH₃CN under constant voltage (0.2 V) at 40 °C. A variety of phosphorothioates **4.18** were produced in good yields under these conditions.



Scheme 4.11. Electrochemical oxidative coupling of trialkyl phosphites with thiols.

A novel and powerful protocol for the S–P bond formation through the combination of both electricity and ultrasound has been also developed in 2021 by Xu and co-workers.^[26] This oxidative cross-coupling was achieved in one-pot, three component fashion involving thiocyanate **4.21** with dialkyl phosphite **4.4** and (hetero)arenes **4.20** to generate the *S*-(hetero)aryl phosphorothioates products **4.22** in moderate to excellent yields. This substrate combinations with *n*Bu₄NHSO₄/CH₃CN as the electrolytic solution and 1,8-diazabicyclo[5.4.0]undec-7-ene (DBU) were charged into undivided batch cell, with platinum plates as anode and cathode under constant current (15 mA) and ultrasonic irradiation (50 W, 40 kHz) conditions at room temperature. In this case, different (hetero)arene substrates **4.20** were tolerated, but only alkyl phosphites delivered the desired products.

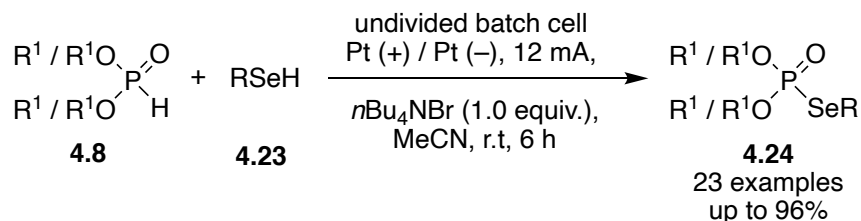


Scheme 4.12. Electrochemical thiophosphination of heterocycles **4.20**.

4.3.3. Electrochemical selenium–phosphorus bond formation

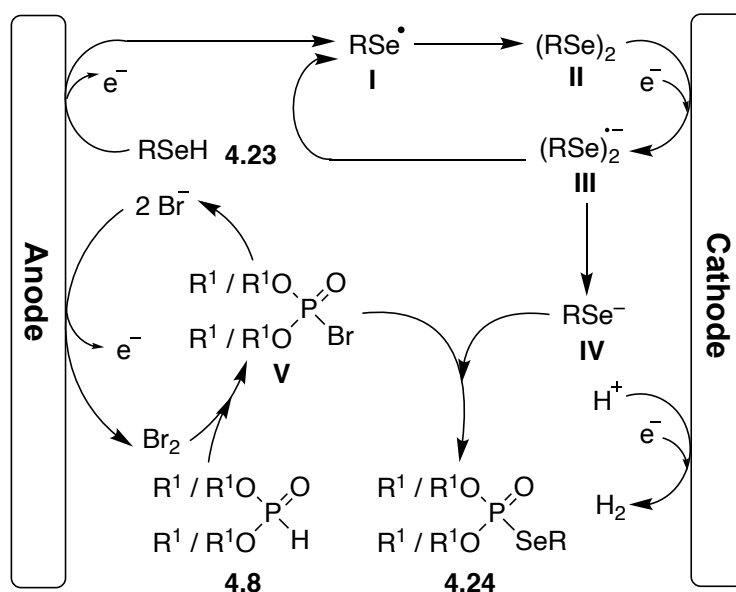
In 2020, Cai and co-authors described an electrochemical cross-coupling method for the Se–P bond formation using *n*Bu₄NBr as the redox mediator (Scheme 4.13).^[27] This electrochemical method uses selenols **4.23** and phosphites or phosphine oxides **4.8** to generate valuable

selenophosphites **4.24** in good to excellent yields. The electrolysis was carried out in an undivided cell under constant current of 12 mA using $n\text{Bu}_4\text{NBr}$ as the supporting electrolyte with platinum electrodes at room temperature. Under these conditions, vast range of phosphites **4.8** were efficiently tolerated, leading to the products **4.24** in good to excellent yields.



Scheme 4.13. Electrochemical synthesis of selenophosphites **4.24** in batch cell.

The proposed mechanism for this reaction is illustrated in Scheme 4.13. At the anode, selenol **4.23** is first oxidized to generate selenyl radical **I**, which is then dimerized to produce diselenide **II**. At the cathode, **II** is reduced to generate radical anion **III**, which can generate **I** and selenyl anion **IV**. Meanwhile, molecular bromine (Br_2) is produced from bromide anion (Br^-) at the anode, which subsequently oxidizes phosphite **4.8** to generate the phosphoryl bromide intermediate **V**, which is then attacked by **IV** to form a new Se–P bond in the products **4.10**.



Scheme 4.14. Plausible mechanism for electrochemical Se–P bond formation *via* bromide mediator.

4.4. Flow electrochemical synthesis of chalcogenophosphites

The flow electrochemical processes have not been investigated to generate chalcogenophosphites derivatives. As described in the above sections, several methods including electrochemical techniques have been carried out to synthesize chalcogenophosphites compounds, but these methods have some drawbacks such as the use of

toxic or expensive catalysts, long reactions time and the requirement of excess amounts of electrolytes. Hence, exploiting our previous experiences in flow transformations for selenenylations of alkene using integrated flow electrochemical reactor in an automated manner,^[28] the synthesis of chalcogenophosphite derivatives is purposed. The same methodology is used in this study for the efficient synthesis of phosphorus–selenium and phosphorus–sulfur bonds (Figure 4.2).

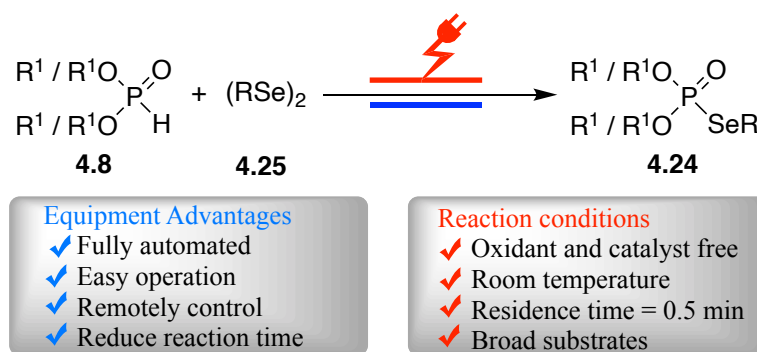


Figure 4.2. Automated flow electrochemical synthesis of chalcogenophosphites.

The Vapourtec automated flow machine with combined Ion electrochemical flow reactor offers unique properties that speeds up the reaction process while minimising the needed manpower. The system can self-load the desired starting materials, self-collect the reaction products, and auto-clean itself while maintaining precise temperature, flow rate, and current control in each reaction. It can also be controlled remotely from other locations with an internet connection. This system is only limited to the accessible number of loading and collecting vials.

4.4.1. Results and discussions

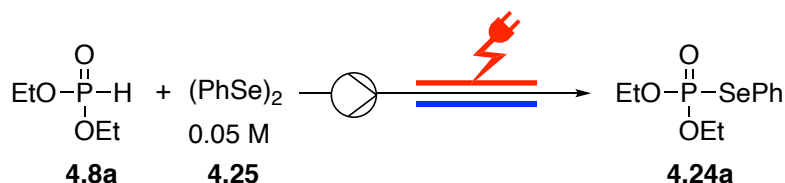
4.4.1.1. Optimisation of the reaction conditions

Initially the reaction between diethylphosphite (**4.8a**) and diphenyl diselenide (**4.25**) in acetonitrile as a model reaction was studied using different reaction conditions such as electrode materials, solvents, flow rates, and electrolytes.

In this process, different concentration of diethylphosphite (**4.8a**) from 0.1 M to 0.25 M were screened and 0.2 M exhibited the best yield of 90% (Table 4.1, entries 1–3). Next, various supporting electrolytes such as *n*Et₄NI, *n*Et₄NBr, *n*Et₄NCl, *n*Bu₄NBF₄ and *n*Bu₄NClO₄ were tested, and *n*Et₄NCl provided the optimum yield of 97 % (Table 4.1, entries 4–7). To reduce the reaction time, the flow rate was raised from 1.0 mL/min to 1.8 mL/min. However, at 1.2 mL/min, 97 % yield was obtained, while higher flow rates resulted in lower yields (Table 4.1, entries 8–10). Acetonitrile was found as the preferred solvent, while dichloromethane, methanol

and dimethylformamide resulted in lower yields (Table 4.1, entries 11–13). Change in electrode combinations showed a small effect on the product yields (Table 4.1, entries 14–15).

Table 4.1. Reaction of **4.8a** and **4.25** to *O,O*-diethyl *Se*-phenyl phosphoroselenoate **4.24a** under flow electrolysis.^[a]



Entry	Electrolyte	Flow rate [ml/min]	Current [mA]	4.24a Yield[%] ^[b]
1 ^[c]	Bu ₄ NI	1.0	80	66
2 ^[d]	Bu ₄ NI	1.0	80	83
3	Bu ₄ NI	1.0	80	90
4	Et ₄ NBr	1.0	80	94
5	Et ₄ NCl	1.0	80	97
6	Bu ₄ NBF ₄	1.0	80	52
7	Bu ₄ NClO ₄	1.0	80	44
8	Et₄NCl	1.2	96	97
9	Et ₄ NCl	1.4	112	94
10	Et ₄ NCl	1.8	144	90
11 ^[e]	Et ₄ NCl	1.2	96	68
12 ^[f]	Et ₄ NCl	1.2	96	56
13 ^[g]	Et ₄ NCl	1.2	96	50
14 ^[h]	Et ₄ NCl	1.2	96	92
15 ^[i]	Et ₄ NCl	1.2	96	87

[a] Reaction conditions: Graphite anode, Pt cathode, **4.8a** (0.2 M), **4.25** (0.05 M), electrolyte (0.01 M), acetonitrile was used as solvent. [b] Determined by using ¹H NMR with 1,3,5-trimethoxybenzene as an internal standard. [c] 0.1 M of **4.8a**. [d] 0.15 M of **4.8a**. [e] Dichloromethane was used as solvent. [f] Methanol was used as solvent. [g] Dimethylformamide was used as solvent. [h] Glassy carbon anode, Pt cathode. [i] Pt anode, Pt cathode.

4.4.1.2. Substrate scope

The optimum reaction conditions with the maximum space-time yield are shown in entry 8 of Table 4.1, where diethylphosphite (**4.8a**, 0.2 M) and diphenyl diselenide (**4.25**, 0.05 M) were reacted in the presence of graphite and platinum electrodes with a flow rate of 1.2 mL/min, and applied current

of 96 mA. These conditions are now being used in the automated synthesis of a wide range of products to study the usefulness and broad application of this electrochemical technique (Figure 4.3).

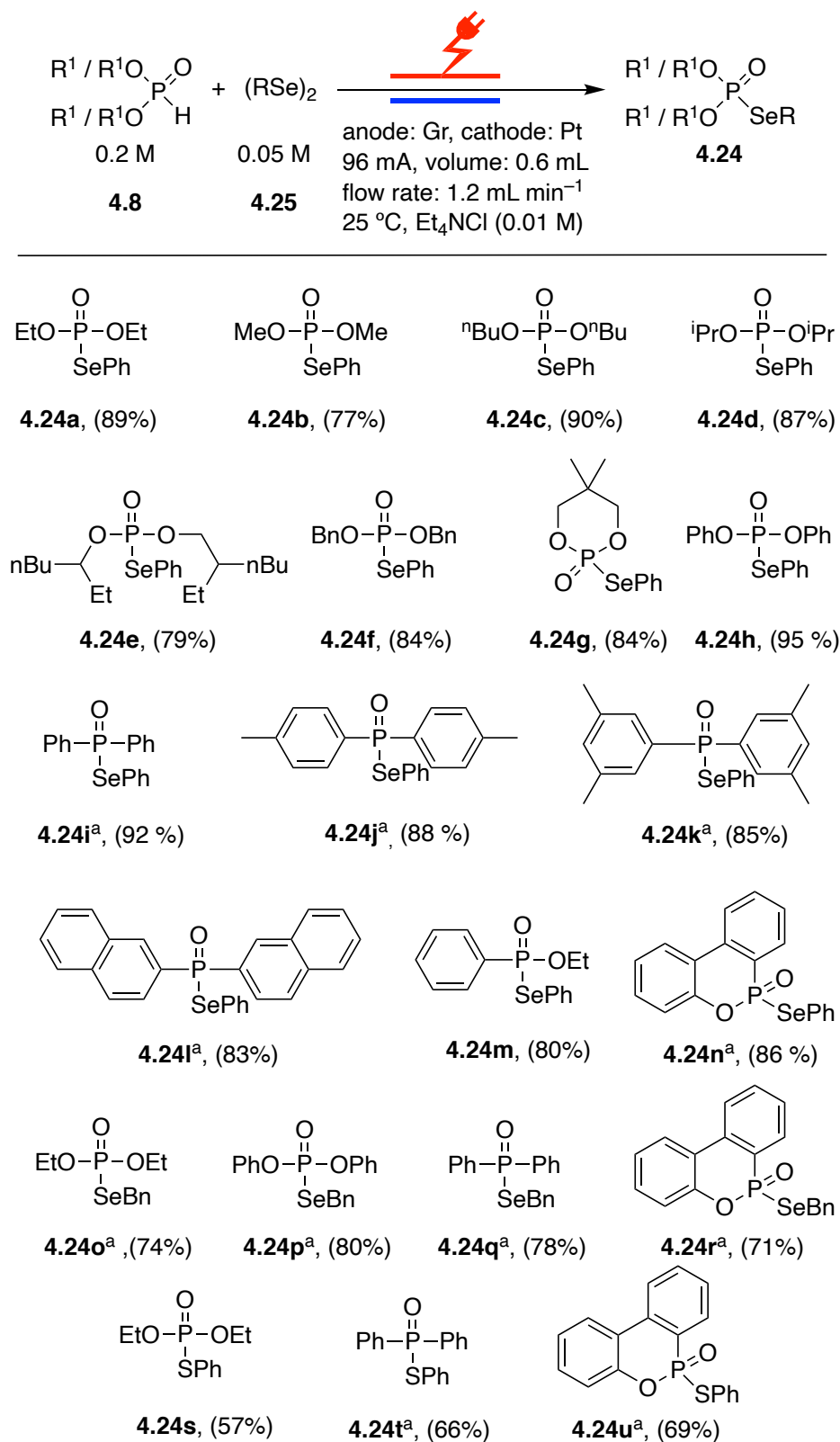


Figure 4.3. Substrate scope for the electrochemical selenenylation and thiolation of phosphites. [a] Mixture of CH₃CN / THF (1:1) was used.

Phosphite derivatives such as ethoxy (**4.8a**), methoxy (**4.8b**), *n*-butoxy (**4.8c**), isopropoxy (**4.8d**), 2-ethylhexyl (**4.8e**) and benzyl (**4.8f**) provided the products in good yields. A cyclic phosphite was investigated and formed the product **4.24g** with 84% isolated yield. Similarly, the phenoxy substituted product **4.24h** was formed in an excellent yield of 95%. Among different phosphine oxide derivatives, the phenyl (**4.8i**), tolyl (**4.8j**), 3,5-dimethyl benzene (**4.8k**) and 2-naphthyl (**4.8l**) the corresponding substituted products were isolated in good yields. Also, unsymmetrical phosphonates bearing ethoxy and phenyl substituents provided the product **4.24m** in 80% yield. Cyclic phosphine **4.24n** was formed in 86% yield. Similar to diphenyl diselenide, other dichalcogenides such as dibenzyl diselenide and diphenyl disulfide could be employed to give phosphorselenoates **4.24o–4.24r** and phosphorsulfonates **4.24s–4.24u**, but the yields of the phosphorsulfonates were found to be slightly lower than the yields of the corresponding phosphorselenoates.

4.4.1.3. Reaction mechanism

In order to get some insight into the mechanism, we studied the electrooxidation properties of each compound (Figure 4.4). From cyclic voltammetry (CV) measurements, diethyl phosphite (**4.8a**) shows no oxidation peak (Figure 4.4, yellow line) and diphenyl diselenide (**4.25**) shows two oxidation peaks at $E_p = 1.46$ V and $E_p = 1.8$ V vs Ag/AgCl (Figure 4.4, dark green line) while Et_4NCl showed an obvious oxidation peak at $E_p = 1.41$ V vs Ag/AgCl (Figure 4.4, blue line).

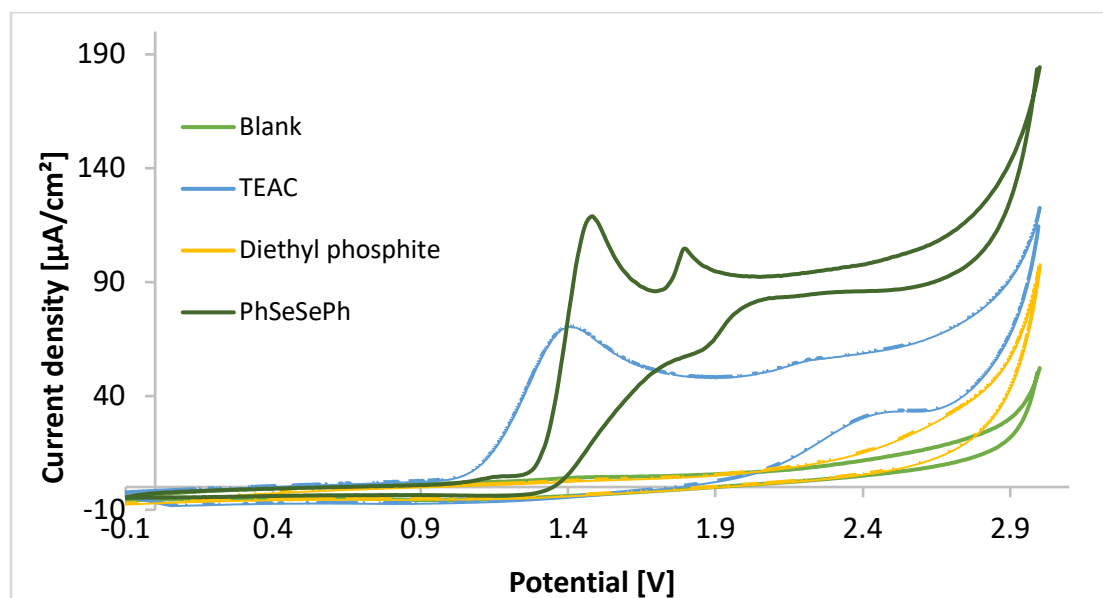
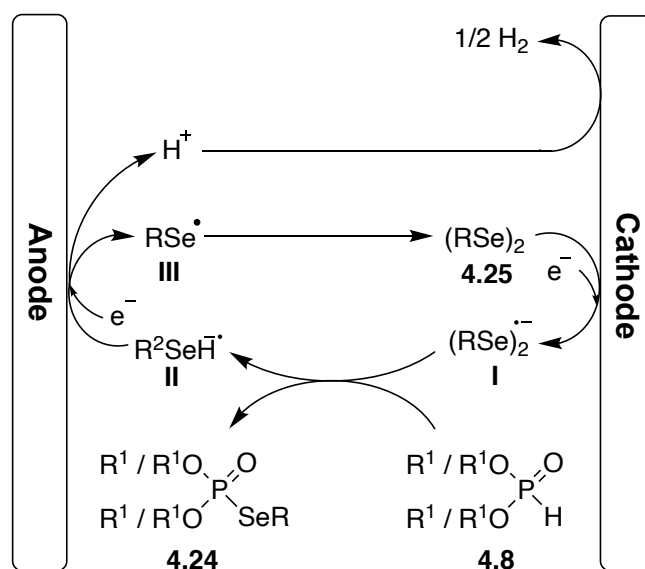


Figure 4.4. Cyclic voltammogram (CV) of substrate diethyl phosphite (5m M); diphenyl diselanide (5m M) and Et_4NCl (5m M) in 0.1M LiClO_4 / MeCN electrolyte (20 mV s^{-1} scan rate). Working electrode: glassy carbon electrode tip (3 mm diameter); Counter electrode: platinum wire; Reference electrode: Ag/AgCl in 3 M KCl.

According to the previous literature reports and our preliminary studies,^[20–27] the hypothesized mechanism involved in the selenenylation of phosphites is illustrated in Scheme 4.15. The diselenide **4.25** is reduced at the cathode to produce the radical anion **I**, which then reacts with the phosphite **4.8** to generate the selenophosphite **4.24** and the radical anion **II**. This intermediate **II** is then oxidized to the selenyl radical **III** which dimerises to **4.25** and a proton, which will be finally reduced to hydrogen at the cathode. Other mechanisms in the literature suggest the involvement of elemental halides^[20,24,27] or halide radicals^[29] produced from the supporting electrolyte. This cannot be excluded here, but according to the work published by Zheng *et al.*^[23] (Explained in section 4.3.2, Scheme 4.9) and the fact that the reaction proceeds also without halide anions (Table 4.1, entries 6 and 7) indicate that a different mechanism should be operating for such reaction.



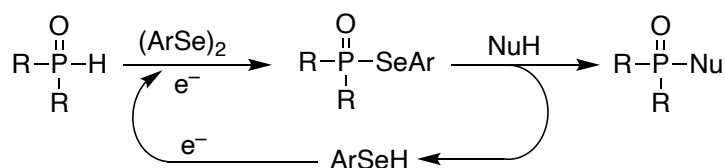
Scheme 4.15. Proposed mechanism for the electrochemical synthesis of selenophosphites.

4.5. Conclusion and outlook

In conclusion, the direct anodic cross-coupling of phosphites with diselenide and disulfide to the corresponding phosphorselenoates and phosphorsulfonates, respectively has been developed. In this protocol, there is only need for tiny amounts of supporting electrolyte. The use of an automated flow system combined with electrochemical microreactor shows the capability and advantages of flow electrochemistry and efficiently improves the outcome the reported process for the formation of P–Se and P–S bonds. The scope and limitation of the technique was demonstrated with a vast range of substrates. Compared to previous procedures, this method is fast, inexpensive, metal-free, and environmentally friendly and most

importantly, automated. This advanced method can be useful for future research in synthesizing organic compounds electrochemically through automation techniques.

In future, this type of cross-coupling can be further extended to the formation of carbon-phosphorus and oxygen-phosphorus bonds. Also, the use of diselenide as catalyst for the nucleophilic functionalization of phosphites can be developed under the flow electrochemical setup (Scheme 4.16).^[30] Certainly, the remote-controlled technique has been demonstrated to accelerate the reaction optimization and preparation in a short time. This easy-to-use automated tool can be explored in further electrochemical transformations as well.



Scheme 4.16. Organocatalytic activation of phosphites.

This work has already been published^[31]

4.6. References

- [1] L. D. Quin, *A Guide to Organophosphorus Chemistry*, New York, **2000**.
- [2] M. Dekker, *Handbook of Organophosphorus Chemistry*, **1992**.
- [3] G. Hua, J. D. Woollins, *Angew. Chem. Int. Ed.* **2009**, *48*, 1368–1377.
- [4] G. Mugesh, W.-W. du Mont, H. Sies, *Chem. Rev.* **2001**, *101*, 2125–2180.
- [5] W. R. Morton, S. M. Drance, M. Fairclough, *Am. J. Ophthalmol.* **1969**, *68*, 1003–1010.
- [6] A. Masahiro, *Patent JP*, 53095946, 1978, **1978**, JP 53095946.
- [7] L.-B. Han, N. Choi, M. Tanaka, *J. Am. Chem. Soc.* **1996**, *118*, 7000–7001.
- [8] Q. Xu, C.-G. Liang, X. Huang, *Synth. Commun.* **2003**, *33*, 2777–2785.
- [9] D.-J. Chen, Z.-C. Chen, *J. Chem. Res.* **2000**, 370–371.
- [10] Y.-X. Gao, G. Tang, Y. Cao, Y.-F. Zhao, *Synthesis*. **2009**, 1081–1086.
- [11] S. Mitra, S. Mukherjee, S. K. Sen, A. Hajra, *Bioorg. Med. Chem. Lett.* **2014**, *24*, 2198–2201.
- [12] J. Wang, X. Wang, H. Li, J. Yan, *J. Organomet. Chem.* **2018**, *859*, 75–79.
- [13] S. K. Bhunia, P. Das, R. Jana, *Org. Biomol. Chem.* **2018**, *16*, 9243–9250.
- [14] M. Mondal, A. Saha, *Tetrahedron Lett.* **2019**, *60*, 150965.
- [15] N. Sbei, G. M. Martins, B. Shirinfar, N. Ahmed, *Chem. Rec.* **2020**, *20*, 1530–1552.
- [16] Z. Du, Q. Qi, W. Gao, L. Ma, Z. Liu, R. Wang, J. Chen, *Chem. Rec.* **2021**, *21*, 1–19.
- [17] J. Wang, C. Ma, X. Mu, W. Cai, L. Liu, X. Zhou, W. Hu, Y. Hu, *J. Hazard. Mater.* **2018**, *352*, 36–46.
- [18] S. S. Le Corre, N. Belmadi, M. Berchel, T. Le Gall, J.-P. Haelters, P. Lehn, T. Montier, P.-A. Jaffrès, *Org. Biomol. Chem.* **2015**, *13*, 1122–1132.
- [19] Q. Li, T. R. Swaroop, C. Hou, Z. Wang, Y. Pan, H. Tang, *Adv. Synth. Catal.* **2019**, *361*, 1761–1765.
- [20] L. Deng, Y. Wang, H. Mei, Y. Pan, J. Han, *J. Org. Chem.* **2019**, *84*, 949–956.
- [21] S. Guo, S. Li, W. Yan, Z. Liang, Z. Fu, H. Cai, *Green Chem.* **2020**, *22*, 7343–7347.
- [22] Q.-L. Wu, X.-G. Chen, C.-D. Huo, X.-C. Wang, Z.-J. Quan, *New J. Chem.* **2019**, *43*, 1531–1535.
- [23] Y. Li, Q. Yang, L. Yang, N. Lei, K. Zheng, *Chem. Commun.* **2019**, *55*, 4981–4984.
- [24] C.-Y. Li, Y.-C. Liu, Y.-X. Li, D. M. Reddy, C.-F. Lee, *Org. Lett.* **2019**, *21*, 7833–7836.
- [25] L. Zhao, X. Liu, S. Shi, Z. Wu, X. Guo, Z. Shen, M. Li, *Electrochim. Acta* **2021**, *389*,

-
- 138748.
- [26] Z.-Y. Meng, C.-T. Feng, L. Zhang, Q. Yang, D.-X. Chen, K. Xu, *Org. Lett.* **2021**, *23*, 4214–4218.
- [27] S. Guo, S. Li, Z. Zhang, W. Yan, H. Cai, *Tetrahedron Lett.* **2020**, *61*, 151566.
- [28] N. Amri, T. Wirth, *Synthesis* **2020**, *52*, 1751–1761.
- [29] X. Dong, R. Wang, W. Jin, C. Liu, *Org. Lett.* **2020**, *22*, 3062–3066.
- [30] Handoko, Z. Benslimane, P. S. Arora, *Org. Lett.* **2020**, *22*, 5811–5816.
- [31] N. Amri, T. Wirth, *Synlett* **2020**, *31*, 1894–1898.

CHAPTER 5

Electrochemical Oxidation of Organosulfur Compounds

CHAPTER 5: Electrochemical oxidation of organosulfur compounds.....	136
5.1. Organosulfur compounds.....	138
5.2. Results and discussion	139
5.2.1. Electrochemical oxidation of sulfides to sulfoxides.....	140
5.2.1.1. Electrode screening	140
5.2.1.2. Solvent screening	141
5.2.1.3. Flow rate screening	142
5.2.1.4. Concentration screening	143
5.2.1.5. Substrate scope.....	144
5.2.2. Electrochemical oxidation of sulfides to sulfones.....	146
5.2.2.1. Effect of charge on the selectivity of the anodic oxidation of sulfides	147
5.2.2.2. Substrate scope.....	148
5.2.3. Electrochemical oxidation of sulfoxides to sulfoximines.....	149
5.2.3.1. Electrode screening	150
5.2.3.2. Solvent and supporting electrolyte screening	150
5.2.3.3. Flow rate and charge screening.....	151
5.2.3.4. Substrate scope.....	153
5.2.4. Reaction mechanism	155
5.3. Conclusions and outlook	157
5.4. References	158

5.1. Organosulfur compounds

Since ancient times, organosulfur compounds have attracted the attention of chemists due to their importance in medicine and pharmaceutical products.^[1,2] Various bioactive sulfur compounds and natural products incorporate sulfoximine, sulfoxide, or sulfone moieties. Notably, sulfoximine, sulfoxide, or sulfone functional groups are very important in antibiotics, musculoskeletal, metabolism, alimentary tract, or anti-inflammatory drugs (Figure 5.1).^[3–6]

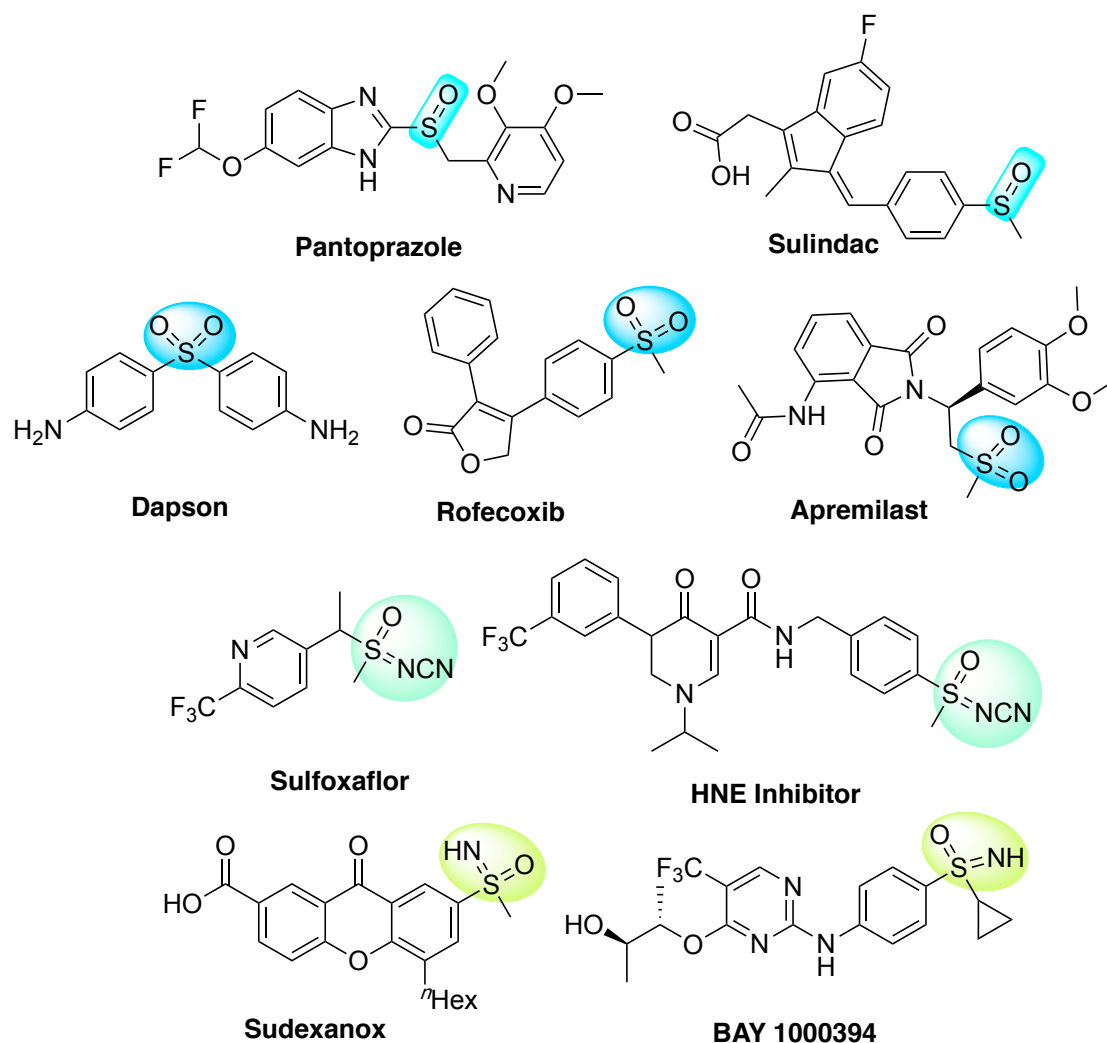


Figure 5.1. Examples of bioactive organosulfur compounds containing sulfoxide, sulfone, and sulfoximine moieties.

Additionally, the chemical applications of organosulfur compounds in organic synthesis are tremendous. The oxygen of the sulfinyl group has the ability to coordinate with different carbon ligands and metal ions, in addition to the stereoelectronic effects and the conformational stability of the sulfinyl group. Chiral sulfoximines and sulfoxides are easily accessible stable functional groups that have been used as ligands in stereoselective synthesis.^[7–10]

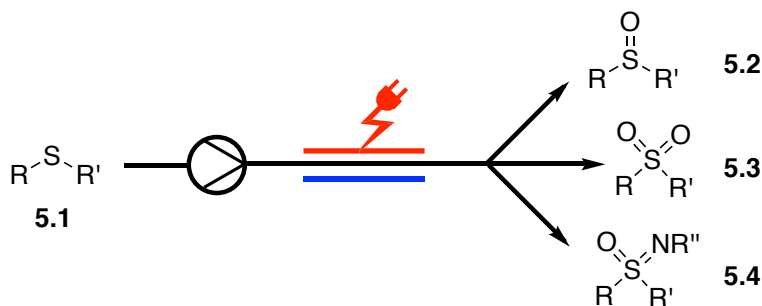
A wide range of oxidation protocols of the organosulfur compounds has been developed enabling access to various sulfur-containing function groups. Generally, such oxidation processes can be performed using different oxidants such as peroxides,^[11,12] photocatalytic processes,^[8,13] or hypervalent iodine reagents.^[14–16] Continuous flow processes have been investigated as well.^[17] Despite these developments in organosulfur oxidation processes, most lack industrial interest owing to sustainability, scaling-up, and safety concerns.

Recently, a resurgence of organic electrosynthesis has been observed in the context of modern synthesis.^[18–22] As a sustainable tool, electricity can be used to perform oxidation and reduction processes in clean and often environmentally benign procedures by replacing chemical oxidants and reductants with inexpensive electricity.^[23,24] Anodic oxidation of sulfur compound has been successfully applied through controlled potential electrolysis.^[25] Noël and co-workers have reported the direct oxidation of thioethers to the corresponding sulfoxides or sulfones in the presence of supporting electrolytes under flow reaction conditions.^[26] Yudin *et al.* reported a method for the amination of sulfoxides in batch electrolysis using a divided cell.^[27] Potentiostatic anodic oxidation have been applied in these reactions. Generally, using a divided cell leads to increased cell potentials.^[28]

There has been significant growth in the field of electroorganic synthesis over the last few years. Electroorganic synthesis in a flow reactor is a highly useful tool to perform redox transformations, in a more proficient manner while overcoming some of the constraints such as low reaction rates, large current gradients, and low conductivity of organic solvents in batch electrolysis. In addition, there have been innovations in flow cells that have permitted selective and successful synthesis exploiting the usually high electrode surface-to-reactor volume ratio, which in turn translates to a higher mass transfer and higher productivity.^[29–32]

5.2. Results and discussion

This chapter focuses on the diversification of organic sulfides *via* electrochemical oxidation under automated flow conditions (Scheme 5.1).



Scheme 5.1. Flow electrochemical diversification of sulfides.

In the following sections our studies on the flow electrochemical oxidation of sulfides **5.1** to the corresponding sulfoxides **5.2**, sulfones **5.3**, and sulfoximines **5.4** will be discussed in detail.

5.2.1. Electrochemical oxidation of sulfides to sulfoxides

The electrochemical of thioanisol (**5.1a**) to the corresponding sulfoxide **5.2a** was chosen as a model reaction for the process optimization using the Ion electrochemical flow cell -described previously- under galvanostatic operation. Various reaction parameters such as electrode materials, current, charge, solvent, supporting electrolyte and concentration were studied.

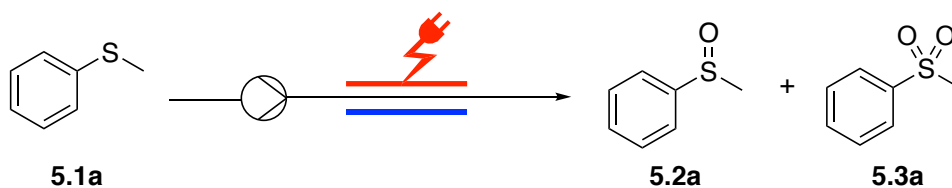
5.2.1.1. Electrode screening

Electrodes play a crucial role in efficiency and selectivity of electrochemical transformations. Hence, various electrode materials / combinations were studied to achieve efficient selective electrochemical oxidation of the model substrate, thioanisole (**5.1a**) to the corresponding sulfoxide **5.2a** (Table 5.1). A solution of thioanisole (**5.1a**) in a mixture of acetonitrile and water (9:1, 0.1 M) was pumped through the ion electrochemical reactor at a flow rate of 0.2 mL/min and electrolysed under constant current of 64 mA (2F).

The results (Table 5.1) show that the conversion of thioanisole (**5.1a**) to the corresponding sulfoxide **5.2a** proceeded smoothly with high conversion and selectivity in most cases. Using a pair of platinum electrodes led to the formation of the desired product **5.2a** in 83% yield, along with the overoxidation product, sulfone **5.3a** in 7% yield (Table 5.1, entry 1). Changing the cathode from Pt to the cheaper platinum on titanium electrode (Table 5.1, entry 2) led to the increase of the desired product **5.2a** to 92% and reduction of the sulfone **5.3a** to 3%. While changing the cathode from platinum to graphite led to 86% yield of sulfoxide **5.2a** and increased amount (12%) of sulfone **5.3a** (Table 5.1, entry 3). While reversing the polarity of the electrode pair used in entry 2 led to the selective formation of **5.2a** (90%) without observing **5.3a** (Table 5.1, entry 4). Replacing the platinum electrodes with graphite (Gr) led to a further improvement of the reaction outcome, where sulfoxide **5.2a** was formed selectively in 96% yield (Table 5.1, entry 5). Keeping graphite as anode and changing the cathode to platinum and then to iron led to slight improvement and the selective formation of **5.2a** in 98% in both cases (Table 5.1, entries 6,7). The same result was also obtained when glassy carbon (GC) was used as working electrode with platinum as a counter electrode (Table 5.1, entry 8). Using a pair of stainless-steel electrodes (Table 5.1, entry 9) led to big reduction of the conversion of **5.1a** to sulfoxide **5.2a**, that was formed selectively, but in low yield (48%). Among the various electrode

pairs that gave excellent results, the cheap pair of graphite anode and stainless-steel cathode (Table 5.1, entry 7) was chosen as optimum and was used for studying the reaction further.

Table 5.1. Electrochemical oxidation of thioanisole (**5.1a**) to sulfoxide **5.2a**: Electrode screening.



Entry	Anode	Cathode	Yield% (5.2a) ^[a]	Yield% (5.3a) ^[a]
1	Pt	Pt	83	7
2	Pt	Pt on Ti	92	3
3	Pt	Gr	86	12
4	Pt on Ti	Pt	90	0
5	Gr	Gr	96	0
6	Gr	Pt	98	0
7	Gr	SS	98	0
8	GC	Pt	98	0
9	SS	SS	48	0

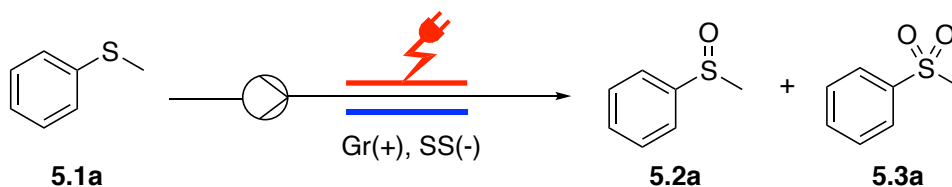
General Procedure: Ion reactor, FEP spacer (0.5 mm thickness; reactor volume: 600 μ L; active electrode surface area: 12 cm²); [**5.1a**] = 0.1 M, MeCN/H₂O (9:1); flow rate = 0.2 mL/min; I = 64 mA (2.0 F); calculated residence time = 3.0 min. [a] Determine by ¹H NMR with 1,3,5-trimethoxybenzene as internal standard. Gr = graphite; GC = glassy carbon, SS = stainless-steel.

5.2.1.2. Solvent screening

Although excellent results were obtained using a solvent mixture of acetonitrile/water (9:1), other solvent systems were also investigated. Using the conditions of entry 7 (Table 5.1), some other solvent systems were screened. The results (Table 5.2) showed that the initially used solvent system (MeCN/H₂O, 9:1) gave the highest yield and selectivity of sulfoxide **5.2a** (Table 5.2, entry 1). However, replacing acetonitrile with methanol led to comparable outcome, albeit giving **5.2a** in slightly lower yield (Table 5.2, entry 2). Using a mixture of acetonitrile, methanol, and water in an 8:1:1 ratio or 2:2:1 ratio led to reduction of the sulfoxide yield to 88%, but without observing the formation of sulfone **5.3a** (Table 5.2, entries 3,4). Using a

mixture of acetonitrile, HFIP, and water in 8:1:1 ratio (Table 5.2, entry 5) led to further reduction of the sulfoxide **5.2a** yield to 84% and the formation of the sulfone **5.3a** in 9% yield.

Table 5.2. Electrochemical oxidation of thioanisole (**5.1a**) to sulfoxide **5.2a**: Solvent screening.

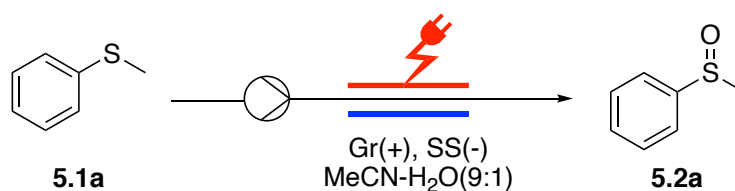


Entry	Solvent	Yield% (5.2a) ^[a]	Yield% (5.3a) ^[a]
1	MeCN-H ₂ O (9:1)	98	0
2	MeOH-H ₂ O (9:1)	95	0
3	MeCN-MeOH-H ₂ O (8:1:1)	88	0
4	MeCN-MeOH-H ₂ O (2:2:1)	88	0
5	MeCN-HFIP-H ₂ O (8:1:1)	84	9

General Procedure: Ion reactor, Anode = graphite, cathode = stainless-steel, FEP spacer (0.5 mm thickness; reactor volume: 600 μ L; active electrode surface area: 12 cm²); [**5.1a**] = 0.1 M; flow rate = 0.2 mL/min; I = 64 mA (2.0 F); calculated residence time = 3.0 min. [a] Determine by ¹H NMR with 1,3,5-trimethoxybenzene as internal standard. Gr = graphite; SS = stainless-steel.

5.2.1.3. Flow rate screening

To explore the reaction productivity, several flow rates were tested. The substrate solution (0.1 M) MeCN/H₂O (9:1) was pumped at various flow rates through the Ion electrochemical reactor equipped with graphite anode and stainless-steel cathode and passing a fixed charge of 2 F/mol in all cases. The results (Table 5.3) showed that lowering the flow rate from 0.2 mL/min to 0.15 mL/min and 0.1 mL/min i.e increasing the residence time didn't impact the reaction outcome and sulfoxide **5.2a** was formed in 98% yield in the three cases (Table 5.3, entries 1-3). On the other hand, increasing the flowrate above 0.2 mL/min to 0.25 mL/min and 0.3 mL/min (Table 5.3, entries 4,5) led to reuction of the sulfoxide yield to 92% and 89%, respectively.

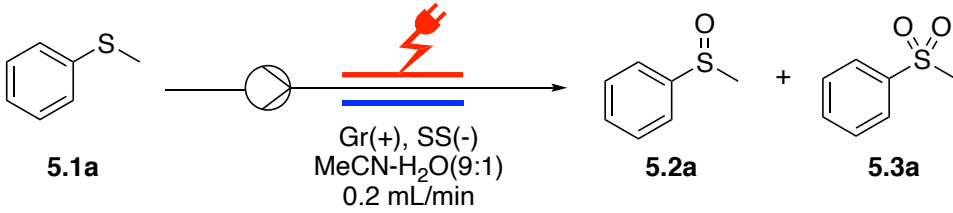
Table 5.3. Electrochemical oxidation of thioanisole (**5.1a**) to sulfoxide **5.2a**: Flow rate screening.

Entry	Flow rate (mL/min)	Current (mA)	Residence time (min)	Yield% (5.2a) ^[a]
1	0.1	32 (2.0 F)	6	98
2	0.15	48 (2.0 F)	4	98
3	0.2	64 (2.0 F)	3	98
4	0.25	80 (2.0 F)	2.4	92
5	0.3	96 (2.0 F)	2	89

General Procedure: Ion reactor, Anode = graphite, cathode = stainless-steel, FEP spacer (0.5 mm thickness; reactor volume: 600 μ L; active electrode surface area: 12 cm²); [**5.1a**] = 0.1 M, MeCN-H₂O (9:1); flow rate = 0.2 mL/min; Charge = 2.0 F/mol. [a] Determine by ¹H NMR with 1,3,5-trimethoxybenzene as internal standard. Gr = graphite; SS = stainless-steel.

5.2.1.4. Concentration screening

Finally, attempts to increase the reaction productivity by increasing the substrate concentration were tested. Under the optimised conditions, electrolysing solutions of thioanisole (**5.1a**) at higher concentrations than the previously tested 0.1 M concentration led to reduction of the yield of product **5.2a** (Table 5.4).

Table 5.4. Electrochemical oxidation of thioanisole (**5.1a**) to sulfoxide **5.2a**: substrate concentration screening.


Entry	[5.1a] (M)	Current (mA)	Yield% (5.2a)	Yield% (5.3a) ^[a]
1	0.1	64 (2.0 F)	98	0
2	0.15	96 (2.0 F)	89	6
3	0.2	128 (2.0 F)	88	6

General Procedure: Ion reactor, Anode = graphite, cathode = stainless-steel, FEP spacer (0.5 mm thickness; reactor volume: 600 μ L; active electrode surface area: 12 cm²); MeCN-H₂O (9:1); flow rate = 0.2 mL/min; Charge = 2.0 F/mol. [a] Determine by ¹H NMR with 1,3,5-trimethoxybenzene as internal standard. Gr = graphite; SS = stainless-steel.

Therefore, the optimum conditions for the selective electrochemical oxidation of the model substrate, thioanisole (**5.1a**) to the corresponding sulfoxide **5.2a** are as follows:

Anode: graphite, Cathode: stainless-steel, Solvent: MeCN-H₂O (9:1), Substrate concentration: 0.1 M, Flow rate: 0.2 mL/min, Calculated residence time: 3 min, Current: 64 mA (2.0 F).

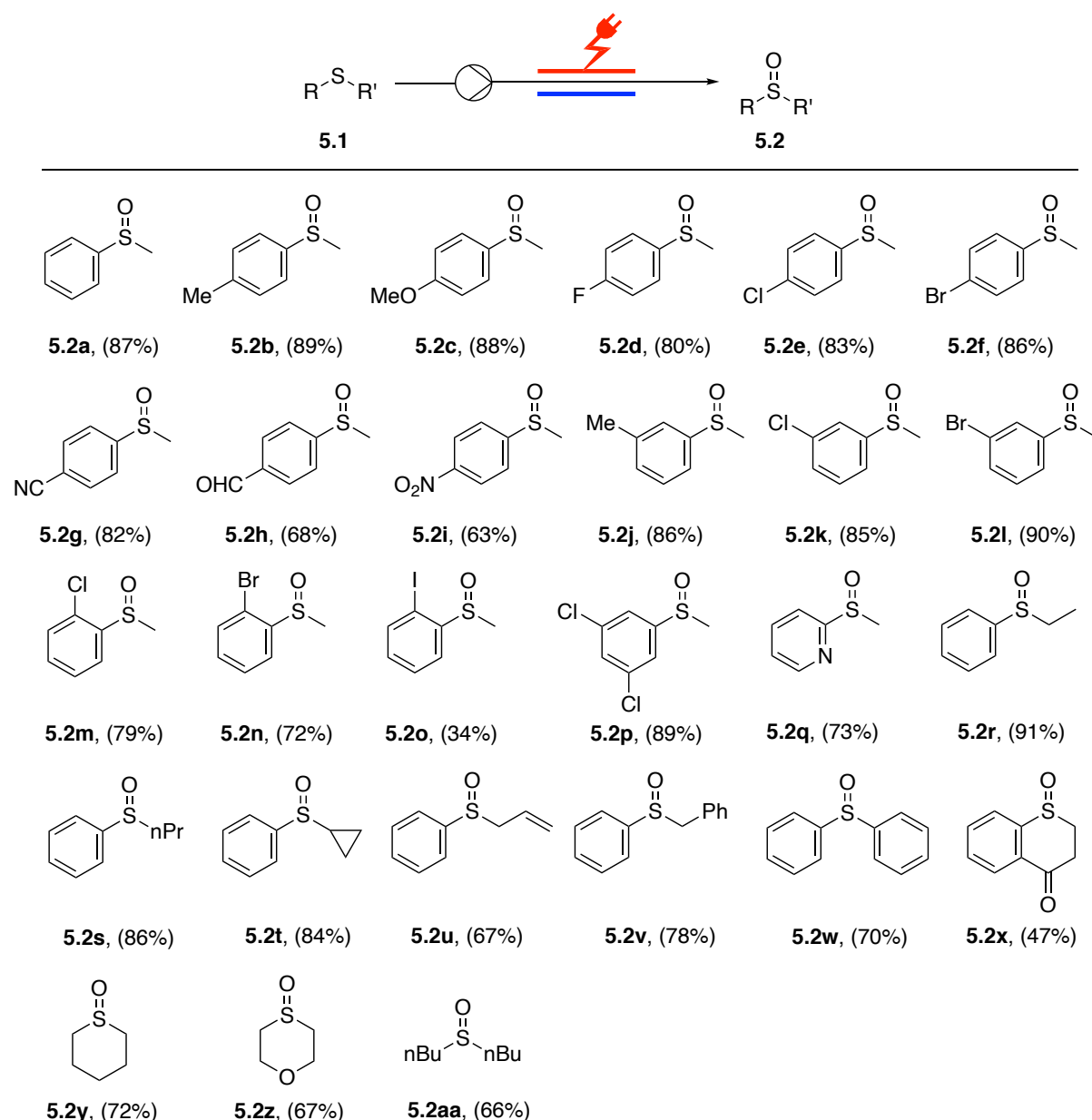
5.2.1.5. Substrate scope

Having the optimised reaction conditions in hand, the reaction scope was studied using a wide range of organic sulfide substrates. Varying the two groups attached to the sulfur in the substrates **5.1**, 27 sulfoxide products were obtained in generally good to excellent yields ranging from 37% to 90% with average yield of 76%. At 1.5 mmol scale, thioanisole **5.1a** was converted to the corresponding sulfoxide **5.2a** that was isolated in 87% yield. Thioanisole derivatives **5.1b-p** with different substituents in the aromatic moiety were easily oxidized to the corresponding sulfoxides **5.2b-p** in high yields in most cases. All para-substituted substrates **5.1b-i** were easily oxidised to the desired sulfoxides **5.2b-i** in very good yield, >80% in all cases except the formyl and nitro derivatives **5.1h,i** that led to the corresponding sulfoxides **5.2h,i** in 68% and 63%, respectively. Similar outcomes were obtained for meta- and ortho-substituted substrates **5.1j-o** leading to the corresponding products **5.2j-o** in high yields, except 2-iodothioanisole (**5.1o**) that gave the corresponding sulfoxide **5.2o** in low yield (34%), which might be due to competitive anodic oxidation of the iodine substituent.^[33,34] While the dichloro derivative **5.2p** was formed in excellent yield (89%). Oxidation of the

heterocyclic pyridine analogue **5.1q** under the same condition was also successful leading to the corresponding sulfoxide **5.2q** in 73% yield.

Furthermore, substrates containing other aliphatic groups attached to the sulfur **5.1r-u** were also easily oxidized to the corresponding sulfoxides **5.2r-u** in very good yields. Ethyl phenyl sulfide (**5.1r**) led to sulfoxide **5.2r** in excellent yield (91%). The *n*-propyl, cyclopropyl, and allyl derivatives led to the corresponding products in 86%, 84%, and 67% yields, respectively. In addition, substrate **5.1v** containing benzylic group, amenable to anodic oxidation,^[35,36] underwent smooth oxidation to the corresponding sulfoxide in very good yield (78%). While diphenyl sulfide (**5.1w**) afforded sulfoxide **5.2w** in 70% yield.

In addition, the oxidation of cyclic sulfides was also satisfactory under the optimised reaction conditions. Substrate **5.1x** lead to the corresponding cyclic sulfoxide **5.2x** in relatively lower yield (47%), while the aliphatic cyclic substrate **5.1y** and the heterocyclic sulfide **5.1z** afforded the corresponding cyclic sulfoxides **5.2y** and **5.2z** in better yields, 72% and 67%, respectively. Similarly, dibutyl sulfide **5.1aa** was oxidized to the corresponding sulfoxide **5.2aa** in 66% yield.



Conditions: Ion reactor, Anode = graphite, cathode = stainless-steel, FEP spacer (0.5 mm thickness; reactor volume: 600 μ L; active electrode surface area: 12 cm^2); **[5.1]** = 0.1 M, MeCN- H_2O (9:1); flow rate = 0.2 mL/min (75 min, 1.5 mmol); current = 64 mA (2.0 F/mol).

Scheme 5.2. Substrate scope of selective flow electrochemical oxidation of sulfides **5.1** to sulfoxides **5.2**.

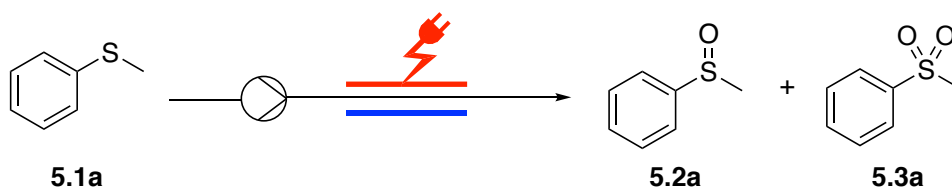
5.2.2. Electrochemical oxidation of sulfides to sulfones

The formation of sulfone **5.3a** was observed as a side product during the optimization of the flow electrochemical oxidation of thioanisole (**5.1a**) to the corresponding sulfoxide **5.2a**. After achieving an efficient selective electrochemical oxidation of sulfides **5.1** to the corresponding sulfoxides **5.2** under flow conditions, the focus turned into modifying the optimized conditions to achieve selective electrochemical oxidation of the same substrates, sulfides **5.1** to the corresponding sulfones **5.3**.

5.2.2.1. Effect of charge on the selectivity of the anodic oxidation of sulfides

Based on the optimized conditions, screening of charge and electrodes to flip the oxidation selectivity towards the sulfone products was studied (Table 5.5).

Table 5.5. Electrochemical oxidation of thioanisole (**5.1a**) to sulfone **5.3a**.



Entry	Anode	Cathode	Current (mA)	Yield% (5.2a) ^[a]	Yield% (5.3a) ^[a]
1	Gr	Fe	64 (2.0 F)	98	0
2	Gr	Fe	128 (4.0 F)	27	73
3	Pt	Fe	128 (4.0 F)	40	58
4	Pt	Fe	160 (5.0 F)	11	87
5	Pt	Fe	192 (6.0 F)	12	87

General Procedure: Ion reactor, FEP spacer (0.5 mm thickness; reactor volume: 600 μ L; active electrode surface area: 12 cm²); [**5.1a**] = 0.1 M, MeCN-H₂O (9:1); flow rate = 0.2 mL/min; calculated residence time = 3.0 min. [a] Determine by ¹H NMR with 1,3,5-trimethoxybenzene as internal standard. Gr = graphite; SS = stainless-steel.

The results (Table 5.5) showed that doubling the current from 64 mA (Table 5.4, entry 1) to 128 mA (4.0 F/mol) led to the formation of sulfone **5.3a** as the major product with 73% yield along with 27% yield of sulfoxide **5.2a** (Table 5.5, entry 2). Changing the working electrode from graphite to platinum, applying the same current (128 mA), reduced the reaction selectivity, where sulfone **5.3a** and sulfoxide **5.2a** were both formed in an approximately 1.5:1 ratio (Table 5.5, entry 3). Increasing the current from 128 mA to 160 mA, *i.e.*, increasing the charge from 4 F/mol to 5 F/mol (Table 5.5, entry 4), led to improvement of the reaction selectivity, where the desired sulfone **5.3a** was formed in 87% yield and the yield of sulfoxide **5.2a** decreased to 11%. Increasing the charge further didn't impact the reaction outcome (Table 5.5, entry 5).

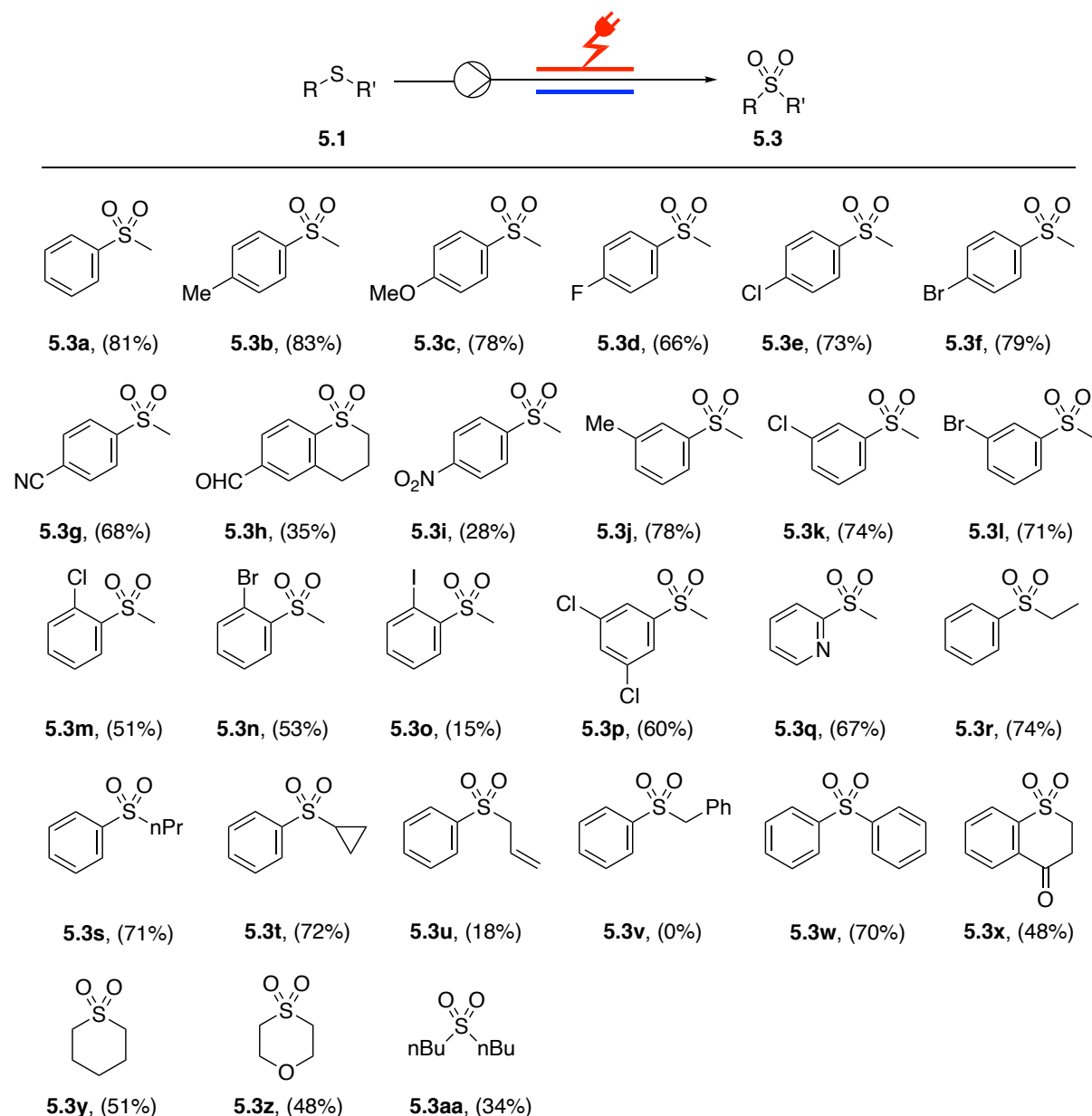
Therefore, the optimum conditions for the electrochemical oxidation of the model substrate, thioanisole (**5.1a**) to the corresponding sulfone **5.3a** are as follows:

Anode: platinum, Cathode: stainless-steel, Solvent: MeCN/H₂O (9:1), Substrate concentration: 0.1 M, Flow rate: 0.2 mL/min, Calculated residence time: 3 min, Current: 160 mA (5.0 F).

5.2.2.2. Substrate scope

Having the new set of conditions that favours the sulfone formation over sulfoxides, the reaction scope was studied using the same sulfide substrates used for studying the scope of the electrochemical oxidation of sulfides to sulfoxides discussed earlier (Scheme 5.2). Twenty-seven sulfone products **5.3** were obtained in generally good to high yields (Scheme 5.3), with an average yield of 57%, which is about 19% lower than the average yield obtained for the corresponding sulfoxide products **5.2** presented in Scheme 5.2. At 1.5 mmol scale, thioanisole **5.1a** was converted to the corresponding sulfone **5.3a** in 81% yield. Thioanisole derivatives **5.1b-p** with different substituents in the aromatic moiety were easily oxidized to the corresponding sulfones **5.3b-p** in good to high yields in most cases. All *para*-substituted substrates **5.1b-i** were easily oxidised to the desired sulfones **5.3b-i** in very good yields, in all cases except the formyl and nitro derivatives **5.1h,i** that led to the corresponding sulfones **5.3h,i** in low yields, 35% and 28%, respectively. Similar outcomes were obtained for *meta*- and *ortho*-substituted substrates **5.1j-o** leading to the corresponding products **5.3j-o** in good yields, except 2-iodothioanisole (**5.1o**) that gave the corresponding sulfone **5.3o** in low yield (15%), which might be due to competitive anodic oxidation of the iodine substituent.^[33,34] While the dichloro derivative **5.3p** was formed in good yield (60%). Oxidation of the heterocyclic pyridine analogue **5.1q** resulted in the formation of the corresponding sulfone **5.3q** in good yield (67%).

Moreover, substrates containing different aliphatic groups attached to the sulfur, **5.1r-t** were also easily oxidized to the corresponding sulfones **5.3r-t** in very good yields. Ethyl phenyl sulfide (**5.1r**) led to sulfone **5.3r** in 74% yield. The *n*-propyl and cyclopropyl derivatives led to the corresponding products in comparable yields, 72% and 71%, respectively. The allyl substituted substrate **5.1u** was not well-tolerated under these conditions and led to the formation of the corresponding sulfone **5.3u** in only 18% yield. Also, substrate **5.1v** containing benzylic group, amenable to anodic oxidation,^[35,36] was not tolerated and the corresponding sulfone **5.3v** was not obtained. While diphenyl sulfide (**5.1w**) was well-tolerated, leading to sulfone **5.3w** in good yield (70%). Furthermore, the oxidation of cyclic sulfides was also satisfactory leading to the desired sulfone products in moderate yields. Substrate **5.1x** afforded the corresponding cyclic sulfone **5.3x** in 48% yield. Similarly, the aliphatic cyclic sulfide **5.1y** and the heterocyclic substrate **5.1z** led to the corresponding cyclic sulfones **5.3y** and **5.3z** in comparable yields, 51% and 48%, respectively. While dibutyl sulfide **5.1aa** was oxidized to the corresponding sulfone **5.3aa** in lower yield (34%).



Conditions: Ion reactor, Anode = platinum, cathode = stainless-steel, FEP spacer (0.5 mm thickness; reactor volume: 600 μ L; active electrode surface area: 12 cm^2); **5.1** = 0.1 M, MeCN-H₂O (9:1); flow rate = 0.2 mL/min (75 min, 1.5 mmol); current = 160 mA (5.0 F/mol).

Scheme 5.3. Substrate scope of flow electrochemical oxidation of sulfides **5.1** to the corresponding sulfones **5.3**.

5.2.3. Electrochemical oxidation of sulfoxides to sulfoximines

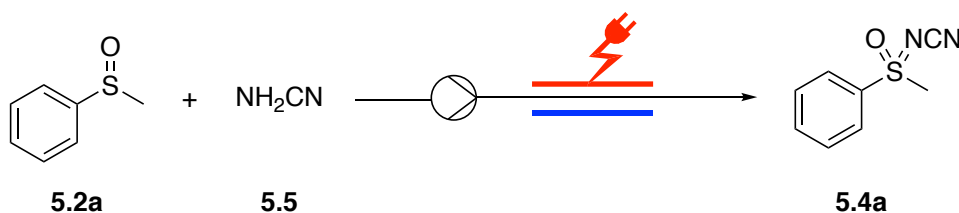
After developing two protocols for the selective electrochemical oxidation of sulfides to the corresponding sulfoxides and sulfones under flow condition, the anodic oxidation of sulfides to sulfoximines was attempted. Initial trials of direct conversion sulfides into sulfoximines by applying the two sets of optimized conditions, discussed above, were not successful and only sulfoxides and sulfones were obtained. Therefore, the transformation was then studied in more

detail using the sulfoxides **5.2** prepared electrochemically (Scheme 5.1) as the starting material instead of sulfides.

5.2.3.1. Electrode screening

A solution of sulfoxide (**5.2a**) in HFIP (0.05 M), cyanamide (**5.5**, 1.5 equiv.) and Et₄NCl (0.01 M) in HFIP was pumped through the ion electrochemical reactor at a flow rate of 0.1 mL/min and electrolysed under constant current of 24 mA (3.0 F).

Table 5.6. Electrochemical oxidation of sulfoxide (**5.2a**) to sulfoximine **5.4a**: Electrode screening.



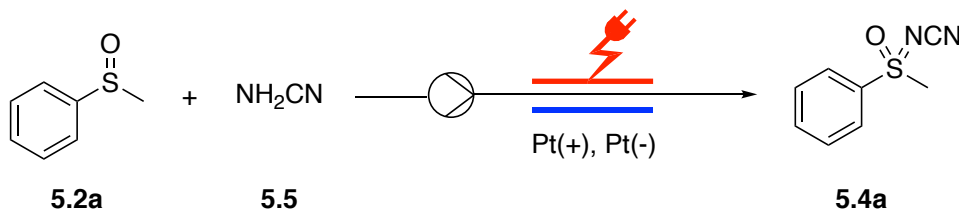
Entry	Anode	Cathode	Conversion% (5.4a) ^[a]
1	Gr	Pt	NR
2	Gr	Gr	NR
3	Gr	SS	NR
4	Pt	Gr	8
5	Pt	Pt	25

General Procedure: Ion reactor, FEP spacer (0.25 mm thickness; reactor volume: 300 μ L; active electrode surface area: 12 cm²); [**5.2a**] = 0.05 M, NH₂CN (0.075 M), Et₄NCl (0.01 M) in HFIP; flow rate = 0.1 mL/min; I = 24 mA (3.0 F); calculated residence time = 3.0 min. [a] Determine by ¹H NMR. Gr = graphite; SS = stainless-steel. HFIP = 1,1,1,3,3,3-hexafluoro-2-propanol. NR = no reaction (starting material recovered).

The results (Table 5.6) showed no reaction when graphite was used as anode with Pt, graphite or stainless-steel as cathode (Table 5.6, entries 1-3). Changing the anode material to platinum with graphite as cathode led to poor conversion (8%) of the starting material to the desired product (Table 5.6, entry 4). The conversion was improved to 25% using a pair of platinum electrodes (Table 5.6, entry 5). Hence, platinum anode and cathode were chosen for further optimization experiments.

5.2.3.2. Solvent and supporting electrolyte screening

Using a pair of platinum electrodes, applying the condition of entry 5 of table 5.7, the effect of solvent and supporting electrolytes on the reaction outcome was studied.

Table 5.7. Electrochemical oxidation of sulfoxide (**5.2a**) to sulfoximine **5.4a**: Solvent and supporting electrolyte screening.

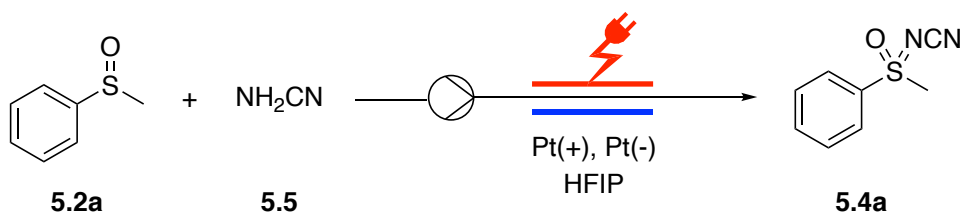
Entry	Solvent	Supporting Electrolyte	Conversion% (5.4a) ^[a]
1	HFIP	Et ₄ NCl	25
2	TFE	Et ₄ NCl	6
3	MeCN	Et ₄ NCl	18
4	CHCl ₃	Et ₄ NCl	11
5	CH ₂ Cl ₂	Et ₄ NCl	NR
6	MeOH	Et ₄ NCl	4
7	HFIP	Et ₄ NI	NR
8	HFIP	Et ₄ NBr	NR
9	HFIP	<i>n</i> Bu ₄ NBr	NR
10	HFIP	none	34

General Procedure: Ion reactor, FEP spacer (0.25 mm thickness; reactor volume: 300 μ L; active electrode surface area: 12 cm²); [**5.2a**] = 0.05 M, NH₂CN (0.075 M), SE (0.01 M); flow rate = 0.1 mL/min; I = 24 mA (3.0 F); calculated residence time = 3.0 min. [a] Determine by ¹H NMR. HFIP = 1,1,1,3,3,3-Hexafluoro-2-propanol, TFE = 2,2,2-Trifluoroethanol. NR = no reaction (starting material recovered).

The results (Table 5.7) showed that in the presence of Et₄NCl as supporting electrolyte, none of the tested solvents, TFE, MeCN, CHCl₃, DCM, or MeOH (Table 5.7, entries 2-7) gave better results than HFIP (Table 5.7, entry 1). Hence, HFIP was chosen as the reaction solvent for the coming experiments. Replacing Et₄NCl with other supporting electrolytes (Table 5.7, entries 7-9) led to no reaction at all. While running the reaction in HFIP without adding any supporting electrolyte led to improvement of the conversion to 34%. Therefore, the optimization process will continue using HFIP as a solvent in the absence of added electrolytes.

5.2.3.3. Flow rate and charge screening

Applying the condition of entry 10 of table 5.6, the effect of flow rate and passed charge on the reaction outcome was studied.

Table 5.8. Electrochemical oxidation of sulfoxide (**5.2a**) to sulfoximine **5.4a**: Flow rate and charge screening.

Entry	Flow rate (mL/min)	Current (mA)	Charge (F/mol)	Conversion%(5.4a) ^[a]
1	0.1	24	3.0	34
2	0.1	32	4.0	41
3	0.1	48	6.0	63
4	0.075	18	3.0	33
5	0.075	24	4.0	48
6	0.075	36	6.0	62
7	0.15	36	3.0	33
8	0.15	48	4.0	48
9	0.15	72	6.0	68
10	0.2	48	3.0	17
11	0.2	64	4.0	42
12	0.2	92	6.0	62

General Procedure: Ion reactor, FEP spacer (0.25 mm thickness; reactor volume: 300 μL ; active electrode surface area: 12 cm^2); [**5.2a**] = 0.05 M and NH_2CN (0.075 M) in HFIP; [a] Determine by ^1H NMR. HFIP = 1,1,1,3,3,3-Hexafluoro-2-propanol.

The results (Table 5.8) showed that at flow rate of 0.1 mL/min increasing the passed charge from 3.0 to 4.0 to 6. F/mol led to improvement of the conversion from 34% to 41% to 63%, respectively (Table 5.8, entries 1-3). The same trend was observed with lower flow rate (0.075 mL/min) and higher flow rates, 0.25 and 0.2 mL/min (Table 5.8, entries, 4-12). The highest conversion (68%) was achieved at 0.15 mL/min, applying 6.0 F/mol (Table 5.8, entry 9). Increasing the substrate concentration to 0.1 M led to big increase of the cell voltage and maintaining constant current was not possible.

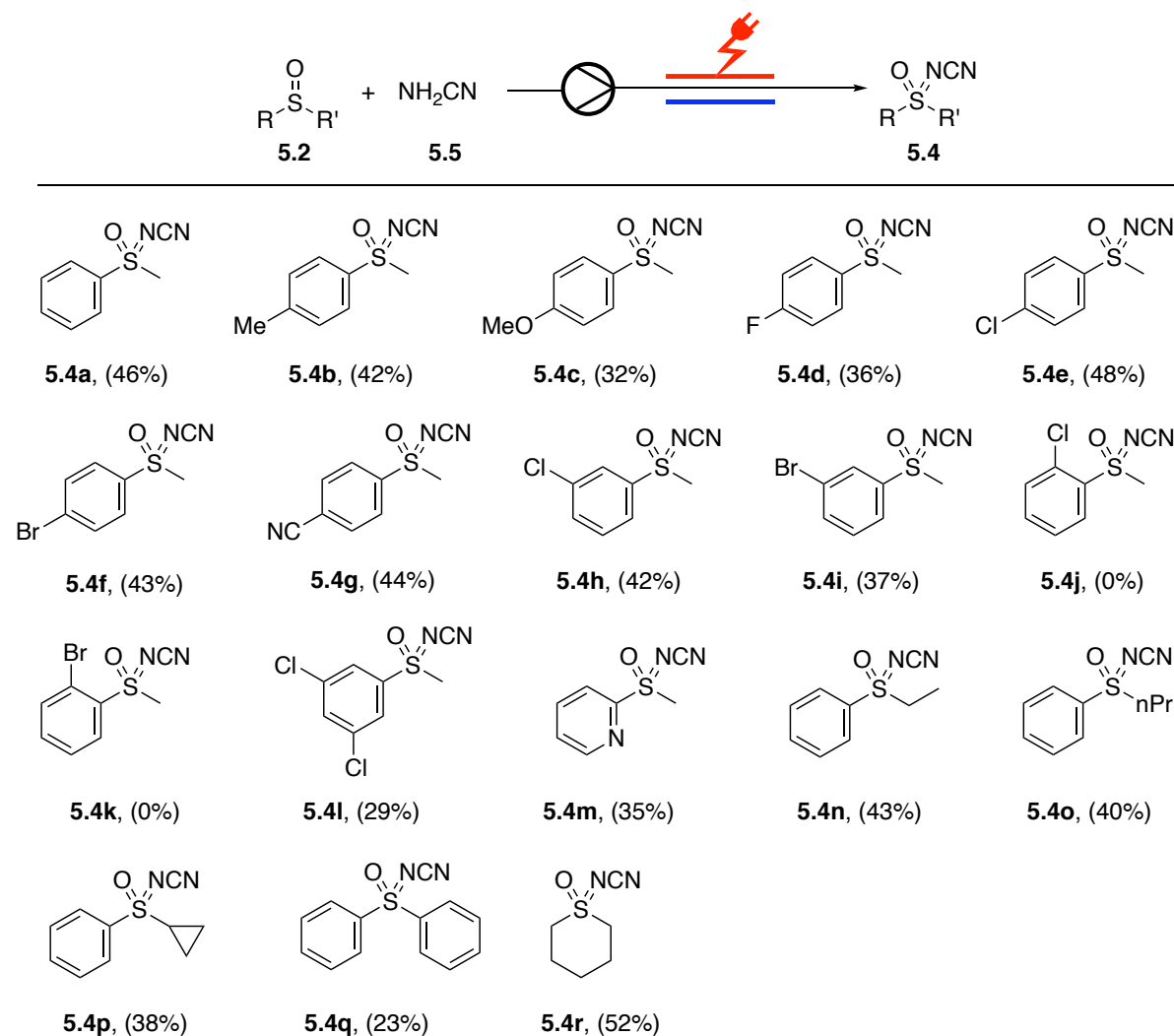
Therefore, the optimum conditions for the electrochemical oxidation of the model substrate, sulfoxide **5.2a** to the corresponding sulfoximine **5.4a** are as follows:

Anode: platinum, Cathode: platinum, Solvent: HFIP, Substrate concentration: 0.05 M, Flow rate: 0.15 mL/min, Calculated residence time: 2 min, Current: 72 mA (6.0 F).

5.2.3.4. Substrate scope

Applying the optimized conditions (Table 5.8, entry 9), the reaction scope was studied using sulfoxide substrates **5.2** prepared earlier and presented in Scheme 5.2. The yields of the electrochemically generated sulfoximine **5.4** were generally moderate, with an average yield of 35%, for 18 products (Scheme 5.4). All the reactions were performed on 0.5 mmol scale. Sulfoxide **5.2a** was converted to the corresponding sulfoximine **5.4a** in 46% yield. All *para*- and *meta*-substituted substrates **5.2b-i** produced the sulfoximines **5.4b-i** in moderate yields, ranging between 32% and 48%. In contrast the *ortho*-substituted substrates **5.2j,k** failed to react under these conditions and the corresponding products **5.4j,k** were not formed, while the dichloro-derivative **5.4l** was formed in 29% yield.

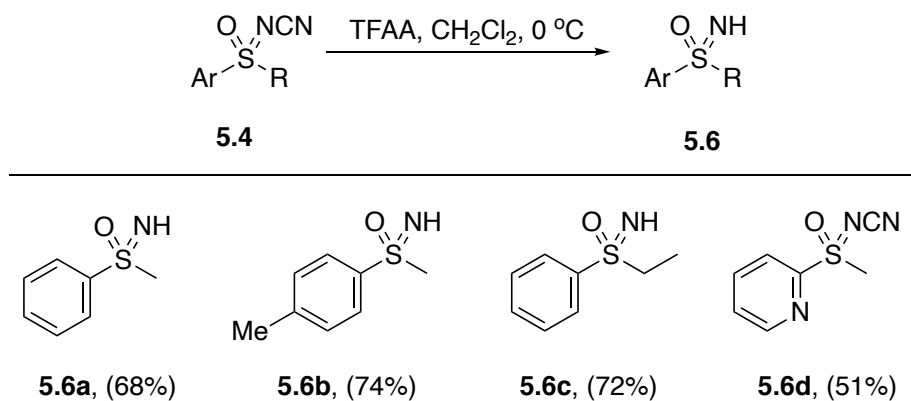
In addition, substrates containing different aliphatic groups attached to the sulfur, **5.2n-p** were oxidized to the corresponding sulfoximine **5.4n-p** in moderate yields (38%-43%). Diphenyl sulfoxide (**5.2q**) was converted to the corresponding sulfoximine **5.4q** in 29% yield. The cyclic sulfoximine **5.4r** was obtained in satisfactory yield (52%).



Conditions: Ion reactor, Anode = platinum, cathode = platinum, FEP spacer (0.25 mm thickness; reactor volume: 300 μ L; active electrode surface area: 12 cm²); [**5.2**] = 0.05 M and NH₂CN (0.075 M) in HFIP; flow rate = 0.15 mL/min (66.7 min, 0.5 mmol); current = 72 mA (6.0 F/mol).

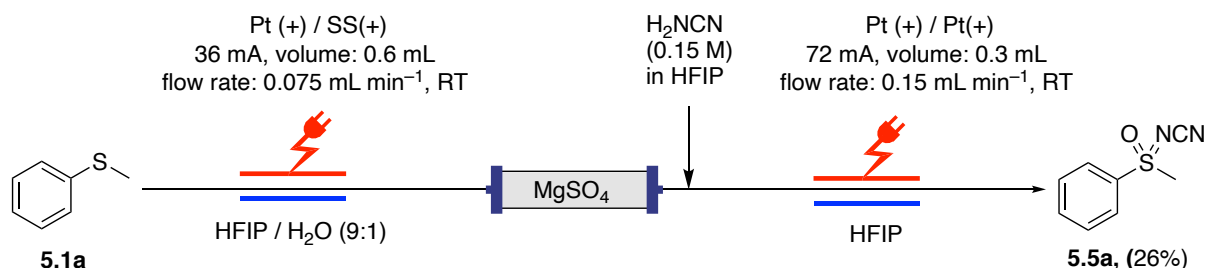
Scheme 5.4. Substrate scope of flow electrochemical oxidation of sulfoxides **5.2** to the corresponding sulfoximines **5.4**.

In addition, some of the prepared *N*-cyanosulfoximines **5.4** were converted to the corresponding NH-sulfoximine **5.6** upon treatment with trifluoroacetic acid anhydride (TFAA) (Scheme 5.5).



Scheme 5.5 Conversion of *N*-cyanosulfoximines **5.4** to NH-sulfoximine **5.6**.

As mentioned earlier, attempts to convert sulfides **5.1** directly to sulfoximines **5.4** were not successful, and sulfoxides **5.2** were used as substrates for this transformation, an attempt has been made to achieve the oxidation of sulfides into sulfoximines in two connected flow electrochemical steps in a coupled flow/flow manner. With this setup (Scheme 5.6), initial promising result was obtained, where thioanisole (**5.1a**) was converted to the corresponding sulfoximine **5.4a** in 26% yield.



Scheme 5.6 Conversion of thioanisole (**5.1a**) to the corresponding sulfoximine **5.4a** in a coupled flow/flow setup.

5.2.4. Reaction mechanism

To explore the reaction mechanism, the electrochemical oxidation of **5.1a** was carried out in the absence of water with the addition of Bu_4NBF_4 as added electrolyte. This experiment failed to produce sulfoxide **5.2a** and the starting material remained unreacted, showing the crucial role of water in this process. Also, the oxidation of thioanisole (**5.1a**) was conducted in the presence of H_2^{18}O under the same reaction conditions. The sulfoxide product contained ^{18}O which was confirmed by HRMS analysis, proving that the oxygen in water is the oxygen source, not the dissolved oxygen gas.

Additionally, cyclic voltammetry studies of sulfide **5.1a** and sulfoxide **5.2a** in acetonitrile and HFIP were measured to obtain insight into the reaction mechanism in various solutions. Two electron oxidation peaks of thioanisole (**5.1a**) were observed in acetonitrile at $E_p = 1.57\text{ V}$ and

$E_p = 1.9$ V (Figure 5.2a, yellow line), while there was only one apparent oxidation peak for sulfoxide **5.2a** at $E_p = 2.05$ V (Figure 5.2a, blue line). Also, the cyclic voltammetry of sulfoxide **5.2a** in HFIP showed one oxidation peak at $E_p = 2.1$ V (Figure 5.2b, orange line), while there was no oxidation peak for cyanamide **5.4** (Figure 5.2b, gray line).

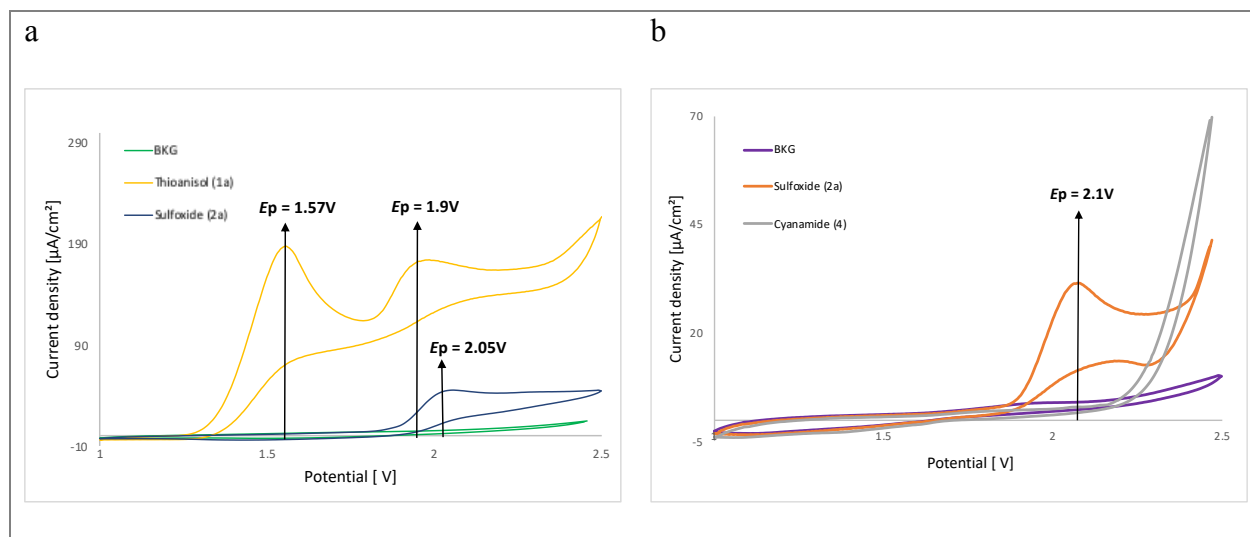
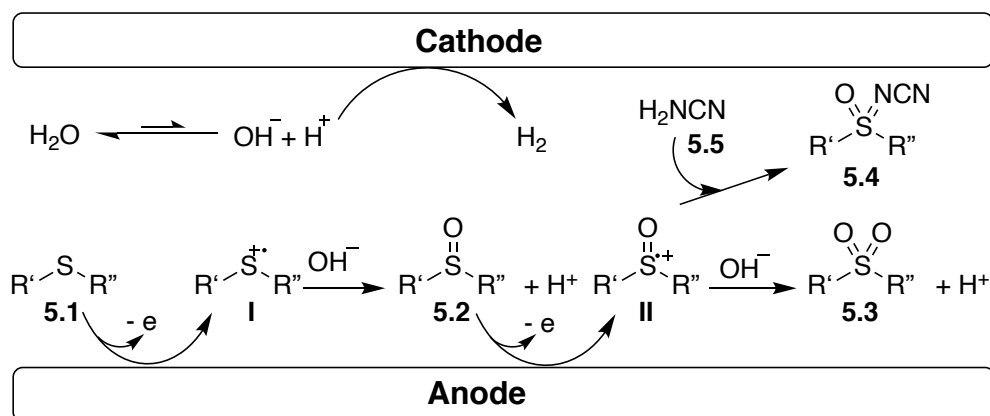


Figure 5.2. Cyclic voltammetry (CV) studies of thioanisole (**5.1a**) (yellow line) and sulfoxide **5.2a** (blue line) in MeCN (a). Sulfoxide **5.2a** (orange line) and cyanamide **5.4** (gray line) in HFIP (b). GC carbon disk working electrode (immersed surface area: 3 mm²), Pt counter electrode (immersed surface area: 1.2 mm²), Ag/0.01 M AgCl reference electrode, 20 mV s⁻¹.

Based on our initial studies and according to various literature reports on oxygenation of sulfides,^[37–39] a plausible mechanism is proposed (Scheme 5.7). Initially, sulfides **5.1** anodically oxidized to produce radical cation intermediate **I**, that reacts with hydroxide ions (OH⁻) generated from reduction of water, producing sulfoxides **5.2**. Subsequently, the sulfoxide **5.2** undergoes a similar transformation to produce sulfones **5.3** *via* intermediate **II**, that can lead also to *N*-cyanosulfoximines **5.4** upon reaction with react with cyanamide **5.5**. Ultimately, protons generated in this process are reduced to hydrogen at the cathode.



Scheme 5.7 Proposed mechanism for anodic oxidation of sulfides to the corresponding sulfoxides, sulfones, and sulfoximines.

5.3. Conclusions and outlook

In conclusion, electrochemical flow protocols for the diversification of organic to sulfoxides, sulfones and sulfoximines *via* anodic oxidation have been developed. A broad range of sulfoxides (27 examples), sulfones (26 examples), and *N*-cyanosulfoximines (16 examples) were synthesized in moderate to excellent yields using an automated electrochemical flow system in the absence of added electrolytes. Depending on the charge passed, the selectivity of the oxidation of sulfides can be controlled to achieve sulfoxides or sulfones using the same protocol in very good yields. Direct oxidation of sulfides to sulfoximines was not successful but using the electrochemically prepared sulfoxides in the presence of cyanamide led to successful transformation to the desired sulfoximines in moderate yields.

Although the developed protocols for sulfoxides and sulfones are selective and high yielding, the protocol to sulfoximines needs improvements. Which could be done by using Design of Experiment (DoE) approach for better exploration of the chemical space and finding good balance between the various reaction parameters to achieve better efficiency. In addition, the initial results of the electrochemical oxidation of sulfides to sulfoximines through a coupled flow/flow setup is promising, but more work is needed for better integration of the two steps in one connected protocol.

This work has already been published.^[40]

5.4. References

- [1] R. J. Cremllyn, *An Introduction to Organosulfur Chemistry*, John Wiley & Sons, Chichester, **1996**.
- [2] N. A. Meanwell, *J. Med. Chem.* **2011**, *54*, 2529–2591.
- [3] M. Feng, B. Tang, S. H. Liang, X. Jiang, *Curr. Top. Med. Chem.* **2016**, *16*, 1200–1216.
- [4] A. S. Surur, L. Schulig, A. Link, *Arch. Pharm.* **2018**, 1800248.
- [5] P. Mäder, L. Kattner, *J. Med. Chem.* **2020**, *63*, 14243–14275.
- [6] H. Narode, M. Gayke, G. Eppa, J. S. Yadav, *Org. Process Res. Dev.* **2021**, *25*, 1512–1523.
- [7] B. M. Trost, M. Rao, *Angew. Chem. Int. Ed.* **2015**, *54*, 5026–5043.
- [8] V. Bizet, C. M. M. Hendriks, C. Bolm, *Chem. Soc. Rev.* **2015**, *44*, 3378–3390.
- [9] M. Reggelin, C. Zur, *Synthesis*. **2000**, 1–64.
- [10] T. Toru, C. Bolm, Eds., *Organosulfur Chemistry in Asymmetric Synthesis*, Wiley, **2008**.
- [11] R. Fareghi-Alamdari, N. Zekri, A. J. Moghadam, M. R. Farsani, *Catal. Commun.* **2017**, *98*, 71–75.
- [12] K. E. Cantwell, P. E. Fanwick, M. M. Abu-Omar, *ACS Omega* **2017**, *2*, 1778–1785.
- [13] H. Lebel, H. Piras, M. Borduy, *ACS Catal.* **2016**, *6*, 1109–1112.
- [14] A. Tota, S. St John-Campbell, E. L. Briggs, G. O. Estévez, M. Afonso, L. Degennaro, R. Luisi, J. A. Bull, *Org. Lett.* **2018**, *20*, 2599–2602.
- [15] G. Zhang, H. Tan, W. Chen, H. C. Shen, Y. Lu, C. Zheng, H. Xu, *ChemSusChem* **2020**, *13*, 922–928.
- [16] M. Zenzola, R. Doran, R. Luisi, J. A. Bull, *J. Org. Chem.* **2015**, *80*, 6391–6399.
- [17] J. P. Colomer, M. Traverssi, G. Oksdath-Mansilla, *J. Flow Chem.* **2020**, *10*, 123–138.
- [18] O. Hammerich, B. Speiser, Editors., *Organic Electrochemistry: Revised and Expanded, Fifth Edition.*, CRC Press, **2016**.
- [19] T. Fuchigami, M. Atobe, S. Inagi, Editors., *Fundamentals and Applications of Organic Electrochemistry: Synthesis, Materials, Devices.*, Wiley, **2014**.
- [20] J. Yoshida, K. Kataoka, R. Horcajada, A. Nagaki, *Chem. Rev.* **2008**, *108*, 2265–2299.
- [21] S. R. Waldvogel, B. Janza, *Angew. Chem. Int. Ed.* **2014**, *53*, 7122–7123.
- [22] M. Yan, Y. Kawamata, P. S. Baran, *Chem. Rev.* **2017**, *117*, 13230–13319.
- [23] S. Möhle, M. Zirbes, E. Rodrigo, T. Gieshoff, A. Wiebe, S. R. Waldvogel, *Angew. Chem. Int. Ed.* **2018**, *57*, 6018–6041.

-
- [24] B. A. Frontana-Urbe, R. D. Little, J. G. Ibanez, A. Palma, R. Vasquez-Medrano, *Green Chem.* **2010**, *12*, 2099.
- [25] N. Amri, T. Wirth, *Chem. Rec.* **2021**, *21*, 2526–2537.
- [26] G. Laudadio, N. J. W. Straathof, M. D. Lanting, B. Knoops, V. Hessel, T. Noël, *Green Chem.* **2017**, *19*, 4061–4066.
- [27] T. Siu, A. K. Yudin, *Org. Lett.* **2002**, *4*, 1839–1842.
- [28] J. Chen, W.-Q. Yan, C. M. Lam, C.-C. Zeng, L.-M. Hu, R. D. Little, *Org. Lett.* **2015**, *17*, 986–989.
- [29] M. Elsherbini, T. Wirth, *Acc. Chem. Res.* **2019**, *52*, 3287–3296.
- [30] T. Noël, Y. Cao, G. Laudadio, *Acc. Chem. Res.* **2019**, *52*, 2858–2869.
- [31] S. Maljuric, W. Jud, C. O. Kappe, D. Cantillo, *J. Flow Chem.* **2020**, *10*, 181–190.
- [32] D. Pletcher, R. A. Green, R. C. D. Brown, *Chem. Rev.* **2018**, *118*, 4573–4591.
- [33] M. Elsherbini, B. Winterson, H. Alharbi, A. A. Folguez-Amador, C. Génot, T. Wirth, *Angew. Chem. Int. Ed.* **2019**, *58*, 9811–9815.
- [34] M. Elsherbini, T. Wirth, *Chem. A Eur. J.* **2018**, *24*, 13399–13407.
- [35] J. A. Marko, A. Durgham, S. L. Bretz, W. Liu, *Chem. Commun.* **2019**, *55*, 937–940.
- [36] D. Wang, P. Wang, S. Wang, Y.-H. Chen, H. Zhang, A. Lei, *Nat. Commun.* **2019**, *10*, 2796.
- [37] Z. Cheng, P. Sun, A. Tang, W. Jin, C. Liu, *Org. Lett.* **2019**, *21*, 8925–8929.
- [38] Y. Li, S. A. Rizvi, D. Hu, D. Sun, A. Gao, Y. Zhou, J. Li, X. Jiang, *Angew. Chem. Int. Ed.* **2019**, *58*, 13499–13506.
- [39] L. Ma, H. Zhou, M. Xu, P. Hao, X. Kong, H. Duan, *Chem. Sci.* **2021**, *12*, 938–945.
- [40] N. Amri, T. Wirth, *J. Org. Chem.* **2021**, DOI: [acs.joc.1c00860](https://doi.org/10.1021/acs.joc.1c00860).

CHAPTER 6

Experimental Part

CHAPTER 6: Experimental Part	161
6.1. General methods	163
6.2. Automated flow and electrochemical reactor setup	165
6.3. Experimental Data for Chapter 2.....	167
6.3.1. Synthesis of <i>N,O</i> -acetals	167
6.3.1.1. Monoalkoxylation of <i>N</i> -Formylpyrrolidine.....	167
6.3.1.2. Dialkoxylation of <i>N</i> -Formylpyrrolidine.....	169
6.4. Experimental Data for Chapter 3.....	173
6.4.1. Oxyselelenylations of alkenes	173
6.4.2. Intramolecular selenocyclisations of alkenes.....	191
6.5. Experimental Data for Chapter 4.....	194
6.6. Experimental Data for Chapter 5.....	202
6.6.1. Electrochemical oxidation of sulfides to sulfoxides.....	202
6.6.2. Electrochemical oxidation of sulfides to sulfones.....	212
6.6.3. Electrochemical imination of sulfoxides:	221
6.6.4. Reduction of <i>N</i> -cyanosulfoximines	227
6.7. References:	230
Appendix: GC Method and Data for Chapter 2.....	233

6.1. General methods

The reactions were performed using standard laboratory equipment. In all the reactions, standard reagent grade solvents and chemicals from Sigma Aldrich, Alfa Aesar, Acros Organic and FluoroChem were used without further purification, unless otherwise specified. All air sensitive reactions were carried out under argon or nitrogen atmosphere using oven dried glassware. All reactions were stirred using a stirrer plate and a magnetic stirrer bar and heating if necessary over a hotplate with a temperature probe control and adapted heating block. Lower temperatures were achieved using ice/water bath (0 °C) or dry ice/acetone bath (-78 °C). Dry ether and THF were collected from a solvent purification system (SPS) from the company MBRAUN (MB SPS-800). Dry CH₂Cl₂ was distilled over calcium hydride under nitrogen atmosphere. Büchi rotavapors were used for solvent evaporations (reduced pressure up to 8 mbar) and a high vacuum apparatus was used to further dry the products.

Thin-layer chromatography (TLC) was performed on pre-coated aluminium sheets of Merck silica gel 60 F254 (0.20 mm) and visualised by UV radiation (254 nm). Automated column chromatography was performed on a Biotage® Isolera Four using Biotage® cartridges SNAP Ultra 10 g, SNAP Ultra 25 g, SNAP Ultra 50 g, SNAP Ultra 100 g, Telos® 12 g and Telos® 20 g. The solvents used for the purification are indicated in the text and were purchased from Fischer Scientific as laboratory grade.

¹H NMR and ¹³C NMR spectra were measured on Bruker DPX 300, 400 or 500 apparatus and were referenced to the residual proton solvent peak (¹H: CDCl₃, δ 7.26 ppm; DMSO-*d*₆, δ 2.54 ppm) and solvent ¹³C signal (CDCl₃, δ 77.2 ppm, DMSO-*d*₆, δ 39.5 ppm). Chemical shifts δ were reported in ppm downfield of tetramethylsilane (δ = 0 ppm), multiplicity of the signals was declared as followed: s = singlet, d = doublet, t = triplet, q = quartet, quin = quintet, sex = sextet, hep = septet, dd = doublet of doublets, m = multiplet, b = broad; and coupling constants (J) in Hertz.

Mass spectrometric measurements were performed by R. Jenkins, R. Hick, T. Williams and S. Waller at Cardiff University on a Water LCR Premier XEtof. Ions were generated by the Atmospheric Pressure Ionisation Techniques (APCI), Electrospray (ESI), Electron Ionisation (EI) or Nanospray Ionisation (NSI). The molecular ion peak values quoted for either molecular ion [M]⁺, molecular ion plus hydrogen [M+H]⁺ or molecular ion plus sodium [M+Na]⁺

IR spectra were recorded on a Shimadzu FTIR Affinity-1S apparatus. Wavenumbers are quoted in cm^{-1} . All compounds were measured neat directly on the crystal of the IR machine. Melting points were measured using a Gallenkamp variable heater with samples in open capillary tubes.

X-Ray crystallographic studies were carried out at the X-Ray Crystallography Service at Cardiff University. The data were collected on an Agilent SuperNova Dual Atlas diffractometer with a mirror monochromator, equipped with an Oxford cryosystems cooling apparatus. Crystal structures were solved and refined using SHELX. Non-hydrogen atoms were refined with anisotropic displacement parameters. Hydrogen atoms were inserted in idealised positions. The structure was solved by a direct method and refined by a full matrix least-squares procedure on F2 for all reflections (SHELXL-97).

In the flow set-ups, the syringe pumps that were used were KR Analytical Ltd Fusion 200 syringe pumps and FEP tubing (OD: 1/16", ID: 0.2–1 mm). The electrochemical reactions were carried out in galvanostatic mode using a Vapourtec Ion Electrochemical flow reactor^[1] powered up by an Ion reaction controller, GWINSTEK GPR-30H10D or Aim-tti bench power supply. The cyclic voltammogram studies were performed in an Orygalys OGF500 Potentiostat/ Galvanostat with OGFPWR power supply. The electrode materials were purchased from Vapourtec and goodfellow suppliers.

6.2. Automated flow and electrochemical reactor setup:

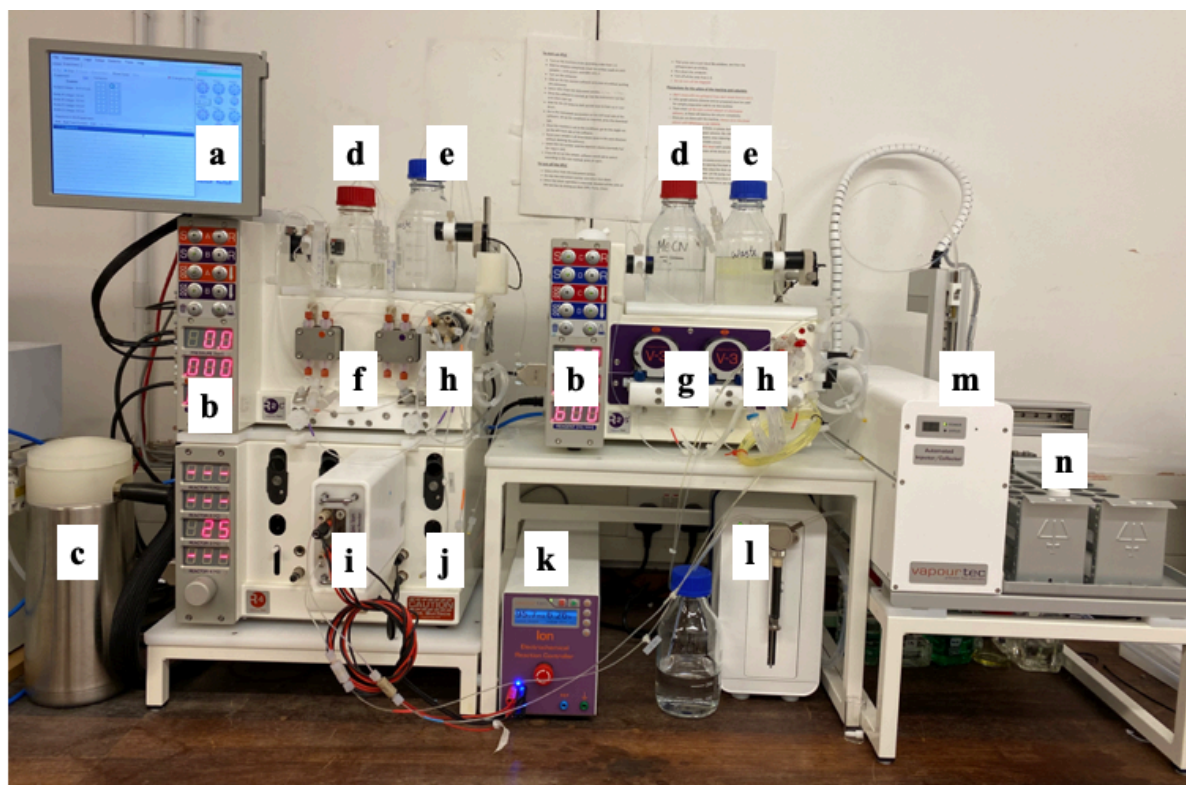


Figure 6.1. Actual flow set-up of the Ion electrochemical reactor combined with an R⁴-Series Vapourtec system.

The automated flow system consists of:

- | | |
|---|----------------------------------|
| a) Display | h) 4 sample loops |
| b) Pressure, flow rate and temperature display. | i) Ion electrochemical reactor. |
| c) Cooling system. | j) Reactor heating system. |
| d) Solvents or reagents bottle. | k) Ion potentiostat. |
| e) Waste bottle. | l) Autosampler pump. |
| f) 2 HPLC pumps. | m) Autosampler. |
| g) 2 V-3 pumps. | n) loading and collection racks. |

Ion electrochemical reactor

The undivided electrochemical flow cell developed by Vapourtec Ltd was used to carry out the electrochemical transformation (Figure 6.2). The body of the microreactor consists of two stainless steel parts (**a**), each part can accommodate a (50 mm x 50 mm) electrode (**b**), the two electrodes are separated by a 500 μm fluorinated ethylene propylene (FEP) spacer (**c**) and clamp to tighten the reactor (**d**).

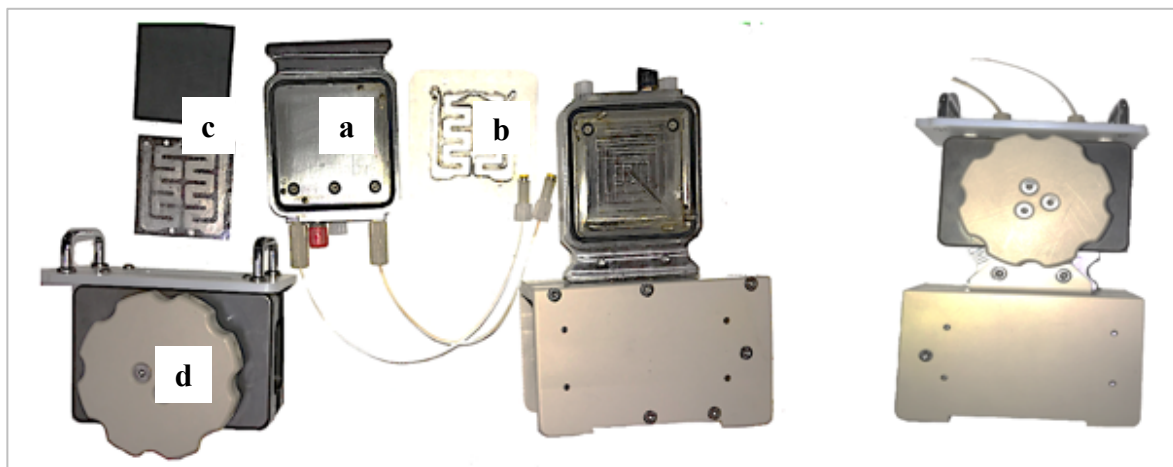


Figure 6.2. Ion electrochemical reactor.

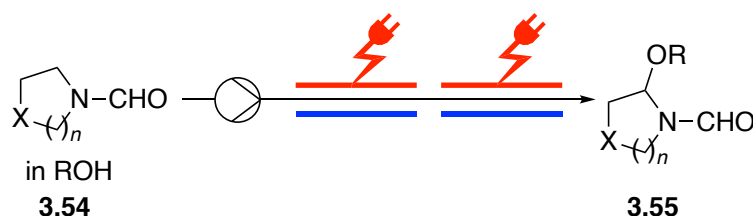
6.3. Experimental Data for Chapter 2:

Electrochemical Alkoxylation of *N*-Formylpyrrolidine in a Flow Cell

6.3.1. Synthesis of *N,O*-acetals

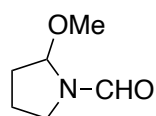
6.3.1.1. Monoalkoxylation of *N*-Formylpyrrolidine

General Procedure 1 (GP1):



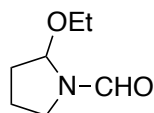
A solution of **3.54** (0.1 M, 60 mL) in MeOH containing Et₄NBF₄ (0.05 M); with alcohol (EtOH, PrOH, BuOH and PentOH) was sonicated prior to the electrolysis to ensure complete dissolution. Two microreactors were connected and the aforementioned solution was pumped at 0.5 mL/min using a syringe pump or the Vapourtec E series, applying a constant current of 160 mA on each reactor. The first 5 mL were discarded, then the reaction mixture was collected for 110 min (55 mL). The alcohol was removed under reduced pressure, and the crude product was washed with water (50 mL) to remove the supporting electrolyte and extracted with CH₂Cl₂ (3 x 30 mL). The organic layers were combined, dried over anhydrous MgSO₄, filtered, evaporated and dried under high vacuum. The residue was chromatographed through silica gel eluting with hexane / ethyl acetate.

2-Methoxypyrrolidine-1-carbaldehyde (**3.55a**):



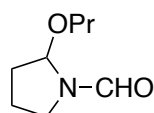
Compound **3.55a** was synthesized following GP1, using *N*-formylpyrrolidine **3.54a** (545 mg, 5.5 mmol) to give the product as a colorless oil (629 mg, 89%), chromatography: hexane/ ethyl acetate (1:1). NMR spectra show a mixture of rotamers (~ 5:1).

¹H NMR (400 MHz, CDCl₃): δ = 8.40_{maj} and 8.29_{min} (s, 1H), 5.37_{min} and 4.92_{maj} (d, *J* = 4.8 Hz, 1H), 3.58 – 3.40 (m, 2H), 3.38_{min} and 3.26_{maj} (s, 3H), 2.13 – 1.79 (m, 4H) ppm. ¹³C NMR (101 MHz, CDCl₃): δ = 162.6_{min} and 161.4_{maj}, 89.7_{maj} and 85.5_{min}, 56.6_{min} and 54.4_{maj}, 45.2_{min} and 42.7_{maj}, 31.9_{min} and 31.8_{maj}, 22.1_{min} and 21.4_{maj} ppm. The spectroscopic data are in agreement with the literature.^[2]

2-Ethoxypyrrolidine-1-carbaldehyde (3.55b):

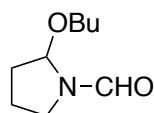
Compound **3.55b** was synthesized following GP1, using *N*-formylpyrrolidine **3.54a** (545 mg, 5.5 mmol) to give the product as a colorless oil (609 mg, 77%), chromatography: hexane/ ethyl acetate (1:1). NMR spectra show a mixture of rotamers ($\sim 5:1$).

^1H NMR (400 MHz, CDCl_3): $\delta = 8.38_{\text{maj}}$ (s, 1H), 8.26_{min} (s, 1H), 5.46_{min} (d, $J = 3.4$ Hz, 1H), 5.03_{maj} (d, $J = 4.8$ Hz, 1H), $3.66 - 3.25$ (m, 4H), $2.24 - 1.68$ (m, 4H), $1.35 - 1.06$ (m, 3H) ppm. ^{13}C NMR (101 MHz, CDCl_3): $\delta = 162.8_{\text{min}}$, 161.7_{maj} , 88.3_{maj} , 84.1_{min} , 64.5_{min} , 62.5_{maj} , 45.2_{min} , 42.7_{maj} , 32.2_{min} , 32.2_{maj} , 22.2_{min} , 21.5_{maj} , 15.4_{min} , 15.1_{maj} ppm; IR (neat): 2976, 2885, 1666, 1386, 1066 cm^{-1} ; HRMS (ESI): m/z calcd for $\text{C}_7\text{H}_{13}\text{NO}_2^+$: 143.0946; found: 143.0954.

2-Propoxypyrrolidine-1-carbaldehyde (3.55c):

Compound **3.55c** was synthesized following GP1, using *N*-formylpyrrolidine **3.54a** (545 mg, 5.5 mmol) to give the product as a colorless oil (553 mg, 64%), chromatography: hexane/ ethyl acetate (1:1). NMR spectra show a mixture of rotamers ($\sim 5:1$).

^1H NMR (500 MHz, CDCl_3): $\delta = 8.37_{\text{maj}}$, 8.25_{min} (s, 1H), 5.44_{min} and 5.00_{maj} (d, $J = 4.7$ Hz, 1H), $3.61 - 3.18$ (m, 4H), $2.28 - 1.69$ (m, 4H), $1.69 - 1.34$ (m, 2H), 0.88 (q, $J = 7.9$ Hz, 3H) ppm; ^{13}C NMR (126 MHz, CDCl_3): $\delta = 162.42_{\text{min}}$ and 161.34_{maj} , 88.37_{maj} and 84.22_{min} , 70.70_{min} and 68.68_{maj} , 45.12_{min} and 42.62_{maj} , 32.11_{min} and 32.08_{maj} , 23.05_{min} and 22.78_{maj} , 22.19_{min} and 21.47_{maj} , 13.65_{min} and 10.66_{maj} ppm; IR (neat): 2962, 2877, 1668, 1386, 1074 cm^{-1} ; HRMS (ESI): m/z calcd for $\text{C}_8\text{H}_{16}\text{NO}_2^+$: 158.1176; found: 158.1181.

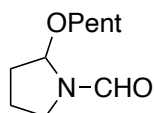
2-Butoxypyrrolidine-1-carbaldehyde (3.55d):

Compound **3.55d** was synthesized following GP1, using *N*-formylpyrrolidine **3.54a** (545 mg, 5.5 mmol) to give the product as a colorless oil (457 mg, 48%), chromatography: hexane/ ethyl acetate (1:1).

^1H NMR (400 MHz, CDCl_3): $\delta = 8.38_{\text{maj}}$ and 8.26_{min} (s, 1H), 5.43_{min} and 5.00_{maj} (d, $J = 4.8$ Hz, 1H), $3.62 - 3.35$ (m, 4H), 3.27 (dt, $J = 8.8, 6.5$ Hz, 1H), $2.20 - 1.75$ (m, 4H), $1.68 - 1.41$ (m,

2H), 1.36 – 1.22 (m, 2H), 0.99 – 0.65 (m, 3H) ppm. ^{13}C NMR (101 MHz, CDCl_3): δ = 162.4_{min}, 161.4_{maj}, 88.4_{maj}, 84.2_{min}, 68.8_{min}, 66.8_{maj}, 45.1_{min}, 42.6_{maj}, 32.11_{maj}, 31.9_{min}, 31.5_{maj}, 22.2_{min}, 21.5_{maj}, 19.4, 14.0_{min}, 13.9_{maj} ppm. IR (neat): 2956, 2872, 1670, 1384, 1076 cm^{-1} ; HRMS (ESI): m/z calcd for $\text{C}_9\text{H}_{18}\text{NO}_2^+$: 172.1332; found: 172.1338.

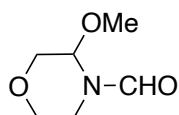
2-(Pentyloxy)pyrrolidine-1-carbaldehyde (3.55e):



Compound **3.55e** was synthesized following GP1, using *N*-formylpyrrolidine **3.54a** (545 mg, 5.5 mmol) to give the product as a colorless oil (431 mg, 42%), chromatography: hexane/ ethyl acetate (1:1).

^1H NMR (400 MHz, CDCl_3): δ = 8.38_{maj} and 8.26_{min} (s, 1H), 5.45_{min} – 5.0_{maj} (d, J = 4.8 Hz, 1H), 3.62 – 3.35 (m, 3H), 3.27 (dt, J = 8.8, 6.5 Hz, 1H), 2.20 – 1.75 (m, 4H), 1.60 – 1.46 (m, 3H), 1.34 – 1.20 (m, 4H), 0.91 – 0.83 (m, 3H) ppm. ^{13}C NMR (101 MHz, CDCl_3): δ = 162.4_{min}, 161.4_{maj}, 88.4_{maj}, 84.2_{min}, 77.80, 69.1_{min}, 67.45_{maj}, 45.1_{min}, 42.6_{maj}, 32.14_{min}, 32.11_{maj}, 29.5_{min}, 29.2_{maj}, 28.4_{maj}, 22.6_{min}, 22.5_{maj}, 22.2_{min}, 21.5_{maj}, 14.15_{min}, 14.11_{maj} ppm. IR (neat): 2954, 2860, 1670, 1384, 1076 cm^{-1} ; HRMS (ESI): m/z calcd for $\text{C}_{10}\text{H}_{20}\text{NO}_2^+$: 186.1493; found: 186.1494.

3-Methoxymorpholine-4-carbaldehyde (3.55f):

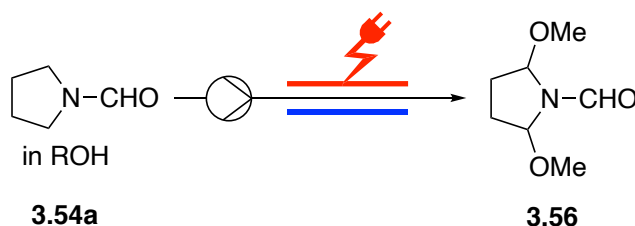


Compound **3.55f** was synthesized following GP1, using *N*-formylmorpholine (633 mg, 5.5 mmol) to give the product as a colorless oil (534 mg, 67%), chromatography: hexane/ ethyl acetate (1:1).

trans-Atropisomer (70%): ^1H NMR (500 MHz, CDCl_3): δ = 8.19 (s, 1H), 4.46 (s, 1H), 4.0 (dd, J = 11.6, 3.4 Hz, 1H), 3.90–4.12 (m, 2H), 3.41–3.63 (m, 2H), 3.27 (s, 3H), 3.14 (td, J = 12.8, 3.9 Hz, 1H). ^{13}C NMR (126 MHz, CDCl_3): δ = 161.2, 83.4, 70.0, 66.2, 54.6, 36.5 ppm. cis-Atropisomer (30%): ^1H NMR (500 MHz, CDCl_3): δ = 8.18 (s, 1H), 5.31 (m, 1H), 3.90–4.12 (m, 2H), 3.60–3.65 (m, 1H), 3.41–3.63 (m, 2H), 3.33 (s, 3H) ppm. ^{13}C NMR (126 MHz, CDCl_3): δ = 162.2, 77.0, 69.4, 67.0, 55.8, 41.6 ppm. IR (neat): 2943, 2885, 1664, 1415, 1064, 1033 cm^{-1} . The spectral data are in agreement with the literature.^[3]

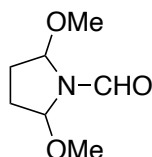
6.3.1.2. Dialkoxylation of *N*-Formylpyrrolidine

General Procedure 2 (GP 2):



A solution of **3.54a** (0.1 M, 60 mL) in MeOH containing Et₄NBF₄ (0.05 M); with alcohol (EtOH, PrOH, BuOH and PentOH) was sonicated prior to the electrolysis to ensure complete dissolution. The aforementioned solution was pumped through one microreactor at 0.5 mL min⁻¹ using a syringe pump or the Vapourtec E series, applying a constant current of 640 mA. The first 5 mL were discarded, then the reaction mixture was collected for 110 min (55 mL). MeOH was removed under reduced pressure, and the crude product was washed with water (50 mL) to remove the supporting electrolyte and extracted with CH₂Cl₂ (3 x 30 mL). The organic layers were combined, dried over anhydrous MgSO₄, filtered, evaporated and dried under high vacuum. The residue was chromatographed through silica gel eluting with hexane / ethyl acetate.

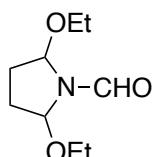
2,5-Dimethoxypyrrolidine-1-carbaldehyde (3.56a):



Compound **3.56a** was synthesized following GP2, using *N*-formylpyrrolidine **3.54a** (545 mg, 5.5 mmol) to give the product as a colorless oil (723 mg, 83%), chromatography: hexane/ ethyl acetate (2:3).

NMR spectra show a mixture of rotamers. ¹H NMR (500 MHz, CDCl₃): δ = 8.49_{min} and 8.40_{maj} (s, 1H), 5.40_{maj} and 5.30_{min} (d, *J* = 3.1 Hz, 1H), 5.00_{maj} and 4.97_{min} (d, *J* = 5.4 Hz, 1H), 3.41_{maj} and 3.39_{min} (s, 3H), 3.30_{maj}, 3.29_{min} (s, 3H), 2.15 – 1.80 (m, 4H) ppm; ¹³C NMR (126 MHz, CDCl₃): δ = 162.9, 162.8, 90.6, 89.5, 86.4, 86.3, 57.1, 56.8, 54.7, 54.2, 30.4, 30.0, 28.9, 28.3 ppm; IR (neat): 2987, 2833, 1681, 1363, 1076 cm⁻¹. The spectroscopic data are in agreement with the literature.^[4]

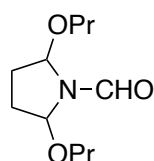
2,5-Diethoxypyrrolidine-1-carbaldehyde (3.56b):



Compound **3.56b** was synthesized following GP2, using *N*-formylpyrrolidine **3.54a** (545 mg, 5.5 mmol) to give the product as a colorless oil (527 mg, 51%), chromatography: hexane/ ethyl acetate (1:1).

^1H NMR (500 MHz, CDCl_3): δ = 8.48_{min} and 8.38_{maj} (s, 1H), 5.65 – 5.36 (m, 1H), 5.08 (dd, J = 13.0, 5.5 Hz, 1H), 3.75 – 3.51 (m, 3H), 3.46 – 3.31 (m, 1H), 2.21 – 1.86 (m, 4H), 1.27 – 1.13 (m, 6H) ppm. ^{13}C NMR (126 MHz, CDCl_3): δ = 162.8, 89.2, 84.7, 64.5, 62.0, 30.8, 30.2, 15.4, 15.1 ppm.

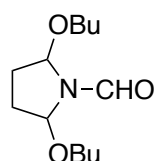
2,5-Dipropoxypyrrolidine-1-carbaldehyde (3.56c):



Compound **3.56c** was synthesized following GP2, using *N*-formylpyrrolidine **3.54a** (545 mg, 5.5 mmol) to give the product as a colorless oil (413 mg, 35%), chromatography: hexane/ ethyl acetate (1:1).

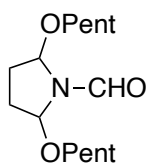
^1H NMR (500 MHz, CDCl_3): δ = 8.37 (s, 1H), 5.46 (d, J = 2.7 Hz, 1H), 5.08 (d, J = 5.4 Hz, 1H), 3.58 – 3.48 (m, 2H), 3.44 (q, J = 7.4 Hz, 1H), 3.27 (q, J = 7.4 Hz, 1H), 2.15 – 1.91 (m, 4H), 1.65 – 1.49 (m, 4H), 0.94 – 0.82 (m, 6H) ppm. ^{13}C NMR (126 MHz, CDCl_3): δ = 162.8, 89.3, 84.9, 70.7, 68.2, 30.8, 30.1, 23.0, 22.8, 10.74, 10.72 ppm; IR (neat): 2960, 2875, 1683, 1367, 1072 cm^{-1} ; HRMS (ESI): m/z calcd for $\text{C}_{11}\text{H}_{21}\text{NO}_3^+$: 215.1521; found: 215.1521.

2,5-Dibutoxypyrrolidine-1-carbaldehyde (3.56d):



Compound **3.56d** was synthesized following GP1, using *N*-formylpyrrolidine **3.54a** (545 mg, 5.5 mmol) to give the product as a colorless oil (364 mg, 27%), chromatography; hexane/ ethyl acetate (1:1).

^1H NMR (400 MHz, CDCl_3): δ = 8.38 (s, 1H), 5.47 (m, 1H), 5.08 (dd, J = 5.5, 2.5 Hz, 1H), 3.65 – 3.43 (m, 3H), 3.35 – 3.27 (m, 1H), 2.25 – 1.91 (m, 4H), 1.54 (ddd, J = 21.9, 10.8, 6.6 Hz, 4H), 1.42 – 1.28 (m, 4H), 0.90 (dt, J = 13.6, 6.8 Hz, 6H) ppm. ^{13}C NMR (101 MHz, CDCl_3): δ = 162.8, 89.3, 84.8, 68.8, 66.3, 31.9, 31.6, 30.7, 30.1, 19.48, 19.45, 14.0, 13.9 ppm. IR (neat): 2962, 2877, 1668, 1386, 1074 cm^{-1} ; HRMS (ESI): m/z calcd for $\text{C}_{13}\text{H}_{26}\text{NO}_3^+$: 244.1913; found: 244.1913.

2,5-Pis(pentyloxy)pyrrolidine-1-carbaldehyde (3.56e):

Compound **3.56e** was synthesized following GP1, using *N*-formylpyrrolidine **3.54a** (545 mg, 5.5 mmol) to give the product as a colorless oil (342 mg, 22%), chromatography: hexane/ ethyl acetate (1:1).

^1H NMR (400 MHz, CDCl_3): δ = 8.37 (s, 1H), 5.49 – 5.42 (m, 1H), 5.07 (dd, J = 5.6, 2.5 Hz, 1H), 3.65 – 3.40 (m, 3H), 3.34 – 3.24 (m, 1H), 2.15 – 1.94 (m, 4H), 1.54 (ddd, J = 21.1, 14.0, 6.9 Hz, 4H), 1.37 – 1.21 (m, 8H), 0.92 – 0.81 (m, 6H) ppm. ^{13}C NMR (101 MHz, CDCl_3): δ = 162.8, 89.3, 84.8, 68.8, 66.3, 31.9, 31.6, 30.7, 30.1, 29.5, 29.2, 28.4, 22.6, 22.5, 14.13, 14.10 ppm. IR (neat): 2954, 2860, 1685, 1379, 1087 cm^{-1} ; HRMS (ESI): m/z calcd for $\text{C}_{15}\text{H}_{30}\text{NO}_3^+$: 271.2174; found: 272.2226.

General Procedure 3 (GP 3): Divided flow cell

The anolyte solution of **3.54a** (0.1 M, 60 mL) in MeOH containing Et_4NBF_4 (0.05 M) and the catholyte solution, MeOH (60 mL) containing Et_4NBF_4 (0.05 M) were sonicated prior to the electrolysis to ensure complete dissolution. The aforementioned solutions were pumped through one microreactor divided by Nafion membrane (Nafion[®] N-324 membrane, 0.15 mm thick, Teflon[®] fabric reinforced $\text{Rf}[\text{OCF}_2(\text{CF}_3)_2]_n\text{OCF}_2\text{SO}_3\text{H}$) at 0.5 mL min^{-1} each using syringe pump or the Vapourtec E series, applying a constant current of 160 mA. The first 5 mL were discarded, then the reaction mixture was collected for 110 min (55 mL). MeOH was removed under reduced pressure, and the crude product was washed with water (50 mL) to remove the supporting electrolyte and extracted with CH_2Cl_2 (3 x 30 mL). The organic layers were combined, dried over anhydrous MgSO_4 , filtered, evaporated and dried under high vacuum. The residue was chromatographed through silica gel eluting with hexane / ethyl acetate to afford **3.55a**.

Procedure 4 (GP4): Batch reaction

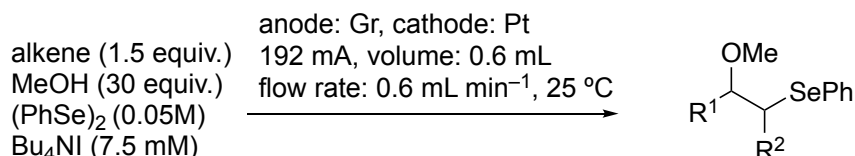
A solution of **3.54a** (0.1 M, 60 mL) in MeOH containing Et_4NBF_4 (0.05 M) was sonicated prior to the electrolysis to ensure complete dissolution. The solution was electrolyzed (304 stainless steel cathode and graphite anode, both 1.0 cm^2) stirred and electrolyzed for 160 min, applying a constant current of 10 mA. Then the reaction mixture of **3.54a** and **3.55a** was analyzed using GC to determine the conversion.

6.4. Experimental Data for Chapter 3:

Electrochemical Selenofunctionalization of Alkenes

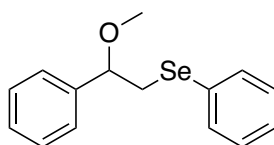
6.4.1. Oxyseleenylation of alkenes

General procedure 5 (GP 5):

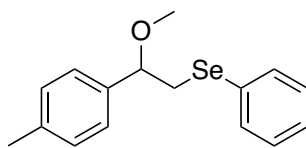


The electrolysis was performed in an undivided cell using a Vapourtec Ion Electrochemical Flow Reactor (reactor volume = 0.6 mL, spacer 0.5 mm) using a Graphite (Gr) electrode as the anode and a platinum (Pt) electrode as the cathode (active surface area: 2 x 12 cm²). A solution of alkene (0.15 M in CH₃CN) placed in vial A and mixture of diphenyl diselenide (0.05 M), alcohol (30 equiv) and TBAI (0.0075 M) in CH₃CN was placed in vial B. Each solution was injected into an 8 mL sample loop. After that, the reactor temperature was set at 25 °C with the flow rate 0.6 mLmin⁻¹ and the current was set at 192 mA to turn on automatically. Then, both solutions were pumped into a PTFE coil (1 mm internal diameter) and mixed *via* a T-piece connected to a 30 cm PTFE coil before the inlet of the electrochemical reactor. After reaching a steady state, the solution (12 mL) was collected automatically into a collection glass vial. The solvent was removed under vacuum. The crude product was purified by column chromatography (EtOAc/hexane).

(2-Methoxy-2-phenylethyl)(phenyl)selane (**3.55**):

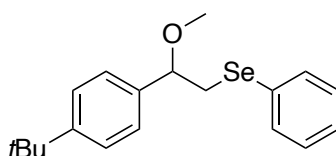


Compound **3.55** was synthesised following GP5 as a colourless oil. It was purified by column chromatography on silica gel using hexane/ethyl acetate (30:1) to obtain 165 mg (95% yield). ¹H NMR (500 MHz, CDCl₃): δ = 7.50 – 7.45 (m, 2H), 7.38 – 7.29 (m, 5H), 7.26 – 7.22 (m, 3H), 4.35 (dd, *J* = 8.4, 5.0 Hz, 1H), 3.33 (dd, *J* = 12.3, 8.4 Hz, 1H), 3.25 (s, 3H), 3.11 (dd, *J* = 12.3, 5.0 Hz, 1H) ppm. ¹³C NMR (126 MHz, CDCl₃): δ = 141.0, 132.7, 130.8, 129.2, 128.7, 128.2, 126.9, 126.8, 83.3, 57.2, 35.5 ppm. The spectroscopic data are in agreement with the literature.^[5]

(2-Methoxy-2-(*p*-tolyl)ethyl)(phenyl)selane (3.56):

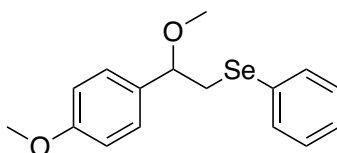
Compound **3.56** was synthesised following GP5 as a colourless oil. It was purified by column chromatography on silica gel using hexane/ethyl acetate (30:1) to obtain 167 mg (91% yield).

^1H NMR (400 MHz, CDCl_3): δ = 7.49 – 7.44 (m, 2H), 7.26 – 7.14 (m, 7H), 4.33 (dd, J = 8.4, 5.1 Hz, 1H), 3.33 (dd, J = 12.2, 8.4 Hz, 1H), 3.24 (s, 3H), 3.10 (dd, J = 12.2, 5.1 Hz, 1H), 2.36 (s, 3H) ppm. ^{13}C NMR (101 MHz, CDCl_3): δ = 137.7, 132.6, 130.9, 129.4, 129.1, 126.9, 126.8, 83.1, 57.0, 35.5, 21.3 ppm. The spectroscopic data are in agreement with the literature.^[6]

(2-(4-(*tert*-Butyl)phenyl)-2-methoxyethyl)(phenyl)selane (3.57):

Compound **3.57** was synthesised following GP5 as a yellow oil. It was purified by column chromatography on silica gel using hexane/ethyl acetate (20:1) to obtain 184 mg (88% yield).

^1H NMR (500 MHz, CDCl_3): δ = 7.51 – 7.43 (m, 2H), 7.40 – 7.38 (m, 2H), 7.26 – 7.18 (m, 5H), 4.35 (dd, J = 8.5, 4.9 Hz, 1H), 3.33 (dd, J = 12.3, 8.5 Hz, 1H), 3.25 (s, 3H), 3.11 (dd, J = 12.3, 4.9 Hz, 1H), 1.32 (s, 9H) ppm. ^{13}C NMR (126 MHz, CDCl_3): δ = 151.2, 138.0, 132.7, 130.9, 129.1, 126.9, 126.5, 125.5, 83.3, 57.2, 35.5, 34.7, 31.6 ppm. The spectroscopic data are in agreement with the literature.^[7]

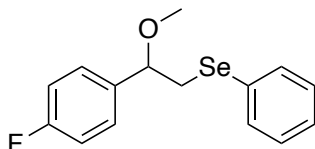
(2-Methoxy-2-(4-methoxyphenyl)ethyl)(phenyl)selane (3.58):

Compound **3.58** was synthesised following GP5 as a colourless oil. It was purified by column chromatography on silica gel using hexane/ethyl acetate (30:1) to obtain 122 mg (63% yield).

^1H NMR (500 MHz, CDCl_3): δ = 7.49 – 7.43 (m, 2H), 7.26 – 7.20 (m, 5H), 6.89 – 6.82 (m, 2H), 4.31 (dd, J = 8.2, 5.3 Hz, 1H), 3.81 (s, 3H), 3.33 (dd, J = 12.2, 8.3 Hz, 1H), 3.22 (s, 3H), 3.09 (dd, J = 12.2, 5.3 Hz, 1H) ppm. ^{13}C NMR (126 MHz, CDCl_3): δ = 159.6, 133.0, 132.6,

130.9, 129.1, 128.0, 126.9, 114.0, 82.8, 56.9, 55.4, 35.5 ppm. The spectroscopic data are in agreement with the literature.^[6]

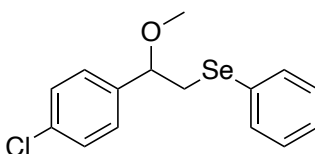
(2-(4-Fluorophenyl)-2-methoxyethyl)(phenyl)selane (3.59):



Compound **3.59** was synthesised following GP5 as a colourless oil. It was purified by column chromatography on silica gel using hexane/ethyl acetate (30:1) to obtain 156 mg (84% yield).

¹H NMR (500 MHz, CDCl₃): δ = 7.50 – 7.42 (m, 2H), 7.29 – 7.20 (m, 5H), 7.07 – 6.97 (m, 2H), 4.33 (dd, J = 8.0, 5.5 Hz, 1H), 3.30 (dd, J = 12.3, 8.0 Hz, 1H), 3.23 (s, 3H), 3.07 (dd, J = 12.3, 5.5 Hz, 1H) ppm. ¹³C NMR (126 MHz, CDCl₃): δ = 162.6 (d, J = 243.7 Hz), 136.7 (d, J = 3.7 Hz), 132.8, 129.2, 128.4 (d, J = 8.7 Hz), 127.0, 115.5 (d, J = 22.5 Hz), 82.7, 56.1, 35.4 ppm. The spectroscopic data are in agreement with the literature.^[7]

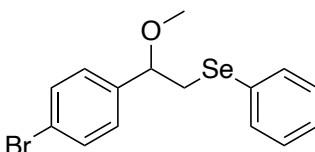
(2-(4-Chlorophenyl)-2-methoxyethyl)(phenyl)selane (3.60):



Compound **3.60** was synthesised following GP5 as a colourless oil. It was purified by column chromatography on silica gel using hexane/ethyl acetate (30:1) to obtain 144 mg (74% yield).

¹H NMR (400 MHz, CDCl₃): δ = 7.49 – 7.44 (m, 2H), 7.32 – 7.28 (m, 2H), 7.26 – 7.16 (m, 5H), 4.31 (dd, J = 7.9, 5.5 Hz, 1H), 3.29 (dd, J = 12.3, 8.0 Hz, 1H), 3.23 (s, 3H), 3.06 (dd, J = 12.3, 5.5 Hz, 1H) ppm. ¹³C NMR (101 MHz, CDCl₃): δ = 139.5, 133.9, 132.8, 130.5, 129.2, 128.9, 128.2, 127.1, 82.7, 57.2, 35.2 ppm. The spectroscopic data are in agreement with the literature.^[6]

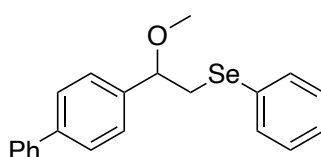
(2-(4-Bromophenyl)-2-methoxyethyl)(phenyl)selane (3.61):



Compound **3.61** was synthesised following GP5 as a yellow oil. It was purified by column chromatography on silica gel using hexane/ethyl acetate (20:1) to obtain 194 mg (87% yield).

^1H NMR (500 MHz, CDCl_3): δ = 7.49 – 7.43 (m, 4H), 7.26 – 7.20 (m, 3H), 7.18 – 7.14 (m, 2H), 4.30 (dd, J = 7.9, 5.5 Hz, 1H), 3.28 (dd, J = 12.4, 7.9 Hz, 1H), 3.23 (s, 3H), 3.06 (dd, J = 12.4, 5.5 Hz, 1H) ppm. ^{13}C NMR (126 MHz, CDCl_3): δ = 140.0, 132.9, 131.8, 130.5, 129.2, 128.9, 127.1, 122.1, 82.7, 57.2, 35.2 ppm. The spectroscopic data are in agreement with the literature.^[7]

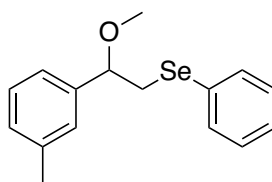
(2-([1,1'-Biphenyl]-4-yl)-2-methoxyethyl)(phenyl)selane (3.62):



Compound **3.62** was synthesised following GP5 as a pale yellow oil. It was purified by column chromatography on silica gel using hexane/ethyl acetate (30:1) to obtain 184 mg (83% yield).

^1H NMR (500 MHz, CDCl_3): δ = 7.60 – 7.57 (m, 4H), 7.50 – 7.44 (m, 4H), 7.39 – 7.34 (m, 3H), 7.26 – 7.22 (m, 3H), 4.41 (dd, J = 8.3, 5.2 Hz, 1H), 3.37 (dd, J = 12.3, 8.3 Hz, 1H), 3.30 (s, 3H), 3.15 (dd, J = 12.3, 5.2 Hz, 1H) ppm. ^{13}C NMR (126 MHz, CDCl_3): δ = 141.2, 140.9, 140.0, 132.8, 130.8, 129.1, 128.9, 127.4, 127.4, 127.2, 127.2, 126.9, 83.1, 57.2, 35.5 ppm. IR (neat): 3055, 2819, 1485, 1477, 1085, 732, 692 cm^{-1} . HRMS (ESI) $^+$ calcd. for $\text{C}_{20}\text{H}_{17}\text{Se}[\text{M}-\text{OMe}]^+$: 333.0522, found: 333.0525.

(2-Methoxy-2-(*m*-tolyl)ethyl)(phenyl)selane (3.63):

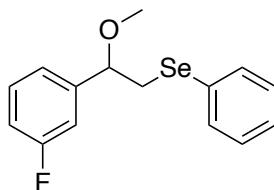


Compound **3.63** was synthesised following GP5 as a yellow oil. It was purified by column chromatography on silica gel using hexane/ethyl acetate (30:1) to obtain 170 mg (93% yield).

^1H NMR (500 MHz, CDCl_3): δ = 7.50 – 7.44 (m, 2H), 7.26 – 7.20 (m, 4H), 7.12 – 7.09 (m, 3H), 4.32 (dd, J = 8.5, 5.0 Hz, 1H), 3.32 (dd, J = 12.2, 8.5 Hz, 1H), 3.25 (s, 3H), 3.10 (dd, J = 12.2, 5.0 Hz, 1H), 2.35 (s, 3H) ppm. ^{13}C NMR (126 MHz, CDCl_3): δ = 141.0, 138.4, 132.7, 130.9, 129.1, 129.0, 128.6, 127.4, 126.9, 123.9, 83.4, 57.2, 35.5, 21.6 ppm. IR (neat): 2981,

2820, 1477, 1437, 1084, 731 cm^{-1} . HRMS (ESI)⁺ calcd. for $\text{C}_{15}\text{H}_{15}\text{Se}[\text{M}-\text{OMe}]^+$: 271.0366, found: 271.0374.

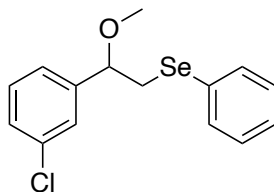
(2-(3-Fluorophenyl)-2-methoxyethyl)(phenyl)selane (3.64):



Compound **3.64** was synthesised following GP5 as a yellow oil. It was purified by column chromatography on silica gel using hexane/ethyl acetate (30:1) to obtain 114 mg (61% yield).

^1H NMR (500 MHz, CDCl_3): δ = 7.50 – 7.44 (m, 2H), 7.32 – 7.25 (m, 1H), 7.24 – 7.21 (m, 3H), 7.09 – 6.96 (m, 3H), 4.33 (dd, J = 8.1, 5.2 Hz, 1H), 3.29 (dd, J = 12.4, 8.2 Hz, 1H), 3.26 (s, 3H), 3.08 (dd, J = 12.4, 5.2 Hz, 1H) ppm. ^{13}C NMR (126 MHz, CDCl_3): δ = 163.2 (d, J = 245.0 Hz), 143.9 (d, J = 6.2 Hz), 132.9, 130.5, 130.2 (d, J = 7.5 Hz), 129.2, 127.1, 122.5 (d, J = 2.5 Hz), 115.1 (d, J = 21.2 Hz), 113.7 (d, J = 25.0 Hz), 113.52, 82.8 (d, J = 2.5 Hz), 57.3, 35.2 ppm. ^{19}F NMR (471 MHz, CDCl_3): δ = -112.69 (s) ppm. IR (neat): 2932, 2822, 1477, 1436, 1089, 1072, 733 cm^{-1} .

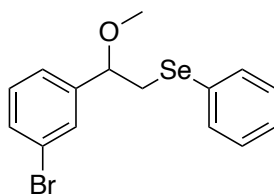
(2-(3-Chlorophenyl)-2-methoxyethyl)(phenyl)selane (3.65):



Compound **3.65** was synthesised following GP5 as a yellow oil. It was purified by column chromatography on silica gel using hexane/ethyl acetate (30:1) to obtain 138 mg (70% yield).

^1H NMR (500 MHz, CDCl_3): δ = 7.49 – 7.43 (m, 2H), 7.29 – 7.27 (m, 1H), 7.27 – 7.21 (m, 5H), 7.19 – 7.14 (m, 1H), 4.30 (dd, J = 8.1, 5.3 Hz, 1H), 3.27 (dd, J = 12.4, 8.1 Hz, 1H), 3.24 (s, 3H), 3.06 (dd, J = 12.4, 5.3 Hz, 1H) ppm. ^{13}C NMR (126 MHz, CDCl_3): δ = 143.2, 134.7, 133.0, 130.5, 130.0, 129.2, 128.4, 127.1, 127.0, 125.0, 82.8, 57.4, 35.2 ppm. IR (neat): 2986, 2821, 1475, 1437, 1099, 1074, 733 cm^{-1} . HRMS (ESI)⁺ calcd. for $\text{C}_{14}\text{H}_{12}\text{ClSe}[\text{M}-\text{OMe}]^+$ 290.9820, found: 290.9810.

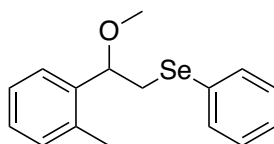
(2-(3-Bromophenyl)-2-methoxyethyl)(phenyl)selane (3.66):



Compound **3.66** was synthesised following GP5 as a yellow oil. It was purified by column chromatography on silica gel using hexane/ethyl acetate (30:1) to obtain 187 mg (84% yield).

^1H NMR (500 MHz, CDCl_3): δ = 7.48 – 7.40 (m, 4H), 7.26 – 7.18 (m, 5H), 4.30 (dd, J = 8.1, 5.3 Hz, 1H), 3.28 (dd, J = 12.4, 8.1 Hz, 1H), 3.25 (s, 3H), 3.06 (dd, J = 12.4, 5.3 Hz, 1H) ppm. ^{13}C NMR (126 MHz, CDCl_3): δ = 143.5, 132.9, 131.3, 130.4, 130.3, 129.9, 129.2, 127.2, 125.5, 122.9, 82.8, 57.4, 35.2 ppm. IR (neat): 2984, 2819, 1476, 1436, 1082, 1070, 732, 688 cm^{-1} .

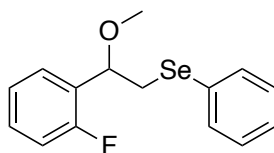
(2-Methoxy-2-(o-tolyl)ethyl)(phenyl)selane (3.67):



Compound **3.67** was synthesised following GP5 as a yellow oil. It was purified by column chromatography on silica gel using hexane/ethyl acetate (30:1) to obtain 154 mg (84% yield).

^1H NMR (400 MHz, CDCl_3): δ = 7.53 – 7.50 (m, 2H), 7.40 – 7.38 (m, 1H), 7.25 – 7.11 (m, 6H), 4.60 (dd, J = 9.0, 4.2 Hz, 1H), 3.31 – 3.17 (m, 4H), 3.07 (dd, J = 12.5, 4.2 Hz, 1H), 2.22 (s, 3H) ppm. ^{13}C NMR (101 MHz, CDCl_3): δ = 139.1, 135.7, 133.2, 130.7, 130.6, 129.1, 127.8, 127.1, 126.5, 126.0, 79.7, 57.1, 34.7, 19.1 ppm. IR (neat): 2980, 2820, 1477, 1437, 1022, 729 cm^{-1} . HRMS (ESI) $^+$ calcd. for $\text{C}_{15}\text{H}_{15}\text{Se}[\text{M}-\text{OMe}]^+$: 271.0366, found: 271.0374.

(2-(2-Fluorophenyl)-2-methoxyethyl)(phenyl)selane (3.68):

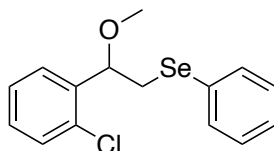


Compound **3.68** was synthesised following GP5 as a pale yellow oil. It was purified by column chromatography on silica gel using hexane/ethyl acetate (30:1) to obtain 120 mg (64% yield).

^1H NMR (500 MHz, CDCl_3): δ = 7.51 – 7.48 (m, 2H), 7.44 – 7.40 (m, 1H), 7.29 – 7.22 (m, 4H), 7.18 – 7.14 (m, 1H), 7.04 – 7.00 (m, 1H), 4.75 (dd, J = 8.2, 4.9 Hz, 1H), 3.32 – 3.25 (m, 4H), 3.20 (dd, J = 12.7, 4.6 Hz, 1H) ppm. ^{13}C NMR (126 MHz, CDCl_3): δ = 160.5 (d, J = 245.0 Hz),

132.8, 130.6, 129.5 (d, $J = 8.7$ Hz), 129.1, 128.0 (d, $J = 13.7$ Hz), 127.7 (d, $J = 3.7$ Hz), 127.0, 124.5 (d, $J = 3.7$ Hz), 115.5 (d, $J = 22.5$ Hz), 76.6 (d, $J = 1.3$ Hz), 57.5, 34.1 ppm. ^{19}F NMR (471 MHz, CDCl_3) $\delta = -119.2$ ppm. IR (neat): 3086, 2824, 1477, 1436, 1105, 1088, 734 cm^{-1} .

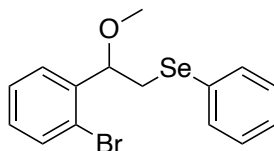
(2-(2-Chlorophenyl)-2-methoxyethyl)(phenyl)selane (3.69):



Compound **3.69** was synthesised following GP5 as a yellow oil. It was purified by column chromatography on silica gel using hexane/ethyl acetate (30:1) to obtain 134 mg (69% yield).

^1H NMR (500 MHz, CDCl_3): $\delta = 7.55 - 7.49$ (m, 3H), 7.34 – 7.28 (m, 2H), 7.26 – 7.19 (m, 4H), 4.85 (dd, $J = 8.7, 3.9$ Hz, 1H), 3.29 (s, 3H), 3.23 (dd, $J = 12.5, 3.9$ Hz, 1H), 3.16 (dd, $J = 12.5, 8.7$ Hz, 1H) ppm. ^{13}C NMR (101 MHz, CDCl_3): $\delta = 138.6, 133.2, 133.1, 130.6, 129.7, 129.1, 127.4, 127.4, 127.0, 79.3, 57.6, 34.1$ ppm. IR (neat): 2985, 2823, 1475, 1436, 1072.1034, 733 cm^{-1} . HRMS (ESI) $^+$ calcd. for $\text{C}_{14}\text{H}_{12}\text{ClSe}[\text{M}-\text{OMe}]^+$: 290.9820, found: 290.9812.

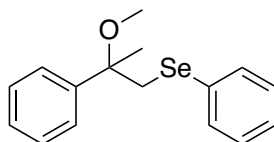
(2-(2-Bromophenyl)-2-methoxyethyl)(phenyl)selane (3.70):



Compound **3.70** was synthesised following GP5 as a yellow oil. It was purified by column chromatography on silica gel using hexane/ethyl acetate (30:1) to obtain 178 mg (80% yield).

^1H NMR (500 MHz, CDCl_3): $\delta = 7.56 - 7.53$ (m, 2H), 7.52 – 7.47 (m, 2H), 7.36 – 7.32 (m, 1H), 7.25 – 7.20 (m, 3H), 7.16 – 7.13 (m, 1H), 4.79 (dd, $J = 8.9, 3.7$ Hz, 1H), 3.29 (s, 3H), 3.22 (dd, $J = 12.6, 3.7$ Hz, 1H), 3.13 (dd, $J = 12.6, 8.9$ Hz, 1H) ppm. ^{13}C NMR (126 MHz, CDCl_3): $\delta = 143.5, 133.0, 131.3, 130.4, 130.3, 129.9, 129.2, 127.2, 125.5, 122.9, 82.8, 57.4, 35.2$ ppm. IR (neat): 3055, 2824, 1475, 1435, 1072.1022, 732, 690 cm^{-1} . HRMS (ESI) $^+$ calcd. for $\text{C}_{14}\text{H}_{12}\text{BrSe}[\text{M}-\text{OMe}]^+$ 334.9315, found: 334.9301.

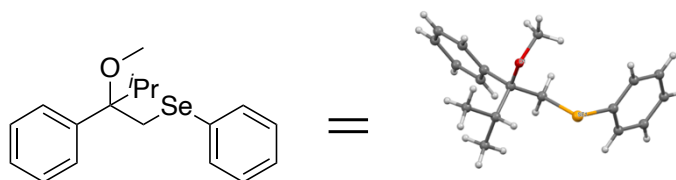
(2-Methoxy-2-phenylpropyl)(phenyl)selane (3.71):



Compound **3.71** was synthesised following GP5 as a yellow oil. It was purified by column chromatography on silica gel using hexane/ethyl acetate (30:1) to obtain 138 mg (75% yield).

^1H NMR (500 MHz, CDCl_3): δ = 7.43 – 7.39 (m, 4H), 7.36 – 7.32 (m, 2H), 7.29 – 7.25 (m, 1H), 7.20 – 7.16 (m, 3H), 3.43 (d, J = 11.3 Hz, 1H), 3.28 (d, J = 11.8 Hz, 1H), 3.13 (s, 3H), 1.72 (s, 3H) ppm. ^{13}C NMR (126 MHz, CDCl_3): δ = 143.8, 132.8, 131.5, 129.0, 128.4, 127.5, 126.8, 126.4, 79.1, 51.2, 42.6, 23.3 ppm. The spectroscopic data are in agreement with the literature.^[8]

(2-Methoxy-3-methyl-2-phenylbutyl)(phenyl)selane (3.72):



Compound **3.72** was synthesised following GP5 as a colourless solid. It was purified by column chromatography on silica gel using hexane/ethyl acetate (30:1) to obtain 32 mg (16% yield), m.p. = 87 – 88 °C.

^1H NMR (500 MHz, CDCl_3): δ = 7.60 – 7.55 (m, 2H), 7.36 – 7.24 (m, 8H), 3.79 (d, J = 12.0 Hz, 1H), 3.62 (d, J = 12.0 Hz, 1H), 3.26 (s, 3H), 2.41 (dt, J = 13.6, 6.8 Hz, 1H), 0.79 (d, J = 6.7 Hz, 3H), 0.75 (d, J = 6.9 Hz, 3H) ppm. ^{13}C NMR (126 MHz, CDCl_3): δ = 139.3, 133.3, 131.0, 129.2, 128.0, 127.6, 127.1, 127.1, 83.7, 50.9, 35.4, 34.8, 18.2, 16.9 ppm. IR (neat): 2966, 2818, 1471, 1170, 1070, 761, 744, 705, 690 cm^{-1} .

Crystal Informations:

Formula: $\text{C}_{13.09} \text{H}_{16} \text{O}_{0.73} \text{Se}_{0.73}$

Space Group: P b c n

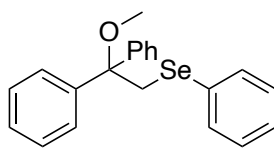
Cell length: a 32.7678(15) b 12.0858(5) c 8.0479(3)

Cell angles: α 90 β 90 γ 90

Cell volume: 3187.17

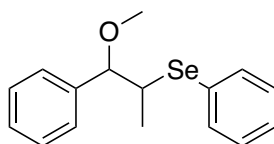
Z, Z' : Z : 11 Z' : 0

R-factor (%): 7.66

(2-Methoxy-2,2-diphenylethyl)(phenyl)selane (3.73):

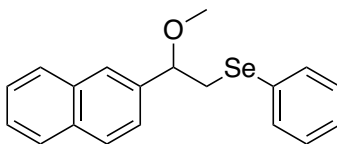
Compound **3.73** was synthesised following GP5 as a colourless solid. It was purified by column chromatography on silica gel using hexane/ethyl acetate (30:1) to obtain 56 mg (25% yield), m.p. = 76 – 78 °C.

^1H NMR (500 MHz, CDCl_3): δ = 7.44 – 7.34 (m, 6H), 7.33 – 7.28 (m, 4H), 7.26 – 7.17 (m, 5H), 3.96 (s, 2H), 3.16 (s, 3H) ppm. ^{13}C NMR (126 MHz, CDCl_3): δ = 144.3, 133.3, 130.9, 129.0, 128.1, 127.3, 127.1, 127.0, 82.2, 50.9, 37.9 ppm. The spectroscopic data are in agreement with the literature.^[9]

(1-Methoxy-1-phenylpropan-2-yl)(phenyl)selane (3.74):

Compound **3.74** was synthesised following GP5 as a yellow oil. It was purified by column chromatography on silica gel using hexane/ethyl acetate (30:1) to obtain 153 mg (84% yield).

^1H NMR (400 MHz, CDCl_3): δ = 7.56 – 7.53 (m, 2H), 7.38 – 7.22 (m, 8H), 4.41 (d, J = 4.5 Hz, 1H), 3.48 (qd, J = 7.0, 4.5 Hz, 1H), 3.30 (s, 3H), 1.35 (d, J = 7.1 Hz, 3H) ppm. ^{13}C NMR (101 MHz, CDCl_3): δ = 139.8, 134.7, 130.1, 129.1, 128.4, 127.9, 127.5, 127.2, 86.5, 57.7, 45.9, 16.5 ppm. The spectroscopic data are in agreement with the literature.^[10]

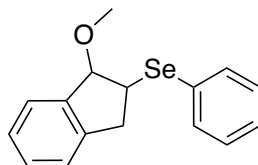
(2-Methoxy-2-(naphthalen-2-yl)ethyl)(phenyl)selane (3.77):

Compound **3.77** was synthesised following GP5 as an orange oil. It was purified by column chromatography on silica gel using hexane/ethyl acetate (30:1) to obtain 177 mg (86% yield).

^1H NMR (400 MHz, CDCl_3): δ = 7.87 – 7.81 (m, 3H), 7.75 (s, 1H), 7.52 – 7.42 (m, 5H), 7.25 – 7.14 (m, 3H), 4.52 (dd, J = 8.3, 5.2 Hz, 1H), 3.40 (dd, J = 12.3, 4.0 Hz, 1H), 3.29 (s, 3H), 3.19 (dd, J = 12.3, 5.2 Hz, 1H) ppm. ^{13}C NMR (126 MHz, CDCl_3): δ = 138.5, 134.4, 133.5,

133.4, 132.9, 130.8, 129.2, 128.8, 128.2, 127.9, 127.1, 126.5, 126.4, 126.3, 124.3, 83.6, 77.3, 57.3, 35.4 ppm. IR (neat): 3050, 2931, 1477, 1437, 1101, 1022, 735 cm^{-1} . HRMS (ESI)⁺ calcd. for $\text{C}_{18}\text{H}_{15}\text{Se}[\text{M}-\text{OMe}]^+$: 307.0366, found: 307.0359.

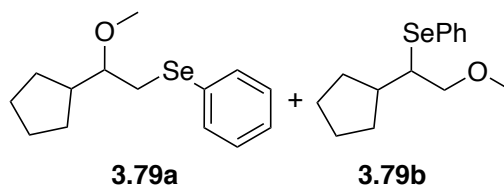
(1-Methoxy-2,3-dihydro-1*H*-inden-2-yl)(phenyl)selane (3.78):



Compound **3.78** was synthesised following GP5 as a orange oil. It was purified by column chromatography on silica gel using hexane/ethyl acetate (30:1) to obtain 168 mg (92% yield).

¹H NMR (400 MHz, CDCl_3): δ = 7.62 – 7.57 (m, 2H), 7.39 (d, J = 7.1 Hz, 1H), 7.32 – 7.19 (m, 6H), 4.76 (d, J = 2.8 Hz, 1H), 4.08 – 3.97 (m, 1H), 3.60 (dd, J = 17.0, 7.4 Hz, 1H), 3.36 (s, 3H), 2.94 (dd, J = 17.0, 3.7 Hz, 1H) ppm. ¹³C NMR (101 MHz, CDCl_3): δ = 142.3, 140.9, 134.4, 129.6, 129.3, 129.1, 127.8, 127.0, 125.7, 125.3, 90.3, 57.0, 44.8, 38.4 ppm. The spectroscopic data are in agreement with the literature.^[7]

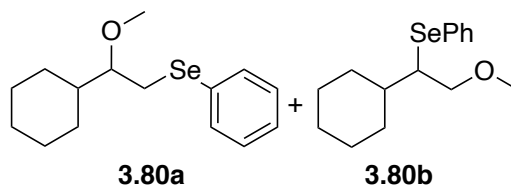
(2-Cyclopentyl-2-methoxyethyl)(phenyl)selane (3.79a) and (1-Cyclopentyl-2-methoxyethyl)(phenyl)selane (3.79b):



Compounds **3.79a** and **3.79b** were synthesised following GP5 as a colourless oil. It was purified by column chromatography on silica gel using hexane/ethyl acetate (30:1) to obtain 127 mg (75% yield).

¹H NMR (500 MHz, CDCl_3): δ = 7.60 – 7.56 (**a**; m, 3H), 7.54 – 7.51 (**b**; m, 2H), 7.28 – 7.20 (**a** + **b**; m, 8H), 3.59– 3.56 (**a** + **b**; m, 3H), 3.38 (**b**; s, 3H), 3.32 (**a**; s, 3H), 3.32 – 3.22 (**a** + **b**; m, 3H), 3.16 (**a**; dd, J = 12.3, 4.8 Hz, 1H), 3.08 (**a**; dd, J = 12.3, 5.8 Hz, 1H), 2.31 – 2.09 (**a** + **b**; m, 2.6H), 1.94 – 1.15 (**a** + **b**; m, 20H) ppm. ¹³C NMR (126 MHz, CDCl_3): δ = 134.6, 132.7, 131.1, 130.10, 129.2, 129.1, 127.4, 126.9, 84.4, 75.71, 58.9, 58.0, 51.85, 44.3, 42.1, 31.7, 31.5, 31.2, 29.35, 28.7, 25.7, 25.6, 25.64, 25.38 ppm. IR (neat): 2947, 2866, 1577, 1475, 1436, 1095, 906, 729, 690 cm^{-1} . HRMS (ESI)⁺ calcd. for $\text{C}_{13}\text{H}_{17}\text{Se}[\text{M}-\text{OMe}]^+$: 249.0522, found: 249.0524.

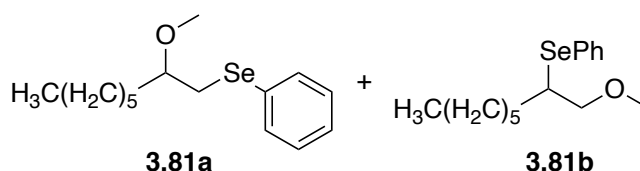
(2-cyclohexyl-2-methoxyethyl)(phenyl)selane (3.80a) and (1-cyclohexyl-2-methoxyethyl)-(phenyl)selane (3.80b):



Compounds **3.80a** and **3.80b** was synthesised following the GP5 as pale yellow oil. It was purified by column chromatography on silica gel using hexane/ethyl acetate (30:1) to obtain 43% isolated yield (76 mg).

^1H NMR (500 MHz, CDCl_3): δ = 7.59 – 7.51 (**a** + **b**; m, 3.6H), 7.29 – 7.20 (**a** + **b**; m, 6H), 3.68 (**a**; dd, J = 10.1, 8.5 Hz, 1H), 3.56 (**a**; dd, J = 10.1, 5.1 Hz, 1H), 3.38 (**b**; s, 3H), 3.30 (**a**; s, 3H), 3.26 – 3.22 (**a**; m, 1H), 3.21 – 3.03 (**a** + **b**; m, 2.5H), 1.89 – 1.40 (**a** + **b**; m, 12H), 1.35 – 1.05 (**a** + **b**; m, 8H) ppm. ^{13}C NMR (126 MHz, CDCl_3): δ = 134.2, 132.7, 131.1, 130.5, 129.1, 129.1, 127.2, 126.8, 85.2, 74.0, 58.7, 58.3, 53.1, 41.4, 39.3, 31.7, 30.1, 30.0, 29.0, 28.3, 26.6, 26.5, 26.54, 26.4, 26.3 ppm. IR (neat): 2974, 2920, 2850, 1577, 1475, 1436, 1097, 1083, 1022, 734, 690 cm^{-1} . HRMS (ESI) $^+$ calcd. for $\text{C}_{14}\text{H}_{19}\text{Se}[\text{M}-\text{OMe}]^+$ 263.0679, found: 263.0685.

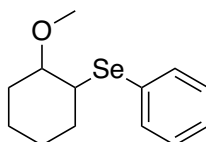
(2-Methoxyoctyl)(phenyl)selane (3.81a) and (1-Methoxyoctan-2-yl)(phenyl)selane (3.81b):



Compounds **3.81a** and **3.81b** were synthesised following GP5 as a colourless oil. It was purified by column chromatography on silica gel using hexane/ethyl acetate (30:1) to obtain 75 mg (42% yield).

^1H NMR (500 MHz, CDCl_3): δ = 7.50 – 7.44 (**a** + **b**; m, 2H), 7.20 – 7.14 (**a** + **b**; m, 4H), 3.48 (**b**; dd, J = 9.9, 5.2 Hz, 1H), 3.42 (**b**; dd, J = 9.9, 7.5 Hz, 1H), 3.33 – 3.27 (**a**; m, 1H), 3.26 (**a**; s, 3H), 3.25 (**b**; s, 3H), 3.23 – 3.18 (**b**; s, 1H), 3.03 (**a**; dd, J = 12.2, 5.5 Hz, 1H), 2.94 (**a**; dd, J = 12.2, 6.1 Hz, 1H), 1.58 – 1.13 (**a** + **b**; m, 12.5H), 0.80 (**a** + **b**; m, 3.75H) ppm. ^{13}C NMR (126 MHz, CDCl_3): δ = 134.9, 133.0, 132.8, 130.9, 129.2, 129.1, 127.6, 126.9, 80.6, 76.0, 58.8, 57.1, 45.0, 32.3, 32.1, 31.9, 31.8, 29.4, 29.2, 27.8, 25.4, 22.7, 14.2 ppm. IR (neat): 2926, 2854, 1577, 1477, 1436, 1091, 1074, 734, 690 cm^{-1} .

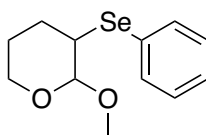
(2-Methoxycyclohexyl)(phenyl)selane (3.82):



Compound **3.82** was synthesised following GP5 as a yellow oil. It was purified by column chromatography on silica gel using hexane/ethyl acetate (30:1) to obtain 130 mg (80% yield).

^1H NMR (500 MHz, CDCl_3): δ = 7.56–7.56 (m, 2H), 7.28 – 7.23 (m, 3H), 3.38 (s, 3H), 3.27 (m, 1H), 3.18 (m, 1H), 2.15 (m, 1H), 2.04 – 1.97 (m, 1H), 1.76 – 1.45 (m, 3H), 1.38 – 1.19 (m, 3H) ppm. ^{13}C NMR (126 MHz, CDCl_3): δ = 135.5, 129.1, 128.9, 127.5, 82.4, 56.5, 47.5, 32.3, 30.4, 25.9, 23.6 ppm. The spectroscopic data are in agreement with the literature.^[11]

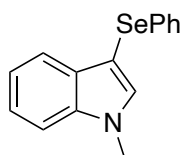
2-Methoxy-3-(phenylselanyl)tetrahydro-2H-pyran (**3.83**):



Compound **3.83** was synthesised following GP5 as a yellow oil. It was purified by column chromatography on silica gel using hexane/ethyl acetate (30:1) to obtain 23 mg (14% yield).

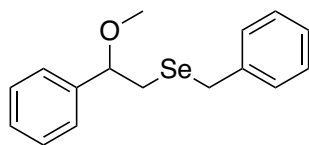
^1H NMR (500 MHz, CDCl_3): δ = 7.59 – 7.54 (m, 2H), 7.30 – 7.23 (m, 3H), 4.51 (d, J = 4.9 Hz, 1H), 3.90 (ddd, J = 11.2, 7.4, 3.6 Hz, 1H), 3.58 – 3.49 (m, 1H), 3.42 (s, 3H), 3.27 (dt, J = 7.4, 4.6 Hz, 1H), 2.20 (ddd, J = 16.9, 8.1, 3.9 Hz, 1H), 1.86 – 1.68 (m, 2H), 1.57 – 1.48 (m, 1H) ppm. ^{13}C NMR (126 MHz, CDCl_3): δ = 134.9, 129.1, 129.0, 127.7, 103.2, 62.9, 55.7, 44.2, 27.5, 24.4 ppm. The spectroscopic data are in agreement with the literature.^[12]

1-Methyl-3-(phenylselanyl)-1H-indole (**3.84**):



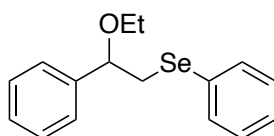
Compound **3.84** was synthesised following GP5 as a colourless oil. It was purified by column chromatography on silica gel using hexane/ethyl acetate (9:1) to obtain 125 mg (72% yield).

^1H NMR (500 MHz, CDCl_3): δ = 7.58 – 7.55 (m, 1H), 7.31 (dt, J = 8.2, 0.9 Hz, 1H), 7.26 – 6.95 (m, 8H), 3.78 (s, 3H) ppm. ^{13}C NMR (101 MHz, CDCl_3): δ = 137.6, 135.8, 134.4, 130.8, 129.0, 128.8, 125.6, 122.6, 120.6, 120.6, 109.7, 96.1, 33.2 ppm. The spectroscopic data are in agreement with the literature.^[13]

Benzyl(2-methoxy-2-phenylethyl)selane (3.85):

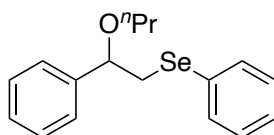
Compound **3.85** was synthesised following GP5 as a pale yellow oil. It was purified by column chromatography on silica gel using hexane/ethyl acetate (30:1) to obtain 76 mg (41% yield).

^1H NMR (500 MHz, CDCl_3): δ = 7.38 – 7.33 (m, 2H), 7.32 – 7.23 (m, 7H), 7.23 – 7.17 (m, 1H), 4.20 (dd, J = 8.0, 5.4 Hz, 1H), 3.70 (d, J = 2.3 Hz, 2H), 3.22 (s, 3H), 2.90 (dd, J = 12.7, 8.0 Hz, 1H), 2.67 (dd, J = 12.7, 5.4 Hz, 1H) ppm. ^{13}C NMR (101 MHz, CDCl_3): δ = 141.3, 139.5, 129.1, 128.6, 128.5, 128.1, 126.8, 126.8, 84.3, 57.0, 31.0, 28.0 ppm. The spectroscopic data are in agreement with the literature.^[7]

(2-Ethoxy-2-phenylethyl)(phenyl)selane (3.86):

Compound **3.86** was synthesised following GP5 as a yellow oil. It was purified by column chromatography on silica gel using hexane/ethyl acetate (30:1) to obtain 157 mg (86% yield).

^1H NMR (400 MHz, CDCl_3): δ = 7.56 – 7.43 (m, 2H), 7.38 – 7.19 (m, 8H), 4.47 (dd, J = 8.5, 5.1 Hz, 1H), 3.38 (m, 3H), 3.10 (dd, J = 12.2, 5.1 Hz, 1H), 1.19 (t, J = 7.0 Hz, 3H) ppm. ^{13}C NMR (101 MHz, CDCl_3): δ = 141.8, 132.7, 131.0, 129.1, 128.6, 128.1, 126.9, 126.7, 81.5, 64.8, 35.7, 15.4 ppm. The spectroscopic data are in agreement with the literature.^[5]

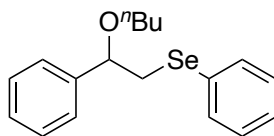
Phenyl(2-phenyl-2-propoxyethyl)selane (3.87):

Compound **3.87** was synthesised following GP5 as a yellow oil. It was purified by column chromatography on silica gel using hexane/ethyl acetate (30:1) to obtain 152 mg (79% yield).

^1H NMR (400 MHz, CDCl_3): δ = 7.51 – 7.30 (m, 2H), 7.28 – 7.06 (m, 8H), 4.36 (dd, J = 8.6, 4.9 Hz, 1H), 3.19 (m, 3H), 2.99 (dd, J = 12.2, 4.9 Hz, 1H), 1.58 – 1.39 (m, 2H), 0.81 (t, J = 7.4

Hz, 3H) ppm. ^{13}C NMR (101 MHz, CDCl_3): δ = 141.9, 132.6, 131.2, 129.1, 128.6, 128.1, 126.8, 126.7, 81.7, 71.2, 35.9, 23.1, 10.8 ppm. IR (neat): 2958, 2874, 1477, 1091, 734, 700 cm^{-1} .

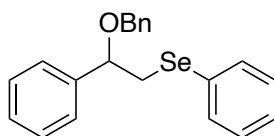
(2-Butoxy-2-phenylethyl)(phenyl)selane (3.88):



Compound **3.88** was synthesised following GP5 as a yellow oil. It was purified by column chromatography on silica gel using hexane/ethyl acetate (30:1) to obtain 148 mg (74% yield).

^1H NMR (400 MHz, CDCl_3): δ = 7.53 – 7.41 (m, 2H), 7.38 – 7.16 (m, 8H), 4.46 (dd, J = 8.7, 4.9 Hz, 1H), 3.40 – 3.23 (m, 3H), 3.09 (dd, J = 12.2, 4.9 Hz, 1H), 1.54 (m, 2H), 1.43 – 1.31 (m, 2H), 0.89 (t, J = 7.3 Hz, 3H) ppm. ^{13}C NMR (101 MHz, CDCl_3): δ = 141.9, 132.6, 131.2, 129.1, 128.6, 128.1, 126.8, 126.7, 81.7, 69.3, 35.9, 32.0, 19.5, 14.0 ppm. The spectroscopic data are in agreement with the literature.^[5]

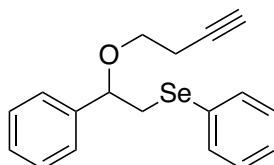
(2-(Benzyloxy)-2-phenylethyl)(phenyl)selane (3.89):



Compound **3.89** was synthesised following GP5 as a yellow oil. It was purified by column chromatography on silica gel using hexane/ethyl acetate (30:1) to obtain 119 mg (54% yield).

^1H NMR (400 MHz, CDCl_3): δ = 7.48 – 7.42 (m, 2H), 7.40 – 7.27 (m, 10H), 7.25 – 7.17 (m, 3H), 4.58 (dd, J = 8.4, 5.0 Hz, 1H), 4.50 (d, J = 11.8 Hz, 1H), 4.32 (d, J = 11.8 Hz, 1H), 3.45–3.83 (m, 1H), 3.12–3.18 (m, 1H) ppm. ^{13}C NMR (126 MHz, CDCl_3): δ = 141.2, 138.2, 132.6, 130.9, 129.1, 128.8, 128.5, 128.3, 128.0, 127.7, 126.9, 126.9, 80.9, 71.0, 35.7 ppm. The spectroscopic data are in agreement with the literature.^[5]

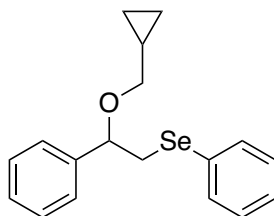
(2-(But-3-yn-1-yloxy)-2-phenylethyl)(phenyl)selane (3.90):



Compound **3.90** was synthesised following GP5 as a yellow oil. It was purified by column chromatography on silica gel using hexane/ethyl acetate (30:1) to obtain 112 mg (57% yield).

^1H NMR (500 MHz, CDCl_3): δ = 7.50 – 7.47 (m, 2H), 7.37 – 7.28 (m, 5H), 7.25 – 7.20 (m, 3H), 4.51 (dd, J = 8.5, 5.0 Hz, 1H), 3.52–3.42(m, 2H), 3.35 (dd, J = 12.4, 8.5 Hz, 1H), 3.09 (dd, J = 12.4, 5.0 Hz, 1H), 2.50–2.40 (m, 2H), 1.95 (t, J = 2.7 Hz, 1H) ppm. ^{13}C NMR (126 MHz, CDCl_3): δ = 141.2, 132.7, 130.9, 129.1, 128.7, 128.3, 126.9, 126.8, 82.1, 81.3, 69.5, 67.4, 35.5, 20.0 ppm. IR (neat): 3057, 2868, 1477, 1437, 1095, 733, 700 cm^{-1} . HRMS (ESI) $^+$ calcd. for $\text{C}_{18}\text{H}_{18}\text{OSeNa}$ $[\text{M}+\text{Na}]^+$: 349.0447, found: 349.0448.

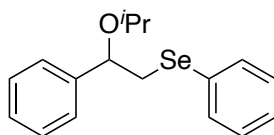
(2-(Cyclopropylmethoxy)-2-phenylethyl)(phenyl)selane (3.91):



Compound **3.91** was synthesised following GP5 as a yellow oil. It was purified by column chromatography on silica gel using hexane/ethyl acetate (30:1) to obtain 150 mg (75% yield).

^1H NMR (500 MHz, CDCl_3): δ = 7.44 – 7.41 (m, 2H), 7.29 – 7.13 (m, 8H), 4.44 (dd, J = 8.4, 5.2 Hz, 1H), 3.31 (dd, J = 12.2, 8.5 Hz, 1H), 3.15 – 3.07 (m, 2H), 3.04 (dd, J = 12.2, 5.1 Hz, 1H), 1.03 – 0.93 (m, 1H), 0.47 – 0.38 (m, 2H), 0.12 – 0.01 (m, 2H) ppm. ^{13}C NMR (126 MHz, CDCl_3): δ = 141.7, 132.6, 131.0, 129.1, 128.6, 128.1, 126.8, 126.7, 81.22, 74.0, 35.8, 10.8, 3.4, 3.1 ppm. IR (neat): 3003, 2858, 1477, 1437, 1089, 1022, 733, 700 cm^{-1} . HRMS (ESI) $^+$ calcd. for $\text{C}_{18}\text{H}_{20}\text{OSeNa}$ $[\text{M}+\text{Na}]^+$: 351.0604, found: 351.0615.

(2-Isopropoxy-2-phenylethyl)(phenyl)selane (3.92):

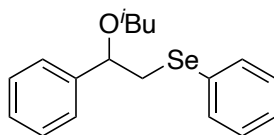


Compound **3.92** was synthesised following GP5 as a yellow oil. It was purified by column chromatography on silica gel using hexane/ethyl acetate (30:1) to obtain 134 mg (70% yield).

^1H NMR (400 MHz, CDCl_3): δ = 7.54 – 7.40 (m, 2H), 7.35 – 7.11 (m, 8H), 4.59 (dd, J = 9.9, 3.6 Hz, 1H), 3.60 – 3.44 (m, 1H), 3.31 (dd, J = 12.1, 8.8 Hz, 1H), 3.08 (dd, J = 12.1, 4.8 Hz, 1H), 1.17 (d, J = 6.0 Hz, 3H), 1.08 (d, J = 6.2 Hz, 3H) ppm. ^{13}C NMR (101 MHz, CDCl_3) δ

142.6, 132.5, 131.2, 129.1, 128.6, 128.0, 126.7, 78.9, 69.9, 36.2, 23.4, 21.5 ppm. The spectroscopic data are in agreement with the literature.^[8]

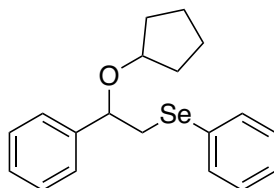
(2-Isobutoxy-2-phenylethyl)(phenyl)selane (3.93):



Compound **3.93** was synthesised following GP5 as a yellow oil. It was purified by column chromatography on silica gel using hexane/ethyl acetate (30:1) to obtain 150 mg (75% yield).

¹H NMR (400 MHz, CDCl₃): δ = 7.56 – 7.43 (m, 2H), 7.38 – 7.18 (m, 8H), 4.46 (dd, J = 8.8, 4.8 Hz, 1H), 3.36 (dd, J = 12.1, 8.8 Hz, 1H), 3.16 – 3.01 (m, 3H), 1.86 (m, 1H), 0.98 – 0.81 (m, 6H) ppm. ¹³C NMR (101 MHz, CDCl₃): δ = 142.6, 132.4, 131.2, 129.1, 128.5, 127.9, 126.7, 78.9, 69.9, 36.2, 23.4, 21.5 ppm. The spectroscopic data are in agreement with the literature.^[5]

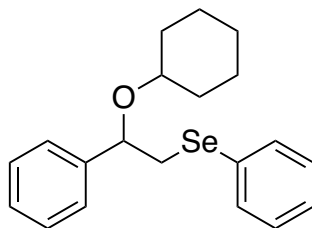
(2-(Cyclopentyloxy)-2-phenylethyl)(phenyl)selane (3.94):



Compound **3.94** was synthesised following GP5 as a yellow oil. It was purified by column chromatography on silica gel using hexane/ethyl acetate (30:1) to obtain 148 mg (71% yield).

¹H NMR (500 MHz, CDCl₃): δ = 7.45 – 7.37 (m, 2H), 7.29 – 7.10 (m, 8H), 4.47 (dd, J = 9.2, 4.4 Hz, 1H), 3.92 – 3.52 (m, 1H), 3.22 (dd, J = 12.2, 9.2 Hz, 1H), 2.99 (dd, J = 12.2, 4.5 Hz, 1H), 1.74 – 1.34 (m, 8H) ppm. ¹³C NMR (126 MHz, CDCl₃): δ = 142.5, 132.4, 131.4, 129.1, 128.6, 127.9, 126.8, 126.7, 79.6, 79.4, 36.2, 33.2, 31.7, 23.5 ppm. IR (neat): 3057, 2868, 1476, 1437, 1072, 1022, 732, 700 cm⁻¹.

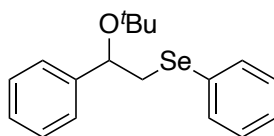
(2-(Cyclohexyloxy)-2-phenylethyl)(phenyl)selane (3.95):



Compound **3.95** was synthesised following GP5 as a yellow oil. It was purified by column chromatography on silica gel using hexane/ethyl acetate (30:1) to obtain 135 mg (62% yield).

^1H NMR (500 MHz, CDCl_3): δ = 7.40 (m, 2H), 7.29 – 7.09 (m, 8H), 4.57 (dd, J = 9.0, 4.6 Hz, 1H), 3.24 (dd, J = 12.1, 9.0 Hz, 1H), 3.16 – 3.07 (m, 1H), 2.99 (dd, J = 12.1, 4.6 Hz, 1H), 1.68 (m, 4H), 1.42 – 0.92 (m, 6H) ppm. ^{13}C NMR (126 MHz, CDCl_3): δ = 142.8, 132.3, 131.4, 129.1, 128.5, 127.9, 126.7, 126.6, 78.5, 75.7, 36.4, 33.5, 31.4, 25.9, 24.2, 24.0 ppm. IR (neat): 2927, 2854, 1477, 1436, 1070, 733, 700 cm^{-1} . The spectroscopic data are in agreement with the literature.^[14]

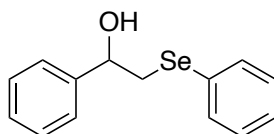
(2-(*tert*-Butoxy)-2-phenylethyl)(phenyl)selane (3.96):



Compound **3.96** was synthesised following GP5 as a yellow oil. It was purified by column chromatography on silica gel using hexane/ethyl acetate (30:1) to obtain 93 mg (47% yield).

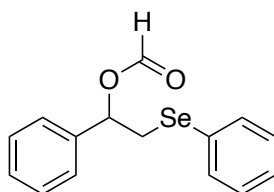
^1H NMR (400 MHz, CDCl_3): δ = 7.41 – 7.31 (m, 2H), 7.27 – 7.06 (m, 8H), 4.60 (dd, J = 8.6, 4.8 Hz, 1H), 3.14 (dd, J = 12.1, 8.6 Hz, 1H), 2.95 (dd, J = 12.1, 4.8 Hz, 1H), 1.02 (s, 9H) ppm. ^{13}C NMR (101 MHz, CDCl_3): δ = 145.3, 132.2, 131.5, 129.1, 128.4, 127.4, 126.6, 126.3, 75.0, 74.2, 37.4, 28.9 ppm. IR (neat): 2972, 2931, 1477, 1436, 1072, 1190, 731, 700 cm^{-1} . The spectroscopic data are in agreement with the literature.^[14]

1-Phenyl-2-(phenylselanyl)ethan-1-ol (3.97):



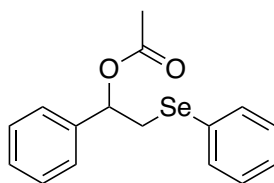
Compound **3.97** was synthesised following GP5 as a colourless oil. It was purified by column chromatography on silica gel using hexane/ethyl acetate (9:1) to obtain 134 mg (81% yield).

^1H NMR (500 MHz, CDCl_3): δ = 7.60 – 7.51 (m, 2H), 7.38 – 7.32 (m, 4H), 7.32 – 7.26 (m, 4H), 4.76 (dd, J = 9.4, 3.5 Hz, 1H), 3.31 (dd, J = 12.8, 3.7 Hz, 1H), 3.15 (dd, J = 12.8, 9.4 Hz, 1H), 2.79 (s, 1H) ppm. ^{13}C NMR (126 MHz, CDCl_3): δ = 142.6, 133.3, 129.4, 129.3, 128.7, 128.1, 127.6, 125.9, 72.4, 38.6 ppm. The spectroscopic data are in agreement with the literature.^[5]

1-Phenyl-2-(phenylselanyl)ethyl formate (3.98):

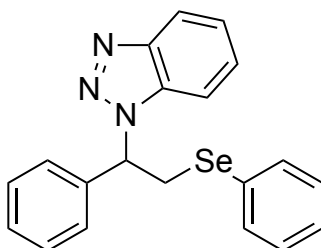
Compound **3.98** was synthesised following GP5 as a colourless oil. It was purified by column chromatography on silica gel using hexane/ethyl acetate (4:1) to obtain 76 mg (41% yield).

^1H NMR (500 MHz, CDCl_3): δ = 8.00 (s, 1H), 7.44 – 7.40 (m, 2H), 7.30 – 7.13 (m, 8H), 5.94 (dd, J = 8.9, 5.8 Hz, 1H), 3.32 (dd, J = 12.9, 8.0 Hz, 1H), 3.18 (dd, J = 13.2, 6.1 Hz, 1H). ^{13}C NMR (126 MHz, CDCl_3): δ = 160.0, 138.8, 135.5, 133.4, 129.3, 128.8, 128.7, 127.5, 126.8, 75.1, 33.2 ppm. The spectroscopic data are in agreement with the literature.^[5]

1-Phenyl-2-(phenylselanyl)ethyl acetate (3.99):

Compound **3.99** was synthesised following GP5 as a colourless oil. It was purified by column chromatography on silica gel using hexane/ethyl acetate (4:1) to obtain 92 mg (46% yield).

^1H NMR (500 MHz, CDCl_3): δ = 7.46 – 7.40 (m, 2H), 7.28 – 7.16 (m, 8H), 5.87 (dd, J = 8.0, 5.7 Hz, 1H), 3.31 (dd, J = 12.8, 8.0 Hz, 1H), 3.16 (dd, J = 12.8, 5.7 Hz, 1H), 1.95 (s, 3H) ppm. ^{13}C NMR (126 MHz, CDCl_3): δ = 170.1, 139.5, 133.2, 129.9, 129.2, 128.6, 128.5, 127.3, 126.7, 75.3, 33.5, 21.2 ppm. The spectroscopic data are in agreement with the literature.^[5]

1-(1-Phenyl-2-(phenylselanyl)ethyl)-1*H*-benzo[*d*][1,2,3]triazole (3.100):

Compound **3.100** was synthesised following GP5 as a colourless oil. It was purified by column chromatography on silica gel using hexane/ethyl acetate (9:1) to obtain 147 mg (65% yield).

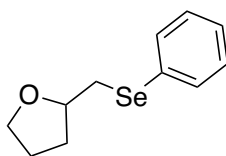
^1H NMR (500 MHz, CDCl_3): δ = 8.10 – 7.94 (m, 1H), 7.46 – 7.39 (m, 2H), 7.38 – 7.19 (m, 11H), 5.85 (dd, J = 9.4, 5.8 Hz, 1H), 4.25 (dd, J = 13.1, 9.4 Hz, 1H), 3.82 (dd, J = 13.1, 5.8 Hz, 1H) ppm. ^{13}C NMR (126 MHz, CDCl_3): δ = 146.1, 138.4, 133.7, 133.1, 129.3, 129.0, 129.0, 128.8, 127.8, 127.3, 126.9, 124.0, 120.1, 109.6, 63.6, 32.6 ppm. The spectroscopic data are in agreement with the literature.^[5]

6.4.2. Intramolecular selenocyclisations of alkenes.

General Procedure 6 (GP 6):

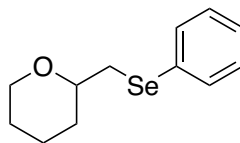
The electrolysis was performed in an undivided cell using a Vapourtec Ion Electrochemical Flow Reactor (reactor volume = 0.6 mL, spacer 0.5 mm) using a Graphite (Gr) electrode as the anode and a platinum (Pt) electrode as the cathode (immersed surface area: $A = 12 \text{ cm}^2$). A solution of alkene (0.15 M in CH_3CN) placed in vial A and mixture of diphenyl diselenide (0.05 M) and TBAI (0.0075 M) in CH_3CN was placed in vial B. Each solution was injected to 8 ml sample loop. After that, the reactor temperature was set at 25°C with the flow rate 0.6 mLmin^{-1} and the current set at 192 mA turn on automatically. Then, both solutions were pumped into a PTFE coil (1 mm internal diameter) and mix via a T-piece connected to 30 cm PTFE coil before the inlet of the electrochemical reactor. After reaching a steady state, the solution (12 mL) was collected automatically into a collection glass vial. The solvent was removed under vacuum. The crude product was purified by column chromatography (EtOAc/hexane).

2-((Phenylselenanyl)methyl)tetrahydrofuran (4.101):



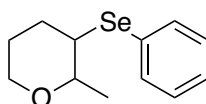
Compound **4.101** was synthesised following GP6 as a pale yellow oil. It was purified by column chromatography on silica gel using hexane/ethyl acetate (4:1) to obtain 105 mg (73% yield).

^1H NMR (500 MHz, CDCl_3): δ = 7.59 – 7.50 (m, 2H), 7.30 – 7.22 (m, 3H), 4.30 – 4.03 (m, 1H), 4.01 – 3.88 (m, 1H), 3.84 – 3.66 (m, 1H), 3.15 (dd, J = 12.2, 5.8 Hz, 1H), 3.01 (dd, J = 12.2, 6.9 Hz, 1H), 2.14 – 2.05 (m, 1H), 2.03 – 1.80 (m, 2H), 1.65 (m, 1H) ppm. ^{13}C NMR (126 MHz, CDCl_3): δ = 137.4, 132.7, 129.2, 127.0, 78.4, 78.4, 33.2, 31.7, 26.1 ppm. The spectroscopic data are in agreement with the literature.^[15]

2-((Phenylselanyl)methyl)tetrahydro-2H-pyran (4.102):

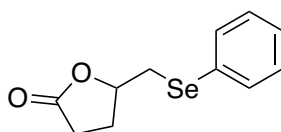
Compound **4.102** was synthesised following GP6 as a pale yellow oil. It was purified by column chromatography on silica gel using hexane/ethyl acetate (4:1) to obtain 103 mg (67% yield).

^1H NMR (500 MHz, CDCl_3): δ = 7.55 – 7.46 (m, 2H), 7.29 – 7.18 (m, 3H), 4.04 – 3.95 (m, 1H), 3.92 – 3.26 (m, 2H), 3.07 (dd, J = 12.2, 6.9 Hz, 1H), 2.93 (dd, J = 12.2, 5.7 Hz, 1H), 1.99 – 1.68 (m, 2H), 1.61 – 1.43 (m, 3H), 1.37 – 1.26 (m, 1H) ppm. ^{13}C NMR (126 MHz, CDCl_3): δ = 132.5, 130.9, 129.1, 126.8, 77.2, 68.9, 33.8, 31.9, 25.9, 23.5 ppm. The spectroscopic data are in agreement with the literature.^[15]

2-((Phenylselanyl)methyl)tetrahydro-2H-pyran (4.103):

Compound **4.103** was synthesised as a 1:1 mixture (*cis* : *trans*) following GP6 as a colourless oil. It was purified by column chromatography on silica gel using hexane/ethyl acetate (9:1) to obtain 89 mg (58% yield).

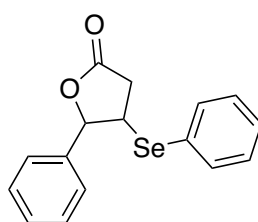
^1H NMR (500 MHz, CDCl_3): δ = 7.61 – 7.55 (m, 4H), 7.31 – 7.23 (m, 6H), 3.96 – 3.86 (m, 3H), 3.78 (dt, J = 9.4, 6.6 Hz, 1H), 3.46 – 3.29 (m, 3H), 2.99 – 2.89 (m, 1H), 2.22 – 2.10 (m, 1H), 2.09 – 1.99 (m, 1H), 1.95 – 1.83 (m, 2H), 1.75 – 1.53 (m, 4H), 1.44 (d, J = 7.0 Hz, 3H), 1.35 (d, J = 6.1 Hz, 3H) ppm. ^{13}C NMR (126 MHz, CDCl_3): δ = 135.6, 135.3, 134.9, 129.1, 129.0, 128.2, 127.9, 127.6, 83.0, 78.4, 68.6, 68.2, 47.2, 44.4, 32.5, 30.4, 28.2, 26.3, 21.3, 18.9 ppm. The spectroscopic data are in agreement with the literature.^[12]

5-((Phenylselanyl)methyl)dihydrofuran-2(3H)-one (104):

Compound **4.104** was synthesised following GP6 as a pale yellow oil. It was purified by column chromatography on silica gel using hexane/ethyl acetate (4:1) to obtain 101 mg (65% yield).

^1H NMR (500 MHz, CDCl_3): δ = 7.62 – 7.46 (m, 2H), 7.33 – 7.26 (m, 3H), 4.69 – 4.61 (m, 1H), 3.29 (dd, J = 12.9, 4.8 Hz, 1H), 3.01 (dd, J = 12.9, 8.0 Hz, 1H), 2.62 – 2.36 (m, 3H), 2.00 – 1.90 (m, 1H) ppm. ^{13}C NMR (126 MHz, CDCl_3): δ = 176.7, 133.4, 129.5, 128.9, 127.8, 79.5, 32.0, 28.9, 27.8 ppm. The spectroscopic data are in agreement with the literature.^[11]

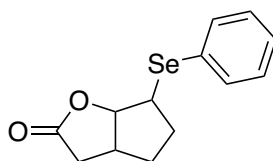
5-Phenyl-4-(phenylselanyl)dihydrofuran-2(3H)-one (4.105)



Compound **4.105** was synthesised following GP6 as a colourless oil. It was purified by column chromatography on silica gel using hexane/ethyl acetate (4:1) to obtain 58 mg (30% yield).

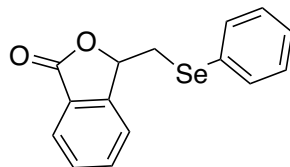
^1H NMR (400 MHz, CDCl_3): δ = 7.55 – 7.52 (m, 2H), 7.40 – 7.28 (m, 8H), 5.38 (d, J = 6.9 Hz, 1H), 3.79– 3.71 (m, 1H), 3.04 (dd, J = 18.0, 8.3 Hz, 1H), 2.67 (dd, J = 18.0, 8.4 Hz, 1H) ppm. ^{13}C NMR (101 MHz, CDCl_3): δ = 174.7, 137.4, 136.3, 129.7, 129.2, 129.1, 128.9, 126.1, 125.9, 86.3, 42.38, 36.1 ppm. The spectroscopic data are in agreement with the literature.^[16]

6-(Phenylselanyl)hexahydro-2H-cyclopenta[b]furan-2-one (4.106):



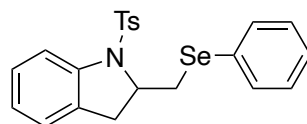
Compound **4.106** was synthesised following GP6 as a colourless oil. It was purified by column chromatography on silica gel using hexane/ethyl acetate (4:1) to obtain 115 mg (68% yield).

^1H NMR (500 MHz, CDCl_3): δ = 7.64 – 7.42 (m, 2H), 7.34 – 7.25 (m, 3H), 4.90 (d, J = 6.3 Hz, 1H), 3.97 – 3.78 (m, 1H), 3.15 – 3.04 (m, 1H), 2.87 – 2.73 (m, 1H), 2.34 (dd, J = 18.4, 2.5 Hz, 1H), 2.28 – 2.18 (m, 2H), 1.91 – 1.71 (m, 1H), 1.61 – 1.51 (m, 1H) ppm. ^{13}C NMR (126 MHz, CDCl_3): δ = 177.0, 133.8, 129.5, 128.8, 127.9, 90.7, 46.4, 37.2, 36.1, 32.6, 30.2 ppm. The spectroscopic data are in agreement with the literature.^[17]

3-((Phenylselanyl)methyl)isobenzofuran-1(3H)-one (4.107):

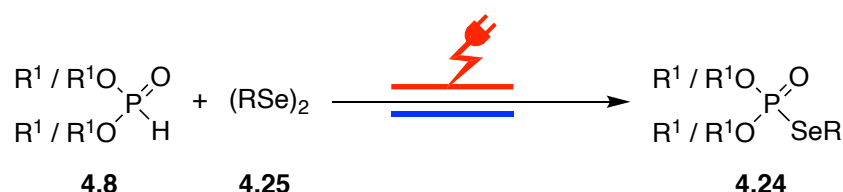
Compound **4.107** was synthesised following GP6 as a colourless oil. It was purified by column chromatography on silica gel using hexane/ethyl acetate (4:1) to obtain 87 mg (48% yield).

^1H NMR (500 MHz, CDCl_3): δ = 7.97 – 7.87 (m, 1H), 7.60 – 7.45 (m, 5H), 7.30 – 7.19 (m, 3H), 5.72 – 5.55 (m, 1H), 3.46 (dd, J = 13.2, 5.0 Hz, 1H), 3.32 (dd, J = 13.2, 6.4 Hz, 1H) ppm. ^{13}C NMR (126 MHz, CDCl_3): δ = 169.9, 148.5, 133.8, 133.6, 129.5, 129.2, 129.0, 127.7, 126.6, 125.7, 122.4, 79.1, 31.8 ppm. The spectroscopic data are in agreement with the literature.^[15]

2-((Phenylselanyl) methyl)-1-tosylindoline (4.108):

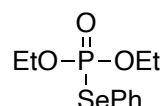
Compound **4.108** was synthesised following GP6 as a yellow solid. It was purified by column chromatography on silica gel using hexane/ethyl acetate (4:1) to obtain 87 mg (33% yield), m.p. = 70 – 72 °C.

^1H NMR (500 MHz, CDCl_3): δ = 7.65 (d, J = 8.1 Hz, 1H), 7.61 – 7.54 (m, 2H), 7.39 – 7.29 (m, 5H), 7.23 – 7.18 (m, 1H), 7.11 – 7.08 (m, 2H), 7.04 – 7.01 (m, 2H), 4.36 – 4.11 (m, 1H), 3.65 (dd, J = 12.5, 3.5 Hz, 1H), 2.96 – 2.81 (m, 3H), 2.32 (s, 3H) ppm. ^{13}C NMR (126 MHz, CDCl_3): δ = 144.0, 141.4, 134.7, 132.6, 131.1, 129.7, 129.4, 128.9, 127.9, 127.2, 127.1, 125.3, 124.8, 117.1, 61.7, 34.2, 33.2, 21.6 ppm. The spectroscopic data are in agreement with the literature.^[18]

6.5. Experimental Data for Chapter 4:**Electrochemical Synthesis of Chalcogenophosphites**General Procedure 7 (GP 7):

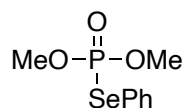
The electrolysis was performed in an undivided cell using a Vapourtec Ion Electrochemical Flow Reactor (reactor volume = 0.6 mL, spacer 0.5 mm) using a Graphite (Gr) anode and a platinum (Pt) cathode (surface area: $A = 12 \text{ cm}^2$). A solution of phosphonate (0.2 M in CH_3CN) is placed in vial A and a mixture of diorganyl dichalcogenides (0.05 M) and Et_4NCl (0.01 M) in CH_3CN placed in vial B. Each solution was injected to 8 mL sample loop. The reactor temperature was set at 25°C with a flow rate of 1.2 mL min^{-1} and the current was set to 96 mA which switched on automatically. Then, both solutions were pumped into a PTFE coil (1 mm internal diameter) and mixed *via* a T-piece connected to a 30 cm PTFE coil before the inlet of the electrochemical reactor. After reaching a steady state, the solution (12 mL) was collected at the reactor outlet automatically into a collection glass vial. The solvent was removed under vacuum. The crude product was purified by column chromatography (EtOAc/cyclohexane).

***O,O*-diethyl *Se*-phenyl phosphoroselenoate (4.24a):**



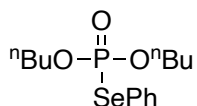
Compound **4.24a** was synthesized following GP7 as a colorless oil. It was purified by column chromatography on silica gel using cyclohexane/ethyl acetate (4:1) to obtain 156 mg (89% yield). ^1H NMR (500 MHz, CDCl_3): $\delta = 7.69 - 7.60$ (m, 2H), $7.38 - 7.29$ (m, 3H), $4.25 - 4.11$ (m, 4H), 1.30 (td, $J = 7.1, 0.8 \text{ Hz}$, 6H) ppm. ^{13}C NMR (126 MHz, CDCl_3): $\delta = 135.7$ (d, $J = 3.7 \text{ Hz}$), 129.6 (d, $J = 1.3 \text{ Hz}$), 128.9 (d, $J = 2.5 \text{ Hz}$), 123.9 (d, $J = 8.7 \text{ Hz}$), 64.0 (d, $J = 6.2 \text{ Hz}$), 16.05 (d, $J = 7.5 \text{ Hz}$) ppm. ^{31}P NMR (202 MHz, CDCl_3): $\delta = 17.92$ ppm. The spectroscopic data are in agreement with the literature.^[19]

***O,O*-dimethyl *Se*-phenyl phosphoroselenoate (4.24b):**



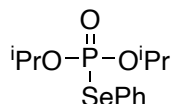
Compound **4.24b** was synthesised following GP7 as a pale yellow oil. It was purified by column chromatography on silica gel using cyclohexane/ethyl acetate (4:1) to obtain 123 mg (77% yield). ^1H NMR (500 MHz, CDCl_3): $\delta = 7.68 - 7.58$ (m, 2H), $7.39 - 7.29$ (m, 3H), 3.81 (s, 3H), 3.78 (s, 3H) ppm. ^{13}C NMR (126 MHz, CDCl_3): $\delta = 135.7$ (d, $J = 3.7 \text{ Hz}$), 129.7 (d, $J = 2.5 \text{ Hz}$), 129.1 (d, $J = 2.5 \text{ Hz}$), 123.4 (d, $J = 8.7 \text{ Hz}$), 54.2 (d, $J = 6.2 \text{ Hz}$) ppm. ^{31}P NMR (202 MHz, CDCl_3): $\delta = 21.88$ ppm. The spectroscopic data are in agreement with the literature.^[20]

***O,O*-dibutyl *Se*-phenyl phosphoroselenoate (4.24c):**



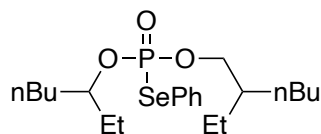
Compound **4.24c** was synthesised following GP7 as a pale yellow oil. It was purified by column chromatography on silica gel using cyclohexane/ethyl acetate (4:1) to obtain 188 mg (90% yield). ^1H NMR (500 MHz, CDCl_3): δ = 7.66 – 7.62 (m, 2H), 7.37 – 7.27 (m, 3H), 4.18 – 4.02 (m, 4H), 1.66 – 1.59 (m, 4H), 1.42 – 1.34 (m, 4H), 0.89 (t, J = 7.4 Hz, 6H) ppm. ^{13}C NMR (126 MHz, CDCl_3): δ = 135.6 (d, J = 4.7 Hz), 129.5 (d, J = 2.0 Hz), 128.8 (d, J = 2.5 Hz), 124.0 (d, J = 8.4 Hz), 67.7 (d, J = 6.4 Hz), 32.2 (d, J = 7.3 Hz), 18.8, 13.69 ppm. ^{31}P NMR (202 MHz, CDCl_3): δ = 18.02 ppm. The spectral data are in agreement with the literature.^[19]

***O,O*-diisopropyl *Se*-phenyl phosphoroselenoate (4.24d):**



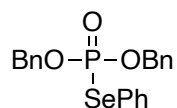
Compound **4.24d** was synthesised following GP7 as a pale yellow oil. It was purified by column chromatography on silica gel using cyclohexane/ethyl acetate (4:1) to obtain 168 mg (87% yield). ^1H NMR (500 MHz, CDCl_3): δ = 7.71 – 7.62 (m, 2H), 7.35 – 7.27 (m, 3H), 4.84 – 4.73 (m, 2H), 1.33 (d, J = 6.2 Hz, 6H), 1.25 (d, J = 6.2 Hz, 6H) ppm. ^{13}C NMR (126 MHz, CDCl_3): δ = 135.3 (d, J = 4.9 Hz), 129.4 (d, J = 1.8 Hz), 128.6 (d, J = 2.3 Hz), 124.7 (d, J = 8.3 Hz), 73.2 (d, J = 6.6 Hz), 24.0 (d, J = 3.8 Hz), 23.6 (d, J = 6.0 Hz) ppm. ^{31}P NMR (202 MHz, CDCl_3): δ = 14.67 ppm. The spectroscopic data are in agreement with the literature.^[20]

***O,O*-bis(2-ethylhexyl) *Se*-phenyl phosphoroselenoate (4.24e):**



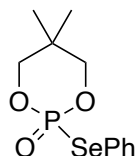
Compound **4.24e** was synthesised following GP7 as a pale yellow oil. It was purified by column chromatography on silica gel using cyclohexane/ethyl acetate (4:1) to obtain 218 mg (79% yield). ^1H NMR (500 MHz, CDCl_3): δ = 7.70 – 7.60 (m, 2H), 7.37 – 7.26 (m, 3H), 4.08 – 3.92 (m, 4H), 1.59 – 1.47 (m, 2H), 1.36 – 1.19 (m, 16H), 0.91 – 0.81 (m, 12H) ppm. ^{13}C NMR (126 MHz, CDCl_3): δ = 135.6 (dt, J = 4.7, 1.8 Hz), 129.5 (d, J = 1.9 Hz), 128.7 (d, J = 2.3 Hz), 124.0 (d, J = 8.4 Hz), 70.0 (dd, J = 7.6, 2.1 Hz), 40.1 (d, J = 1.2 Hz), 30.04 (d, J = 6.9 Hz), 28.9 (d, J = 2.2 Hz), 23.4 (d, J = 5.6 Hz), 23.0, 14.1, 11.0 ppm. ^{31}P NMR (202 MHz, CDCl_3): δ = 17.83 ppm.

***O,O*-dibenzyl *Se*-phenyl phosphoroselenoate (4.24f):**



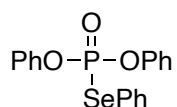
Compound **4.24f** was synthesised following GP7 as a pale yellow oil. It was purified by column chromatography on silica gel using cyclohexane/ethyl acetate (4:1) to obtain 211 mg (84% yield). ^1H NMR (500 MHz, CDCl_3): δ = 7.59 – 7.53 (m, 2H), 7.36 – 7.30 (m, 7H), 7.29 – 7.22 (m, 6H), 5.12 (qd, J = 11.7, 8.7 Hz, 4H) ppm. ^{13}C NMR (126 MHz, CDCl_3): δ = 136.0 (d, J = 4.7 Hz), 135.5 (d, J = 7.9 Hz), 129.7 (d, J = 2.2 Hz), 129.1 (d, J = 2.6 Hz), 128.7, 128.6, 128.3, 123.5 (d, J = 8.6 Hz), 69.3 (d, J = 6.1 Hz) ppm. ^{31}P NMR (202 MHz, CDCl_3): δ = 18.48 ppm. The spectroscopic data are in agreement with the literature.^[20]

5,5-dimethyl-2-(phenylselanyl)-1,3,2-dioxaphosphinane 2-oxide (4.24g):

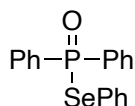


Compound **4.24g** was synthesised following GP7 as a white solid. It was purified by column chromatography on silica gel using cyclohexane/ethyl acetate (4:1) to obtain 154 mg (84% yield). ^1H NMR (500 MHz, CDCl_3): δ = 7.76 – 7.72 (m, 2H), 7.39 – 7.30 (m, 3H), 4.15 (dd, J = 10.6, 4.3 Hz, 2H), 3.87 (ddt, J = 24.7, 11.4, 1.6 Hz, 2H), 1.28 (s, 3H), 0.86 (s, 3H) ppm. ^{13}C NMR (126 MHz, CDCl_3): δ = 136.0 (d, J = 4.7 Hz), 129.8 (d, J = 2.0 Hz), 129.2 (d, J = 2.5 Hz), 122.0 (d, J = 8.0 Hz), 78.2 (d, J = 7.3 Hz), 32.7 (d, J = 7.0 Hz), 22.3, 20.6 (d, J = 1.0 Hz) ppm. ^{31}P NMR (202 MHz, CDCl_3): δ = 9.73 ppm. The spectroscopic data are in agreement with the literature.^[19]

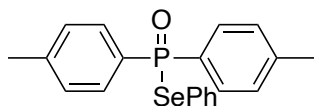
***O,O*,*Se*-triphenyl phosphoroselenoate (4.24h):**



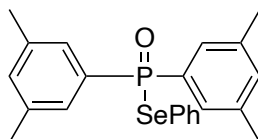
Compound **4.24h** was synthesised following GP7 as a pale yellow oil. It was purified by column chromatography on silica gel using cyclohexane/ethyl acetate (4:1) to obtain 154 mg (95% yield). ^1H NMR (500 MHz, CDCl_3): δ = 7.62 – 7.40 (m, 2H), 7.35 – 7.25 (m, 7H), 7.20 – 7.16 (m, 6H) ppm. ^{13}C NMR (126 MHz, CDCl_3): δ = 150.3 (d, J = 8.6 Hz), 136.3 (d, J = 4.8 Hz), 129.8 (d, J = 1.0 Hz), 129.6 (d, J = 2.5 Hz), 129.4 (d, J = 3.0 Hz), 125.7 (d, J = 1.5 Hz), 122.7 (d, J = 9.1 Hz), 120.7 (d, J = 5.1 Hz) ppm. ^{31}P NMR (202 MHz, CDCl_3): δ = 9.43 ppm. The spectroscopic data are in agreement with the literature.^[20]

Se-phenyl diphenylphosphinoselenoate (4.24i):

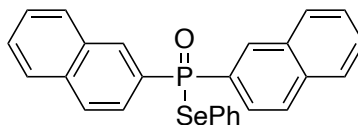
Compound **4.24i** was synthesised following GP7 as a pale yellow oil. It was purified by column chromatography on silica gel using cyclohexane/ethyl acetate (4:1) to obtain 198 mg (92% yield). ^1H NMR (500 MHz, CDCl_3): δ = 7.87 – 7.77 (m, 4H), 7.53 – 7.46 (m, 4H), 7.46 – 7.41 (m, 4H), 7.26 – 7.23 (m, 1H), 7.19 – 7.12 (m, 2H) ppm. ^{13}C NMR (126 MHz, CDCl_3): δ = 136.4 (d, J = 3.3 Hz), 134.0 (s), 133.3 (s), 132.4 (d, J = 3.1 Hz), 131.5 (d, J = 10.6 Hz), 129.4 (d, J = 1.6 Hz), 128.8 (d, J = 2.0 Hz), 128.6 (d, J = 13.2 Hz), 123.9 (d, J = 5.7 Hz) ppm. ^{31}P NMR (202 MHz, CDCl_3): δ = 20.18 ppm. The spectroscopic data are in agreement with the literature.^[21]

Se-phenyl di-*p*-tolylphosphinoselenoate (4.24j):

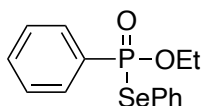
Compound **4.24j** was synthesised following GP7 as white solid. It was purified by column chromatography on silica gel using cyclohexane/ethyl acetate (4:1) to obtain 204 mg (88% yield). ^1H NMR (500 MHz, CDCl_3): δ = 7.73 – 7.66 (m, 4H), 7.52 – 7.46 (m, 2H), 7.25 – 7.19 (m, 5H), 7.18 – 7.13 (m, 2H), 2.37 (s, 6H) ppm. ^{13}C NMR (126 MHz, CDCl_3): δ = 142.9 (d, J = 3.1 Hz), 136.4 (d, J = 3.3 Hz), 131.5 (d, J = 11.0 Hz), 131.1, 130.3, 129.42 (d, J = 13.6 Hz), 129.40 (d, J = 1.5 Hz), 128.7 (d, J = 1.9 Hz), 124.5 (d, J = 5.6 Hz), 21.8 ppm. ^{31}P NMR (202 MHz, CDCl_3): δ = 40.24 ppm. The spectroscopic data are in agreement with the literature.^[22]

Se-phenyl bis(3,5-dimethylphenyl)phosphinoselenoate (4.24k):

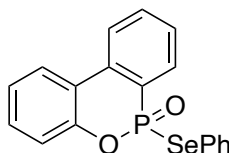
Compound **4.24k** was synthesised following GP7 as colorless oil. It was purified by column chromatography on silica gel using cyclohexane/ethyl acetate (4:1) to obtain 212 mg (85% yield). ^1H NMR (500 MHz, CDCl_3): δ = 7.53 – 7.48 (m, 2H), 7.45 – 7.37 (m, 4H), 7.26 – 7.22 (m, 1H), 7.19 – 7.14 (m, 2H), 7.12 – 7.07 (m, 2H), 2.30 (s, 12H) ppm. ^{13}C NMR (126 MHz, CDCl_3): δ = 138.2 (d, J = 13.9 Hz), 136.4 (d, J = 3.2 Hz), 134.0 (d, J = 3.2 Hz), 133.0, 129.2 (d, J = 1.5 Hz), 128.9 (d, J = 10.5 Hz), 128.7 (d, J = 1.9 Hz), 124.3 (d, J = 5.7 Hz), 21.3 ppm. ^{31}P NMR (202 MHz, CDCl_3): δ = 41.17 ppm. The spectroscopic data are in agreement with the literature.^[22]

***Se*-phenyl di(naphthalen-2-yl)phosphinoselenoate(4.24l):**

Compound **4.24l** was synthesised following GP7 as a white solid. It was purified by column chromatography on silica gel using cyclohexane/ethyl acetate (4:1) to obtain 228 mg (83% yield). ^1H NMR (500 MHz, CDCl_3): δ = 8.45 (d, J = 15.0 Hz, 2H), 7.93 – 7.82 (m, 8H), 7.61 – 7.51 (m, 6H), 7.22 – 7.15 (m, 1H), 7.14 – 7.06 (m, 2H) ppm. ^{13}C NMR (126 MHz, CDCl_3): δ = 136.4 (d, J = 3.2 Hz), 134.9 (d, J = 2.6 Hz), 133.7 (d, J = 9.6 Hz), 132.5 (d, J = 14.4 Hz), 131.0, 130.25, 129.4 (d, J = 1.5 Hz), 129.2, 128.8 (d, J = 1.9 Hz), 128.5 (d, J = 13.3 Hz), 127.9, 127.1, 126.1 (d, J = 12.1 Hz), 123.9 (d, J = 5.7 Hz) ppm. ^{31}P NMR (202 MHz, CDCl_3): δ = 39.81 ppm. The spectroscopic data are in agreement with the literature.^[22]

***O*-ethyl *Se*-phenyl phenylphosphonoselenoate (4.24m):**

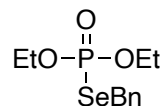
Compound **4.24m** was synthesised following GP7 as a pale yellow oil. It was purified by column chromatography on silica gel using cyclohexane/ethyl acetate (4:1) to obtain 156 mg (80% yield). ^1H NMR (500 MHz, CDCl_3): δ = 7.54 – 7.47 (m, 2H), 7.40 – 7.35 (m, 1H), 7.28 – 7.16 (m, 5H), 7.10 – 7.04 (m, 2H), 4.32 – 4.18 (m, 2H), 1.31 (t, J = 7.1 Hz, 3H) ppm. ^{13}C NMR (126 MHz, CDCl_3): δ = 150.5 (d, J = 3.6 Hz), 133.4, 132.5 (d, J = 3.3 Hz), 132.3, 131.1 (d, J = 11.0 Hz), 129.3 (d, J = 2.1 Hz), 128.8 (d, J = 2.5 Hz), 128.2 (d, J = 14.9 Hz), 124.3 (d, J = 6.6 Hz), 62.7, 16.34 ppm. ^{31}P NMR (202 MHz, CDCl_3): δ = 38.49 ppm.

6-(phenylselanyl)dibenzo[*c,e*][1,2]oxaphosphinine 6-oxide (4.24n):

Compound **4.24n** was synthesised following GP7 as a white solid. It was purified by column chromatography on silica gel using cyclohexane/ethyl acetate (4:1) to obtain 192 mg (86% yield). ^1H NMR (500 MHz, CDCl_3): δ = 7.90 – 7.83 (m, 1H), 7.77 – 7.73 (m, 1H), 7.66 – 7.60 (m, 2H), 7.46 (tdd, J = 7.5, 3.6, 1.0 Hz, 1H), 7.33 – 7.29 (m, 1H), 7.25 – 7.20 (m, 2H), 7.17 – 7.12 (m, 3H), 7.01 – 6.97 (m, 2H) ppm. ^{13}C NMR (126 MHz, CDCl_3): δ = 150.5 (d, J = 9.9 Hz), 137.1 (d, J = 3.6 Hz), 136.0 (d, J = 7.5 Hz), 133.8 (d, J = 2.8 Hz), 130.6 (d, J = 11.0 Hz), 129.19

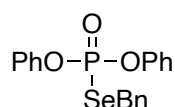
(d, $J = 2.5$ Hz), 129.13 (d, $J = 2.9$ Hz), 128.5 (d, $J = 14.9$ Hz), 126.6, 125.73, 125.0 (d, $J = 1.0$ Hz), 124.8, 123.3 (d, $J = 11.2$ Hz), 122.1 (d, $J = 7.2$ Hz), 122.0 (d, $J = 11.7$ Hz), 120.2 (d, $J = 7.0$ Hz) ppm. ^{31}P NMR (202 MHz, CDCl_3): $\delta = 31.24$ ppm. The spectroscopic data are in agreement with the literature.^[22]

***Se*-benzyl *O,O*-diethyl phosphoroselenoate (4.24o):**



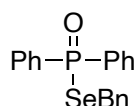
Compound **4.24o** was synthesised following GP7 as a colorless oil. It was purified by column chromatography on silica gel using cyclohexane/ethyl acetate (4:1) to obtain 136 mg (74% yield). ^1H NMR (500 MHz, CDCl_3): $\delta = 7.41 - 7.32$ (m, 2H), 7.32 – 7.27 (m, 2H), 7.26 – 7.20 (m, 1H), 4.16 – 3.98 (m, 6H), 1.30 (td, $J = 7.1, 0.7$ Hz, 6H) ppm. ^{13}C NMR (126 MHz, CDCl_3): $\delta = 138.5$ (d, $J = 4.7$ Hz), 129.0, 128.7, 127.5, 63.5 (d, $J = 5.5$ Hz), 29.5 (d, $J = 4.6$ Hz), 16.0 (d, $J = 7.5$ Hz) ppm. ^{31}P NMR (202 MHz, CDCl_3): $\delta = 20.24$ ppm. The spectroscopic data are in agreement with the literature.^[23]

***Se*-benzyl *O,O*-diphenyl phosphoroselenoate (4.24p):**



Compound **4.24p** was synthesised following GP7 as a colorless oil. It was purified by column chromatography on silica gel using cyclohexane/ethyl acetate (4:1) to obtain 193 mg (80% yield). ^1H NMR (500 MHz, CDCl_3): $\delta = 7.28 - 7.24$ (m, 4H), 7.16 – 7.12 (m, 11H), 4.08 (d, $J = 12.6$ Hz, 2H) ppm. ^{13}C NMR (126 MHz, CDCl_3): $\delta = 137.2$ (d, $J = 6.0$ Hz), 129.9 (d, $J = 1.3$ Hz), 129.2, 128.8, 127.7, 125.8 (d, $J = 1.7$ Hz), 121.0 (d, $J = 4.9$ Hz), 120.45, 30.9 (d, $J = 4.8$ Hz) ppm. ^{31}P NMR (202 MHz, CDCl_3): $\delta = 13.72$ ppm. The spectroscopic data are in agreement with the literature.^[23]

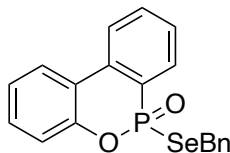
***Se*-benzyl diphenylphosphinoselenoate (4.24q):**



Compound **4.24q** was synthesised following GP7 as a white solid. It was purified by column chromatography on silica gel using cyclohexane/ethyl acetate (4:1) to obtain 174 mg (78% yield). ^1H NMR (500 MHz, CDCl_3): $\delta = 7.94 - 7.78$ (m, 4H), 7.55 – 7.49 (m, 2H), 7.48 – 7.35 (m, 4H), 7.20 – 7.10 (m, 5H), 4.07 (d, $J = 8.3$ Hz, 2H) ppm. ^{13}C NMR (126 MHz, CDCl_3): $\delta =$

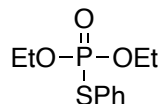
137.7 (d, $J = 4.4$ Hz), 134.6, 133.8, 132.4 (d, $J = 3.1$ Hz), 131.4 (d, $J = 10.9$ Hz), 129.2, 128.8, 128.7 (d, $J = 5.2$ Hz), 127.3, 28.4 (d, $J = 2.5$ Hz) ppm. ^{31}P NMR (202 MHz, CDCl_3): $\delta = 40.03$ ppm. The spectroscopic data are in agreement with the literature.^[24]

6-(benzylselanyl)dibenzo[*c,e*][1,2]oxaphosphinine 6-oxide (4.24r):



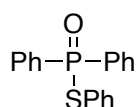
Compound **4.24r** was synthesised following GP7 as a colorless oil. It was purified by column chromatography on silica gel using cyclohexane/ethyl acetate (4:1) to obtain 165 mg (71% yield). ^1H NMR (500 MHz, CDCl_3): $\delta = 7.95 - 7.84$ (m, 3H), 7.70 – 7.65 (m, 1H), 7.49 (tdd, $J = 7.6$, 3.6, 0.9 Hz, 1H), 7.38 – 7.33 (m, 1H), 7.29 – 7.19 (m, 6H), 7.11 – 7.05 (m, 1H), 4.24 – 4.09 (m, 2H) ppm. ^{13}C NMR (126 MHz, CDCl_3) $\delta = 149.4$ (d, $J = 9.8$ Hz), 137.7 (d, $J = 4.4$ Hz), 135.6 (d, $J = 7.6$ Hz), 133.8 (d, $J = 2.7$ Hz), 130.8, 130.4 (d, $J = 11.9$ Hz), 129.18, 128.7 (t, $J = 7.5$ Hz), 127.8, 127.5, 126.8, 125.2 (d, $J = 1.1$ Hz), 125.1 (d, $J = 0.6$ Hz), 123.8 (d, $J = 10.9$ Hz), 122.3 (d, $J = 12.3$ Hz), 120.6 (d, $J = 6.6$ Hz), 29.2 (d, $J = 3.7$ Hz) ppm. ^{31}P NMR (202 MHz, CDCl_3): $\delta = 33.66$ ppm. The spectroscopic data are in agreement with the literature.^[22]

***O,O*-diethyl *S*-phenyl phosphorothioate (4.24s):**



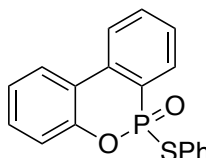
Compound **4.24s** was synthesised following GP7 as a colorless oil. It was purified by column chromatography on silica gel using cyclohexane/ethyl acetate (4:1) to obtain 84 mg (57% yield). ^1H NMR (500 MHz, CDCl_3): $\delta = 7.59 - 7.52$ (m, 2H), 7.37 – 7.31 (m, 3H), 4.25 – 4.12 (m, 4H), 1.30 (td, $J = 7.1$, 0.9 Hz, 6H) ppm. ^{13}C NMR (126 MHz, CDCl_3): $\delta = 134.6$ (d, $J = 5.2$ Hz), 129.5 (d, $J = 2.2$ Hz), 129.1 (d, $J = 2.8$ Hz), 126.7 (d, $J = 7.2$ Hz), 64.2 (d, $J = 6.2$ Hz), 16.1 (d, $J = 7.2$ Hz) ppm. ^{31}P NMR (202 MHz, CDCl_3): $\delta = 22.88$ ppm. The spectroscopic data are in agreement with the literature.^[25]

***S*-phenyl diphenylphosphinothioate (4.24t):**



Compound **4.24t** was synthesised following GP7 as a white solid. It was purified by column chromatography on silica gel using cyclohexane/ethyl acetate (4:1) to obtain 124 mg (66% yield). ^1H NMR (500 MHz, CDCl_3): δ = 7.88 – 7.81 (m, 4H), 7.53 – 7.48 (m, 2H), 7.47 – 7.41 (m, 6H), 7.26 – 7.22 (m, 1H), 7.22 – 7.17 (m, 2H) ppm. ^{13}C NMR (126 MHz, CDCl_3): δ = 135.5 (d, J = 3.9 Hz), 133.1, 132.4 (d, J = 3.0 Hz), 131.7 (d, J = 10.2 Hz), 129.2 (d, J = 1.7 Hz), 129.0 (d, J = 2.2 Hz), 128.6 (d, J = 13.1 Hz), 126.3 (d, J = 5.2 Hz) ppm. ^{31}P NMR (202 MHz, CDCl_3): δ = 41.31 ppm. The spectroscopic data are in agreement with literature.^[19]

6-(phenylthio)dibenzo[*c,e*][1,2]oxaphosphinine 6-oxide (**4.24u**):



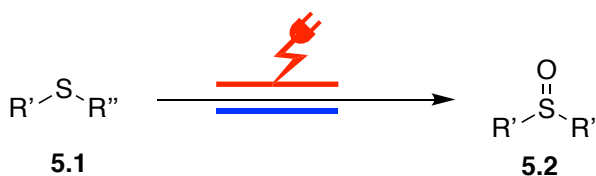
Compound **4.24u** was synthesised following GP7 as a pale yellow oil. It was purified by column chromatography on silica gel using cyclohexane/ethyl acetate (4:1) to obtain 135 mg (69% yield). ^1H NMR (500 MHz, CDCl_3): δ = 7.96 – 7.89 (m, 1H), 7.86 – 7.81 (m, 1H), 7.75 (dd, J = 7.8, 1.6 Hz, 1H), 7.70 – 7.65 (m, 1H), 7.50 (tdd, J = 7.5, 3.6, 1.0 Hz, 1H), 7.38 – 7.34 (m, 1H), 7.28 – 7.16 (m, 5H), 7.12 – 7.06 (m, 2H) ppm. ^{13}C NMR (126 MHz, CDCl_3): δ = 150.6 (d, J = 9.6 Hz), 136.4 (d, J = 7.3 Hz), 136.1 (d, J = 4.3 Hz), 133.8 (d, J = 2.6 Hz), 130.9 (d, J = 10.2 Hz), 130.6, 129.4 (d, J = 3.1 Hz), 129.1 (d, J = 2.6 Hz), 128.5 (d, J = 14.9 Hz), 125.4, 124.7, 124.3 (d, J = 4.9 Hz), 123.3 (d, J = 11.5 Hz), 121.9 (d, J = 11.6 Hz), 120.1 (d, J = 7.1 Hz) ppm. ^{31}P NMR (202 MHz, CDCl_3): δ = 34.20 ppm. The spectroscopic data are in agreement with the literature.^[26]

6.6. Experimental Data for Chapter 5:

Flow Electrosynthesis of Sulfoxides, Sulfones and Sulfoximines

6.6.1. Electrochemical oxidation of sulfides to sulfoxides

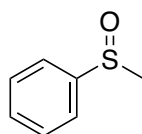
General Procedure 8 (GP 8):



The electrolysis was performed in an undivided cell using a Vapourtec Ion Electrochemical Flow Reactor (reactor volume = 0.6 mL, spacer 0.5 mm) using a graphite (Gr) electrode as the

anode and a stainless steel (Fe) electrode as the cathode (active surface area: $A = 12 \text{ cm}^2$). A solution of sulfide (0.1 M) in mixture of CH_3CN and H_2O (9:1) placed in 20 mL vial screw cap with hole with PTFE/silicone septum. The reaction mixture was injected to 18 mL sample loop. After that, the reactor temperature was set at room temperature with the flow rate 0.2 mL min^{-1} and the current was set at 64 mA turn on automatically. Then, solutions were pumped into the electrochemical reactor. After reaching a steady state, the solution (15 mL, 1.5 mmol) was collected automatically into a glass vial. The solvent was removed under vacuum. The crude product was purified by column chromatography (EtOAc/cyclohexane).

(Methylsulfinyl)benzene (5.2a):

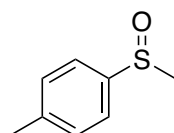


Compound **5.2a** was synthesized following GP8, using methyl(phenyl)sulfane (**5.1a**, 186 mg, 1.5 mmol) to give the product as colourless oil. It was purified by column chromatography on silica gel using ethyl acetate (100 %) to obtain 87% yield (183 mg).

^1H NMR (500 MHz, CDCl_3): $\delta = 7.72 - 7.63$ (m, 2H), $7.57 - 7.48$ (m, 2H), 2.72 (s, 3H) ppm.

$^{13}\text{C}\{^1\text{H}\}$ NMR (126 MHz, CDCl_3): $\delta = 145.7, 131.1, 129.4, 123.6, 44.0$ ppm. The spectroscopic data are in agreement with the literature.^[27]

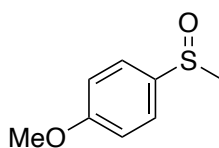
1-Methyl-4-(methylsulfinyl)benzene (5.2b).



Compound **5.2b** was synthesized following GP8, using methyl(*p*-tolyl)sulfane (**5.1b**, 207 mg, 1.5 mmol) to give the product as colourless oil. It was purified by column chromatography on silica gel using ethyl acetate (100 %) to obtain 89% yield (207 mg).

^1H NMR (500 MHz, CDCl_3): $\delta = 7.54$ (d, $J = 7.4$ Hz, 2H), 7.33 (d, $J = 7.6$ Hz, 2H), 2.70 (s, 3H), 2.41 (s, 3H) ppm. ^{13}C NMR (126 MHz, CDCl_3): $\delta = 142.6, 141.7, 130.2, 123.7, 44.1, 21.5$ ppm. The spectroscopic data are in agreement with the literature.^[27]

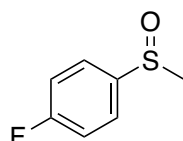
1-Methoxy-4-(methylsulfinyl)benzene (5.2c):



Compound **5.2c** was synthesized following GP8, using (4-methoxyphenyl)(methyl)sulfane (**5.1c**, 231 mg, 1.5 mmol) to give the product as colourless oil. It was purified by column chromatography on silica gel using ethyl acetate (100 %) to obtain 88% yield (224 mg). m.p.: 42-44 °C [Lit.: 42-44 °C].^[28]

¹H NMR (400 MHz, CDCl₃): δ = 7.63 – 7.55 (m, 2H), 7.06 – 6.99 (m, 2H), 3.85 (s, 3H), 2.69 (s, 3H) ppm. ¹³C NMR (101 MHz, CDCl₃): δ = 162.1, 136.8, 125.6, 114.9, 55.6, 44.1 ppm. The spectroscopic data are in agreement with the literature.^[27]

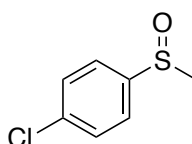
1-Fluoro-4-(methylsulfinyl)benzene (5.2d):



Compound **5.2d** was synthesized following GP8, using (4-fluorophenyl)(methyl)sulfane (**5.1d**, 213 mg, 1.5 mmol) to give the product as yellow oil. It was purified by column chromatography on silica gel using ethyl acetate (100 %) to obtain 80% yield (190 mg).

¹H NMR (500 MHz, CDCl₃): δ = 7.68 – 7.61 (m, 2H), 7.25 – 7.16 (m, 2H), 2.70 (s, 3H) ppm. ¹³C NMR (126 MHz, CDCl₃): δ = 164.4 (d, *J* = 251.4 Hz), 141.2 (d, *J* = 3.1 Hz), 125.9 (d, *J* = 8.9 Hz), 116.8 (d, *J* = 22.6 Hz) ppm. ¹⁹F NMR (471 MHz, CDCl₃): δ = –152.06 ppm. The spectroscopic data are in agreement with the literature.^[29]

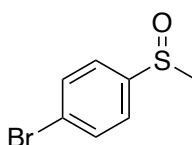
1-Chloro-4-(methylsulfinyl)benzene (5.2e):



Compound **5.2e** was synthesized following GP8, using (4-chlorophenyl)(methyl)sulfane (**5.1e**, 238 mg, 1.5 mmol) to give the product as colourless oil. It was purified by column chromatography on silica gel using ethyl acetate (100 %) to obtain 83% yield (217 mg).

¹H NMR (500 MHz, CDCl₃): δ = 7.58 (d, *J* = 8.5 Hz, 2H), 7.50 (d, *J* = 8.4 Hz, 2H), 2.71 (s, 3H) ppm. ¹³C NMR (126 MHz, CDCl₃): δ = 144.3, 137.4, 129.8, 125.1, 44.2 ppm. The spectroscopic data are in agreement with the literature.^[27]

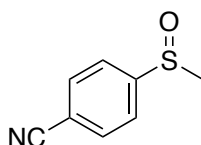
1-Bromo-4-(methylsulfinyl)benzene (5.2f):



Compound **5.2f** was synthesized following GP8, using (4-bromophenyl)(methyl)sulfane (**5.1f**, 305 mg, 1.5 mmol) to give the product as white solid. It was purified by column chromatography on silica gel using ethyl acetate (100 %) to obtain 86% yield (282 mg). m.p.: 86-88 °C [Lit.: 85-87 °C].^[30]

¹H NMR (500 MHz, CDCl₃): δ = 7.67 (d, *J* = 8.3 Hz, 2H), 7.52 (d, *J* = 8.3 Hz, 2H), 2.71 (s, 3H) ppm. ¹³C NMR (126 MHz, CDCl₃): δ = 145.1, 132.8, 125.7, 125.4, 44.2 ppm. The spectroscopic data are in agreement with the literature.^[27]

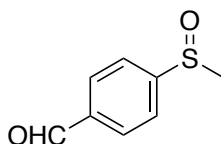
4-(Methylsulfinyl)benzonitrile (**5.2g**):



Compound **5.2g** was synthesized following GP8, using 4-(methylthio)benzonitrile (**5.1g**, 224 mg, 1.5 mmol) to give the product as White solid. It was purified by column chromatography on silica gel using cyclohexane/ethyl acetate (4:6) to obtain 82% yield (204 mg). m.p.: 86-88 °C [Lit.: 87-89 °C].^[28]

¹H NMR (500 MHz, CDCl₃): δ = 7.96 – 7.68 (m, 4H), 2.76 (s, 3H) ppm. ¹³C NMR (126 MHz, CDCl₃): δ = 151.6, 133.1, 124.4, 117.8, 114.9, 44.0 ppm. The spectroscopic data are in agreement with the literature.^[31]

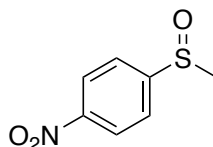
4-(Methylsulfinyl)benzaldehyde (**5.2h**):



Compound **5.2h** was synthesized following GP8, using 4-(methylthio)benzaldehyde (**5.1h**, 228 mg, 1.5 mmol) to give the product as white solid. It was purified by column chromatography on silica gel using cyclohexane/ethyl acetate (4:6) to obtain 68% yield (174 mg). m.p.: 83-86°C [Lit.: 84-87 °C].^[32]

¹H NMR (500 MHz, CDCl₃): δ = 10.09 (s, 1H), 8.05 (d, *J* = 7.7 Hz, 2H), 7.82 (d, *J* = 7.7 Hz, 2H), 2.78 (s, 3H) ppm. ¹³C NMR (126 MHz, CDCl₃): δ = 191.1, 152.4, 138.0, 130.3, 124.1, 43.7 ppm. The spectroscopic data are in agreement with the literature.^[31]

1-(Methylsulfinyl)-4-nitrobenzene (**5.2i**):

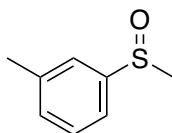


Compound **5.2i** was synthesized following GP8, using methyl(4-nitrophenyl)sulfane (**5.1i**, 254 mg, 1.5 mmol) to give the product as yellow oil. It was purified by column chromatography on silica gel using ethyl acetate (100 %) to obtain 63% yield (174 mg).

^1H NMR (500 MHz, CDCl_3): δ = 8.43 – 8.34 (m, 2H), 7.88 – 7.78 (m, 2H), 2.79 (s, 3H) ppm.

^{13}C NMR (126 MHz, CDCl_3): δ = 153.4, 149.6, 124.8, 124.6, 44.0 ppm. The spectroscopic data are in agreement with the literature.^[27]

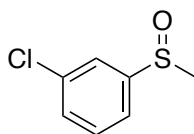
1-Methyl-3-(methylsulfinyl)benzene (**5.2j**):



Compound **5.2j** was synthesized following GP8, using methyl(m-tolyl)sulfane (**5.1j**, 207 mg, 1.5 mmol) to give the product as yellow oil. It was purified by column chromatography on silica gel using ethyl acetate (100 %) to obtain 86% yield (200 mg).

^1H NMR (500 MHz, CDCl_3): δ = 7.49 – 7.45 (m, 1H), 7.41 – 7.36 (m, 2H), 7.30 – 7.26 (m, 1H), 2.70 (s, 3H), 2.41 (s, 3H) ppm. ^{13}C NMR (126 MHz, CDCl_3): δ = 145.6, 139.7, 131.9, 129.2, 123.9, 120.7, 44.0, 21.5 ppm. The spectroscopic data are in agreement with the literature.^[27]

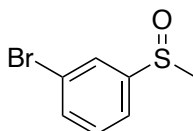
1-Chloro-3-(methylsulfinyl)benzene (**5.2k**):



Compound **5.2k** was synthesized following GP8, using (3-chlorophenyl)(methyl)sulfane (**5.1k**, 238 mg, 1.5 mmol) to give the product as colourless oil. It was purified by column chromatography on silica gel using ethyl acetate (100 %) to obtain 85% yield (224 mg).

^1H NMR (500 MHz, CDCl_3): δ = 7.65 (s, 1H), 7.50 – 7.43 (m, 3H), 2.73 (s, 3H) ppm. ^{13}C NMR (126 MHz, CDCl_3): δ = 148.0, 135.8, 131.3, 130.7, 123.7, 121.7, 44.1 ppm. The spectroscopic data are in agreement with the literature.^[29]

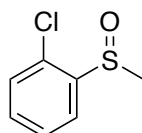
1-Bromo-3-(methylsulfinyl)benzene (**5.2l**):



Compound **5.2l** was synthesized following GP8, using (3-bromophenyl)(methyl)sulfane (**5.1l**, 305 mg, 1.5 mmol) to give the product as yellow oil. It was purified by column chromatography on silica gel using ethyl acetate (100%) to obtain 90% yield (296 mg).

^1H NMR (500 MHz, CDCl_3): δ = 7.84 – 7.76 (m, 1H), 7.64 – 7.50 (m, 2H), 7.42 – 7.36 (m, 1H), 2.72 (s, 3H) ppm. $^{13}\text{C}\{^1\text{H}\}$ NMR (126 MHz, CDCl_3): δ = 148.1, 134.2, 130.9, 126.6, 123.7, 122.2, 44.1 ppm. The spectroscopic data are in agreement with the literature.^[29]

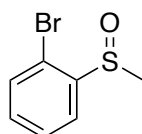
1-Chloro-2-(methylsulfinyl)benzene (5.2m):



Compound **5.2m** was synthesized following GP8, using (2-chlorophenyl)(methyl)sulfane (**5.1m**, 238 mg, 1.5 mmol) to give the product as yellow oil. It was purified by column chromatography on silica gel using cyclohexane/ethyl acetate (4:6) to obtain 79% yield (208 mg).

^1H NMR (500 MHz, CDCl_3): δ = 7.94 (dd, J = 7.8, 1.6 Hz, 1H), 7.53 (td, J = 7.5, 1.2 Hz, 1H), 7.44 (td, J = 7.4, 1.5 Hz, 1H), 7.39 (d, J = 1.2 Hz, 1H), 2.81 (s, 3H) ppm. ^{13}C NMR (126 MHz, CDCl_3): δ = 143.7, 132.1, 129.9, 128.3, 125.4, 41.7 ppm. The spectroscopic data are in agreement with the literature.^[29]

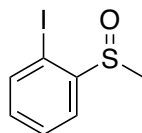
1-Bromo-2-(methylsulfinyl)benzene (5.2n):



Compound **5.2n** was synthesized following GP8, using (2-bromophenyl)(methyl)sulfane (**5.1n**, 305 mg, 1.5 mmol) to give the product as yellow oil. It was purified by column chromatography on silica gel using cyclohexane/ethyl acetate (4:6) to obtain 72% yield (238 mg).

^1H NMR (500 MHz, CDCl_3): δ = 7.94 (dd, J = 7.8, 1.7 Hz, 1H), 7.62 – 7.54 (m, 2H), 7.39 – 7.35 (m, 1H), 2.82 (s, 3H) ppm. ^{13}C NMR (126 MHz, CDCl_3): δ = 145.5, 133.0, 132.4, 128.8, 125.8, 118.5, 42.0 ppm. The spectroscopic data are in agreement with the literature.^[31]

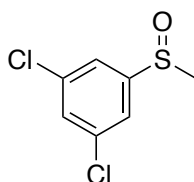
1-Iodo-2-(methylsulfinyl)benzene (5.2o):



Compound **5.2o** was synthesized following GP8, using (2-iodophenyl)(methyl)sulfane (**5.1o**, 375 mg, 1.5 mmol) to give the product as yellow oil. It was purified by column chromatography on silica gel using cyclohexane/ethyl acetate (4:6) to obtain 34% yield (136 mg).

¹H NMR (500 MHz, CDCl₃): δ = 7.89 (t, J = 6.6 Hz, 1H), 7.82 – 7.79 (t, J = 6.6 Hz, 1H), 7.63 – 7.56 (m, 1H), 7.24 – 7.17 (m, 1H), 2.77 (s, 3H) ppm. ¹³C NMR (126 MHz, CDCl₃): δ = 148.4, 139.4, 132.6, 129.7, 125.9, 91.5, 42.3 ppm. The spectroscopic data are in agreement with the literature.^[33]

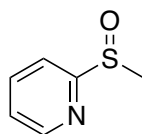
1,3-Dichloro-5-(methylsulfinyl)benzene (**5.2p**):



Compound **5.2p** was synthesized following GP8, using (3,5-dichlorophenyl)(methyl)sulfane (**5.1p**, 290 mg, 1.5 mmol) to give the product as white solid. It was purified by column chromatography on silica gel using ethyl acetate (100 %) to obtain 89% yield (278 mg). m.p.: 71-73°C [Lit.: 72-74 °C].^[34]

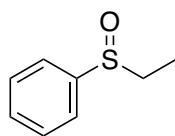
¹H NMR (500 MHz, CDCl₃): δ = 7.50 (d, J = 1.6 Hz, 2H), 7.46 – 7.44 (m, 1H), 2.74 (s, 3H) ppm. ¹³C NMR (126 MHz, CDCl₃): δ = 149.5, 136.4, 131.2, 122.0, 44.1 ppm. The spectroscopic data are in agreement with the literature.^[29]

2-(Methylsulfinyl)pyridine (**5.2q**):



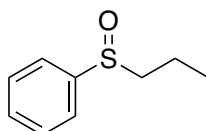
Compound **5.2q** was synthesized following GP8, using 2-(methylthio)pyridine (**5.1q**, 188 mg, 1.5 mmol) to give the product as colourless oil. It was purified by column chromatography on silica gel using cyclohexane/ethyl acetate (4:6) to obtain 73% yield (155 mg).

¹H NMR (500 MHz, CDCl₃): δ = 8.65 – 8.54 (m, 1H), 8.00 (dt, J = 7.9, 1.0 Hz, 1H), 7.93 (td, J = 7.7, 1.7 Hz, 1H), 7.36 (ddd, J = 7.4, 4.8, 1.1 Hz, 1H), 2.83 (s, 3H) ppm. ¹³C NMR (126 MHz, CDCl₃): δ = 166.0, 149.6, 138.3, 124.7, 119.5, 41.4 ppm. The spectroscopic data are in agreement with the literature.^[29]

(Ethylsulfinyl)benzene (5.2r):

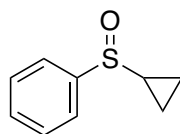
Compound **5.2r** was synthesized following GP8, using ethyl(phenyl)sulfane (**5.1r**, 207 mg, 1.5 mmol) to give the product as yellow oil. It was purified by column chromatography on silica gel using ethyl acetate (100 %) to obtain 91% yield (210 mg).

^1H NMR (500 MHz, CDCl_3): δ = 7.63 – 7.55 (m, 2H), 7.53 – 7.46 (m, 3H), 2.89 (dq, J = 13.3, 7.4 Hz, 1H), 2.76 (dq, J = 13.3, 7.4 Hz, 1H), 1.18 (t, J = 7.4 Hz, 3H) ppm. ^{13}C NMR (126 MHz, CDCl_3): δ = 143.3, 131.0, 129.2, 124.3, 50.4, 6.0 ppm. The spectroscopic data are in agreement with the literature.^[27]

(Propylsulfinyl)benzene (5.2s):

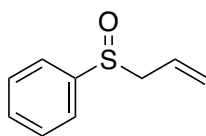
Compound **5.2s** was synthesized following GP8, using phenyl(propyl)sulfane (**5.1s**, 228 mg, 1.5 mmol) to give the product as colourless oil. It was purified by column chromatography on silica gel using ethyl acetate (100 %) to obtain 86% yield (218 mg).

^1H NMR (500 MHz, CDCl_3): δ = 7.67 – 7.53 (m, 2H), 7.52 – 7.41 (m, 3H), 2.81 – 2.69 (m, 2H), 1.83 – 1.72 (m, 1H), 1.69 – 1.59 (m, 1H), 1.02 (t, J = 7.4 Hz, 3H) ppm. ^{13}C NMR (126 MHz, CDCl_3): δ = 144.1, 131.0, 129.3, 124.1, 59.3, 16.0, 13.3 ppm. The spectroscopic data are in agreement with the literature.^[35]

(Cyclopropylsulfinyl)benzene (5.2t):

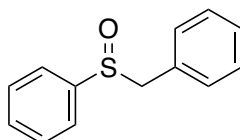
Compound **5.2s** was synthesized following GP8, using cyclopropyl(phenyl)sulfane (**5.1t**, 225 mg, 1.5 mmol) to give the product as colourless. It was purified by column chromatography on silica gel using ethyl acetate (100 %) to obtain 84% yield (209 mg).

^1H NMR (500 MHz, CDCl_3): δ = 7.73 – 7.56 (m, 2H), 7.55 – 7.42 (m, 3H), 2.29 – 2.17 (m, 1H), 1.28 – 1.19 (m, 1H), 1.06 – 0.89 (m, 3H) ppm. ^{13}C NMR (126 MHz, CDCl_3): δ = 144.9, 131.0, 129.2, 124.1, 33.9, 3.5, 2.9 ppm. The spectroscopic data are in agreement with the literature.^[29]

(Allylsulfinyl)benzene (5.2u):

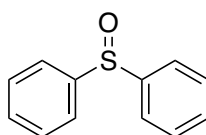
Compound **5.2u** was synthesized following GP8, using allyl(phenyl)sulfane (**5.1u**, 225 mg, 1.5 mmol) to give the product as colourless oil. It was purified by column chromatography on silica gel using cyclohexane/ethyl acetate (4:6) to obtain 67% yield (166 mg).

^1H NMR (500 MHz, CDCl_3): δ = 7.64 – 7.55 (m, 2H), 7.55 – 7.46 (m, 3H), 5.78 – 5.52 (m, 1H), 5.37 – 5.30 (m, 1H), 5.19 (dq, J = 17.0, 1.2 Hz, 1H), 3.54 (ddd, J = 32.0, 12.7, 7.5 Hz, 2H) ppm. ^{13}C NMR (126 MHz, CDCl_3) δ 143.0, 131.2, 129.2, 125.4, 124.4, 124.0, 61.0 ppm. The spectroscopic data are in agreement with the literature.^[36]

(Benzylsulfinyl)benzene (5.2v):

Compound **5.2v** was synthesized following GP8, using allyl(phenyl)sulfane (**5.1v**, 300 mg, 1.5 mmol) to give the product as white solid. It was purified by column chromatography on silica gel using cyclohexane/ethyl acetate (4:6) to obtain 78% yield (254 mg). m.p.: 120-122°C [Lit.: 122-123 °C].^[37]

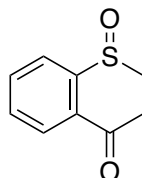
^1H NMR (500 MHz, CDCl_3): δ = 7.51 – 7.33 (m, 3H), 7.32 – 7.22 (m, 2H), 6.98 (d, J = 7.2 Hz, 1H), 4.05 (dd, J = 50.0, 12.6 Hz, 1H) ppm. ^{13}C NMR (126 MHz, CDCl_3): δ = 142.8, 131.3, 130.5, 129.2, 128.9, 128.5, 128.3, 124.6, 63.7 ppm. The spectroscopic data are in agreement with the literature.^[36]

Sulfinyldibenzene (5.2w):

Compound **5.2w** was synthesized following GP8, using diphenylsulfane (**5.1w**, 279 mg, 1.5 mmol) to give the product as white solid. It was purified by column chromatography on silica gel using cyclohexane/ethyl acetate (6:4) to obtain 70% yield (212 mg). m.p.: 68-70°C [Lit.: 69-70 °C].^[34]

^1H NMR (500 MHz, CDCl_3): δ = 7.69 – 7.58 (m, 2H), 7.47 – 7.41 (m, 3H) ppm. ^{13}C NMR (126 MHz, CDCl_3): δ = 145.6, 131.1, 129.3, 124.8 ppm. The spectroscopic data are in agreement with the literature.^[27]

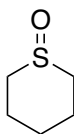
Thiochroman-4-one 1-oxide (5.2x):



Compound **5.2x** was synthesized following GP8, using thiochroman-4-one (**5.1x**, 246 mg, 1.5 mmol) to give the product as yellow oil. It was purified by column chromatography on silica gel using cyclohexane/ethyl acetate (4:6) to obtain 47% yield (128 mg).

^1H NMR (500 MHz, CDCl_3): δ = 8.11 (dd, J = 7.8, 1.2 Hz, 1H), 7.83 (dd, J = 7.7, 0.9 Hz, 1H), 7.72 (td, J = 7.6, 1.3 Hz, 1H), 7.62 (td, J = 7.6, 1.2 Hz, 1H), 3.49 – 3.39 (m, 3H), 2.90 – 2.81 (m, 1H) ppm. ^{13}C NMR (126 MHz, CDCl_3): δ = 192.1, 145.6, 134.7, 132.2, 129.3, 128.9, 128.5, 46.7, 30.4 ppm. The spectroscopic data are in agreement with the literature.^[38]

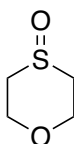
Tetrahydro-2H-thiopyran 1-oxide (5.2y):



Compound **5.2y** was synthesized following GP8, using tetrahydro-2H-thiopyran (**5.1y**, 153 mg, 1.5 mmol) to give the product as colourless oil. It was purified by column chromatography on silica gel using ethyl acetate/methanol (98:2) to obtain 72% yield (128 mg).

^1H NMR (500 MHz, CDCl_3): δ = 2.88 – 2.74 (m, 1H), 2.73 – 2.64 (m, 1H), 2.21 – 2.09 (m, 1H), 1.64 – 1.46 (m, 2H) ppm. ^{13}C NMR (126 MHz, CDCl_3): δ = 48.8, 24.7, 19.0 ppm. The spectroscopic data are in agreement with the literature.^[39]

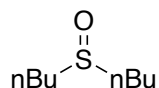
1,4-Oxathiane 4-oxide (5.2z):



Compound **5.2z** was synthesized following GP8, using 1,4-oxathiane (**5.1z**, 156 mg, 1.5 mmol) to give the product as colourless oil. It was purified by column chromatography on silica gel using ethyl acetate/methanol (98:2) to obtain 67% yield (120 mg).

^1H NMR (500 MHz, CDCl_3): δ = 4.36 – 4.23 (m, 1H), 3.80 – 3.70 (m, 1H), 2.92 – 2.78 (m, 1H), 2.73 – 2.60 (m, 1H) ppm. ^{13}C NMR (126 MHz, CDCl_3): δ = 59.1, 46.2 ppm. The spectroscopic data are in agreement with the literature.^[40]

1-(Butylsulfinyl)butane (**5.2aa**):

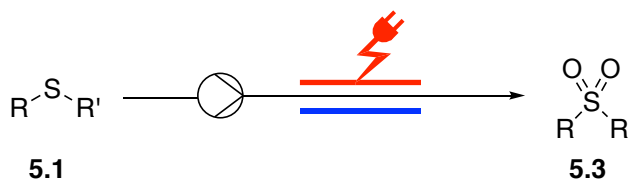


Compound **5.2aa** was synthesized following GP8, using dibutylsulfane (**5.1aa**, 219 mg, 1.5 mmol) to give the product as colourless oil. It was purified by column chromatography on silica gel using ethyl acetate (100 %) to obtain 66% yield (160 mg).

^1H NMR (500 MHz, CDCl_3): δ = 2.67 – 2.54 (m, 4H), 1.76 – 1.62 (m, 4H), 1.51 – 1.33 (m, 4H), 0.90 (t, J = 7.4 Hz, 6H) ppm. ^{13}C NMR (101 MHz, CDCl_3): δ = 52.1, 24.6, 22.1, 13.7 ppm. The spectroscopic data are in agreement with the literature.^[27]

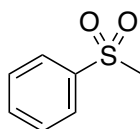
6.6.2. Electrochemical oxidation of sulfides to sulfones

General Procedure 9 (GP 9):



The electrolysis was performed in an undivided cell using a Vapourtec Ion Electrochemical Flow Reactor (reactor volume = 0.6 mL, spacer 0.5 mm) using a graphite (Pt) electrode as the anode and a stainless steel (Fe) electrode as the cathode (active surface area: $A = 12 \text{ cm}^2$). A solution of sulfide (0.1 M) in mixture of CH_3CN and H_2O (9:1) placed in 20 mL vial screw cap with hole with PTFE/silicone septum. The reaction mixture was injected to the 18 mL sample loop. After that, the reactor temperature was set at room temperature with the flow rate 0.2 mL/min and the current was set at 160 mA turn on automatically. Then, solutions were pumped into the electrochemical reactor. After reaching a steady state, the solution (15 mL, 1.5 mmol) was collected automatically into a glass vial. The solvent was removed under vacuum. The crude product was purified by column chromatography (EtOAc/cyclohexane).

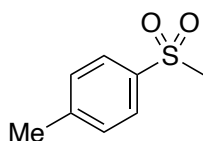
(Methylsulfonyl)benzene (**5.3a**).



Compound **5.3a** was synthesized following GP9, using methyl(phenyl)sulfane (**5.1a**, 186 mg, 1.5 mmol) to give the product as White solid. It was purified by column chromatography on silica gel using cyclohexane/ethyl acetate (6:4) to obtain 81% yield (189 mg). m.p.: 89–91 °C. [Lit.: 88–91 °C].^[34]

¹H NMR (400 MHz, CDCl₃): δ = 7.93 (d, J = 8.2 Hz, 2H), 7.68 – 7.51 (m, 3H), 3.04 (s, 3H) ppm. ¹³C NMR (101 MHz, CDCl₃): δ = 140.7, 133.7, 129.4, 127.4, 44.8 ppm. The spectroscopic data are in agreement with the literature.^[29]

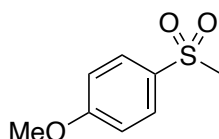
1-Methyl-4-(methylsulfonyl)benzene (5.3b):



Compound **5.3b** was synthesized following GP9, using methyl(*p*-tolyl)sulfane (**5.1b**, 207 mg, 1.5 mmol) to give the product as white solid. It was purified by column chromatography on silica gel using cyclohexane/ethyl acetate (6:4) to obtain 83% yield (212 mg). m.p.: 86–87 °C [Lit.: 87–88 °C].^[41]

¹H NMR (400 MHz, CDCl₃): δ = 7.78 (d, J = 8.2 Hz, 2H), 7.32 (d, J = 7.3 Hz, 2H), 2.99 (s, 3H), 2.40 (s, 3H) ppm. ¹³C NMR (101 MHz, CDCl₃): δ = 144.7, 137.7, 123.0, 127.3, 44.6, 21.6 ppm. The spectroscopic data are in agreement with the literature.^[39]

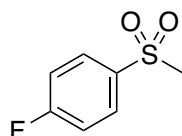
1-Methoxy-4-(methylsulfonyl)benzene (5.3c):



Compound **5.3c** was synthesized following GP9, using (4-methoxyphenyl)(methyl)sulfane (**5.1c**, 231 mg, 1.5 mmol) to give the product as white solid. It was purified by column chromatography on silica gel using cyclohexane/ethyl acetate (6:4) to obtain 78% yield (218 mg). m.p.: 118–120 °C [Lit.: 120–122 °C].^[37]

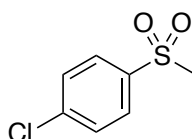
¹H NMR (400 MHz, CDCl₃): δ = 7.93 – 7.72 (m, 2H), 7.10 – 6.90 (m, 2H), 3.86 (s, 3H), 3.01 (s, 3H) ppm. ¹³C NMR (101 MHz, CDCl₃): δ = 163.8, 132.4, 129.6, 114.6, 55.8, 44.9 ppm. The spectroscopic data are in agreement with the literature.^[29]

1-Fluoro-4-(methylsulfonyl)benzene (5.3d):



Compound **5.3d** was synthesized following GP9, using (4-fluorophenyl)(methyl)sulfane (**5.1d**, 213 mg, 1.5 mmol) to give the product as colourless oil. It was purified by column chromatography on silica gel using cyclohexane/ethyl acetate (6:4) to obtain 66% yield (172 mg). ^1H NMR (500 MHz, CDCl_3): δ = 7.98 – 7.90 (m, 2H), 7.26 – 7.20 (m, 2H), 3.04 (s, 3H) ppm. ^{13}C NMR (101 MHz, CDCl_3): δ = 165.8 (d, J = 256.1 Hz), 136.8 (d, J = 3.2 Hz), 130.4 (d, J = 9.6 Hz), 116.7 (d, J = 22.7 Hz), 44.7 (s) ppm. ^{19}F NMR (471 MHz, CDCl_3): δ = –103.59 ppm. The spectroscopic data are in agreement with the literature.^[29]

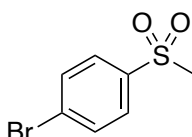
1-Chloro-4-(methylsulfonyl)benzene (**5.3e**):



Compound **5.3e** was synthesized following GP9, using (4-chlorophenyl)(methyl)sulfane (**5.1e**, 238 mg, 1.5 mmol) to give the product as white solid. It was purified by column chromatography on silica gel using cyclohexane/ethyl acetate (6:4) to obtain 73 yield (210 mg). m.p.: 92-94°C. [Lit.: 94-95 °C].^[37]

^1H NMR (400 MHz, CDCl_3): δ = 7.91 – 7.84 (m, 2H), 7.57 – 7.51 (m, 2H), 3.08 – 3.01 (m, 3H) ppm. ^{13}C NMR (101 MHz, CDCl_3): δ = 140.6, 139.2, 129.8, 129.0, 44.6 ppm. The spectroscopic data are in agreement with the literature.^[29]

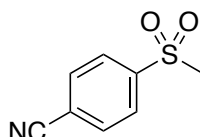
1-Bromo-4-(methylsulfonyl)benzene (**5.3f**):



Compound **5.3f** was synthesized following GP9, using (4-bromophenyl)(methyl)sulfane (**5.1f**, 305 mg, 1.5 mmol) to give the product as white solid. It was purified by column chromatography on silica gel using cyclohexane/ethyl acetate (6:4) to obtain 79% yield (280 mg). m.p.: 100-102°C [Lit.: 100-102 °C].^[37]

^1H NMR (400 MHz, CDCl_3): δ = 7.85 – 7.77 (m, 2H), 7.73 – 7.66 (m, 2H), 3.04 (s, 3H) ppm. $^{13}\text{C}\{^1\text{H}\}$ NMR (101 MHz, CDCl_3): δ = 139.7, 132.8, 129.1, 44.6 ppm. The spectroscopic data are in agreement with the literature.^[29]

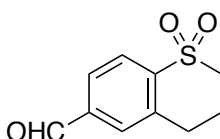
4-(Methylsulfonyl)benzonitrile (**5.3g**):



Compound **5.3g** was synthesized following GP9 using (4-(methylthio)benzonitrile (**5.1g**, 224 mg, 1.5 mmol) to give the product as white solid. It was purified by column chromatography on silica gel using cyclohexane/ethyl acetate (2:8) to obtain 68% yield (68 mg). m.p.: 142–143 °C [Lit.: 142-143 °C].^[42]

¹H NMR (500 MHz, CDCl₃): δ = 8.11 – 8.03 (m, 2H), 7.91 – 7.84 (m, 2H), 3.08 (s, 3H) ppm. ¹³C NMR (101 MHz, CDCl₃): δ = 144.6, 133.3, 128.3, 117.7, 117.1, 44.3 ppm. The spectroscopic data are in agreement with the literature.^[42]

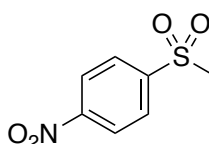
4-(Methylsulfonyl)benzaldehyde (**5.3h**):



Compound **5.3h** was synthesized following GP9, using 4-(methylthio)benzaldehyde (**5.1h**, 228 mg, 1.5 mmol) to give the product as white solid. It was purified by column chromatography on silica gel using cyclohexane/ethyl acetate (6:4) to obtain 35% yield (96 mg). m.p.: 157-158 °C [Lit.: 157-158 °C].^[43]

¹H NMR (400 MHz, CDCl₃): δ = 10.14 (s, 1H), 8.11 (dd, *J* = 19.4, 8.3 Hz, 4H), 3.10 (s, 3H) ppm. ¹³C NMR (101 MHz, CDCl₃): δ = 190.8, 145.5, 139.8, 130.5, 128.4, 44.4 ppm. The spectroscopic data are in agreement with the literature.^[44]

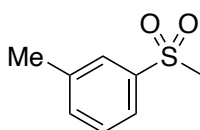
1-(Methylsulfonyl)-4-nitrobenzene (**5.3i**):



Compound **5.3i** was synthesized following GP9, using methyl(4-nitrophenyl)sulfane (**5.1i**, 254 mg, 1.5 mmol) to give the product as yellow oil. It was purified by column chromatography on silica gel using cyclohexane/ethyl acetate (6:4) to obtain 28% yield (85 mg).

¹H NMR (500 MHz, CDCl₃): δ = 8.46 – 8.39 (m, 2H), 8.20 – 8.10 (m, 2H), 3.12 (s, 3H) ppm. ¹³C NMR (101 MHz, CDCl₃): δ = 151.0, 146.1, 129.1, 124.8, 44.5 ppm. The spectroscopic data are in agreement with the literature.^[39]

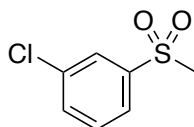
1-Methyl-3-(methylsulfonyl)benzene (**5.3j**):



Compound **5.3j** was synthesized following GP9, using methyl(m-tolyl)sulfane (**5.1j**, 207 mg, 1.5 mmol) to give the product as colourless oil. It was purified by column chromatography on silica gel using cyclohexane/ethyl acetate (6:4) to obtain 78% yield (198 mg).

^1H NMR (500 MHz, CDCl_3): δ = 7.79 – 7.63 (m, 2H), 7.49 – 7.40 (m, 2H), 3.03 (s, 3H), 2.43 (s, 3H) ppm. ^{13}C NMR (126 MHz, CDCl_3): δ = 140.5, 139.8, 134.5, 129.3, 127.7, 124.5, 44.6, 21.4 ppm. The spectroscopic data are in agreement with the literature.^[45]

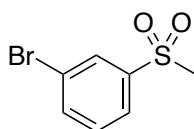
1-Chloro-3-(methylsulfonyl)benzene (5.3k):



Compound **5.3k** was synthesized following GP9, using (3-chlorophenyl)(methyl)sulfane (**5.1k**, 283 mg, 1.5 mmol) to give the product as white solid. It was purified by column chromatography on silica gel using cyclohexane/ethyl acetate (6:4) to obtain 74% yield (212 mg). m.p.: 55–56°C [Lit.: 56–58 °C].^[37]

^1H NMR (500 MHz, CDCl_3): δ = 7.93 (t, J = 1.9 Hz, 1H), 7.85 – 7.81 (m, 1H), 7.64 – 7.60 (m, 1H), 7.52 (t, J = 7.9 Hz, 1H), 3.06 (s, 3H) ppm. ^{13}C NMR (101 MHz, CDCl_3): δ = 142.3, 135.7, 134.0, 130.9, 127.7, 125.6, 44.5 ppm. The spectroscopic data are in agreement with the literature.^[29]

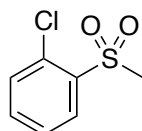
1-Bromo-3-(methylsulfonyl)benzene (5.3l):



Compound **5.3l** was synthesized following GP9, using (3-bromophenyl)(methyl)sulfane (**5.1l**, 305 mg, 1.5 mmol) to give the product as white solid. It was purified by column chromatography on silica gel using cyclohexane/ethyl acetate (6:4) to obtain 71% yield (252 mg). m.p.: 102–103 °C.

^1H NMR (500 MHz, CDCl_3): δ = 8.10 – 8.05 (m, 1H), 7.89 – 7.85 (m, 1H), 7.79 – 7.76 (m, 1H), 7.49 – 7.42 (m, 1H), 3.06 (s, 3H) ppm. ^{13}C NMR (101 MHz, CDCl_3): δ = 142.5, 136.9, 131.1, 130.5, 125.9, 123.4, 44.6. The spectroscopic data are in agreement with the literature.^[46]

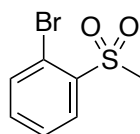
1-Chloro-2-(methylsulfonyl)benzene (5.3m):



Compound **5.3m** was synthesized following GP9, using (2-chlorophenyl)(methyl)sulfane (**5.1m**, 238 mg, 1.5 mmol) to give the product as white solid. It was purified by column chromatography on silica gel using cyclohexane/ethyl acetate (6:4) to obtain 53% yield (152 mg). m.p.: 82-84°C [Lit.: 80-82 °C].^[37]

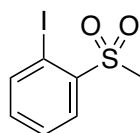
¹H NMR (500 MHz, CDCl₃): δ = 8.13 (dd, *J* = 8.3, 1.5 Hz, 1H), 7.59 – 7.52 (m, 2H), 7.49 – 7.43 (m, 1H), 3.26 (s, 3H) ppm. ¹³C NMR (126 MHz, CDCl₃): δ = 138.1, 134.9, 132.6, 132.0, 130.9, 127.6, 42.8 ppm. The spectroscopic data are in agreement with the literature.^[29]

1-Bromo-2-(methylsulfonyl)benzene (5.3n):



Compound **5.3n** was synthesized following GP9, using (2-bromophenyl)(methyl)sulfane (**5.1n**, 305 mg, 1.5 mmol) to give the product as yellow oil. It was purified by column chromatography on silica gel using cyclohexane/ethyl acetate (6:4) to obtain 51% yield (180 mg). ¹H NMR (500 MHz, CDCl₃): δ = 8.19 (dd, *J* = 7.7, 1.9 Hz, 1H), 7.77 (dd, *J* = 7.8, 1.3 Hz, 1H), 7.50 (dtd, *J* = 17.1, 7.5, 1.5 Hz, 2H), 3.28 (s, 3H) ppm. ¹³C NMR (126 MHz, CDCl₃): δ = 139.8, 135.6, 134.9, 131.3, 128.2, 120.8, 42.5 ppm. The spectroscopic data are in agreement with the literature.^[29]

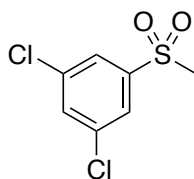
1-Iodo-2-(methylsulfonyl)benzene (5.3o):



Compound **5.3o** was synthesized following GP9, using (2-iodophenyl)(methyl)sulfane (**5.1o**, 375 mg, 1.5 mmol) to give the product as white solid. It was purified by column chromatography on silica gel using cyclohexane/ethyl acetate (6:4) to obtain 15% yield (64 mg). m.p.: 108-109 °C.

¹H NMR (500 MHz, CDCl₃): δ = 8.23 (dd, *J* = 7.9, 1.7 Hz, 1H), 8.11 (dd, *J* = 7.9, 1.2 Hz, 1H), 7.58 – 7.54 (m, 1H), 7.27 (dt, *J* = 7.7, 1.7 Hz, 1H), 3.26 (s, 3H) ppm. ¹³C NMR (101 MHz, CDCl₃): δ = 142.9, 142.9, 134.6, 131.0, 129.0, 92.7, 42.0 ppm.

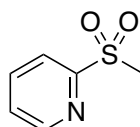
1,3-Dichloro-5-(methylsulfonyl)benzene (5.3p):



Compound **5.3p** was synthesized following GP9, using (3,5-dichlorophenyl)(methyl)sulfane (**5.1p**, 290 mg, 1.5 mmol) to give the product as white solid. It was purified by column chromatography on silica gel using cyclohexane/ethyl acetate (6:4) to obtain 60% yield (204 mg). m.p.: 202-205 °C [Lit.: 201-203 °C].^[34]

¹H NMR (500 MHz, CDCl₃): δ = 7.82 (d, *J* = 1.9 Hz, 2H), 7.62 (t, *J* = 1.9 Hz, 1H), 3.08 (s, 3H) ppm. ¹³C NMR (126 MHz, CDCl₃): δ = 14.4, 136.5, 133.9, 126.0, 44.5 ppm. The spectroscopic data are in agreement with the literature.^[34]

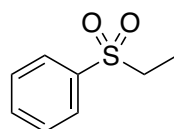
2-(Methylsulfonyl)pyridine (**5.3q**):



Compound **5.3q** was synthesized following GP9, using 2-(methylthio)pyridine (**5.1q**, 188 mg, 1.5 mmol) to give the product as yellow oil. It was purified by column chromatography on silica gel using cyclohexane/ethyl acetate (4:6) to obtain 67% yield (158 mg).

¹H NMR (500 MHz, CDCl₃): δ = 8.75 – 8.69 (m, 1H), 8.07 (dt, *J* = 7.9, 1.0 Hz, 1H), 7.96 (td, *J* = 7.8, 1.7 Hz, 1H), 7.55 (ddd, *J* = 7.7, 4.7, 1.1 Hz, 1H), 3.21 (s, 3H) ppm. ¹³C NMR (101 MHz, CDCl₃): δ = 158.1, 150.1, 138.4, 127.6, 121.1, 40.1 ppm. The spectroscopic data are in agreement with the literature.^[29]

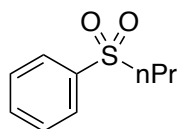
(Ethylsulfonyl)benzene (**5.3r**):



Compound **5.3r** was synthesized following GP9, using ethyl(phenyl)sulfane (**5.1r**, 207 mg, 1.5 mmol) to give the product as yellow oil. It was purified by column chromatography on silica gel using cyclohexane/ethyl acetate (6:4) to obtain 74% yield (188 mg).

¹H NMR (500 MHz, CDCl₃): δ = 7.94 – 7.80 (m, 2H), 7.68 – 7.51 (m, 3H), 3.10 (q, *J* = 7.4 Hz, 2H), 1.25 (t, *J* = 7.4 Hz, 3H) ppm. ¹³C NMR (126 MHz, CDCl₃): δ = 138.6, 133.8, 129.3, 128.3, 50.7, 7.5 ppm. The spectroscopic data are in agreement with the literature.^[39]

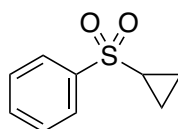
(Propylsulfonyl)benzene (**5.3s**):



Compound **5.3s** was synthesized following GP9, using phenyl(propyl)sulfane (**5.1s**, 228 mg, 1.5 mmol) to give the product as yellow oil. It was purified by column chromatography on silica gel using cyclohexane/ethyl acetate (6:4) to obtain 71% yield (196 mg).

^1H NMR (500 MHz, CDCl_3): δ = 7.90 – 7.84 (m, 2H), 7.64 – 7.59 (m, 1H), 7.56 – 7.51 (m, 2H), 3.06 – 3.00 (m, 2H), 1.75 – 1.66 (m, 2H), 0.95 (t, J = 7.5 Hz, 3H) ppm. ^{13}C NMR (126 MHz, CDCl_3): δ = 139.2, 133.7, 129.3, 128.0, 57.9, 16.5, 12.9 ppm. The spectroscopic data are in agreement with the literature.^[47]

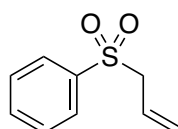
(Cyclopropylsulfonyl)benzene (5.3t):



Compound **5.3t** was synthesized following GP9, using cyclopropyl(phenyl)sulfane (**5.1t**, 225 mg, 1.5 mmol) to give the product as yellow oil. It was purified by column chromatography on silica gel using cyclohexane/ethyl acetate (6:4) to obtain 72% yield (198 mg).

^1H NMR (500 MHz, CDCl_3): δ = 7.93 – 7.80 (m, 2H), 7.65 – 7.58 (m, 1H), 7.57 – 7.47 (m, 2H), 2.51 – 2.36 (m, 1H), 1.35 – 1.27 (m, 2H), 1.04 – 0.94 (m, 2H) ppm. ^{13}C NMR (126 MHz, CDCl_3): δ = 140.7, 133.4, 129.3, 127.5, 32.9, 6.0 ppm. The spectroscopic data are in agreement with the literature.^[29]

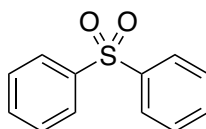
(Allylsulfonyl)benzene (5.3u):



Compound **5.3u** was synthesized following GP9, using allyl(phenyl)sulfane (**5.1u**, 225 mg, 1.5 mmol) to give the product as colourless oil. It was purified by column chromatography on silica gel using cyclohexane/ethyl acetate (6:4) to obtain 18% yield (48 mg).

^1H NMR (500 MHz, CDCl_3): δ = 7.91 – 7.82 (m, 2H), 7.65 (t, J = 7.4 Hz, 1H), 7.56 (t, J = 7.7 Hz, 2H), 5.80 (ddt, J = 17.4, 10.1, 7.4 Hz, 1H), 5.24 (dd, J = 92.6, 13.6 Hz, 2H), 3.81 (d, J = 7.4 Hz, 2H) ppm. ^{13}C NMR (126 MHz, CDCl_3): δ = 138.4, 133.9, 129.2, 128.7, 124.9, 124.8, 61.0 ppm. The spectroscopic data are in agreement with the literature.^[48]

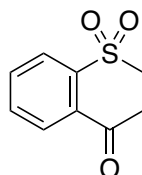
Sulfonyldibenzene (5.3w):



Compound **5.3v** was synthesized following GP9, using diphenylsulfane (**5.1v**, 279 mg, 1.5 mmol) to give the product as white solid. It was purified by column chromatography on silica gel using cyclohexane/ethyl acetate (6:4) to obtain 70% yield (230 mg). m.p.: 121-122°C [Lit.: 117-118 °C].^[49]

¹H NMR (400 MHz, CDCl₃): δ = 8.02 – 7.89 (m, 2H), 7.61 – 7.46 (m, 3H) ppm. ¹³C NMR (101 MHz, CDCl₃): δ = 141.7, 133.3, 129.4, 127.8 ppm. The spectroscopic data are in agreement with the literature.^[29]

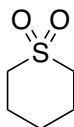
Thiochroman-4-one 1,1-dioxide (5.3x):



Compound **5.3x** was synthesized following GP9, using thiochroman-4-one (**5.1x**, 246 mg, 1.5 mmol) to give the product as white solid. It was purified by column chromatography on silica gel using cyclohexane/ethyl acetate (6:4) to obtain 48% yield (142 mg). m.p.: 142-144°C [Lit.: 142-144 °C].^[50]

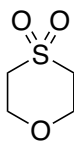
¹H NMR (500 MHz, CDCl₃): δ = 8.09 (d, J = 7.8 Hz, 1H), 7.98 (d, J = 7.8 Hz, 1H), 7.80 (t, J = 7.6 Hz, 1H), 7.72 (t, J = 7.7 Hz, 1H), 3.77 – 3.61 (m, 2H), 3.46 – 3.30 (m, 2H) ppm. ¹³C NMR (126 MHz, CDCl₃): δ = 190.26, 141.5, 135.0, 133.5, 130.3, 128.9, 123.7, 49.3, 36.8 ppm. The spectroscopic data are in agreement with the literature.^[51]

Tetrahydro-2H-thiopyran 1,1-dioxide (5.3y):



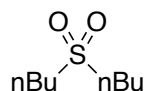
Compound **5.3y** was synthesized following GP9, using tetrahydro-2H-thiopyran (**5.1y**, 153 mg, 1.5 mmol) to give the product as colourless oil. It was purified by column chromatography on silica gel using ethyl acetate (100 %) to obtain 51% yield (102 mg).

¹H NMR (500 MHz, CDCl₃): δ = 3.01 – 2.88 (m, 4H), 2.10 – 2.00 (m, 4H), 1.63 – 1.55 (m, 2H) ppm. ¹³C NMR (101 MHz, CDCl₃): δ = 52.16, 24.28, 23.8 ppm. The spectroscopic data are in agreement with the literature.^[39]

1,4-Oxathiane 4,4-dioxide (5.3z):

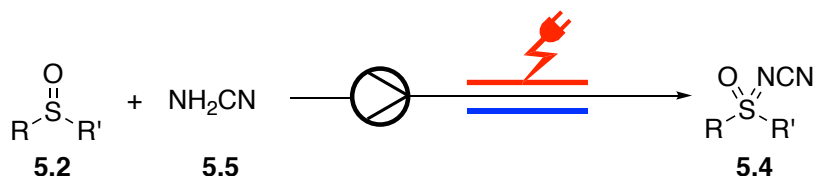
Compound **5.3z** was synthesized following GP9, using 1,4-oxathiane (**5.1z**, 156 mg, 1.5 mmol) to give the product as white solid. It was purified by column chromatography on silica gel using ethyl acetate (100 %) to obtain 48% yield (98 mg). m.p.: 130-132 °C [Lit.: 130-131°C].^[52]

¹H NMR (500 MHz, CDCl₃): δ = 4.14 – 4.08 (m, 2H), 3.13 – 3.05 (m, 2H) ppm. ¹³C NMR (101 MHz, CDCl₃): δ = 66.3, 53.0 ppm. The spectroscopic data are in agreement with the literature.^[53]

1-(Butylsulfonyl)butane (5.3aa):

Compound **5.3aa** was synthesized following GP9, using dibutylsulfane (**5.1aa**, 219 mg, 1.5 mmol) to give the product as colourless oil. It was purified by column chromatography on silica gel using ethyl acetate (100 %) to obtain 34% yield (92 mg).

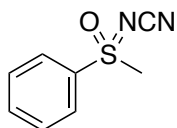
¹H NMR (500 MHz, CDCl₃): δ = 3.11 – 2.80 (m, 2H), 1.84 – 1.76 (m, 2H), 1.50 – 1.42 (m, 2H), 0.95 (t, *J* = 7.4 Hz, 3H) ppm. ¹³C NMR (126 MHz, CDCl₃): δ = 52.6, 24.0, 21.9, 13.7 ppm. The spectroscopic data are in agreement with the literature.^[39]

6.6.3. Electrochemical imination of sulfoxides:General Procedure 10 (GP 10):

The electrolysis was performed in an undivided cell using a Vapourtec Ion Electrochemical Flow Reactor (reactor volume = 0.3 mL, spacer 0.3 mm) using a platinum (Pt) electrode as anode and cathode (active surface area: *A* = 12 cm²). A solution of sulfoxide (0.05 M) and cyanamide (1.5 equiv.) in HFIP (12 mL) was placed in a 20 mL vial screw cap with hole with PTFE/silicone septum. The reaction mixture was injected to the 12 mL sample loop. After that, the reactor temperature was set at room temperature with the flow rate 0.15 mLmin⁻¹ and the current was set at 72 mA turn on automatically. Then, solutions were pumped into the

electrochemical rector. After reaching a steady state, the solution (10 mL, 0.5 mmol) was collected automatically into a glass vial. The solvent was removed under vacuum. The crude product was purified by column chromatography (EtOAc/cyclohexane).

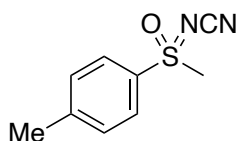
***N*-(Methyl(oxo)(phenyl)- λ^6 -sulfaneylidene)cyanamide (5.4a).**



Compound **5.4a** was synthesized following GP10, using (methylsulfinyl)benzene (**5.2a**, 70 mg, 0.5 mmol) to give the product as yellow oil. It was purified by column chromatography on silica gel using cyclohexane/ethyl acetate (4:6) to obtain 46% yield (42 mg).

^1H NMR (500 MHz, CDCl_3): δ = 7.98 – 7.89 (m, 2H), 7.76 – 7.70 (m, 1H), 7.66 – 7.60 (m, 2H), 3.28 (s, 3H) ppm. ^{13}C NMR (126 MHz, CDCl_3): δ = 136.1, 135.6, 130.4, 128, 112, 44.9 ppm. The spectroscopic data are in agreement with the literature.^[54]

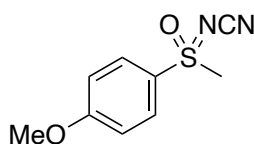
***N*-(Methyl(oxo)(*p*-tolyl)- λ^6 -sulfaneylidene)cyanamide (5.4b):**



Compound **5.4b** was synthesized following GP10, using 1-methyl-4-(methylsulfinyl)benzene (**5.2b**, 77 mg, 0.5 mmol) to give the product as yellow oil. It was purified by column chromatography on silica gel using cyclohexane/ethyl acetate (4:6) to obtain 42% yield (41 mg).

^1H NMR (500 MHz, CDCl_3): δ = 7.86 (d, J = 8.3 Hz, 2H), 7.47 (d, J = 8.2 Hz, 2H), 3.31 (s, 3H), 2.49 (s, 3H) ppm. ^{13}C NMR (126 MHz, CDCl_3): δ = 147.2, 133.0, 131.0, 128.1, 112.2, 45.1, 21.9 ppm. The spectroscopic data are in agreement with the literature.^[54]

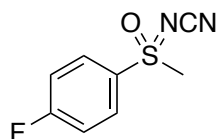
***N*-((4-Methoxyphenyl)(methyl)(oxo)- λ^6 -sulfaneylidene)cyanamide (5.4c):**



Compound **5.4c** was synthesized following GP10, using 1-methoxy-4-(methylsulfinyl)benzene (**5.2c**, 85 mg, 0.5 mmol) to give the product as yellow oil. It was purified by column chromatography on silica gel using cyclohexane/ethyl acetate (4:6) to obtain 32% yield (34 mg).

^1H NMR (500 MHz, CDCl_3): δ = 8.01 – 7.80 (m, 2H), 7.18 – 7.03 (m, 2H), 3.92 (s, 3H), 3.32 (s, 3H) ppm. ^{13}C NMR (126 MHz, CDCl_3): δ = 165.4, 130.4, 126.6, 115.7, 113.8, 56.2, 45.4 ppm. The spectroscopic data are in agreement with the literature.^[54]

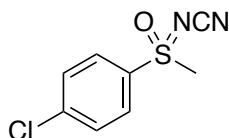
***N*-((4-Fluorophenyl)(methyl)(oxo)- λ^6 -sulfaneylidene)cyanamide (5.4d):**



Compound **5.4d** was synthesized following GP10, start with 1-fluoro-4-(methylsulfinyl)benzene (**5.2d**, 79 mg, 0.5 mmol) to give the product as yellow oil. It was purified by column chromatography on silica gel using cyclohexane/ethyl acetate (4:6) to obtain 36% yield (36 mg).

^1H NMR (500 MHz, CDCl_3): δ = 8.06 – 8.00 (m, 2H), 7.39 – 7.33 (m, 2H), 3.35 (s, 3H) ppm. ^{13}C NMR (126 MHz, CDCl_3): δ = 167.0 (d, J = 260.2 Hz), 132.0 (d, J = 3.2 Hz), 131.2 (d, J = 10.1 Hz), 118.0 (d, J = 23.1 Hz), 112.0, 45.1 ppm. ^{19}F NMR (471 MHz, CDCl_3): δ = –99.69 ppm. The spectroscopic data are in agreement with the literature.^[55]

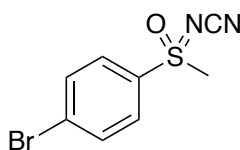
***N*-((4-Chlorophenyl)(methyl)(oxo)- λ^6 -sulfaneylidene)cyanamide (5.4e):**



Compound **5.4e** was synthesized following GP10, using 1-chloro-4-(methylsulfinyl)benzene (**5.2e**, 87 mg, 0.5 mmol) to give the product as yellow oil. It was purified by column chromatography on silica gel using cyclohexane/ethyl acetate (4:6) to obtain 48% yield (52 mg).

^1H NMR (500 MHz, CDCl_3): δ = 8.00 – 7.88 (m, 2H), 7.72 – 7.61 (m, 2H), 3.35 (s, 3H) ppm. $^{13}\text{C}\{^1\text{H}\}$ NMR (126 MHz, CDCl_3): δ = 142.8, 134.5, 130.8, 129.5, 111.6, 45.0 ppm. The spectroscopic data are in agreement with the literature.^[54]

***N*-((4-Bromophenyl)(methyl)(oxo)- λ^6 -sulfaneylidene)cyanamide (5.4f):**

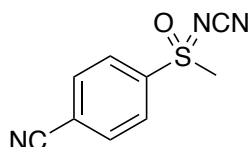


Compound **5.4f** was synthesized following GP10, using 1-bromo-4-(methylsulfinyl)benzene (**5.2f**, 110 mg, 0.5 mmol) to give the product as yellow oil. It was purified by column

chromatography on silica gel using cyclohexane/ethyl acetate (4:6) to obtain 43% yield (56 mg).

^1H NMR (500 MHz, CDCl_3): δ = 7.93 – 7.78 (m, 4H), 3.35 (s, 3H) ppm. ^{13}C NMR (126 MHz, CDCl_3): δ = 135.1, 133.8, 131.4, 129.5, 111.6, 44.8 ppm. The spectroscopic data are in agreement with the literature.^[54]

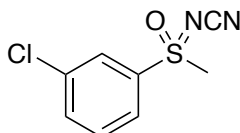
***N*-(4-Cyanophenyl)(methyl)(oxo)- λ^6 -sulfaneylidene)cyanamide (5.5g):**



Compound **5.5g** was synthesized following GP10, using 4-(methylsulfinyl)benzonitrile (**5.2g**, 83 mg, 0.5 mmol) to give the product as yellow oil. It was purified by column chromatography on silica gel using cyclohexane/ethyl acetate (4:6) to obtain 44% yield (45 mg).

^1H NMR (500 MHz, CDCl_3): δ = 8.18 – 8.11 (m, 2H), 8.02 – 7.95 (m, 2H), 3.40 (s, 3H) ppm. ^{13}C NMR (126 MHz, CDCl_3): δ = 140.4, 134.0, 128.9, 119.4, 116.6, 111.0, 44.5 ppm. The spectroscopic data are in agreement with the literature.^[56]

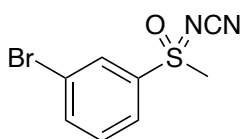
***N*-(3-Chlorophenyl)(methyl)(oxo)- λ^6 -sulfaneylidene)cyanamide (5.4h):**



Compound **5.4h** was synthesized following GP10, using 1-chloro-3-(methylsulfinyl)benzene (**5.2k**, 87 mg, 0.5 mmol) to give the product as yellow oil. It was purified by column chromatography on silica gel using cyclohexane/ethyl acetate (4:6) to obtain 42% yield (45 mg).

^1H NMR (500 MHz, CDCl_3): δ = 7.97 (t, J = 1.9 Hz, 1H), 7.89 (ddd, J = 7.9, 1.9, 1.0 Hz, 1H), 7.75 (ddd, J = 8.1, 2.0, 1.0 Hz, 1H), 7.64 (t, J = 8.0 Hz, 1H), 3.36 (s, 3H) ppm. ^{13}C NMR (101 MHz, CDCl_3): δ = 137.9, 136.8, 135.8, 131.7, 128.1, 126.1, 111.4, 44.8 ppm. The spectroscopic data are in agreement with the literature.^[57]

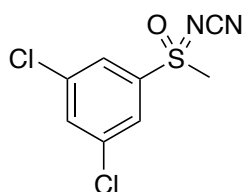
***N*-(3-Bromophenyl)(methyl)(oxo)- λ^6 -sulfaneylidene)cyanamide (5.4i):**



Compound **5.4i** was synthesized following GP10, using 1-bromo-3-(methylsulfinyl)benzene (**5.2l**, 110 mg, 0.5 mmol) to give the product as yellow oil. It was purified by column chromatography on silica gel using cyclohexane/ethyl acetate (4:6) to obtain 37% yield (48 mg).

^1H NMR (500 MHz, CDCl_3): δ = 8.12 (s, 1H), 7.97 – 7.88 (m, 2H), 7.57 (t, J = 8.0 Hz, 1H), 3.36 (s, 3H) ppm. ^{13}C NMR (126 MHz, CDCl_3): δ = 138.7, 138.0, 131.8, 130.8, 126.6, 124.4, 111.4, 44.9 ppm. The spectroscopic data are in agreement with the literature.^[54]

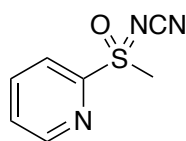
***N*-(3,5-Dichlorophenyl)(methyl)(oxo)- λ^6 -sulfaneylidene)cyanamide (**5.4l**):**



Compound **5.4l** was synthesized following GP10, using 1,3-dichloro-5-(methylsulfinyl)benzene (**5.2p**, 105 mg, 0.5 mmol) to give the product as yellow oil. It was purified by column chromatography on silica gel using cyclohexane/ethyl acetate (4:6) to obtain 29% yield (36 mg).

^1H NMR (500 MHz, CDCl_3): δ = 7.87 (d, J = 1.8 Hz, 2H), 7.75 (t, J = 1.8 Hz, 1H), 3.38 (s, 3H) ppm. ^{13}C NMR (126 MHz, CDCl_3): δ = 139.1, 137.5, 135.7, 126.4, 110.9, 44.7 ppm. IR (neat): 2934, 2185, 1444, 1211, 1167, 1091, 844, 688 cm^{-1} . HRMS (ESI) m/z : $[\text{M}+\text{H}]$ cal for $\text{C}_8\text{H}_7\text{N}_2\text{OSCl}_2$ 248.9656; found 248.9655.

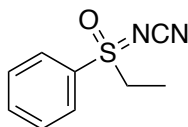
***N*-(Methyl(oxo)(pyridin-2-yl)- λ^6 -sulfaneylidene)cyanamide (**5.4m**):**



Compound **5.4m** was synthesized following GP10, using 2-(methylsulfinyl)pyridine (**5.2q**, 101 mg, 0.5 mmol) to give the product as yellow oil. It was purified by column chromatography on silica gel using cyclohexane/ethyl acetate (4:6) to obtain 35% yield (32 mg).

^1H NMR (500 MHz, CDCl_3): δ = 8.75 (d, J = 4.7 Hz, 1H), 8.10 (d, J = 7.8 Hz, 1H), 7.99 (td, J = 7.8, 1.6 Hz, 1H), 7.62 – 7.53 (m, 1H), 3.24 (s, 3H) ppm. ^{13}C NMR (126 MHz, CDCl_3): δ = 158.2, 150.6, 138.8, 128.0, 121.6, 113.7, 40.5 ppm. The spectroscopic data are in agreement with the literature.^[54]

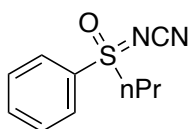
***N*-(Ethyl(oxo)(phenyl)- λ^6 -sulfaneylidene)cyanamide (**5.4n**):**



Compound **5.4n** was synthesized following GP10, using (ethanesulfinyl)benzene (**5.2r**, 77 mg, 0.5 mmol) to give the product as yellow oil. It was purified by column chromatography on silica gel using cyclohexane/ethyl acetate (4:6) to obtain 43% yield (42 mg).

^1H NMR (500 MHz, CDCl_3): δ = 7.98 – 7.90 (m, 2H), 7.82 – 7.77 (m, 1H), 7.71 – 7.66 (m, 2H), 3.52 – 3.33 (m, 2H), 1.34 (t, J = 7.4 Hz, 3H) ppm. ^{13}C NMR (126 MHz, CDCl_3): δ = 135.6, 134.0, 130.3, 128.7, 112.3, 51.7, 7.3 ppm. The spectroscopic data are in agreement with the literature.^[55]

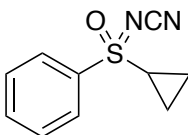
***N*-(Oxo(phenyl)(propyl)- λ^6 -sulfaneylidene)cyanamide (**5.4o**):**



Compound **5.4o** was synthesized following GP10, using (propylsulfinyl)benzene (**5.2s** 84 mg, 0.5 mmol) to give the product as yellow oil. It was purified by column chromatography on silica gel using cyclohexane/ethyl acetate (4:6) to obtain 40% yield (42 mg).

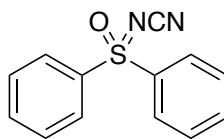
^1H NMR (500 MHz, CDCl_3): δ = 8.01 – 7.88 (m, 2H), 7.80 – 7.75 (m, 1H), 7.71 – 7.64 (m, 2H), 3.40 (ddd, J = 14.2, 10.6, 5.4 Hz, 1H), 3.30 (ddd, J = 14.2, 10.5, 5.5 Hz, 1H), 1.87 – 1.72 (m, 2H), 1.02 (t, J = 7.5 Hz, 3H) ppm. ^{13}C NMR (126 MHz, CDCl_3): δ = 135.5, 134.8, 130.3, 128.6, 112.3, 58.4, 16.3, 12.6 ppm. IR (neat): 2923, 2191, 1447, 1241, 1186, 1091, 825, 683 cm^{-1} . HRMS (ESI) m/z : $[\text{M}+\text{H}]$ cal for $\text{C}_{10}\text{H}_{13}\text{N}_2\text{OS}$ 209.0749; found 209.0746.

***N*-(Cyclopropyl(oxo)(phenyl)- λ^6 -sulfaneylidene)cyanamide (**5.4p**):**



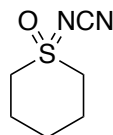
Compound **5.4p** was synthesized following GP10, using (cyclopropylsulfinyl)benzene (**5.2t** 83 mg, 0.5 mmol) to give the product as yellow oil. It was purified by column chromatography on silica gel using cyclohexane/ethyl acetate (4:6) to obtain 38% yield (39 mg).

^1H NMR (500 MHz, CDCl_3): δ = 8.02 – 7.87 (m, 2H), 7.78 – 7.74 (m, 1H), 7.69 – 7.61 (m, 2H), 2.73 – 2.65 (m, 1H), 1.72 – 1.65 (m, 1H), 1.40 – 1.28 (m, 2H), 1.15 – 1.08 (m, 1H) ppm. ^{13}C NMR (126 MHz, CDCl_3): δ = 136.5, 135.2, 130.2, 128.0, 112.2, 33.7, 7.2, 6.1 ppm. The spectroscopic data are in agreement with the literature.^[54]

***N*-(Oxodiphenyl- λ^6 -sulfaneylidene)cyanamide (5.4q):**

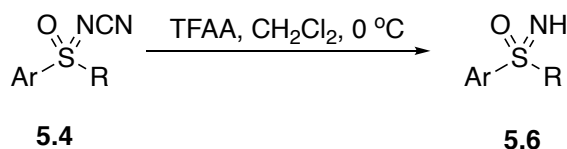
Compound **5.4q** was synthesized following GP10, using sulfinyldibenzene (**5.2w** 101 mg, 0.5 mmol) to give the product as yellow oil. It was purified by column chromatography on silica gel using cyclohexane/ethyl acetate (4:6) to obtain 23% yield (28 mg).

^1H NMR (500 MHz, CDCl_3): δ = 7.72 – 7.64 (m, 2H), 7.63 – 7.55 (m, 3H) ppm. ^{13}C NMR (126 MHz, CDCl_3): δ = 135.8, 133.1, 130.4, 127.6, 113.8 ppm. The spectroscopic data are in agreement with the literature.^[54]

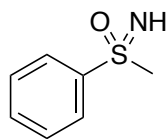
***N*-(1-Oxidotetrahydro-2H-1 λ^6 -thiopyran-1-ylidene)cyanamide (5.4r):**

Compound **5.4r** was synthesized following GP10, using tetrahydro-2H-thiopyran 1-oxide (**5.2y**, 59 mg, 0.5 mmol) to give the product as yellow oil. It was purified by column chromatography on silica gel using ethyl acetate (100%) to obtain 52% yield (41 mg).

^1H NMR (500 MHz, CDCl_3): δ = 3.60 – 3.37 (m, 2H), 3.34 – 3.08 (m, 2H), 2.23 – 2.04 (m, 4H), 1.80 – 1.57 (m, 2H) ppm. ^{13}C NMR (126 MHz, CDCl_3): δ = 112.2, 51.8, 23.8, 22.9 ppm. IR (neat): 2148, 1416, 1174, 872, 756 cm^{-1} . HRMS (ESI) m/z : $[\text{M}+\text{H}]$ cal for $\text{C}_6\text{H}_{11}\text{N}_2\text{OS}$ 159.0592; found 159.0593. The spectroscopic data are in agreement with the literature.

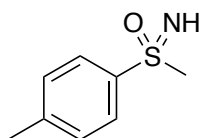
6.6.4. Reduction of *N*-cyanosulfoximines:General Procedure 11 (GP 11):

To a mixture solution of *N*-cyanosulfoximine (0.5 mmol) in CH_2Cl_2 (10 mL) at 0 °C, TFAA (1.5 mmol) was added. The reaction mixture was allowed to stirrer at room temperature until the starting material was consumed (monitored by TLC). The mixture was quenched with water (10 mL). The aqueous layer was extracted with CH_2Cl_2 (3 x 10 mL). The combined organic layers were dried over anhydrous MgSO_4 , filtered and evaporated. The residue was purified by column chromatography (EtOAc/cyclohexane).

Imino(methyl)(phenyl)- λ^6 -sulfanone (5.6a):

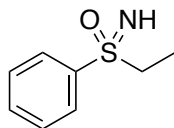
Compound **5.6a** was synthesized following GP11, using *N*-(methyl(oxo)(phenyl)- λ^6 -sulfaneylidene)cyanamide (**5.4a**, 90 mg, 0.5 mmol) to give the product as colourless oil. It was purified by column chromatography on silica gel using ethyl acetate (100 %) to obtain 68% yield (53 mg).

^1H NMR (500 MHz, CDCl_3): δ = 8.02 – 7.90 (m, 2H), 7.61 – 7.55 (m, 1H), 7.55 – 7.45 (m, 2H), 3.06 (s, 3H), 2.70 (s, 1H) ppm. ^{13}C NMR (126 MHz, CDCl_3): δ = 143.5, 133.1, 129.3, 127.7, 46.2 ppm. The spectroscopic data are in agreement with the literature.^[58]

Imino(methyl)(*p*-tolyl)- λ^6 -sulfanone (5.6b):

Compound **5.6b** was synthesized following GP11, using *N*-(methyl(oxo)(*p*-tolyl)- λ^6 -sulfaneylidene)cyanamide (**5.4b**, 97 mg, 0.5 mmol) to give the product as pale-yellow oil. It was purified by column chromatography on silica gel using ethyl acetate (100%) to obtain 74% yield (63 mg).

^1H NMR (500 MHz, CDCl_3): δ = 7.87 (d, J = 8.3 Hz, 2H), 7.33 (d, J = 8.3 Hz, 2H), 3.08 (br.s, 3H), 2.94 (s, 1H), 2.43 (s, 3H) ppm. ^{13}C NMR (126 MHz, CDCl_3): δ = 144.1, 140.6, 130.0, 127.9, 46.4, 21.6 ppm. The spectroscopic data are in agreement with the literature.^[58]

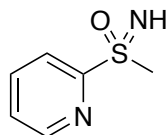
Ethyl(imino)(phenyl)- λ^6 -sulfanone (5.6c):

Compound **5.6c** was synthesized following GP4, using *N*-(ethyl(oxo)(phenyl)- λ^6 -sulfaneylidene)cyanamide (**5.4n**, 97 mg, 0.5 mmol) to give the product as pale-yellow oil. It was purified by column chromatography on silica gel using ethyl acetate (100%) to obtain 72% yield (61 mg).

^1H NMR (500 MHz, CDCl_3): δ = 7.96 – 7.86 (m, 2H), 7.59 – 7.54 (m, 1H), 7.52 – 7.46 (m, 2H), 3.12 (q, J = 7.5 Hz, 2H), 2.69 (s, 1H), 1.20 (t, J = 7.4 Hz, 3H) ppm. ^{13}C NMR (126 MHz,

CDCl₃): δ = 141.3, 133.0, 129.1, 128.5, 51.8, 7.9 ppm. The spectroscopic data are in agreement with the literature.^[58]

Imino(methyl)(pyridin-2-yl)- λ^6 -sulfanone (5.6d):



Compound **5.6d** was synthesized following GP4, using *N*-(methyl(oxo)(pyridin-2-yl)- λ^6 -sulfaneylidene)cyanamide (**5.4m**, 97 mg, 0.5 mmol) to give the product as pale-yellow oil. It was purified by column chromatography on silica gel using CH₂Cl₂/MeOH (20:1) to obtain 51% yield (40 mg).

¹H NMR (500 MHz, CDCl₃): δ = 8.72 (d, J = 4.7 Hz, 1H), 8.12 (dt, J = 7.9, 1.0 Hz, 1H), 7.94 (td, J = 7.8, 1.7 Hz, 1H), 7.50 (ddd, J = 7.6, 4.7, 1.1 Hz, 1H), 3.25 (s, 3H), 2.73 (s, 1H) ppm. ¹³C NMR (126 MHz, CDCl₃): δ = 160.6, 150.7, 138.4, 126.9, 121.2, 42.4 ppm. The spectroscopic data are in agreement with the literature.^[59]

6.7. References:

- [1] “Ion electrochemical reactor,” can be found under <https://www.vapourtec.com/products/flow-reactors/ion-electrochemical-reactor-features/> (accessed Jul 28, 2021).
- [2] R. A. Green, R. C. D. Brown, D. Pletcher, B. Harji, *Org. Process Res. Dev.* **2015**, *19*, 1424–1427.
- [3] F. Liebner, P. Schmid, C. Adelwöhrer, T. Rosenau, *Tetrahedron* **2007**, *63*, 11817–11821.
- [4] M. D. Mitzlaff, K. Warning, H. Jensen, *Eur. J. Org. Chem.* **1978**, *1978*, 1713–1733.
- [5] L. Sun, Y. Yuan, M. Yao, H. Wang, D. Wang, M. Gao, Y.-H. Chen, A. Lei, *Org. Lett.* **2019**, *21*, 1297–1300.
- [6] G. Perin, P. Santoni, A. M. Barcellos, P. C. Nobre, R. G. Jacob, E. J. Lenardão, C. Santi, *Eur. J. Org. Chem.* **2018**, *2018*, 1224–1229.
- [7] C. Yu, H. Shi, J. Yan, *Arkivoc* **2015**, *2015*, 266–276.
- [8] A. A. Vieira, J. B. Azeredo, M. Godoi, C. Santi, E. N. da Silva Júnior, A. L. Braga, *J. Org. Chem.* **2015**, *80*, 2120–2127.
- [9] C. Bosman, A. D’Annibale, S. Resta, C. Trogolo, *Tetrahedron Lett.* **1994**, *35*, 6525–6528.
- [10] M. Tiecco, L. Testaferri, M. Tingoli, D. Chianelli, D. Bartoli, *Tetrahedron* **1988**, *44*, 2261–2272.
- [11] E. S. Conner, K. E. Crocker, R. G. Fernando, F. R. Fronczek, G. G. Stanley, J. R. Ragains, *Org. Lett.* **2013**, *15*, 5558–5561.
- [12] M. Kostić, P. Verdía, V. Fernández-Stefanuto, R. Puchta, E. Tojo, *J. Phys. Org. Chem.* **2019**, *32*, e3928.
- [13] S. Vásquez-Céspedes, A. Ferry, L. Candish, F. Glorius, *Angew. Chemie Int. Ed.* **2015**, *54*, 5772–5776.
- [14] M. Liu, Y. Li, L. Yu, Q. Xu, X. Jiang, *Sci. China Chem.* **2018**, *61*, 294–299.
- [15] Q.-B. Zhang, P.-F. Yuan, L.-L. Kai, K. Liu, Y.-L. Ban, X.-Y. Wang, L.-Z. Wu, Q. Liu, *Org. Lett.* **2019**, *21*, 885–889.
- [16] S. E. Denmark, W. R. Collins, *Org. Lett.* **2007**, *9*, 3801–3804.
- [17] K. C. Nicolaou, S. P. Seitz, W. J. Sipio, J. F. Blount, *J. Am. Chem. Soc.* **1979**, *101*, 3884–3893.
- [18] Y. Ni, H. Zuo, Y. Li, Y. Wu, F. Zhong, *Org. Lett.* **2018**, *20*, 4350–4353.

- [19] R. Choudhary, P. Singh, R. Bai, M. C. Sharma, S. S. Badsara, *Org. Biomol. Chem.* **2019**, *17*, 9757–9765.
- [20] S. K. Bhunia, P. Das, R. Jana, *Org. Biomol. Chem.* **2018**, *16*, 9243–9250.
- [21] S. Kawaguchi, M. Kotani, S. Atobe, A. Nomoto, M. Sonoda, A. Ogawa, *Organometallics* **2011**, *30*, 6766–6769.
- [22] S. Guo, S. Li, Z. Zhang, W. Yan, H. Cai, *Tetrahedron Lett.* **2020**, *61*, 151566.
- [23] J. Wang, X. Wang, H. Li, J. Yan, *J. Organomet. Chem.* **2018**, *859*, 75–79.
- [24] X. Zhang, Z. Shi, C. Shao, J. Zhao, D. Wang, G. Zhang, L. Li, *Eur. J. Org. Chem.* **2017**, *2017*, 1884–1888.
- [25] C.-Y. Li, Y.-C. Liu, Y.-X. Li, D. M. Reddy, C.-F. Lee, *Org. Lett.* **2019**, *21*, 7833–7836.
- [26] D. Wang, J. Zhao, W. Xu, C. Shao, Z. Shi, L. Li, X. Zhang, *Org. Biomol. Chem.* **2017**, *15*, 545–549.
- [27] Q. Xu, X. Liang, B. Xu, J. Wang, P. He, P. Ma, J. Feng, J. Wang, J. Niu, *Chem. – A Eur. J.* **2020**, *26*, 14896–14902.
- [28] Y. Li, S. A. Rizvi, D. Hu, D. Sun, A. Gao, Y. Zhou, J. Li, X. Jiang, *Angew. Chemie Int. Ed.* **2019**, *58*, 13499–13506.
- [29] Z. Cheng, P. Sun, A. Tang, W. Jin, C. Liu, *Org. Lett.* **2019**, *21*, 8925–8929.
- [30] M. M. D. Pramanik, N. Rastogi, *Chem. Commun.* **2016**, *52*, 8557–8560.
- [31] L.-Q. Wei, B.-H. Ye, *ACS Appl. Mater. Interfaces* **2019**, *11*, 41448–41457.
- [32] S. Gan, J. Yin, Y. Yao, Y. Liu, D. Chang, D. Zhu, L. Shi, *Org. Biomol. Chem.* **2017**, *15*, 2647–2654.
- [33] H. Saito, K. Yamamoto, Y. Sumiya, L. Liu, K. Nogi, S. Maeda, H. Yorimitsu, *Chem. – An Asian J.* **2020**, *15*, 2442–2446.
- [34] G. Laudadio, N. J. W. Straathof, M. D. Lanting, B. Knoops, V. Hessel, T. Noël, *Green Chem.* **2017**, *19*, 4061–4066.
- [35] L. Wang, M. Chen, P. Zhang, W. Li, J. Zhang, *J. Am. Chem. Soc.* **2018**, *140*, 3467–3473.
- [36] L. Zhao, H. Zhang, Y. Wang, *J. Org. Chem.* **2016**, *81*, 129–136.
- [37] L. Ma, H. Zhou, M. Xu, P. Hao, X. Kong, H. Duan, *Chem. Sci.* **2021**, *12*, 938–945.
- [38] F. Silva, A. Baker, J. Stansall, W. Michalska, M. S. Yusubov, M. Graz, R. Saunders, G. J. S. Evans, T. Wirth, *European J. Org. Chem.* **2018**, *2018*, 2134–2137.
- [39] C. Li, N. Mizuno, K. Murata, K. Ishii, T. Suenobu, K. Yamaguchi, K. Suzuki, *Green*

- Chem.* **2020**, *22*, 3896–3905.
- [40] L. Chen, Y. Yang, D. Jiang, *J. Am. Chem. Soc.* **2010**, *132*, 9138–9143.
- [41] C. S. Richards-Taylor, D. C. Blakemore, M. C. Willis, *Chem. Sci.* **2014**, *5*, 222–228.
- [42] W.-Y. Fang, H.-L. Qin, *J. Org. Chem.* **2019**, *84*, 5803–5812.
- [43] M. Tabata, K. Moriyama, H. Togo, *Eur. J. Org. Chem.* **2014**, *2014*, 3402–3410.
- [44] P. Hu, M. Tan, L. Cheng, H. Zhao, R. Feng, W.-J. Gu, W. Han, *Nat. Commun.* **2019**, *10*, 2425.
- [45] W. J. Kerr, G. J. Knox, M. Reid, T. Tuttle, J. Bergare, R. A. Bragg, *ACS Catal.* **2020**, *10*, 11120–11126.
- [46] S. Chen, Y. Li, M. Wang, X. Jiang, *Green Chem.* **2020**, *22*, 322–326.
- [47] A. Shavnya, K. D. Hesp, V. Mascitti, A. C. Smith, *Angew. Chemie Int. Ed.* **2015**, *54*, 13571–13575.
- [48] A. Adenot, J. Char, N. von Wolff, G. Lefèvre, L. Anthore-Dalion, T. Cantat, *Chem. Commun.* **2019**, *55*, 12924–12927.
- [49] B. Saavedra, X. Marset, G. Guillena, D. J. Ramón, *Eur. J. Org. Chem.* **2020**, *2020*, 3462–3467.
- [50] M. H. Holshouser, L. J. Loeffler, I. H. Hall, *J. Med. Chem.* **1981**, *24*, 853–858.
- [51] Y. Meng, M. Wang, X. Jiang, *Angew. Chemie Int. Ed.* **2020**, *59*, 1346–1353.
- [52] K. R. Guertin, A. S. Kende, *Tetrahedron Lett.* **1993**, *34*, 5369–5372.
- [53] K. Kamata, K. Sugahara, Y. Kato, S. Muratsugu, Y. Kumagai, F. Oba, M. Hara, *ACS Appl. Mater. Interfaces* **2018**, *10*, 23792–23801.
- [54] C. A. Dannenberg, L. Fritze, F. Krauskopf, C. Bolm, *Org. Biomol. Chem.* **2017**, *15*, 1086–1090.
- [55] W. Hu, F. Teng, H. Peng, J. Yu, S. Sun, J. Cheng, Y. Shao, *Tetrahedron Lett.* **2015**, *56*, 7056–7058.
- [56] F. W. Goldberg, J. G. Kettle, J. Xiong, D. Lin, *Tetrahedron* **2014**, *70*, 6613–6622.
- [57] S. Kim, J. E. Kim, J. Lee, P. H. Lee, *Adv. Synth. Catal.* **2015**, *357*, 3707–3717.
- [58] S. Li, L. Liu, R. Wang, Y. Yang, J. Li, J. Wei, *Org. Lett.* **2020**, *22*, 7470–7474.
- [59] O. García Mancheño, O. Bistri, C. Bolm, *Org. Lett.* **2007**, *9*, 3809–3811.

Appendix: GC Method and Data for Chapter 2

The GC method was performed using a Perkin Elmer Clarus system (Clarus 680 GC, Clarus SQ8C Mass Spec), fitted with a Perkin Elmer Elite 1 30 m x 0.25 mm, 0.25 μ m column. The results were processed using chromatogram software. The carrier flow was 1.0 mL min⁻¹ and split flow was 20 mL min⁻¹. The injection temperature was 100 °C; initial temperature 80 °C kept for 2 min, then 8 °C min⁻¹ to 280 °C, kept for 3 min. Compounds **2.57a** and **2.58a** were observed at 5.6 and 6.6 min; the cis- and trans-**2.59a** were observed at 7.9 and 8.2 min.

Table 2.1, entry 2

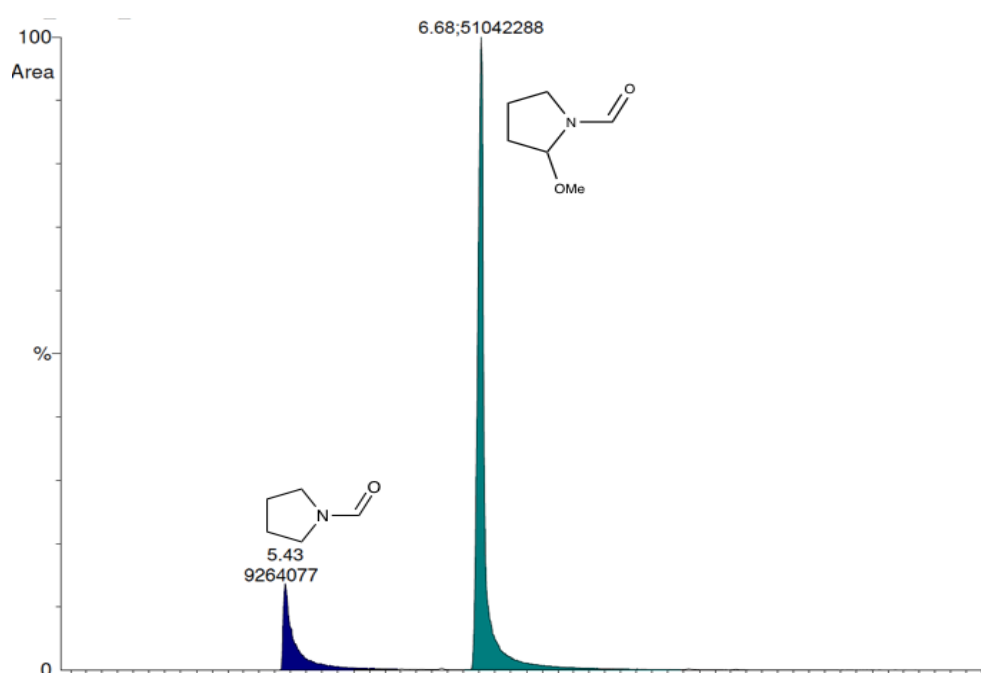


Table 2.1, entry 8

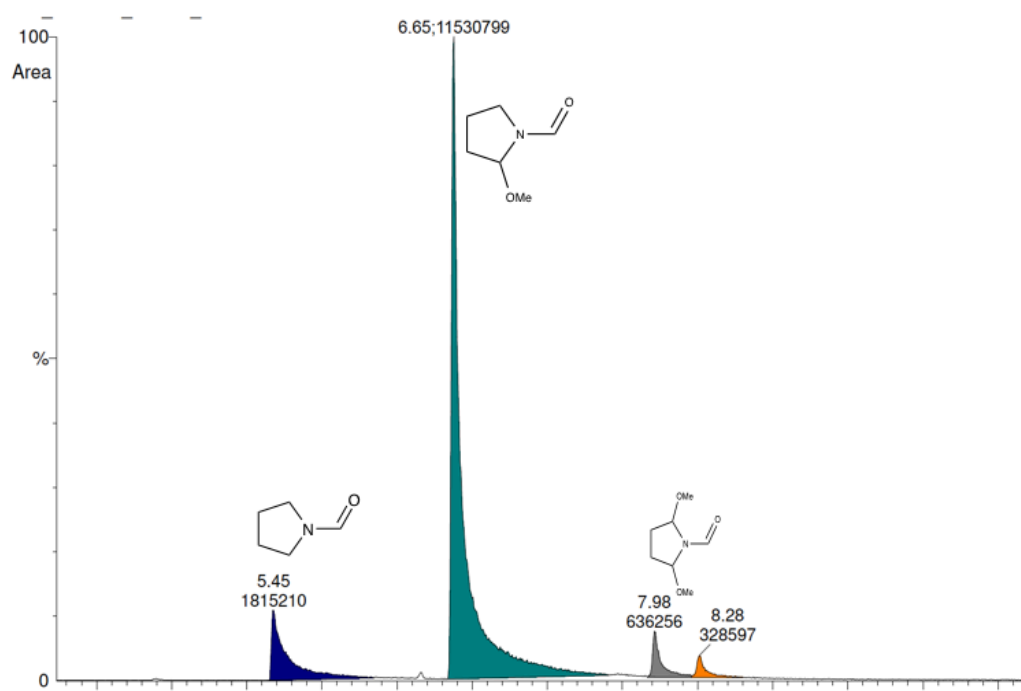


Table 2.1, entry 13

